Phase II
Design Definition of the

Laser Atmospheric Wind Sounder (LAWS)

Contract NAS8-37590

DR-20
Vol. II: FINAL REPORT

November 1992

Prepared for

GEORGE C. MARSHALL SPACE FLIGHT CENTER
MARSHALL SPACE FLIGHT CENTER, AL 35812

Lockheed
Missiles & Space Company
4800 Bradford Blvd., Huntsville, AL 35807

DR-20

PHASE II

DESIGN DEFINITION OF THE

LASER ATMOSPHERIC WIND SOUNDER (LAWS)

VOL II: FINAL REPORT

November 1992

CONTRACT NAS8-37590

Prepared for
National Aeronautics and Space Administration
George C. Marshall Space Flight Center (MSFC)
Marshall Space Flight Center, Alabama 35812

Prepared by _____
D. J. Wilson
LAWS Deputy Program Manager
Chief Engineer

Date 11/17/92

Approved by _____
W. E. Jones
LAWS Program Manager

Date 11/17/92

Submitted by

Lockheed
Missiles & Space Company
4800 Bradford Blvd., Huntsville, AL 35807

FOREWORD

This document presents the final results of the 21-month Phase II Design Definition and 18-month laser breadboard efforts for the Laser Atmospheric Wind Sounder (LAWS). This work was performed for the Marshall Space Flight Center (MSFC) by Lockheed Missiles & Space Company, Inc., Huntsville, Alabama, under Contract NAS8-37590. The study was conducted under the direction of R.G. Beranek, NASA Program Manager, and R.M. Baggett, LAWS Instrument Project Office, JA92. The period of performance was 24 August 1990 to 30 June 1992. Subcontractors contributing to this effort are Textron Defense Systems - Everett, and Itek Optical Systems.

The complete Phase II Final Report consists of the following three volumes:

Volume I	Executive Summary
Volume II	Final Report
Volume III	Program Costs.

Major contributions to this contract at Lockheed-Huntsville were made by T.K. Speer, G.R. Power, Dr. S.C. Kurzius, Dr. W.W. Montgomery, Dr. W.R. Eberle, F.R. Davis, P.G. Porter, A.J. Condino, D.M. Tilley, R.E. Joyce, K.R. Shrider, W.M. Harrison, G.B. Washburn, B.J. Audeh, Dr. F. Wang, W. Dean, Z.S. Karu, J. Dyar, T.L. Sonnenberg, A.S. Stewart, J.T. Steigerwald, T.G. Larson, D.D. Coulter, J.C. Frost, R.G. Raney, and W.S. Johnson.

At Textron Defense Systems-Everett, S. Ghoshroy, PM, was supported by Dr. H.P. Chou, F. Faria-e-Maia, I. Moran, H. Stowe, G. Crawford, M. Fava, M. Nguyen, and T. Christiano.

Itek Optical Systems contributors were S.E. Kendrick, PM, C.M. Ullathorne, and C. Robbert.

Major contributions were also made by Dr. Carl Buczek, Laser Systems & Research Corp., and Dr. C. DiMarzio, Northeastern University.

CONTENTS

CONTENTS
(Continued)

CONTENTS
(Concluded)

ILLUSTRATIONS

ILLUSTRATIONS
(Continued)

ILLUSTRATIONS
(Continued)

ILLUSTRATIONS
(Continued)

TABLES

ACRONYMS AND ABBREVIATIONS

A/D	analog-to-digital
ADP	acceptance data package
AGC	automated gain control
ARTS	automated requirements traceability system
ASE	airborne support equipment
BDU	bus data unit
BW	bandwidth
CART	condition of assembly at release and transfer
CCAM	collision/contamination avoidance maneuver
CCSDS	Consultative Committee for Space Data Systems
C&DH	command and data handling
CEI	contract end item
CG	center of gravity
CIL	critical items list
CPCI	computer program configuration item
CPDP	computer program development plan
CTE	coefficient of thermal expansion
CVCM	collected volatile condensable materials
DPA	destructive physical analysis
DVT	design verification test
EEE	electrical, electronic, and electromagnetic
EI	equipment item
EMC	electromagnetic compatibility
EO	electro-optical
EOS	Earth Observation System
EPS	electrical power subsystem
ESC/ESD	electrostatic compatibility/electrostatic discharge
EU	engineering unit
FFT	fast fourier transformer
FMEA	failure mode effects analysis
FOSR	flexible optical solar reflector
GFE	Government furnished equipment
GIDEP	Government-Industry Data Exchange Program
GIIS	General Instrument Interface Specification
GSE	Ground Support Equipment

ACRONYMS AND ABBREVIATIONS (Continued)

HOSC	Huntsville Operations Support Center
H&S	health and status
HST	Hubble Space Telescope
IARM	input annular reference mirror
IAS	integrated alignment sensor
ICD	Interface Control Document
IMU	inertial measurement unit
LAEPL	LAWS Approved EEE Parts List
LAWS	Laser Atmospheric Wind Sounder
LC&DH	LAWS Command and Data Handling
LO	local oscillator
LOS	line-of-sight
MA	multiple access
MAPTIS	Material Processing Information System
MCS	Manufacturing Control System
MLI	multi-layer insulation
MUA	Material Usage Agreement
NSPAR	Nonstandard Part Approval Request
OARM	output annular reference mirror
OR	obscuration ratio
PA	product assurance
PCP	platform command processor
PDS	power distribution system
PDT	product development team
PFN	pulse forming network
PIND	particle impact noise detection
PLF	payload fairing
PMP	program management plan
POCC	Payload Operations Control Center
PRACA	parts problem reporting and corrective action
PRF	pulse repitition frequency
PRL	program requirements list
PSATS	parallel spacecraft automated test system
PZT	pezio-electric transducer

ACRONYMS AND ABBREVIATIONS (Concluded)

RCS	reaction control system
rms	root mean square
R&RR	range and range rate
SA	single access
SBA	scan bearing assembly
SLM	single longitudinal mode
SMS	structures and mechanical subsystem
SN	space network
SNR	signal-to-noise ratio
SQU	Structural Qualification Unit
STDN/DSN	Spaceflight Tracking and Data Network/Deep Space Network
ST&LO	system test and launch operations
STV	structural test vehicle
TAP	transportation adapter plate
TCS	Thermal Control System
TDRSS	Tracking and Data Relay Satellite System
TML	total mass loss
TWG	test working group
ULE	ultra-low expansion
VCRM	verification cross reference matrix
WFE	wavefront error
WSMC	Western Space and Missile Center

Section 1
INTRODUCTION AND SUMMARY

Lockheed personnel, along with team member subcontractors and consultants, have performed a preliminary design for the LAWS Instrument. Breadboarding and testing of a LAWS class laser have also been performed. These efforts have demonstrated that LAWS is a feasible Instrument and can be developed with existing state-of-the-art technology. Only a commitment to fund the Instrument development and deployment is required to place LAWS in orbit and obtain the anticipated science and operational forecasting benefits.

The LAWS Science Team was selected in 1988-89 as were the competing LAWS Phase I/II contractor teams. The LAWS Science Team developed requirements for the LAWS Instrument, and the NASA/LAWS project office defined launch vehicle and platform design constraints. From these requirements and constraints, several of which are listed in *Figure 1-1*, the Lockheed team developed LAWS Instrument concepts and configurations. A system designed to meet these requirements and constraints is outlined in *Figure 1-2*.

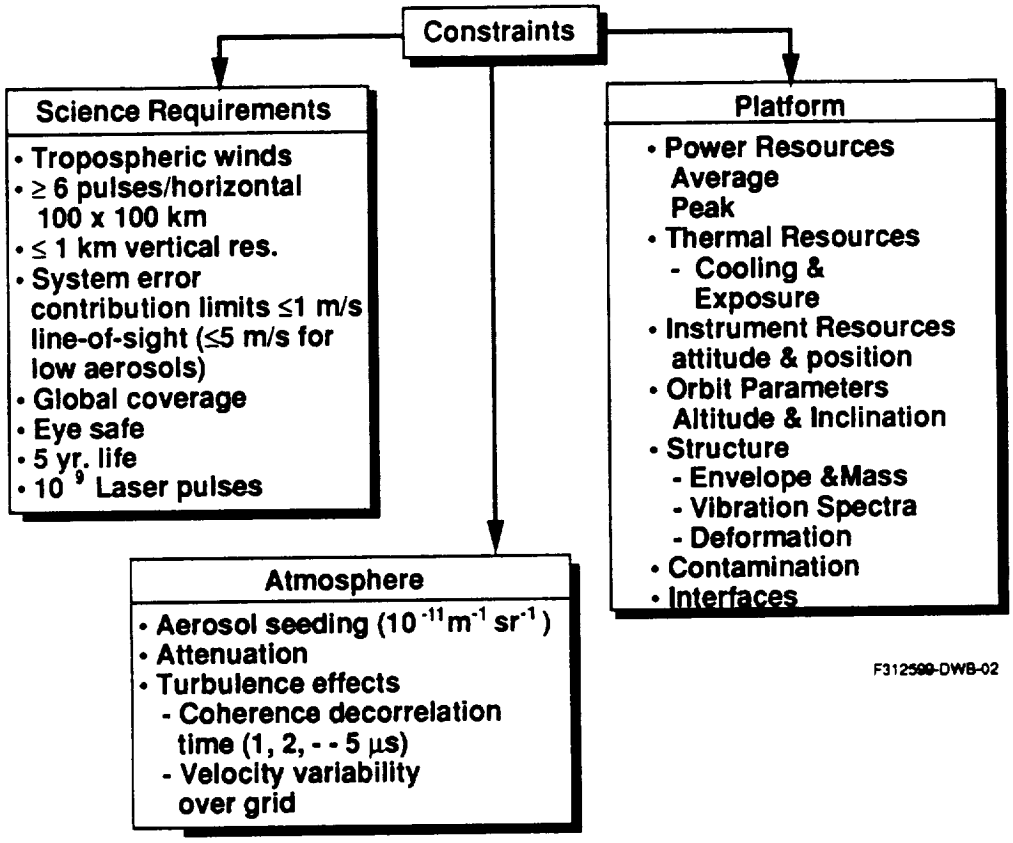

Figure 1-1. LAWS Science Requirements and Constraints

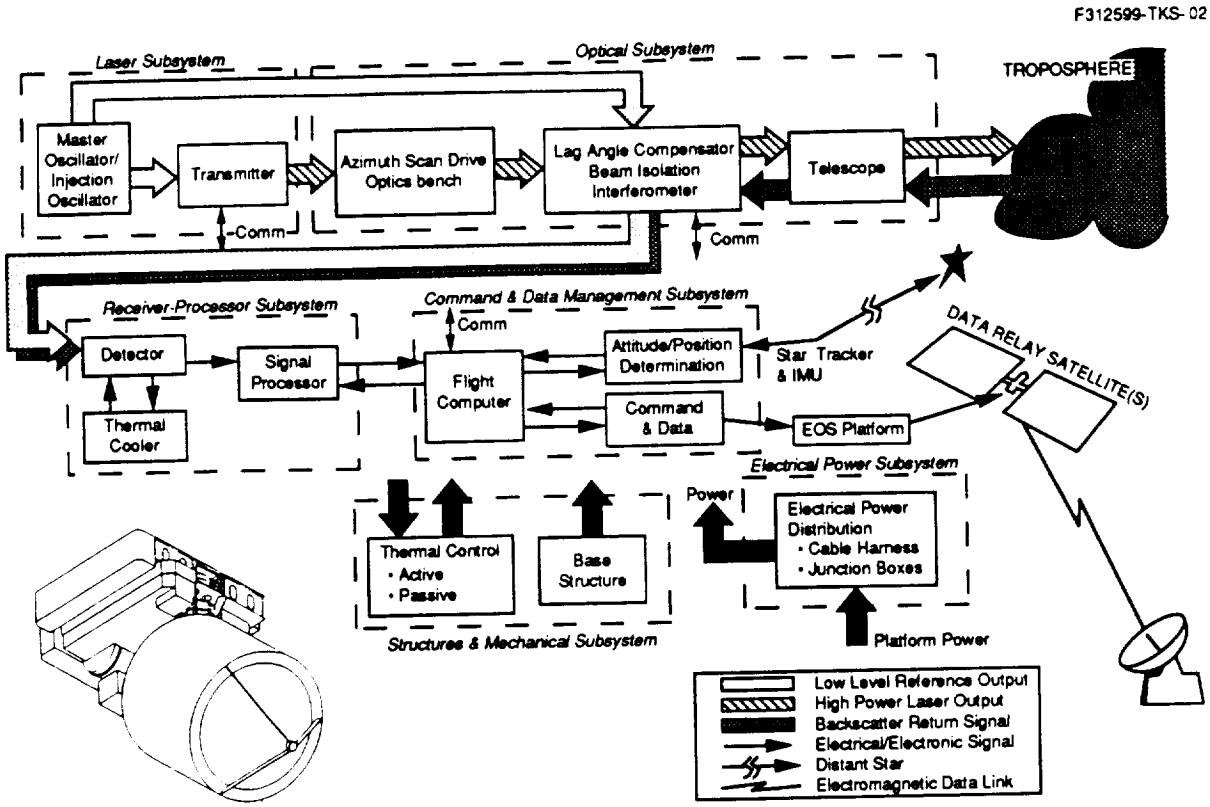

Figure 1-2. LAWS System Diagram

Figure 1-2 identifies the LAWS primary subsystems and interfaces - laser, optical and receiver/processor - required to assemble a lidar. The figure also identifies the support subsystems required for the lidar to function from space: structures and mechanical, thermal, electrical, and command and data management. The Lockheed team has developed a preliminary design of a LAWS Instrument system consisting of these subsystems and interfaces which will meet the requirements and objectives of the Science Team.

This final report provides a summary of the systems engineering analyses and trades of the LAWS (Section 2). Summaries of the configuration, preliminary designs of the subsystems, testing recommendations, and performance analysis are presented in Section 3. Sections 4 and 5 discuss environmental considerations associated with deployment of LAWS. Finally, the successful LAWS laser breadboard effort is discussed in Section 6 along with the requirements and test results.

The Lockheed team baseline LAWS Instrument meets all Science Team requirements. The Instrument design is compatible with the Atlas IIAS and, with minor modifications, the Delta launch vehicles. It is also compatible with the MSFC strawman orbital platform.

The team has also investigated the downsized LAWS Instrument, i.e., from a 15 J to 5 J/pulse laser and from a 1.6 m to a 0.75 m aperture telescope. This Instrument can be developed and orbited at a somewhat reduced cost from the baseline LAWS. Our laser breadboard has already been operated at this reduced energy output, and wall plug efficiency, pulse frequency chirp, and performance have been demonstrated to meet these downsized Instrument requirements.

The Lockheed team is ready to proceed with an aggressive program to orbit a LAWS Instrument in the near future. After performing these analyses, design studies, and laser breadboard development, we foresee no technical challenges to disrupt the early deployment of LAWS. We recommend an aggressive 18-month effort in testing the laser breadboards and optimizing detector performance, followed immediately with a Phase C/D program leading to an early year 2001 launch.

Section 2
SYSTEM ENGINEERING AND ANALYSIS

The complexity and sophistication of the NASA LAWS Instrument, including its integration with the satellite platform bus, booster, and supporting ground and space systems, require a systematic application of a sound system engineering process. This process was applied by Lockheed to develop the LAWS Instrument configuration during Phases I and II as shown in *Figure 2-1.*

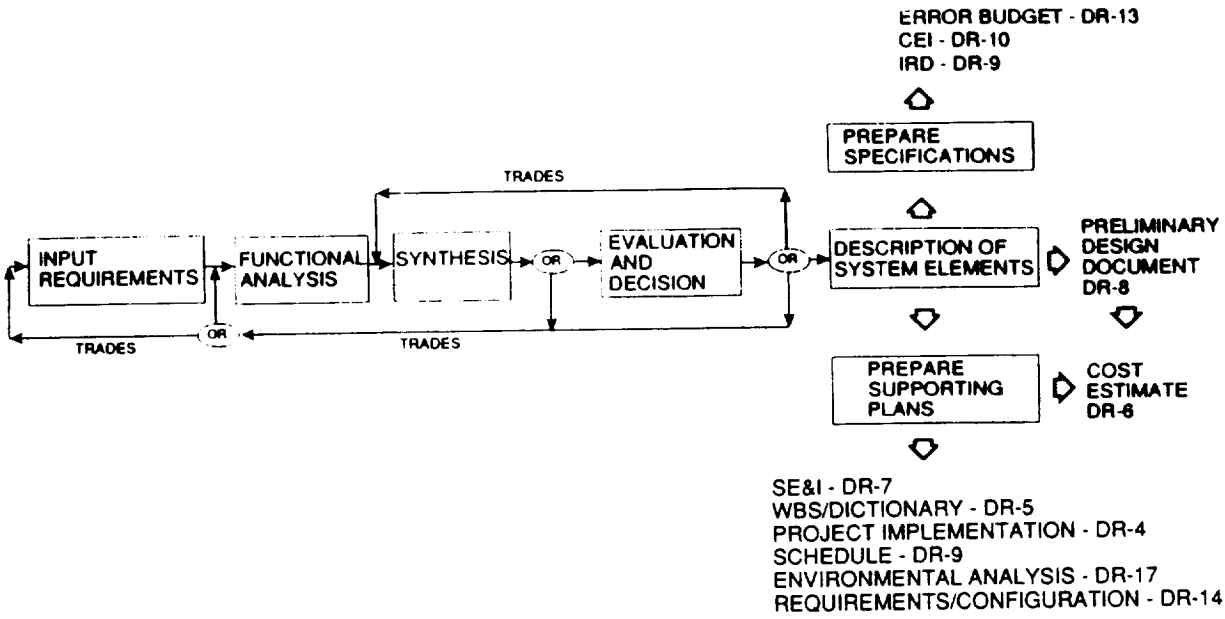

Figure 2-1. System Engineering Process

2.1 REQUIREMENTS

Performance requirements, established by NASA and the Science Team, were analyzed by Lockheed and its subcontractors. These requirements were organized, flowed down, and allocated to different LAWS System functions as shown in *Figure 2-2.* As these requirements were accumulated, identified, and quantified, they were entered into a Lockheed developed computerized data base system known as the Automated Requirements Traceability System (ARTS). ARTS permits easy access for updating existing requirements and for adding new requirements as they are identified. Specification formats, compatible with the requirements of MM 8040.12A, are included in this data base program; these formats can be selected as the requirements are printed as different types of specifications and interface control documents. Requirements collected by this process are listed in the Prime Equipment Detail Specification (DR-10).

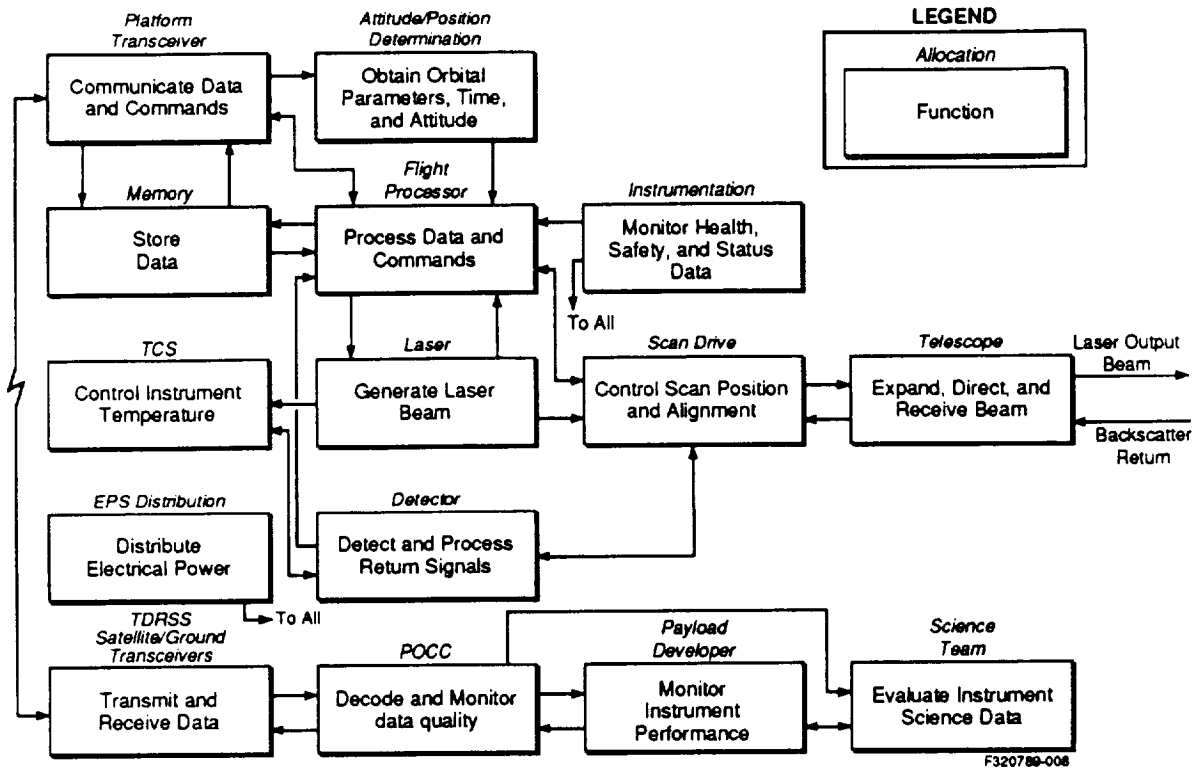

Figure 2-2. LAWS System Functional Flow Diagram

2.2 ANALYSIS AND TRADES (PHASES I AND II)

The functions shown in *Figure 2-2* were individually analyzed to identify each internal subfunction performed to achieve each assigned performance requirement. Interfaces with other functions were analyzed to determine how each function could best be accomplished. These analyses also allowed identification and evaluation of available approaches that could be synthesized by proven hardware and/or software techniques to implement the requirements.

The results of these analyses were evaluated to determine performance compatibility and to establish requirement limits which were entered into the ARTS data base record. When multiple approaches were identified, trade studies were conducted to select the one best suited to perform the required function.

2.3 ERROR BUDGET

The LAWS Instrument will collect large amounts of data from a satellite platform in a sun-synchronous orbit about the Earth. Additional atmospheric phenomena data will be collected from other sensors. These data will be processed with algorithms developed by the Science Team.

Interaction between the collection and processing of these data to produce wind information is shown in *Figure 2-3*. Each block of the error tree is assigned an identification number. These identification numbers allow each of the parameter variation effects to be traced from the bottom of the error tree to the top, where the results of all effects are integrated.

The LAWS Instrument errors are represented by laser frequency factors, pointing factors, and signal-to-noise factors as shown in *Figure 2-3*. Statistical data, produced by selected shot management modes of operation, are also recorded for input to the statistical sampling algorithm. Two types of data are supplied for input to the velocity algorithm. These data are related to pointing errors and to factors that affect the signal-to-noise ratio (SNR).

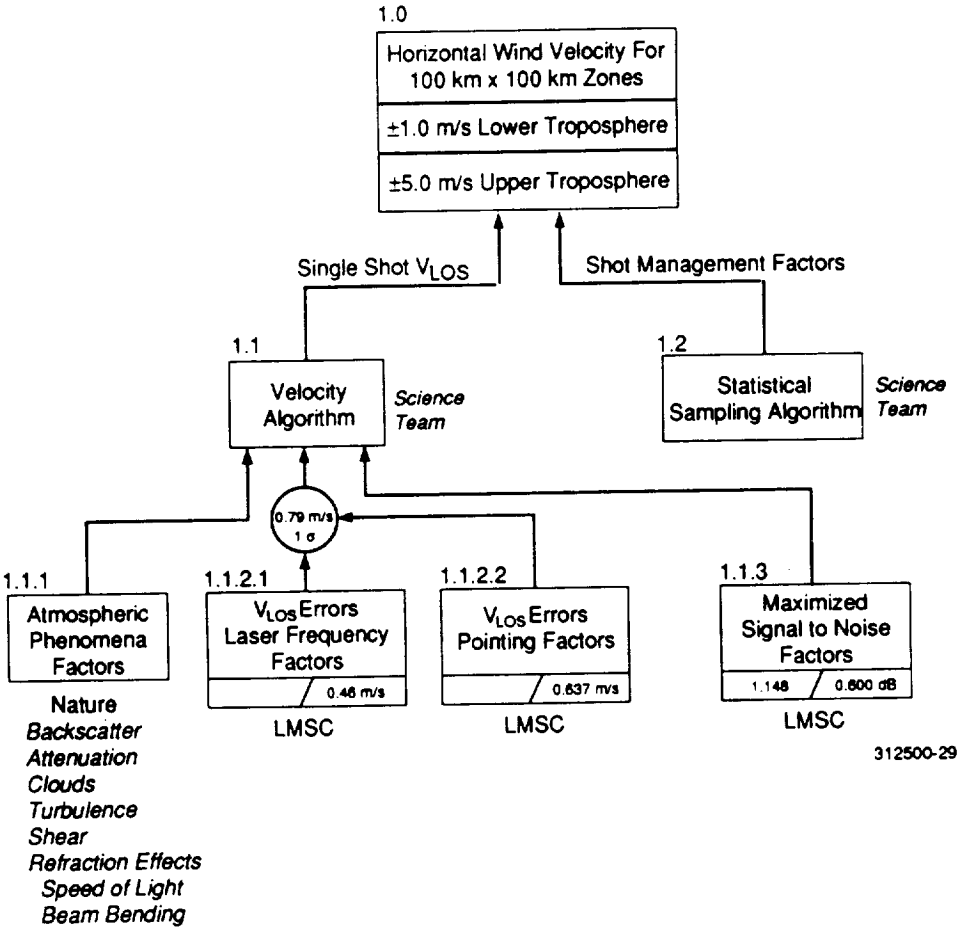

Figure 2-3. LAWS Instrument Data Collected for Processing with the Science Team Algorithm

Errors introduced by undesired variations in the laser frequency are shown in *Figure 2-4*. These errors appear as incorrect shifts in the LOS doppler velocity measurement values. Pointing factor error sources are shown in *Figure 2-5*. The angular error values and the equivalent velocity errors are also shown in this figure.

The ability to extract doppler shifted velocity information from low level signals that contain high levels of noise provides a useful measure of LAWS system performance. Because of the low signal levels expected to be received by the LAWS Instrument from suspended aerosols, design efforts are required to maximize the effective SNR. An SNR equation, recognized by NASA and members of the Science Team, is shown in *Figure 2-6*. This equation includes LAWS Instrument parameters which can be controlled by design to maximize the Instrument SNR. Factors which contribute to the maximization of the SNR are shown in *Figure 2-7*. The LAWS Instrument Error Budget Report was delivered to NASA as DR-13. Note that the SNR equation presented in *Figure 2-6* contains the pulse length (which is controlled by the contractor) and not the processing bandwidth (controlled by the Science Team). As such, this narrow band SNR is ~14 dB greater than the wide band SNR.

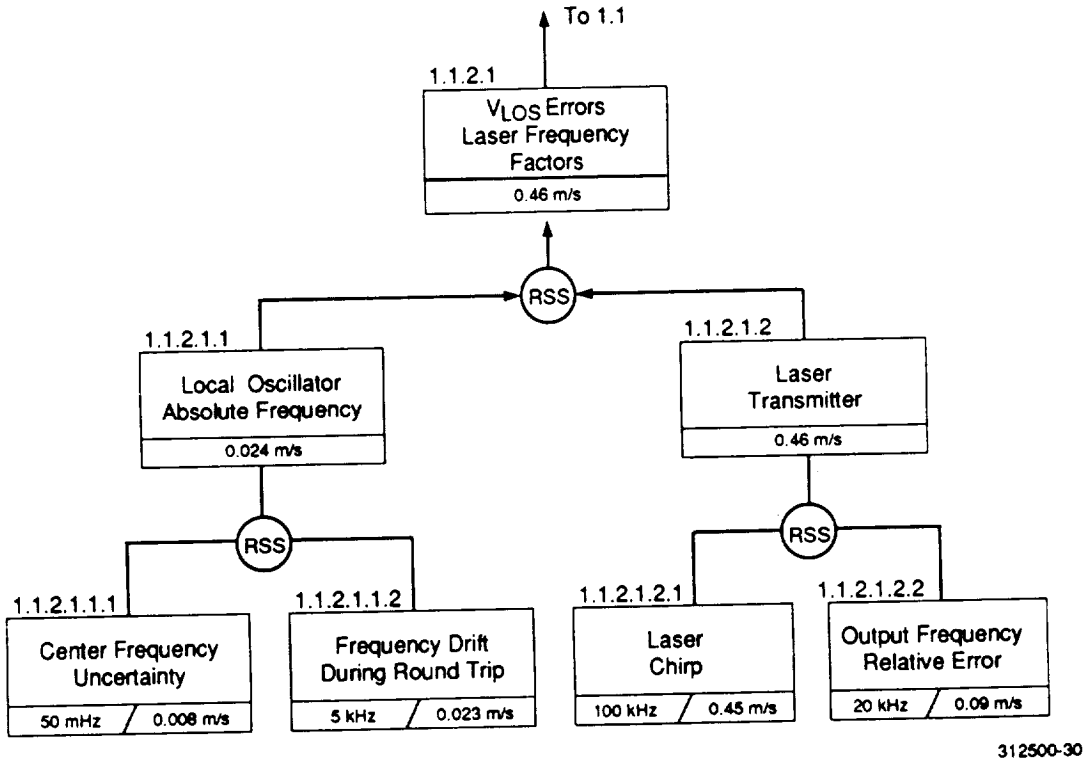

Figure 2-4. Laser Frequency Variations Introduce LOS Wind Velocity Errors

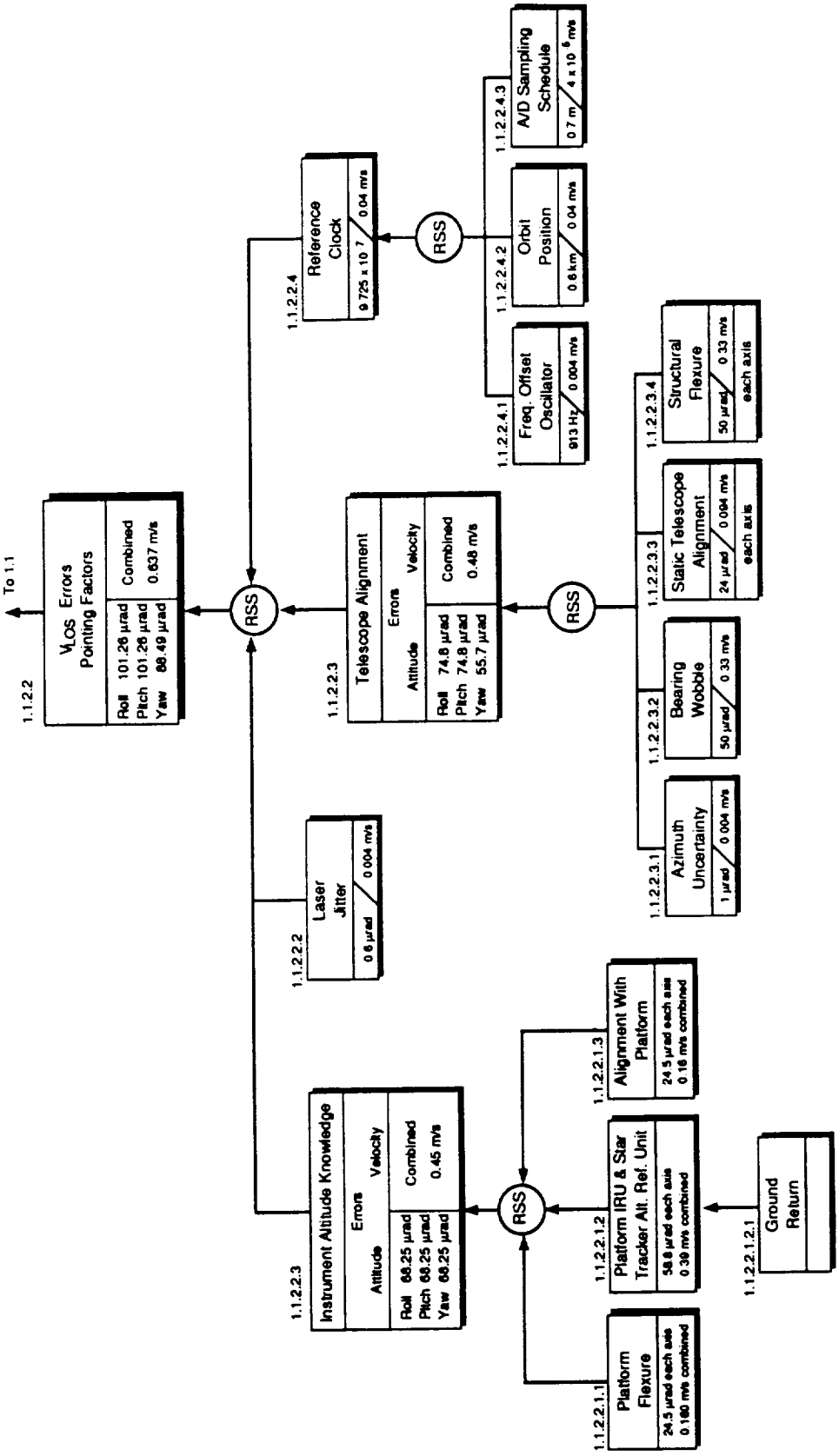

Figure 2-5. LOS Pointing Errors Introduce Errors into Wind Velocity Vector Measurements

$$SNR = \frac{1}{h\upsilon}\ \frac{\pi D^2}{4R^2}\ J\ \frac{c\tau}{2}\ \beta\ \frac{[\text{Absorption Effects}]}{[\text{Turbulence Effects}]}\ [\text{Efficiencies}]$$

Where:

$h\upsilon$ = Photon Energy = 2.18E - 20 J (for 9.11 μm)

$\frac{\pi D^2}{4}$ = Aperture Area

J = Pulse Energy

$\frac{c\tau}{2}$ = Pulse Half Length (for Distributed Target)

R = Range to Target

β = Backscatter Coefficient (Given)

Absorption Effects (Given)

Turbulence Effects (Small Number at these Ranges)

η = Combined Efficiencies

For LAWS

$\eta = \eta$ Transmit Optics $\cdot\ \eta$ Receiver Optics $\cdot\ \eta$ Heterodyne Efficiency $\cdot\ \eta$ Effective Quantum Efficiency

312500-32

Reference: EB23/W. Jones, November 1990, Modification for Turbulence to D. Emmitt's October 1990 memo.

Figure 2-6. Signal-to-Noise Ratio Equation Used to Evaluate LAWS Instrument Performance

2.4 RISK ASSESSMENT

Lockheed is very sensitive to risk factors involved in the development, fabrication, testing, and extended, unattended operation of the LAWS Instrument in space. Because of this sensitivity, Lockheed has selected a risk assessment technique that has proven to be effective on other successful Lockheed space programs.

Three interrelated elements associated with program risks for the LAWS Program are technical performance, cost, and schedule. Recognition and identification of potential program risks are the first steps required to circumvent or minimize problems that could seriously affect the outcome of the program. This analysis begins with three steps:

- Identification of potential hardware, software, and support system risk elements using a structured approach to ensure that all system areas have been considered
- Quantitative assessment of the risk and ranking of items to determine those of most concern
- Definition of alternate paths to minimize risk and establish criteria for initiation or termination of these activities.

The LAWS Instrument Work Breakdown Structure (WBS) is used for evaluation purposes to identify possible development risks for every element of the program down to the fourth level (other than elements listed under Project Management). The risk assessment employed considers two factors: probability of failure (P_F) and consequence of failure (C_F).

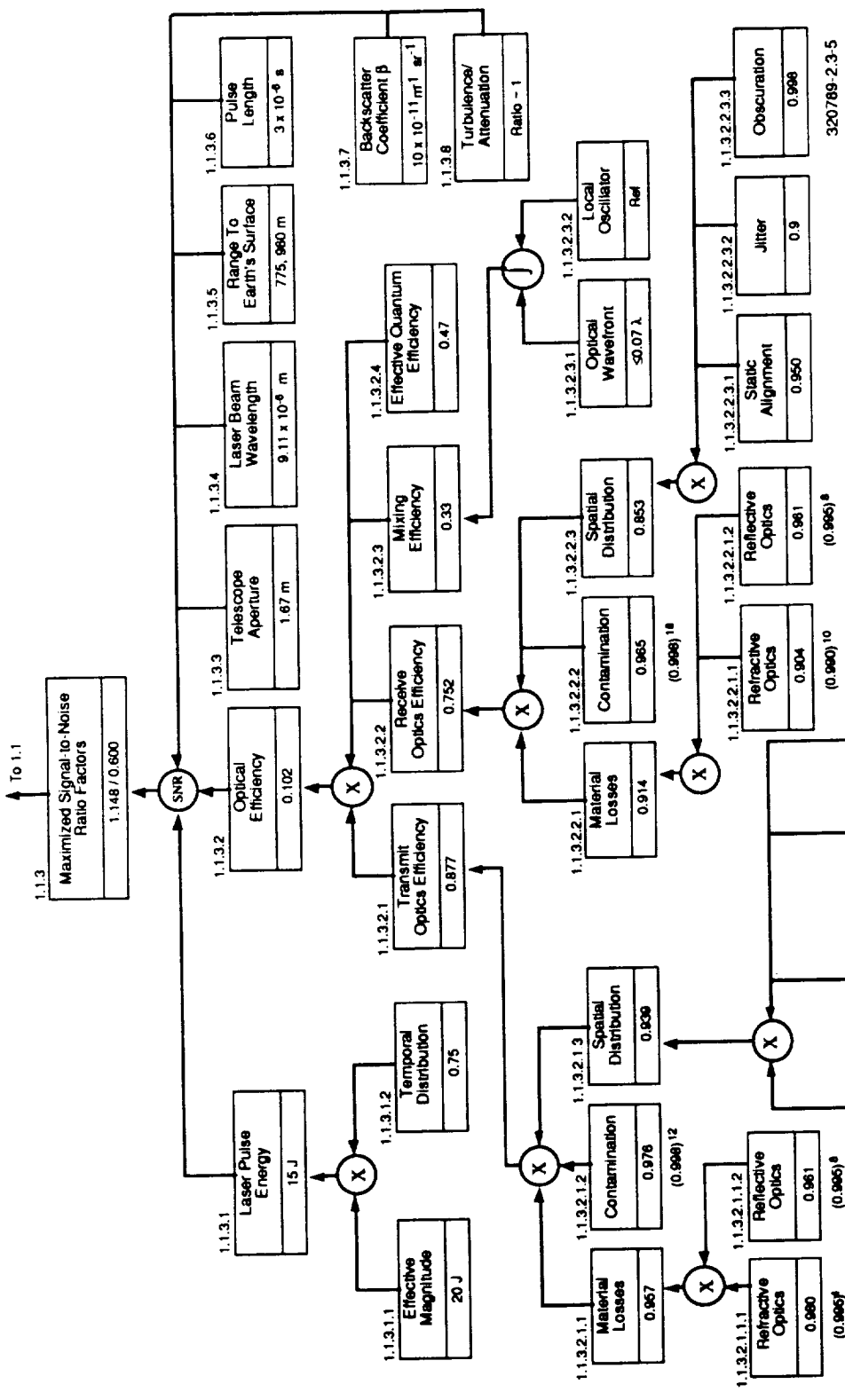

Figure 2-7. Contributing Factors for Maximized Signal-to-Noise Ratio

P_F considers the technical risks associated with a hardware or software item's potential failure to achieve technical performance specification requirements due to the item's state of maturity, degree of complexity, or dependency on interfacing items. Hardware and software designs are evaluated to determine whether potential technical problems exist, and the extent of these problems. P_F is obtained from the ratings given in *Tables 2-1, 2-2,* and *2-3* for the five different problem categories as follows:

$$P_F = \frac{P_{M_H} + P_{M_{SW}} + P_{C_H} + P_{C_{SW}} + P_D}{5}$$

where

P_{M_H} = Probability of failure due to degree of maturity of hardware

P_{MSW} = Probability of failure due to degree of maturity of software

P_{C_H} = Probability of failure due to degree of complexity of hardware

P_{CSW} = Probability of failure due to degree of complexity of software

P_D = Probability of failure due to dependency on other items.

Where no software is involved, those two factors are omitted, and the denominator becomes 3.

The C_F factor considers the impact on the LAWS Instrument system if an item fails to meet technical, cost, or schedule requirements. The C_F is determined by using values given in *Table 2-4* for the three factors (technical, cost, and schedule) and calculating the average of these factors:

$$CF = \frac{C_{F_S} + C_{F_C} + C_{F_T}}{3}$$

where:

C_{F_T} =Consequences of failure due to technical factors

C_{F_C} = Consequences of failure due to changes in cost

C_{F_S} = Consequences of failure due to changes in schedule.

The Risk Factor (R_F) is calculated using the equation:

$$R_F = P_F + C_F - P_F \times C_F.$$

The risk evaluation process is shown in *Figure 2-8.* Risks are ranked from minimal to high according to established criteria, as in the following example:

$R_F < 0.3$ risk is low

$R_F > 0.3 < 0.7$ risk is medium

$R_F > 0.7$ risk is high.

Table 2-1. Probability of Failure - Maturity

Rating	Hardware (P_{M_H})	Software ($P_{M_{SW}}$)
0.1 (low)	Off-the-shelf items; no new hardware required	Existing, proven software or no new software required
0.3	Minor redesign of proven hardware	Some slight change in existing S/W; minor change in modules/lines of code
0.5	Technical feasibility established: change in design and performance requirements of existing hardware	Major change in existing S/W modules/lines of code
0.7	Undergoing exploratory development; complex design and performance requirements; technology available	New software; software similar to existing programs
0.9 (high)	Very limited experience; some research performed; significant change in state-of-the-art	New software; programs pushing state-of-the-art

Table 2-2. Probability of Failure - Complexity

Rating	Hardware (P_{C_H})	Software ($P_{C_{SW}}$)
0.1 (low)	Simple design; no changes required or not applicable	Simple design; no changes required, or not applicable
0.3	Minor increase in complexity or performance requirements	Minor change in program complexity
0.5	Moderate increase in complexity or performance requirements	Large increase in program complexity
0.7	Significant increase in complexity	Significant increase in program complexity; major increase in modules
0.9 (high)	Extremely complex system	Highly complex program; very large data bases and complex, rapidly operating executive programs

*Table 2-3. Probability of Failure - Dependency on Other Factors**

Rating	Description
0.1 (low)	Independent of system/facility or associate contractor's performance or schedule efforts
0.3	Dependent upon the schedule for modification of existing system or facility to meet requirements
0.5	Dependent upon the performance, capacity or interface of system or facility to meet requirements
0.7	Dependent upon the schedule for assembly and test of other items or the system to meet requirements
0.9 (high)	Dependent upon the performance of hardware/software or of interfaces of the system to meet requirements

* Factors include other group hardware/software performance, interfaces, schedule, and availability.

Table 2-4. Consequences of Failure (C_F)

Rating	Technical (C_{F_T})	Costs (C_{F_C})	Schedules (C_{F_S})
0.1 (low)	Minimal or no consequences; unimportant	Budget estimates not exceeded; some transfer of monies	Negligible impact on program; slight development schedule change compensated by available schedule slack
0.3	Some problems anticipated but easily corrected	Cost estimates exceed budget by 1 to 5 percent	Minor slip in schedule (less than one month); some adjustment in item milestones required
0.5	Some reduction in technical performance	Cost estimates increased by 5 to 20 percent	Moderate item development schedule slip (1 to 3 months); impact on item milestones with potential for impact on segment milestones
0.7	Significant degradation in technical performance	Cost estimates increased by 20 to 50 percent	Item development schedule slip in excess of 3 months
0.9 (high)	Technical goals cannot be achieved	Cost estimates increase in excess of 50 percent	Large schedule slip that impacts segment milestones and/or has possible impact on system milestones

Risk abatement activities for moderate and high risk items will then be established based on the above evaluation. These activities may include the following:

- Initiation of parallel development activities
- Initiation of extensive development testing
- Development of simulations to develop performance predictions
- Use of consultants and specialists to review design
- Intensified management review of the development process.

A risk management program will be developed which identifies risk abatement activities to be undertaken, balancing the risk level against the resulting cost and schedule impact on the program. A final review of the selected items and alternatives will be made against current state-of-the-art knowledge and recent experience on other programs to ensure that the development risk for any item has not been under-evaluated.

Inherent in the monitoring and review process is the evaluation of predicted performance against specified requirements. Appropriate performance parameters for risk monitoring purposes are established at the top level, together with their contributors (or allocations) at the lower levels.

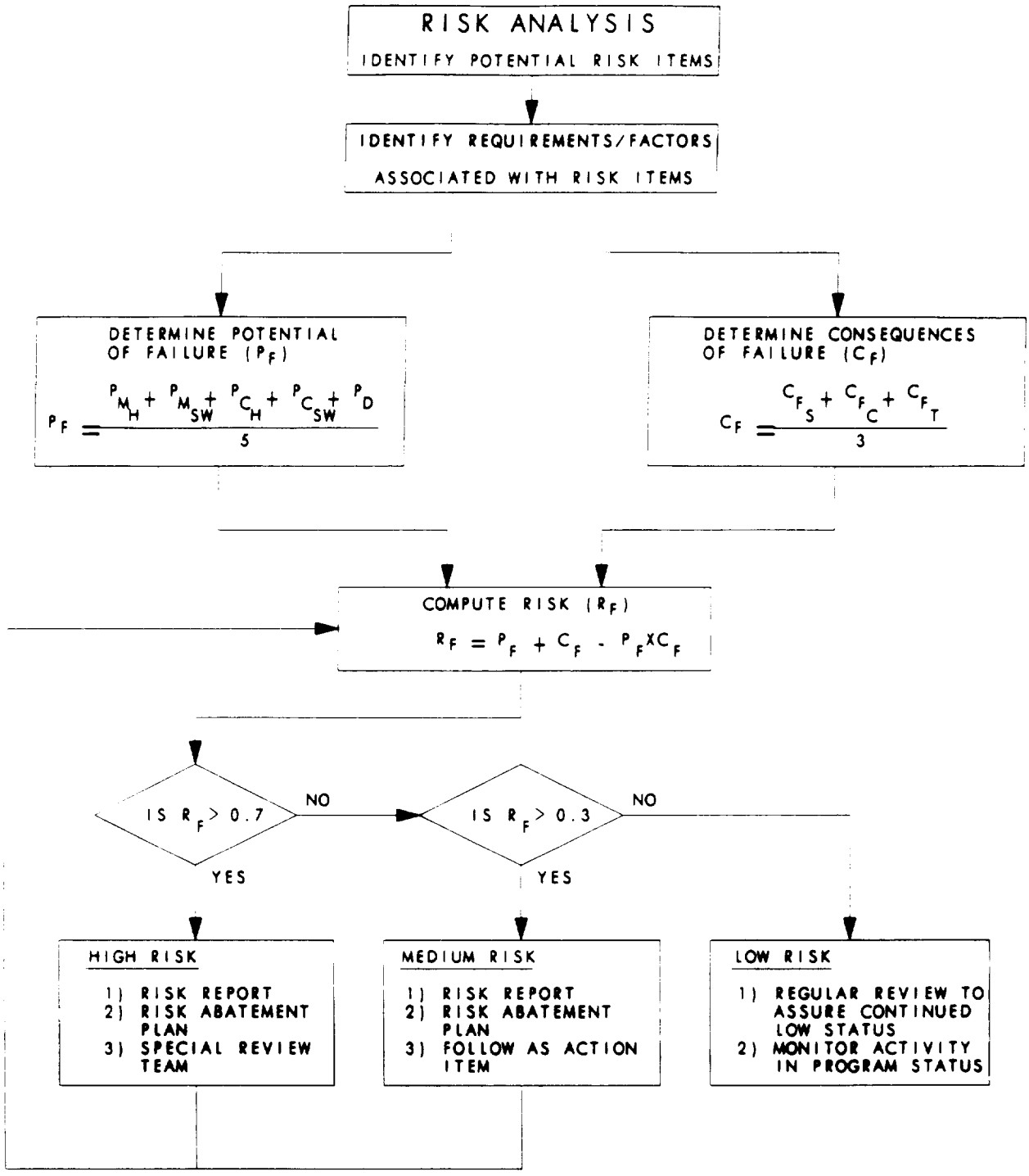

Figure 2-8. Risk Assessment Process

Risk items are continually monitored by Systems Engineering and actions recommended, such as initiation or termination of activities when the capability of an item (or its alternate) to meet performance requirement is established.

A Risk Management Plan will be prepared for moderate and high risk items. The plan shall include the following as a minimum:

- A statement of the risk
- Assessment of the risk and assessment rationale
- Consequence of failure
- Alternatives considered and risk associated with each alternative
- The recommended risk abatement actions
- Implementation impact statement (cost, schedule, technical)
- Implementation start date and key milestone schedule
- Criteria for tracking and closure.

2.5 SPECIFICATION REQUIREMENTS

A Contract End Item Specification was prepared and delivered to NASA as a Contract Data Report (DR-10). This specification was prepared in accordance with the requirements of MM 8040.12A, Standard Contractor Configurations Management Requirements.

To ensure compliance with higher level requirements and compatibility with LAWS interfacing requirements, this specification was prepared using the Lockheed developed Automated Requirements Traceability System (ARTS). ARTS creates a requirement hierarchy as shown in *Figure 2-9*. From the LAWS CEI level, requirements are allocated to lower level subsystems. The requirements matrix resulting from systems design requirements documents (SDRDs) ensures traceability and compliance through all program levels. ARTS is maintained by current data revision.

The CEI specification and lower level SDRDs are maintained by configuration management (CM) and controlled by the LAWS configuration control board (CCB). This CEI specification and SDRDs are maintained by data revision to text in a CM data base and issued as either page revision or as a complete reissue, whichever is most cost effective, to reflect approved program changes. All changes to this specification are processed in accordance with the requirements of MM 8040.12A.

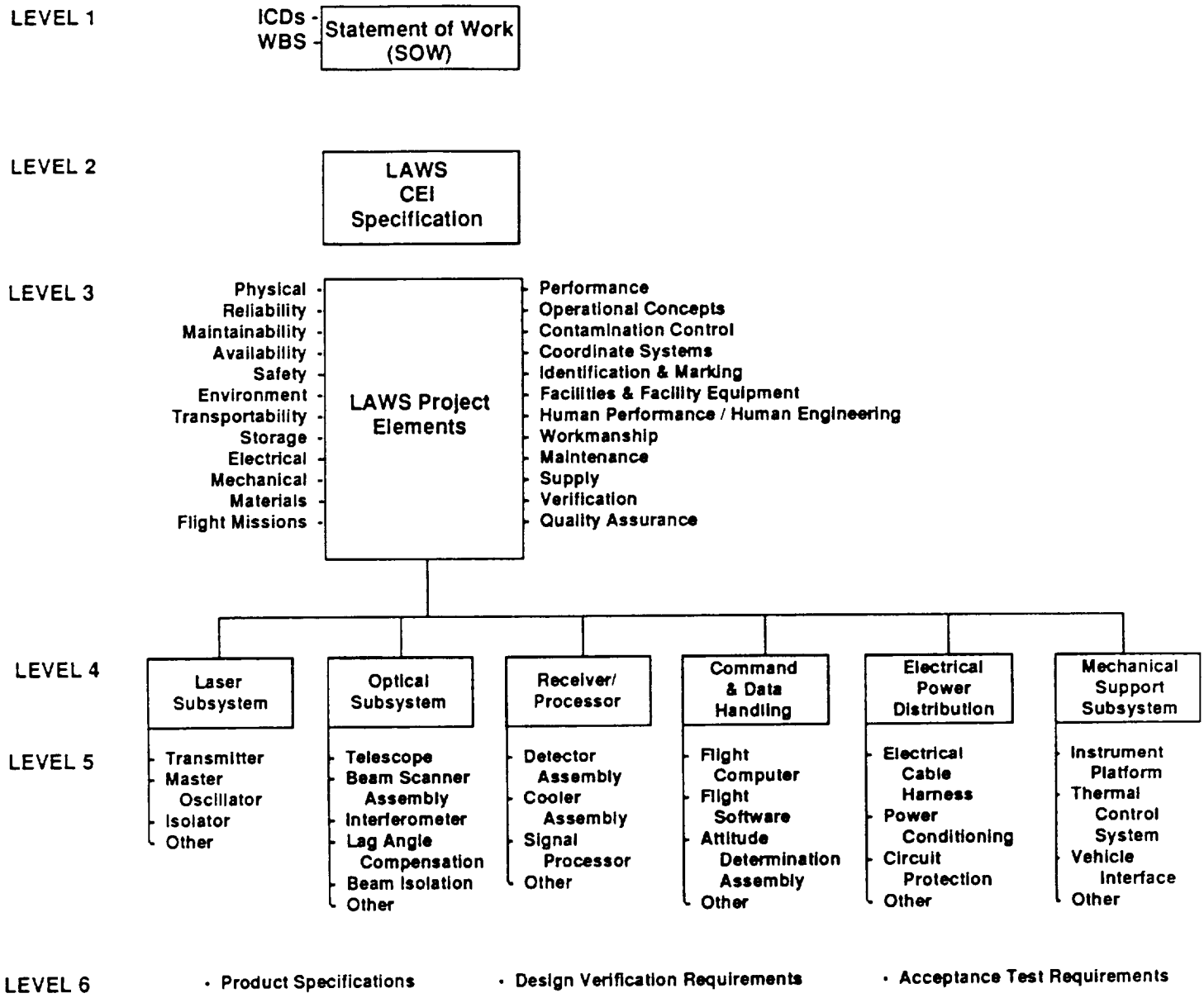

Figure 2-9. ARTS Requirement Hierarchy

2.6 INTERFACE DEFINITION

Three types of LAWS Instrument interface control documents (ICDs) have been identified. These documents will be prepared in accordance with the requirements of MM 8040.12A. Copies of each of these ICDs will be delivered to the MSFC-NASA Project Manager.

One ICD is required to define and control the design of the interfaces between the complete LAWS Instrument assembly and the NASA supplied EDS Platform. This ICD will address all physical, functional, and procedural interfaces. All software, data, and commands will also be addressed to ensure compatible exchanges. This ICD will be mutually approved and controlled by the MSFC-NASA LAWS Project Manager and the Lockheed LAWS Program Manager.

Two ICDs of a slightly different type are required to define and control the design of the interfaces between major subcontractor supplied components of the LAWS Instrument. One of these ICDs will address the physical, functional, procedural, and software interfaces between the LAWS Instrument and the LAWS laser subsystem. The second ICD will address the physical, functional, procedural, and software interfaces between the LAWS Instrument and the LAWS optical subsystem.

Both of these ICDs will address the physical, functional, procedural, and software interfaces between the laser subsystem and the optical subsystem. The Lockheed Program Manager will resolve all design incompatibilities if any are found during the Instrument assembly, integration, and test operations. Both of these ICDs will be prepared and controlled by the Lockheed Program Manager and approved by each of the affected subcontract managers.

The third type of ICD will address the LAWS Instrument Software, Data, and Command interfaces. All software interfaces, both internal and external, will be included in this ICD. The Lockheed Program Manager or his authorized representative will initiate, coordinate, and/or approve all changes to this ICD with the Lockheed subcontractors and with the MSFC-NASA LAWS Project Manager.

2.7 RELIABILITY

The LAWS Instrument has been given a Class B mission designation by the MSFC LAWS Program Office. This designation is based on a 5-year mission life and the fact that the payload will be installed on a free flyer spacecraft which will not be retrievable by use of the Space Transportation System. Lockheed has extensive experience with this type of payload and has determined that a combination of Class S and Class B parts may be acceptable depending on the assurance that system reliability goals are met. Significant cost and schedule savings may be achieved by using Class B parts.

2.7.1 Parts Cost Consideration

Class S parts procurement costs are typically 2 to 8 times higher than Class B parts. Typically, Class B parts have a failure rate of 2 times that of Class S parts. Initial cost typically increases 1.5 times if Class S parts are used, and the reliability increases 1.25 times. The manufacturing cost includes materials procurement, fabrication, assembly, quality assurance, and test. Typically, only 15 percent of the manufacturing cost is for electronic/electrical parts for a high density electronic box. This explains the apparent discrepancy in the increased reliability of only 25 percent if all parts used are Class S.

2.7.2 Manufacturing/Test Cost

Manufacturing costs would increase due to the higher number of failures of Class B parts. As stated above, Class B failure rates are approximately twice Class S rates. Therefore, early failures in manufacturing could be twice the Class S rates. Associated costs include additional failure analysis of failed parts, corrective action, rework, retest, and possible schedule slippage.

2.7.3 Summary

With the Class B mission designation, a mix of Class S and Class B parts will be used. Reliability analyses will be conducted to determine which components can use lower grade parts and still meet LAWS program reliability goals.

Section 3

PRELIMINARY DESIGN

The LAWS Instrument preliminary design has been subdivided into the following six primary subsystems: optical, laser, receiver/processor, command and data management, structures and mechanical (including the thermal control system), and electrical power. *Figure 3-1* identifies the element of these subsystems, which are described in the following pages.

Section 3.1 provides information on the overall system configuration and accommodations, including the overall layouts, envelope drawings, mating with the bus and carrier vehicle, and structural design. Section 3.2 reviews the trades and analyses which were used in defining the system concept/configurations. Section 3.3 presents the preliminary design of the six primary subsystems, as well as of the thermal control system and the attitude determination system. Section 3.4 describes our test and evaluation plan, and Section 3.5 defines LAWS operation requirements and scenarios.

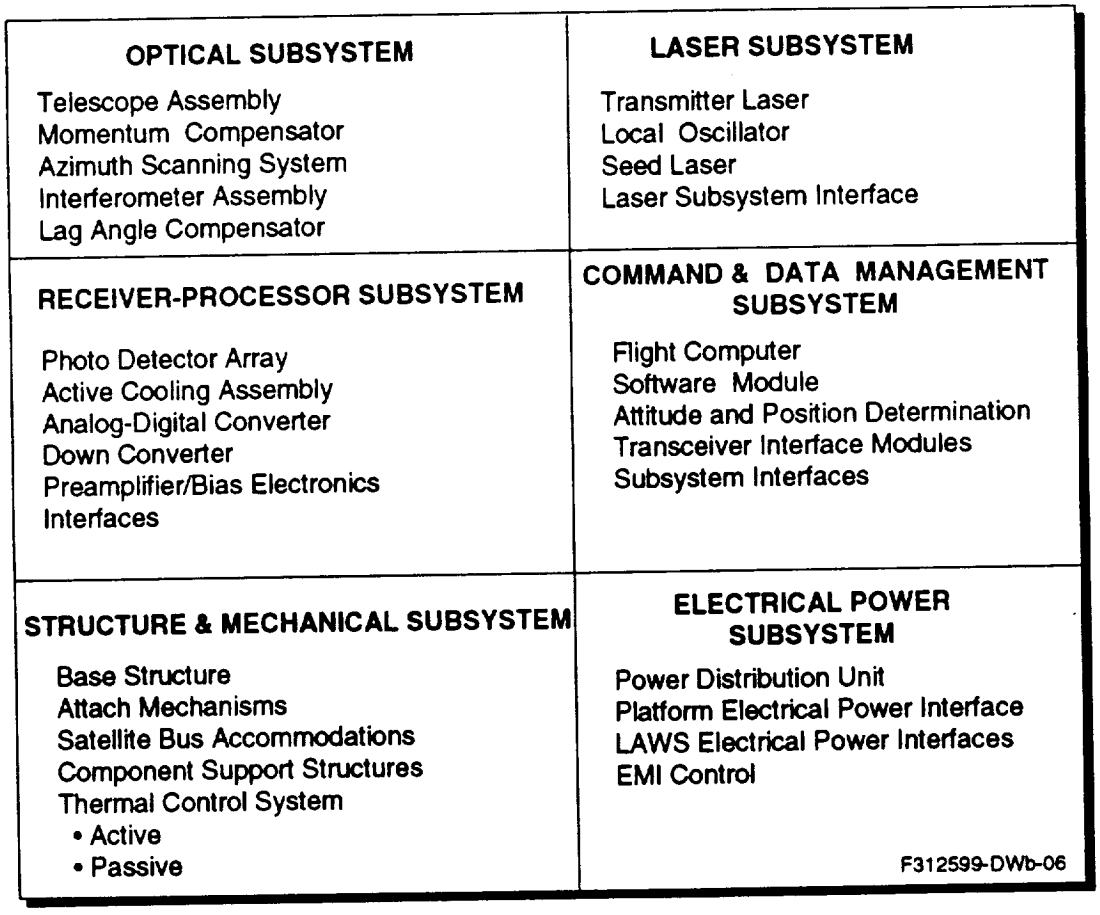

Figure 3-1. LAWS Subsystem Assemblies

3.1 OVERALL CONFIGURATION AND ACCOMMODATIONS

3.1.1 Baseline LAWS

The LAWS Instrument baseline design is illustrated in *Figure 3-2*. The velocity vector is depicted with the telescope bearing on the leading side of the Instrument platform, the laser on the trailing side, and the telescope rotating about nadir. Dual Star Trackers are shown on the cold side of the Instrument in close proximity to the inertial measurement unit (IMU). This configuration meets all packaging requirements for the Atlas IIAS launch vehicle and can be accommodated by the Titan vehicle and, with minor changes, the Delta vehicle. It is designed with clear access for assembly, installation, checkout, and removal of all components. Components are located either around the perimeter of the Instrument base or on the optical platform. The laser tank and telescope bearing are mounted to the Instrument base with critical optical components mounted to the optics bench, which can be isolated from the base. The base is, in turn, kinematically mounted to the spacecraft.

Figure 3-3 depicts the Instrument with the environmental covers removed. Smaller optical elements, including the redundant local oscillator lasers and the redundant receiver coolers, are shown in the figure. The optical bench provides a thermally and structurally stable platform for mounting and alignment of critical optical elements. The telescope motor-bearing assembly and laser pressure vessel are mounted directly to the base structure through cut-outs in the optical bench.

LAWS, in an orbiting configuration, is illustrated in *Figure 3-4*. The solar panels are deployed in the orbital plane. The radiators are deployed facing deep space. The spacecraft closely resembles the generic LAWS spacecraft designed by MSFC personnel.

Figure 3-5 depicts three views of LAWS. Components are located for optimal passive thermal control. Two of the views show the 1.67 m aperture telescope. The telescope secondary mirror is tripod-mounted with spacing for the f:1.5 primary mirror.

The dimensions of the LAWS Instrument are shown with three views in *Figure 3-6*. Instrument volume is optimized with a 2.5 x 2.9 x 3.6 m package size. The 1.67 m aperture telescope provides approximately 1 dB additional SNR over a 1.5 m aperture version. LAWS is packaged as a single integrated Instrument and can be assembled and checked out either with or without the spacecraft.

LAWS is shown within an Atlas IIAS fairing in *Figure 3-7*. A 0.16 m clearance is provided between the telescope spider and the fairing for clearance during launch shock and vibration. A 2.3 m available (longitudinal) space is allowed for the spacecraft envelope. The IIAS payload adapter interface is also shown.

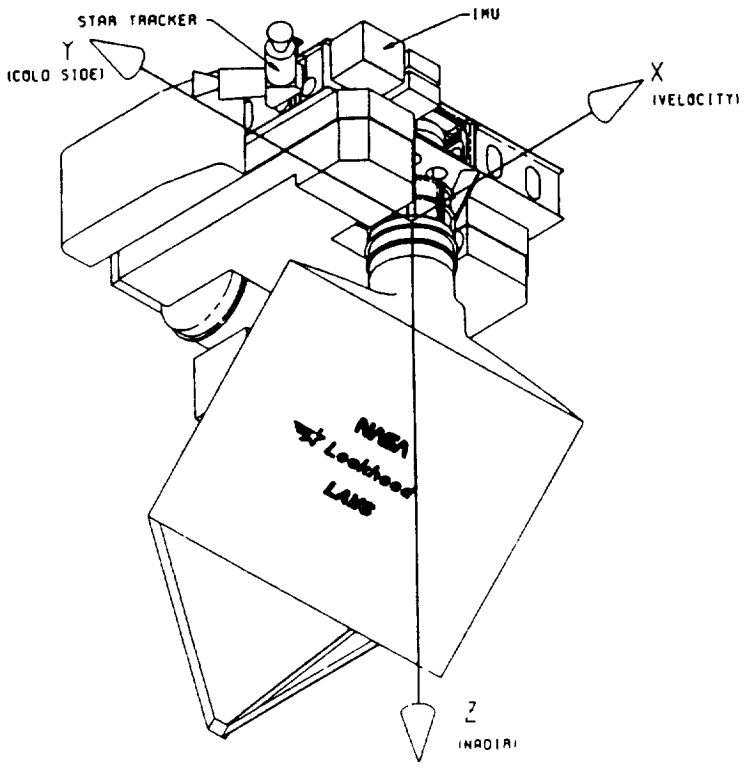

Figure 3-2. LAWS Baseline Design Flight Configuration

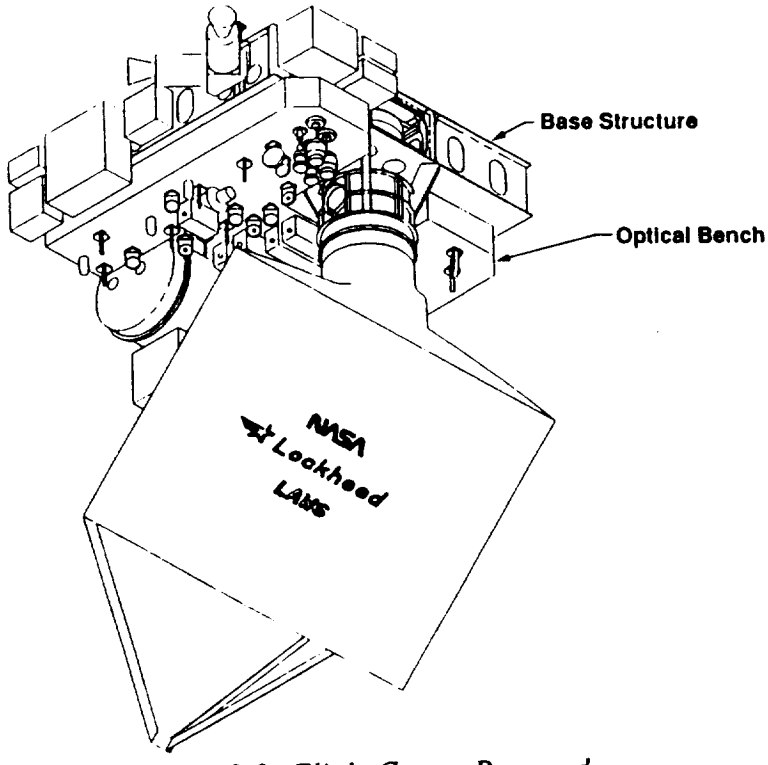

Figure 3-3. Flight Covers Removed

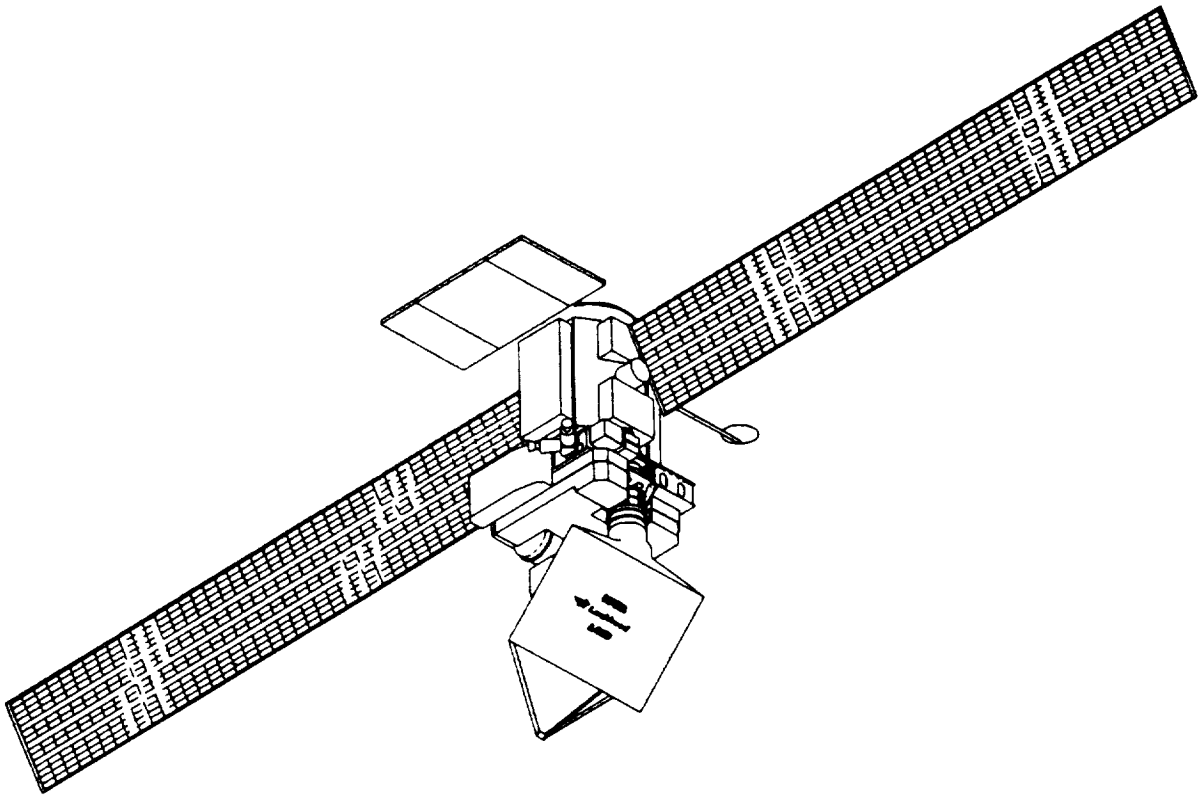

Figure 3-4. LAWS Package on Bus Assembly

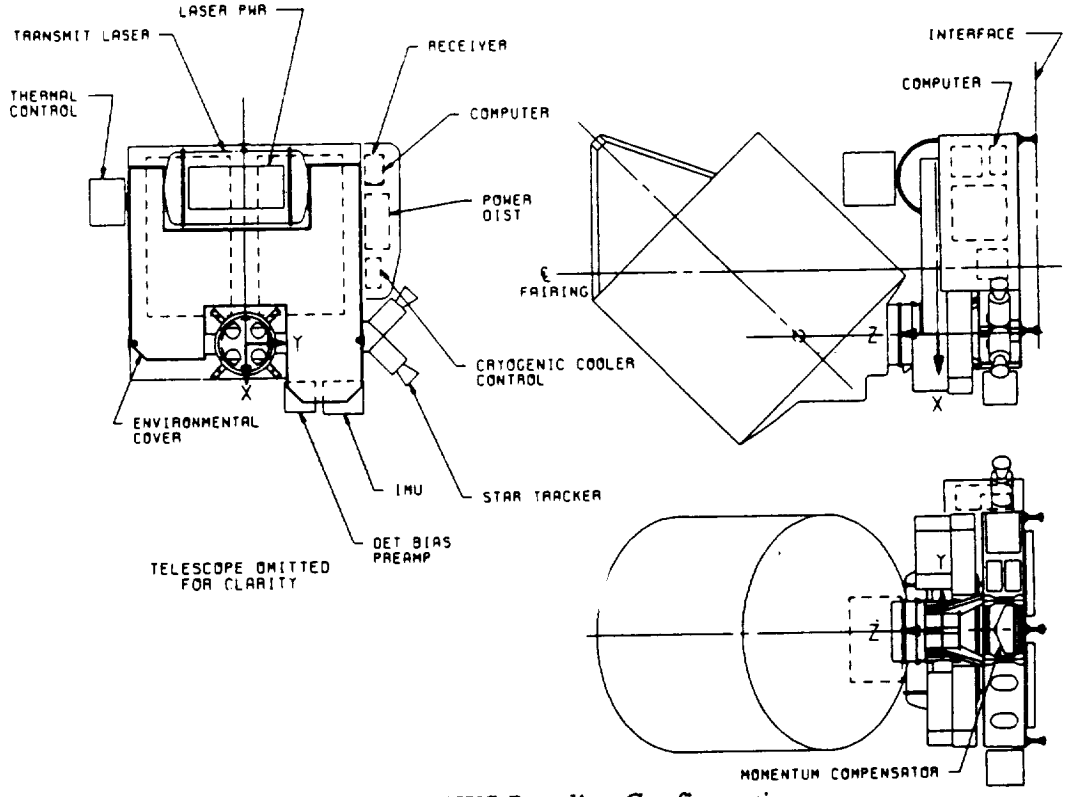

Figure 3-5. LAWS Baseline Configuration

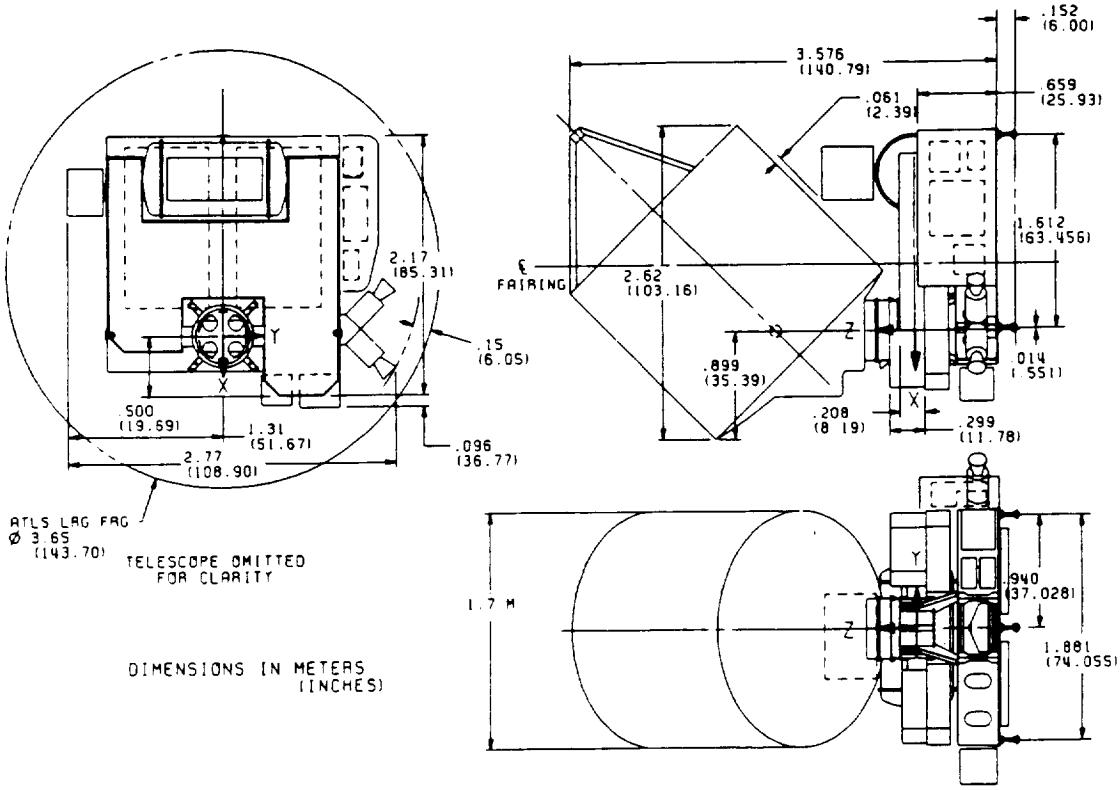

Figure 3-6. LAWS Baseline Dimensions

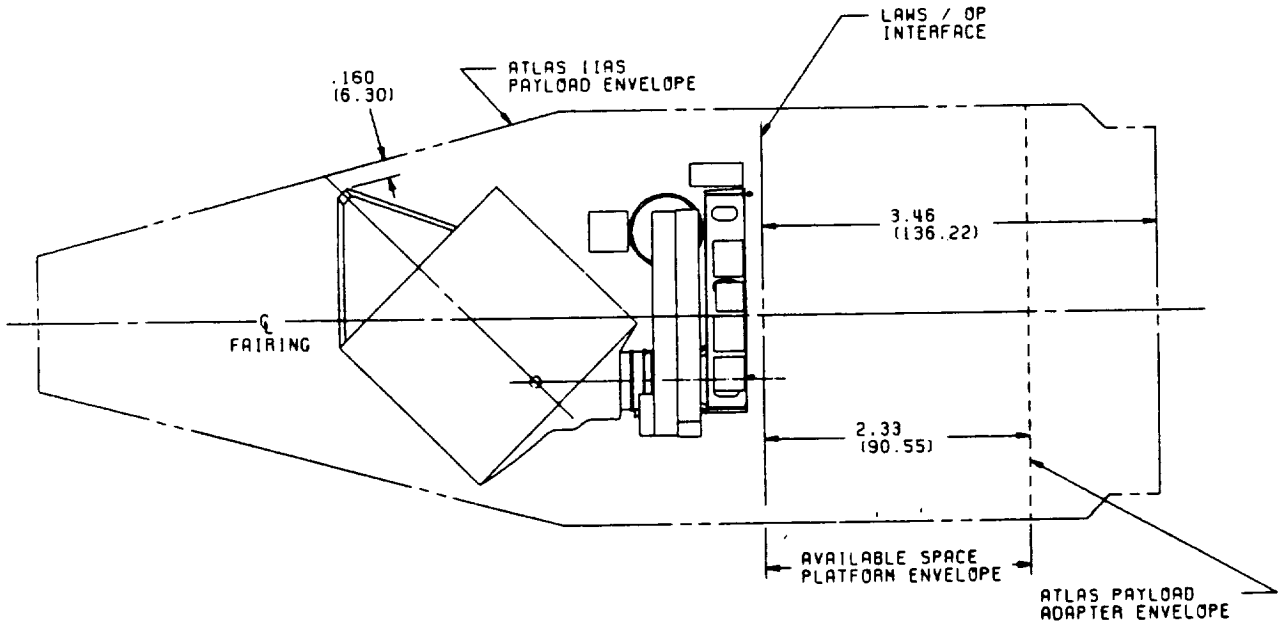

Figure 3-7. LAWS/POP in Atlas IIAS Large Fairing

The Instrument base structure shown in *Figure 3-8* is constructed of graphite epoxy with metallic fittings where necessary. Several base thickness values were analyzed and modeled, with the 0.35 m thick base selected as optimum from weight and stiffness standpoints. Kinematic mounts connect the base to the spacecraft on one side and support the optical bench on the opposite side.

The optical bench is outlined in *Figure 3-9*. The bench is notched for location of the laser pressure vessel and telescope scan bearing. Bench thickness is 0.2 m.

Figures 3-10 and *3-11* depict the optical path layout including redundant local oscillators, seed lasers, and detectors. The transmitter laser pressure vessel is mounted to the base structure and isolated from the optical bench. The telescope bearing assembly is also mounted to the base rather than the optical bench. Only low mass components are mounted to the optical bench. In *Figure 3-10*, the local oscillator and seed laser outputs are mixed and the seed laser is controlled with a specified off set. The seed laser is injected into the transmitter laser and used to control the cavity length prior to transmitter oscillator firing. Output of the transmitter is directed across the optical bench toward the telescope bearing. The 4 cm beam is directed along the scan bearing axis (*Figure 3-11*) and deflected by a pair of mirrors to enter the telescope at an off-set. Prior to entering the rear of the primary, the beam traverses a field corrector lens assembly. The transmitted beam travels to the secondary, fills the primary, and is directed toward Earth.

The returned beam is collected by the telescope approximately 5 ms after transmission. By this time, the telescope has traveled ~ 0.2 deg and the beam is received near on-axis, dependent upon orbit altitude (a variable) and scan rate. The primary condenses the beam onto the secondary, which in turn directs the beam axially through the primary toward a pair of mirrors; these mirrors direct it down the scan bearing, this time parallel to the bearing axis and off-axis. The periscope follows at the lower end of the scan bearing, is driven by an encoder/phase lock-loop, and brings the beam back on-axis where it is directed onto the optical bench again via fixed mirror (*Figure 3-10*). A three element (refracture) pupil relay is inserted in the receive optical assembly as El_1, El_2, and El_3, with the pupil coincident with the dynamic lag-angle compensator tip-tilt mirror. The receive beam is directed off a beamsplitter toward the detectors. The local oscillator beam is also fed through the beamsplitter to combine with the received radiation at the detectors. Cryocoolers driven by redundant compressors chill the detectors to the 80 K operating temperature.

Figure 3-12 depicts the environmental cover which assists in the control of the optical bench environment. With partitions and vents, this cover helps to stabilize component temperatures and protects from contamination.

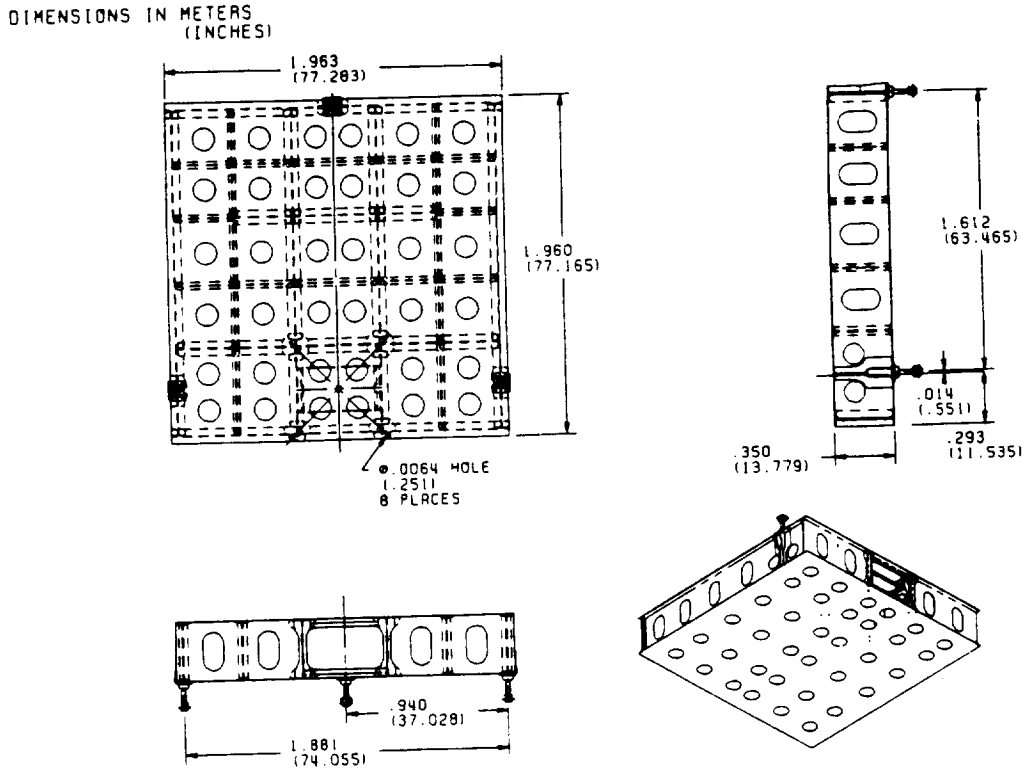

Figure 3-8. Structure, LAWS Medium Base

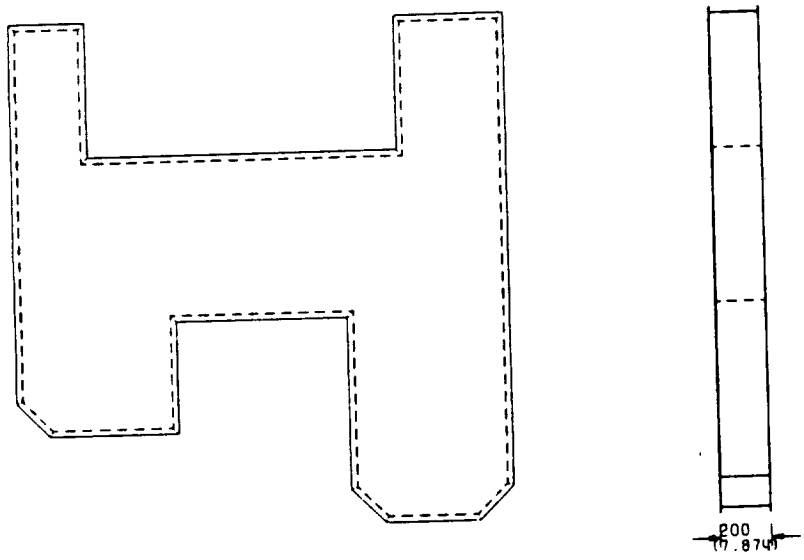

Figure 3-9. Optical Bench Configuration

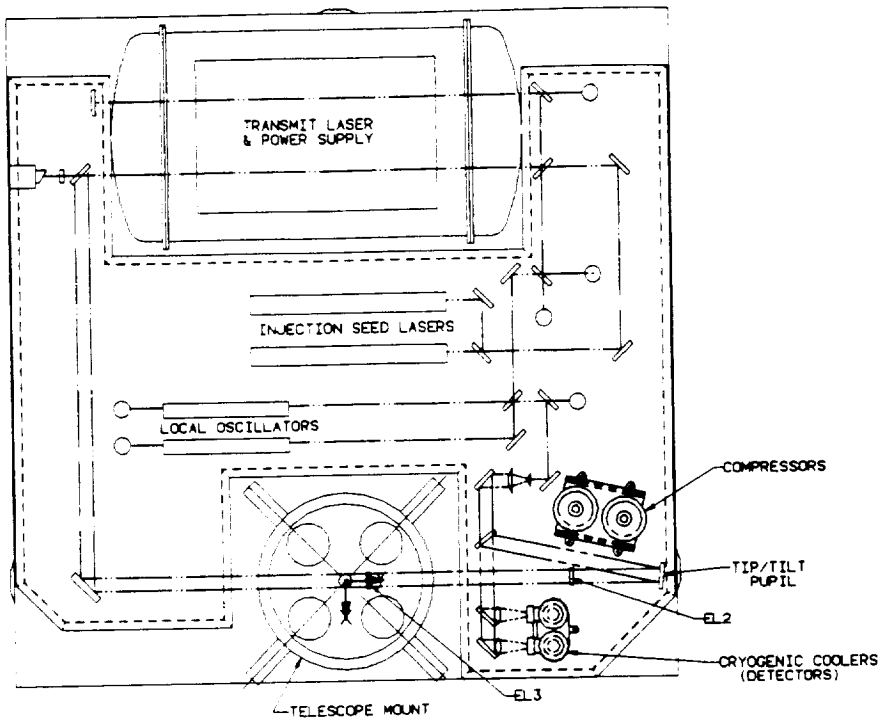

Figure 3-10. LAWS Optical Bench and Schematic

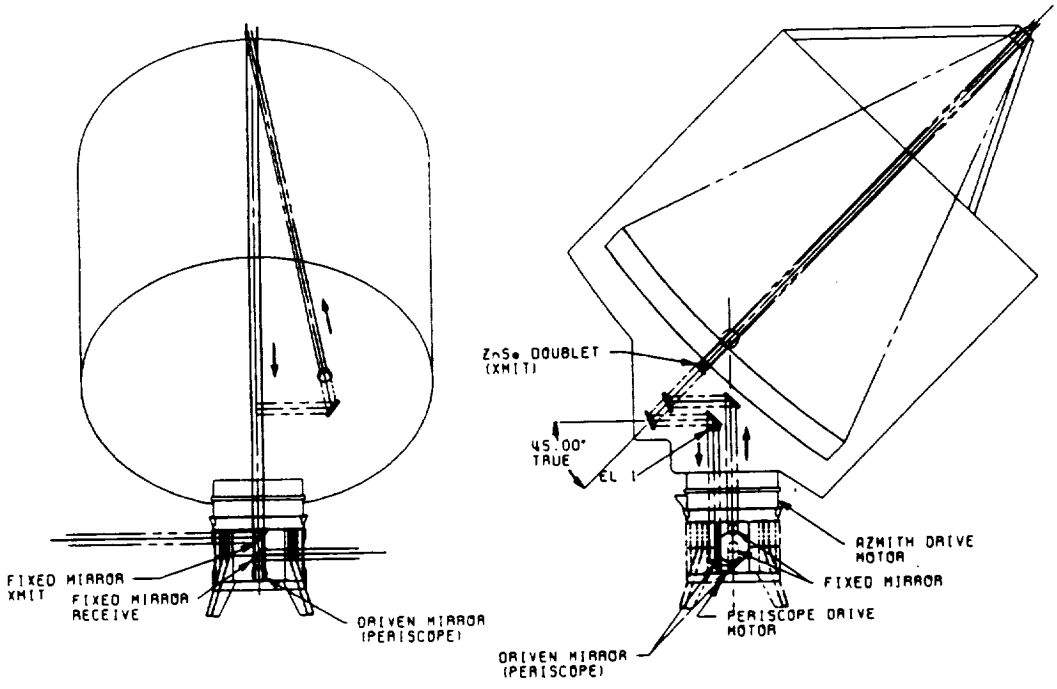

Figure 3-11. LAWS Telescope Assembly

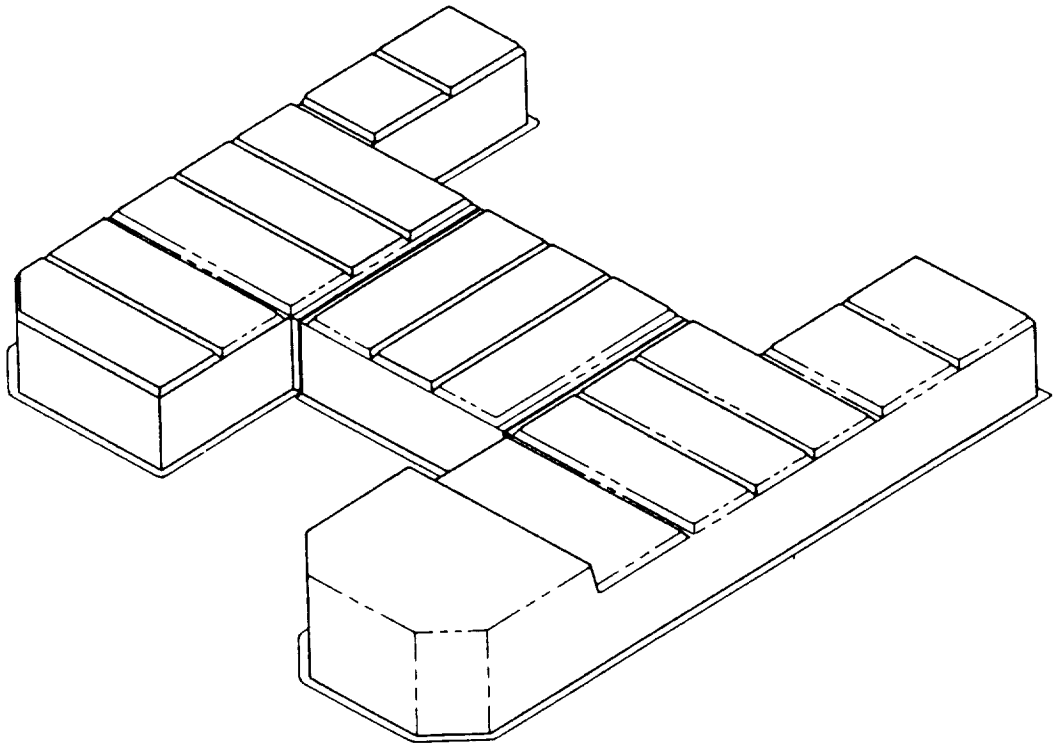

Figure 3-12. LAWS Environmental Cover (Optical Bench)

LAWS signal flow through the laser, optics, and receiver/processor subsystems is shown in *Figure 3-13*. Tip-tilt mirrors are depicted for low bandwidth adjustment of the local oscillator beam; higher bandwidth adjustment is required for the dynamic lag angle compensation. Telescope internal alignment is maintained by an out-of-band alignment assembly. Focus/de-focus capability at the receiver provides increased field-of-view for initial acquisition. Optical paths are dashed, while electrical paths are shown as solid lines. The components shown with a "2" have been tentatively selected for redundancy.

A condensed baseline mass properties table is depicted in *Figure 3-14*. The weight values are based on design analyses or vendor data for selected hardware elements. The weight budget of 800 kg is met, but little contingency is presently available. A major emphasis will be placed on weight reduction in the following months. The CG is located close to the longitudinal (X) centerline. The telescope rotating mass has been minimized to 161.5 kg. The telescope mass CG is located on the axis of rotation for minimum inertia effects. The momentum compensator is included to compensate for telescope rotational momentum.

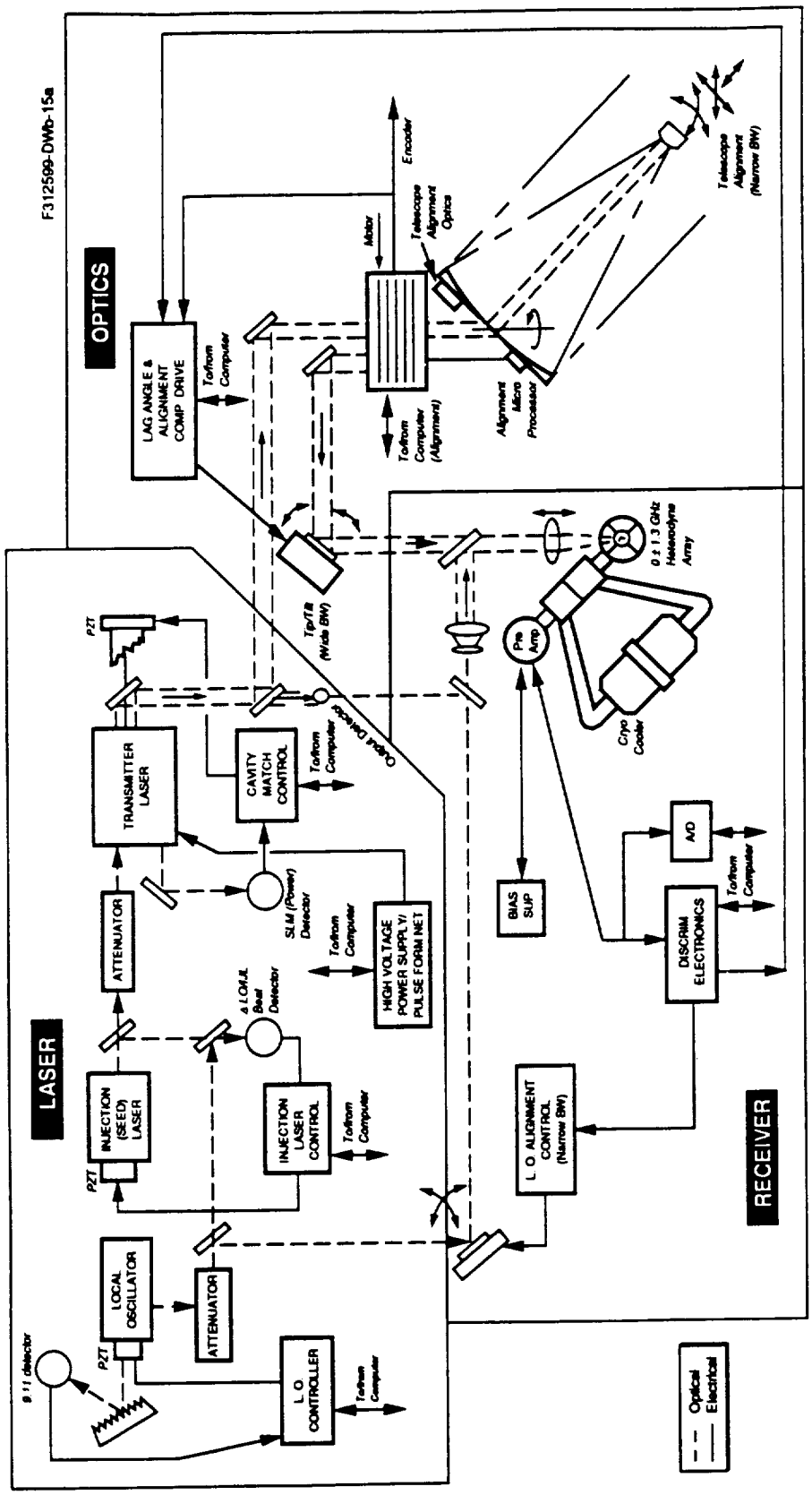

Figure 3-13. LAWS Signal Flow

System	Contents	System Weight (kg)	CG Location (m) X	Y	Z
Structure	Base, Bench, Environmental Cover, Mounts	138.0	0.03	0.57	-0.34
Power	Distributor, Cable	14.0	0.77	0.88	-0.32
Thermal	Pump Package 15.5 *, Heaters, Cable, EOS Cold Plates 21. **, Lines, Misc.	92.95	-0.20	0.82	-0.38
Telescope	Mirrors, Reaction & Metering Structures, TCS, Motor/Bearing, Misc.	212.9	0.0	0.0	0.92
Laser	Laser & Power Supp., Oscillators & Power Supp., Seed Lasers & Power Supp., Misc.	204.3	-0.05	1.20	0.21
Data	Computer, Cables	22.0	0.29	0.79	-0.28
Receiver / Detec.	Electronics, Cryo Cooler, Controller, Compressors, Displacers, Bias, Preamp, Misc.	52.0	0.62	0.26	-0.24
Momentum Comp.	Momentum Compensator, Heat Exchanger	12.9	0.0	0.0	-0.62
Pointing	IMU, Star Trackers ***	41.0	0.97	-0.17	-0.50
Total		790.0 kg	0.08 m	0.55 m	0.16 m

* Can be replaced by platform pump if LAWS goes on dedicated platform.
** Can be replaced with 5 kg heat exchanger if LAWS goes on dedicated platform.
*** Can be replaced with platform instrument if LAWS goes on dedicated platform.

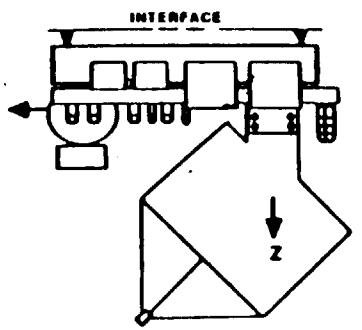

Allotted Budget	800 kg
-Contingency (20%)	160 kg
Target Weight	640 kg

I-XX = 810.7 I-XY = -48.6
I-YY = 678.0 I-XZ = -35.9 (kg-m**2)
I-ZZ = 677.8 I-YZ = -90.9

Contingency Used 150 kg (94%)

Note: Can recover 77 kg instrument weight with dedicated platform.

Figure 3-14. LAWS Baseline Current Mass Properties

Table 3-1 shows our LAWS baseline configuration can be accommodated by Atlas IIAS, Delta, and Titan vehicles with minor changes. Titan load factors were used during preliminary analyses for conservatism.

The LAWS Instrument with telescope can be fitted into a Delta (large) fairing (shown in *Figure 3-15*) by reducing the telescope aperture from 1.67 m to 1.60 m diameter. This size reduction results in a signal-to-noise loss of approximately 0.5 dB.

Conclusions for the LAWS configuration are listed below:

- LAWS configuration fits in the Atlas IIAS payload fairing with adequate room for spacecraft accommodation
- Configuration is easily adaptable to Delta or Titan vehicles
- LAWS is within weight and volume allocations
- LAWS configuration interfaces with preliminary MSFC Orbiting Platform design and other similar spacecraft configurations
- LAWS configuration provides a one piece integrated unit for instrument validation/calibration
- LAWS packaging provides easy access to all components for maintenance and calibration after platform/launch-vehicle integration
- All GIIS interface requirements are met
- Weight reductions are possible with dedicated LAWS spacecraft.

Table 3-1. Potential Launch Vehicles

LAUNCH VEHICLE	FAIRING DIAMETER (m)	DESIGN LOAD FACTORS (g)	LAWS CONFIGURATION
Atlas IIAS	4.19 large	6.0 axial 2.0 lateral	Baseline
Delta	3.0 large	6.3 axial 3.0 lateral	Reduces telescope diameter & base mount height
Titan	5.08	6.5 axial 3.5 lateral	Baseline

F312594-49

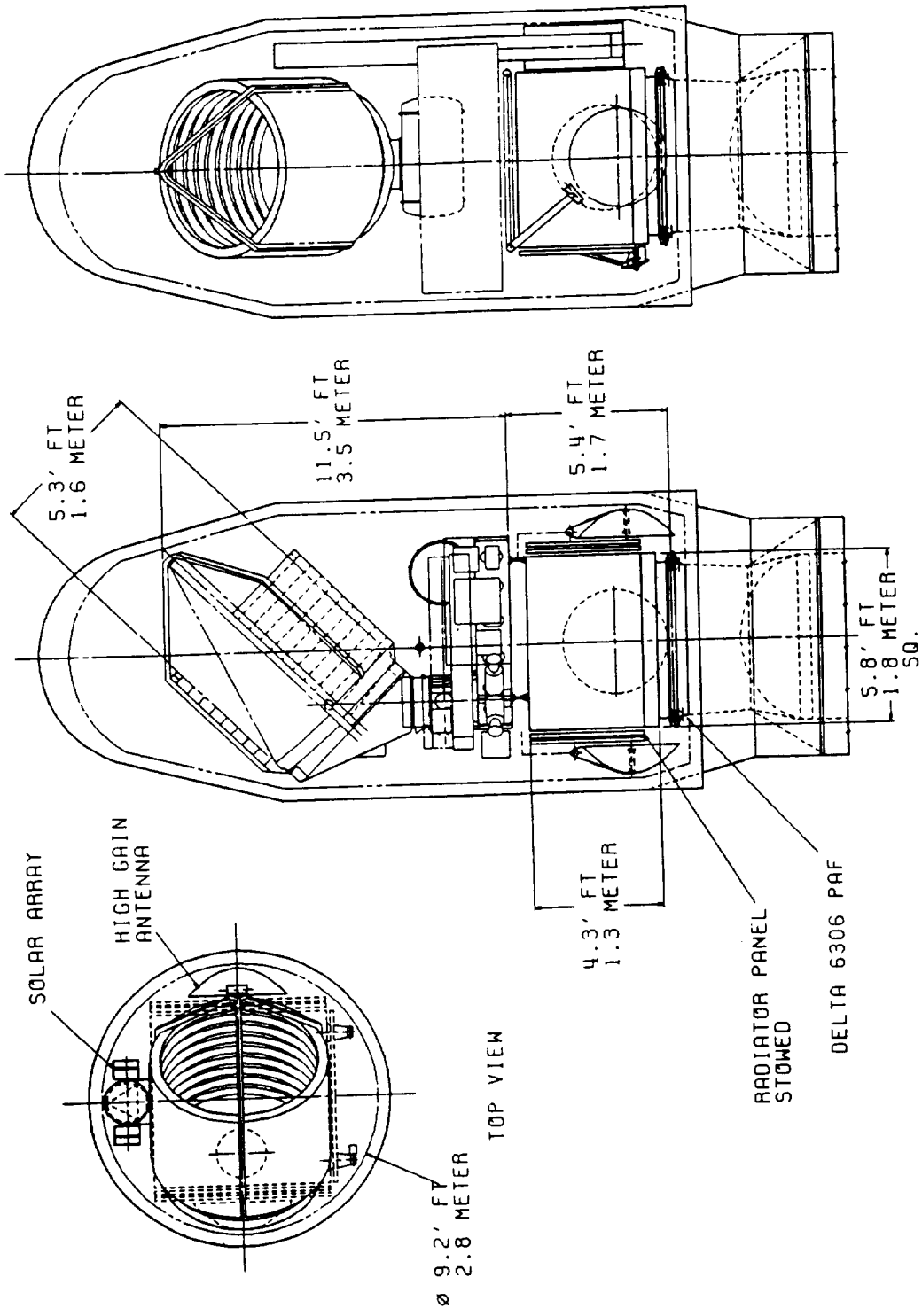

Figure 3-15. LAWS in Delta Large Fairing

3.1.2 Downsized LAWS

NASA Program personnel have indicated that with the overall Earth Observation System budget reductions, a downsized LAWS may be more appropriate for the initial LAWS system rather than the more optimized baseline LAWS. The downsizing presented to the contractors by NASA has been from a 20 J/pulse laser to a 5 J/pulse laser and from a 1.67 m aperture telescope to 0.75 m aperture. These reductions degrade SNR by approximately 13 dB.

Figures 3-16 and *3-17* depict the downsized LAWS Instrument. In developing the downsized configuration, Lockheed has left much of the baseline configuration intact and reduced dimensions and weights of the transmitter laser and telescope. The thermal control system weight along with instrument power requirements have also been reduced accordingly, since with less energy per pulse and similar pulse repetition rates, energy consumption and dissipation rates are reduced. *Figure 3-18* shows the mass budget of the downsized LAWS.

A cross section of the reduced size LAWS Instrument is shown in *Figure 3-16* within the Delta fairing. This configuration allows 3.2 m for the bus (platform) compared with 2.3 m in the Atlas/baseline configuration of *Figure 3-7* and 1.7 m in the Delta/near baseline configuration of *Figure 3-15*.

For the downsized laser shown in *Figure 3-17*, we have reduced the tank dimensions from *Figures 3-6* and *3-10*, but left the resonator intact along with seed laser and local oscillator.

3.2 TRADES AND ANALYSES

The most fundamental system level trades are the selection of laser pulse energy and the selection of telescope diameter. Selection of laser pulse energy is a trade between many pulses of low energy and few pulses of high energy, within constraints of laser weight and maximum pulse energy which can be developed with reasonable technical risk. Selection of telescope diameter is a trade of allocation of available mass into the laser or the telescope within the physical constraints of the launch system and the maximum diameter which can be manufactured.

Initially, in the program, a trade to determine optimal pulse repetition frequency (PRF) was conducted. The objective is the minimization of

$$\sigma_0^2 = (\sigma_V^2 + \sigma_r^2)/N$$

where

σ_0 = characteristic velocity in a 100 km by 100 km grid square

σ_V = standard deviation of measurement error for a single shot

σ_r = standard deviation of wind velocity

N = number of shots in a 100 km by 100 km grid square.

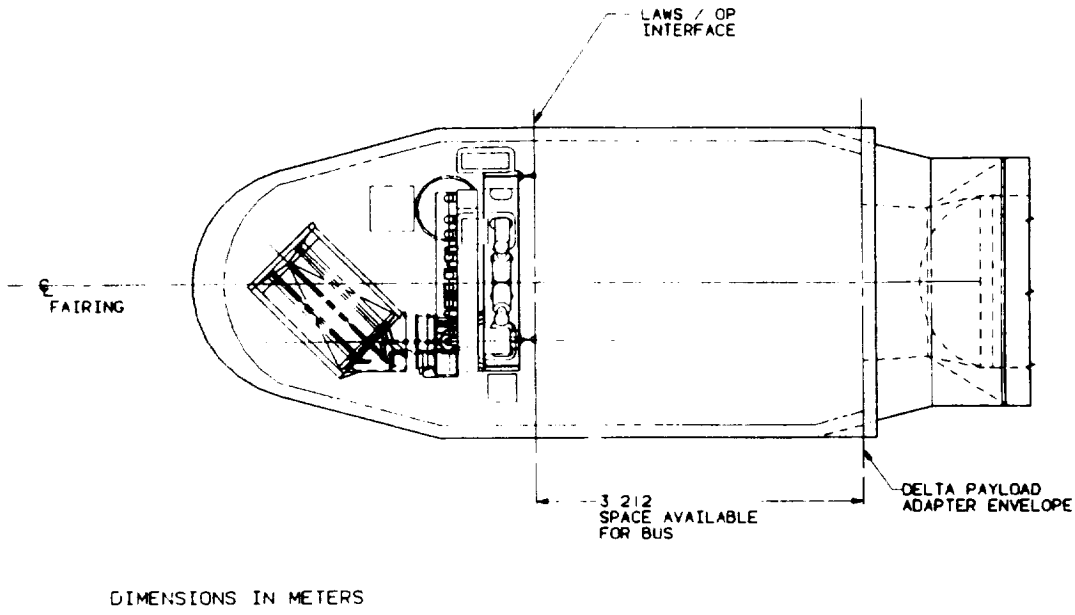

Figure 3-16. LAWS Telescope with 0.75 m Diameter Mirror in Delta Fairing

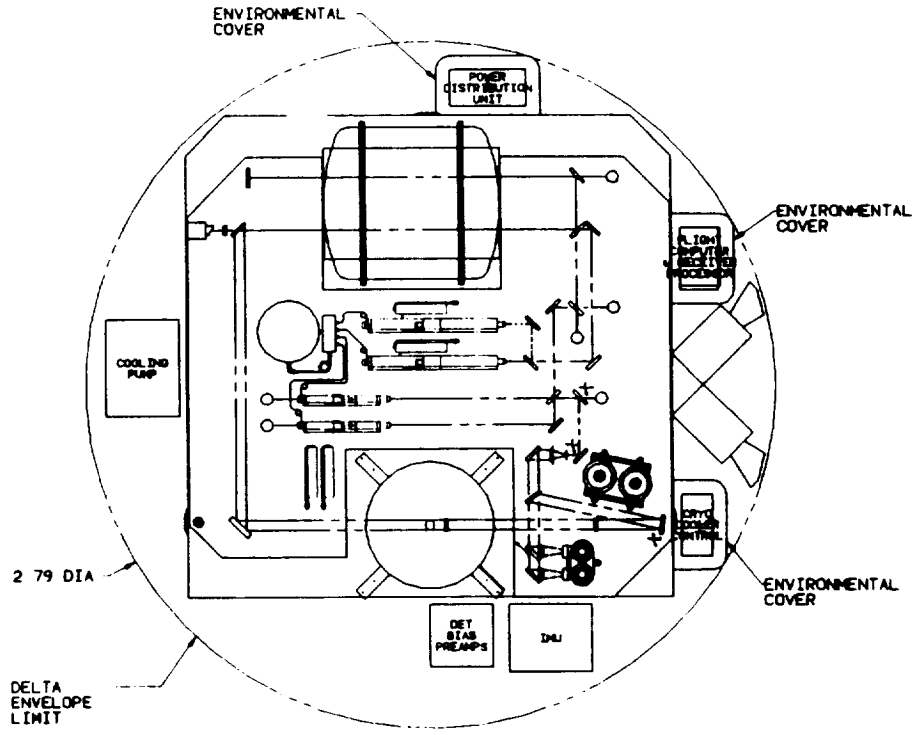

Figure 3-17. LAWS Instrument Fit-Check in Delta Fairing

System	Contents	System Weight (kg)	C. G. Location (m) X	Y	Z
Structure	Base, Bench, Environmental Cover, Mounts	127.5	-0.57	0.03	-0.34
Power	Distributor, Cable	13.6	-0.88	0.77	-0.32
Thermal	Pump Package 15.5 *, Heaters, Cable, EOS Cold Plates 12. **, Lines, Misc.	71.35	-0.82	-0.2	-0.38
Telescope	Mirrors, Reaction & Metering Structures, TCS, Motor/Bearing, Misc.	125.9	0.0	0.0	0.59
Laser	Laser & Power Supp., Oscillators & Power Supp., Seed Lasers & Power Supp., Misc.	134.1	-1.20	-0.05	0.21
Data	Computer, Cables	20.4	-0.79	0.29	-0.28
Receiver / Detec.	Electronics, Cryo Cooler, Controller, Compressors, Displacers, Bias, Preamp, Misc.	52.0	-0.26	0.62	-0.24
Momentum Comp.	Momentum Compensator, Heat Exchanger	12.9	0.0	0.0	-0.62
Pointing	IMU, Star Trackers	41.0	0.17	0.97	-0.50
Total		598.7^kg	-0.54 m	0.12 m	-0.03 m

* Could be replaced by platform pump if LAWS goes on dedicated platform.
**Could be replaced with 5 kg heat exchanger if LAWS goes on dedicated platform.
^ Telescope downsize saves 178.75 kg without telescope contamination cover.

Figure 3-18. LAWS Downsized Mass Properties (6 April 1992)

In a power-limited system, both σv and N are functions of the laser pulse energy. A low PRF gives relatively good velocity measurement for each pulse, but does not allow averaging over a large number of pulses. Conversely, a high PRF gives relatively poor velocity measurement for each pulse, but allows more averaging over a large number of pulses. The results of this trade are shown in *Figure 3-19*. The abscissa shows the pulse repetition rate. The ordinate shows the statistical expectation of standard deviation of velocity measurement (using the Cramer-Rao velocity estimator) for n pulses in a 100 km by 100 km grid square. The left side of the figure is limited by laser pulse energy (with laser power less than the maximum available), and the right side of the figure is limited by power available to the laser (with pulse energy less than the maximum acceptable). The figure shows that velocity measurement error is minimized when both maximum laser pulse energy and maximum laser power are used. In *Figure 3-19*, there is no variance in wind velocity. The analysis was extended to the situation in which there is natural variance of wind velocity in the grid square and it is desired to determine a single value of velocity which is representative of the wind velocity within the grid square. *Figure 3-20* shows these results. The figure shows that for good backscatter (low altitude), overall velocity error is decreased by increasing PRF, allowing more averaging of the natural atmospheric variance. For poor backscatter (high altitude), a lower PRF is preferable. As compared with a high PRF, the

improvement in measurement accuracy for each pulse more than offsets the advantage of averaging over many pulses for natural atmospheric variance. Therefore, the optimal PRF is approximately 5 Hz. During the study, this trade led to the selection of 3 pulse pairs per grid as the appropriate shot density for the survey mode.

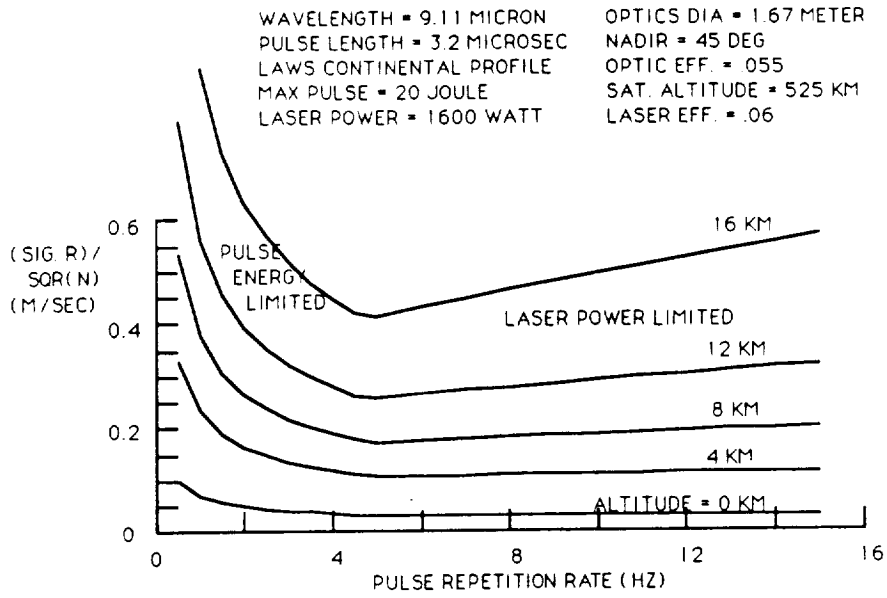

Figure 3-19. Selection of Pulse Repetition Frequency to Minimize Error in Wind Velocity Averaged Over a Grid Square

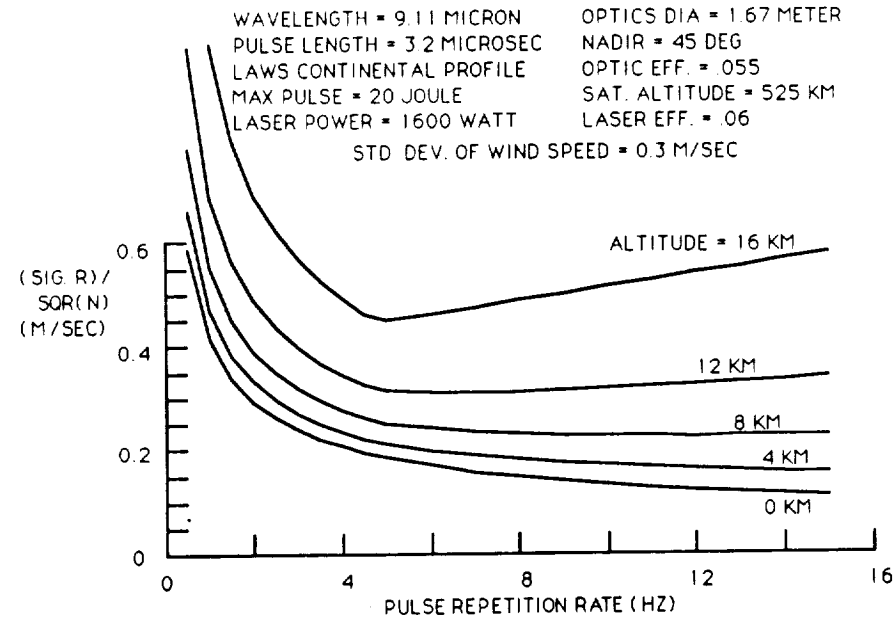

Figure 3-20. Effect of Pulse Repetition Frequency on Error in Averaged Wind Velocity with Variation in Wind Speed Over a Grid Square

The conclusion that a high pulse energy, low PRF system is preferable to a low pulse energy, high PRF system results from the fact that much of LAWS operation is in marginal backscatter conditions. If backscatter were significantly larger, a low pulse energy, high PRF system would be preferable.

Figure 3-21 shows the trade between laser pulse energy and telescope diameter. The 2.1 m limit in telescope diameter is that which can be manufactured with available facilities. The 20 J limit in laser pulse energy is a judgment of the maximum which can be developed with acceptable technical risk. Given the requirement of 3 shot pairs per 100 km by 100 km grid square for the survey mode, the laser pulse energy is also limited by the 2200 W average power for the survey mode. However, this limit is less constraining than is the 20 J maximum pulse energy. Lines of constant instrument mass and lines of constant narrow band SNR are shown. The lines of constant mass indicate that instrument mass is a function of both pulse energy and telescope diameter, and these two parameters must be traded to achieve constant mass.

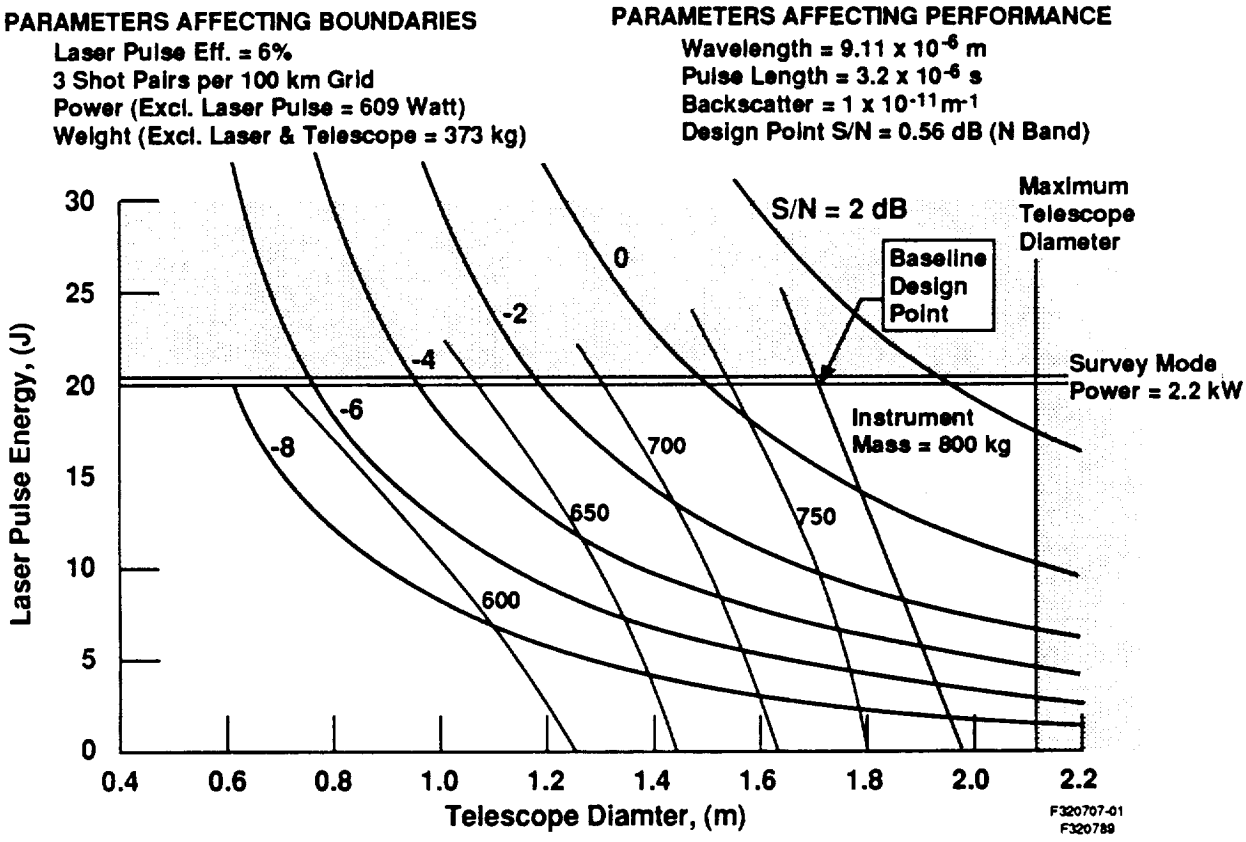

Figure 3-21. Trade Between Laser Pulse Energy and Telescope Diameter to Maximize SNR within Weight Constraints

The figure shows that for an instrument mass of 800 kg, SNR is maximized by using a 20 J laser and maximizing the telescope diameter within the 800 kg mass limit. Therefore, the 20 J laser and 1.67 m diameter have been selected as the baseline design point. The chart permits evaluation of sensitivity of instrument mass and SNR to other candidate design points.

3.3 SUBSYSTEM DESIGNS

3.3.1 Laser Subsystem

This section addresses the design of the laser subsystem, which consists of the following assemblies:

- Optical resonator
- Electrical discharge
- Pulse power supply
- Pressure vessel structure
- Gas flow loop
- Controls and instrumentation
- Injection laser
- Local oscillator.

The physical layout of the transmitter laser subsystem is shown in *Figure 3-22*. Its general configuration is fundamentally that proposed in Phase I. Modifications of note are removal of the resonator optics from the pressure vessel, the addition of a contraction to the flow loop, and relocation of the catalyst beds upstream of the heat exchangers. The functional interactions between the transmitter laser assemblies are outlined in *Figure 3-23* and discussed in the following paragraphs.

3.3.1.1 Optical Resonator

The resonator configuration, shown in *Figure 3-24*, closely resembles that of the breadboard design. Although some design parameters were modified to accommodate the interface of the transmitter with LAWS optical bench, care was taken to ensure that performance parameters such as mode discrimination and sensitivity to misalignment were not adversely affected. The key resonator parameters are listed below:

- Type unstable
- Equiv. fresnel no. 1.56
- Magnification 2.25
- Cavity length 3.0 m
- Gain length 1.5 m
- Beam size 4 x 4 cm.

The resonator is of the unstable type with a conventional concave primary mirror and a lens/grating combination acting as the feedback mirror. A folded cavity configuration was chosen for compactness, with both folding mirrors partially reflecting.

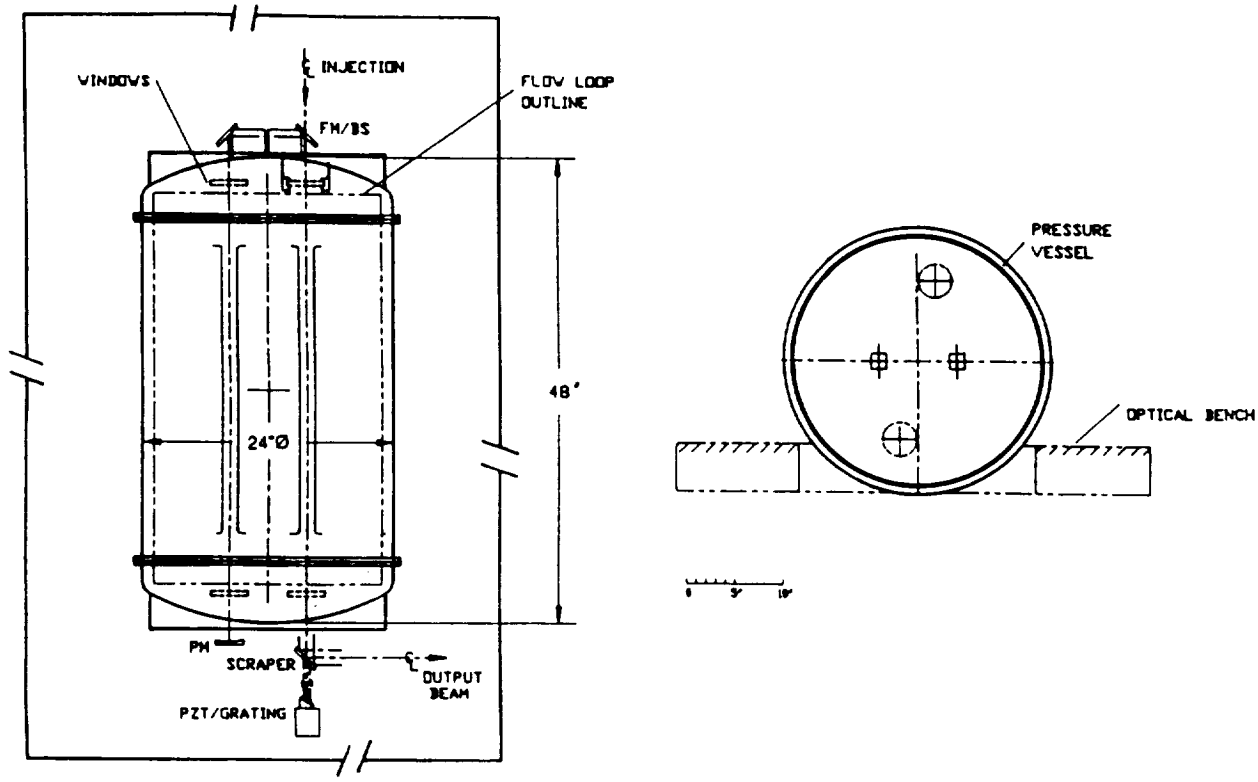

Figure 3-22. Laser Transmitter

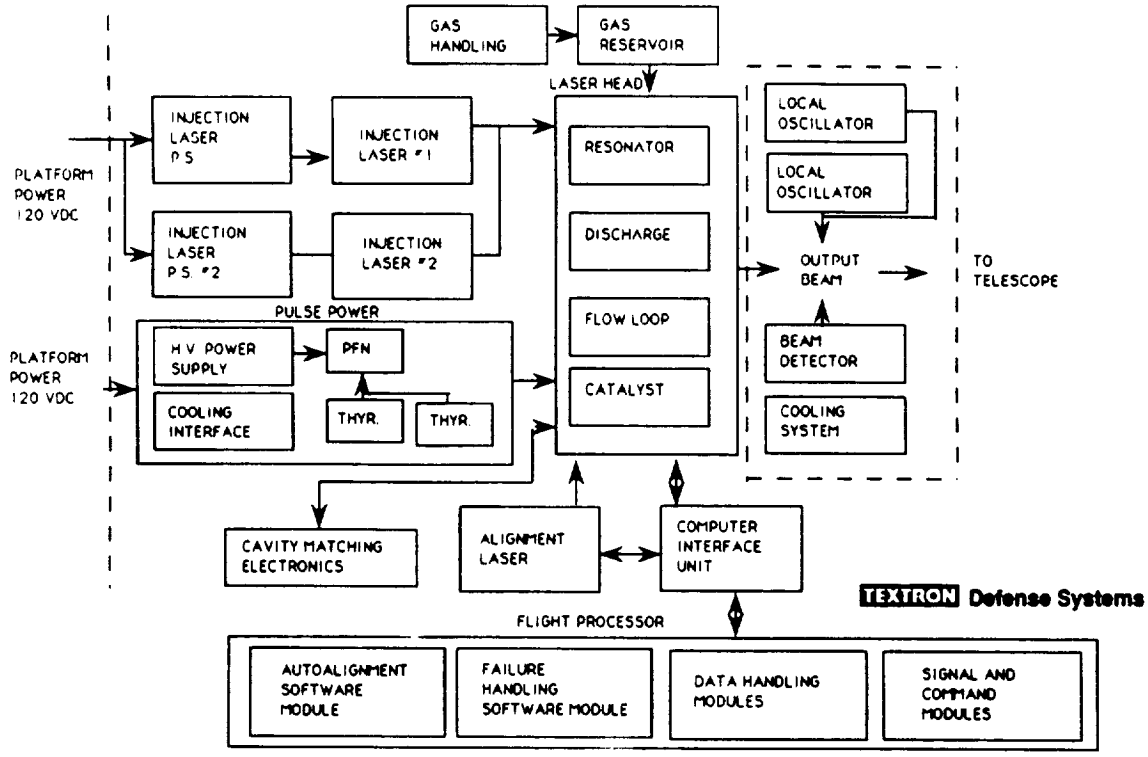

Figure 3-23. Laser Subsystem Block Diagram

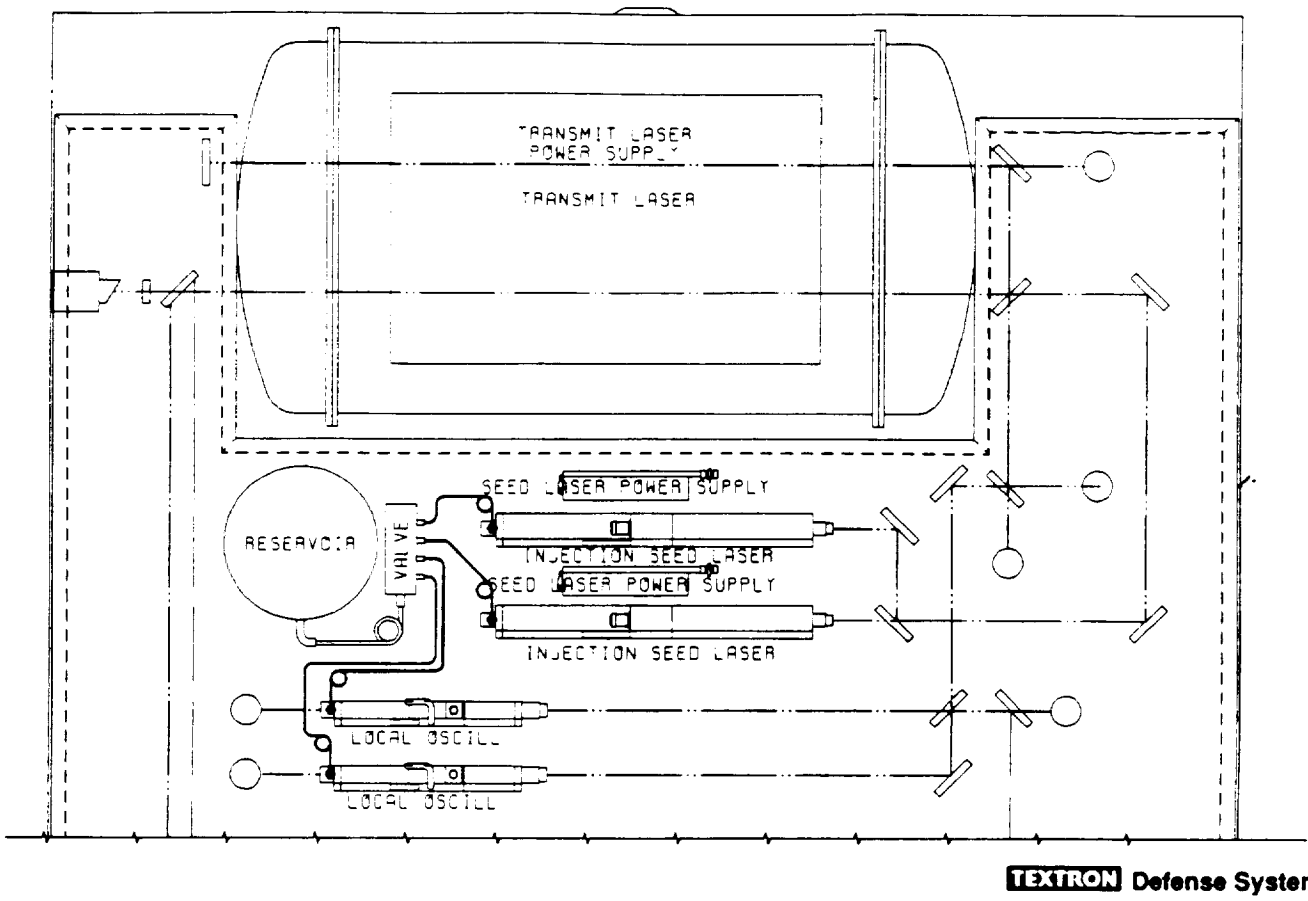

Figure 3-24. Resonator Optics Layout

The seed laser light is injected through one of the folds with the single longitudinal mode (SLM) detector monitoring the light transmitted through the same fold. The intensity of light transmitted through the opposite fold is measured by a cavity matching detector. Information from the "finesse" curve thus obtained is used by the cavity matching electronics to adjust the piezo-electric transducer (PZT) drive on which the feedback assembly is mounted. Use of a dithering system instead of the ramp function used in the resonator design verification test (DVT) and also in the breadboard will be considered.

Laser output energy is extracted by a scraper mirror located near the feedback assembly and measured by a pyrodetector located between the scraper and the telescope.

The primary and scraper mirrors will be made either of copper or dielectrically coated silicon substrates, while the folding mirrors and pressure vessel windows will be made of ZnSe to allow alignment in the visible regime.

3.3.1.2 Flow/Discharge Subsystem

These assemblies have been defined as one subsystem because of their high level of mechanical integration and functional interdependency. As *Figures 3-25* and *3-26* indicate, the layout closely matches that of the breadboard. Differences arise primarily in the choice of materials and addition of redundant components wherever failure mode analysis and breadboard lifetime tests indicate a need.

A UV preionized self-sustained discharge scheme was chosen with four electrode pair modules (two per side) providing redundancy and eliminating alignment and current distribution problems associated with long electrodes. A modified Ernst profile was chosen for the cathode based on extensive electrostatics code calculations substantiated by the DVT results. A flat anode profile was chosen for flow compatibility and compactness. Preionization is achieved through holes in the anode utilizing a dielectric/corona bar assembly. The dielectric material chosen for the preionizer housing can be machined and is impermeable. The relevant operating parameters of the discharge are listed below:

- Gas mixture — 3:1:1 He:CO_2:N_2
- Gas pressure — 0.625 atm
- Discharge dimensions — 4.2 x 4 x 150 cm
- Pulse length — 3.2 - 4.0 μs
- Specific energy loading — 86 J/L
- Discharge voltage — 21-23 kV.

The flow loop is designed to accommodate the discharge assembly described in the previous section. It provides fresh gas to the discharge and moves the used hot gas at the appropriate speed to prevent arcing. This gas is subsequently reconditioned by the catalyst bed, where recombination of CO and O into CO_2 dissociated during the discharge occurs. Subsequently, the thermal energy resulting from the inefficiencies inherent in the laser kinetics processes is removed by a fan and tube heat exchanger. The sidewall mufflers, located in both sides of the cathode, attenuate the acoustic waves generated by the discharge in order to maintain the homogeneity of the lasing medium in the cavity below the levels dictated by beam quality and cavity matching requirements.

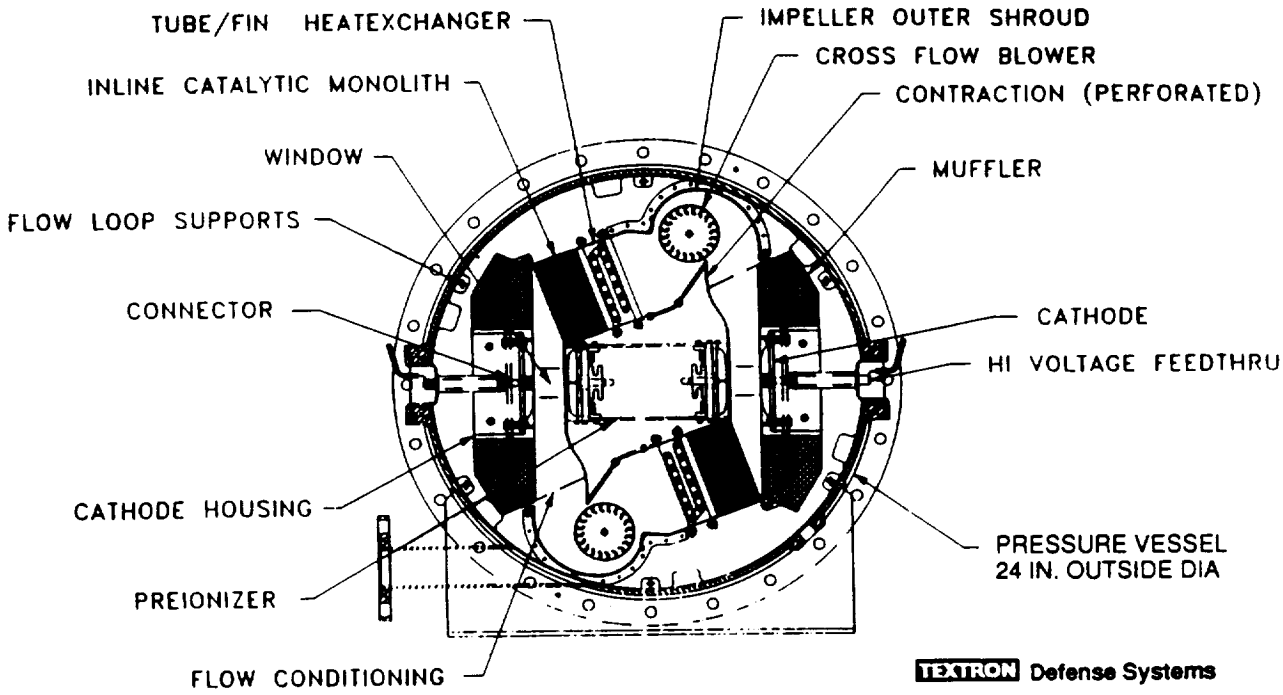

Figure 3-25. LAWS Discharge/Flow Loop, End View

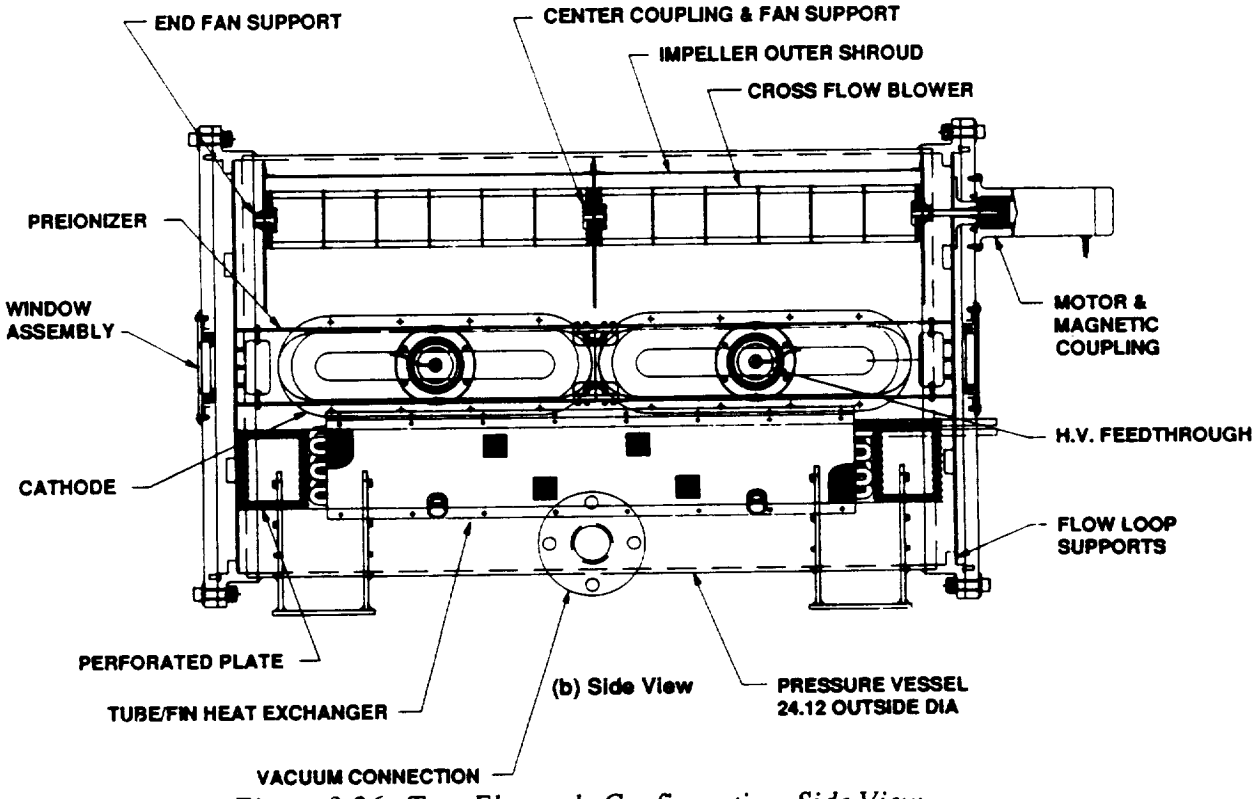

Figure 3-26. Two-Electrode Configuration, Side View

Key features of the flow loop design are the dual tangential fans chosen for both compactness and modularity, the contractions upstream of each discharge which assist in restoring flow uniformity, and the skewed positioning of the catalyst bed and heat exchanger which provides compactness and causes a gradual equilibration and cooling of the hot gas. This last feature minimizes density perturbations to the laser medium which could otherwise affect the medium homogeneity in the cavity. The relevant flow parameters are listed below:

- Mass flow rate — 23 g/s
- Flow velocity in cavity — 1.26 m/s
- Fan speed — 1700 rpm
- Cavity flush factor — 3.0 at 10 Hz
- Available catalyst volume — 12.6 L
- Porosity of muffler wall — 3 percent - no packing resistance
  Backup Design: 30 percent - 1 cgs rays/cm.

3.3.1.3 Pulse Power

The pulse power system in a discharge pumped CO_2 laser is formed by three primary components: a high voltage dc-dc converter, a pulse forming network (PFN), and a thyratron. The function of the high voltage power supply is to step up the 120 Vdc prime power input to the 40 kV charge voltage required by the PFN. The PFN in turn is charged by this power supply and, upon switching by the thyratron, generates a pulse with the desired length as well as voltage and current characteristics. The pulse energy is subsequently discharged into the gas by the discharge assembly described in the previous section. A functional diagram of these processes is shown in *Figure 3-27.*

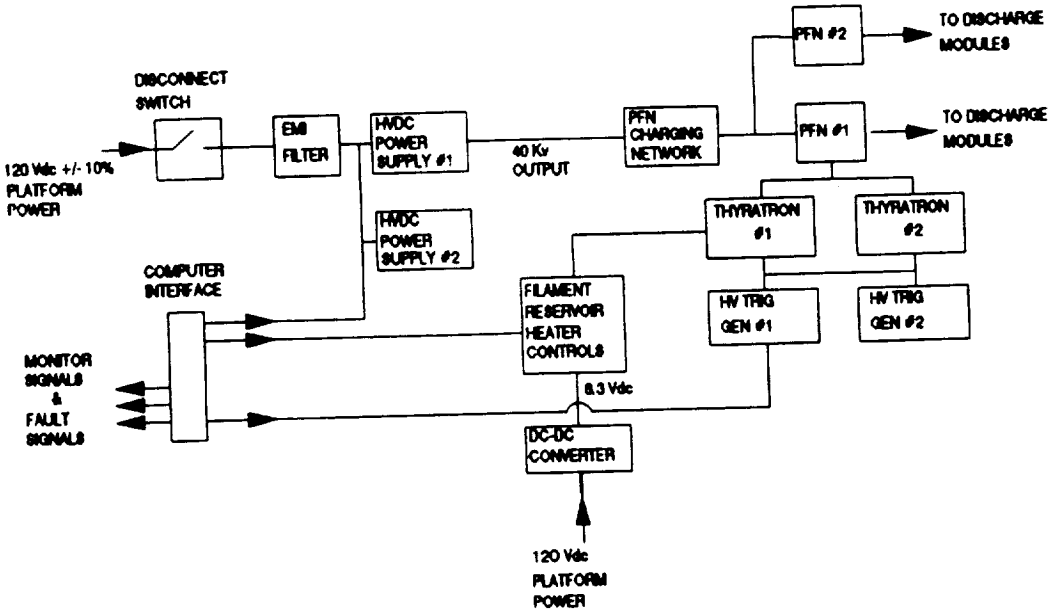

Figure 3-27. Energy Discharge Processes

The configuration of the PFN, shown in *Figure 3-28*, will be an E-type, thyratron switched scheme similar to that utilized in the breadboard. Primary differences arise in the choice of lighter weight, space qualified components, particularly capacitors, and the use of redundant critical components such as the thyratron, capacitors, and diodes. Also, because operating the PFN in a pressurized environment would result in a considerable weight penalty, vacuum operation is anticipated. This requires mounting components on a coldplate and active cooling of the thyratron. The operating parameters of the pulse subsystem are listed below:

- Total energy stored in PFN 264 J
- PFN charge voltage 40 kV max
- PFN current <2.5 kA
- Total capacitance 400 nF
- Pulse length 4.5 μs max
- PRF 10-15 Hz.

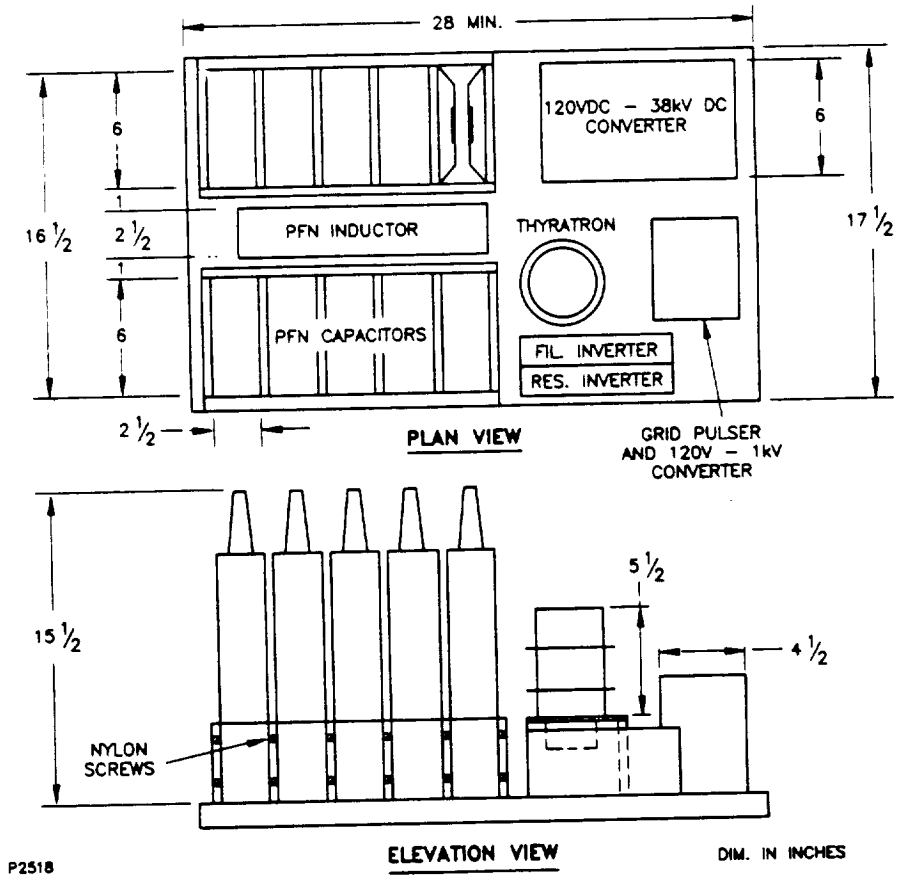

Figure 3-28. Preliminary Layout of Pulsed Power Section

3.3.1.4 Controls and Instrumentation

The controls and instrumentation units needed for the space device have been identified, as have their functions. A computer interface unit will be provided to handle signal and command flow between the transmitter components and LMSC's flight computer. In addition, electronics units for the auto-alignment feedback loop, cavity matching loop, and fan drive will be implemented. Functional diagrams for these loops are shown in *Figures 3-29* and *3-30*, respectively.

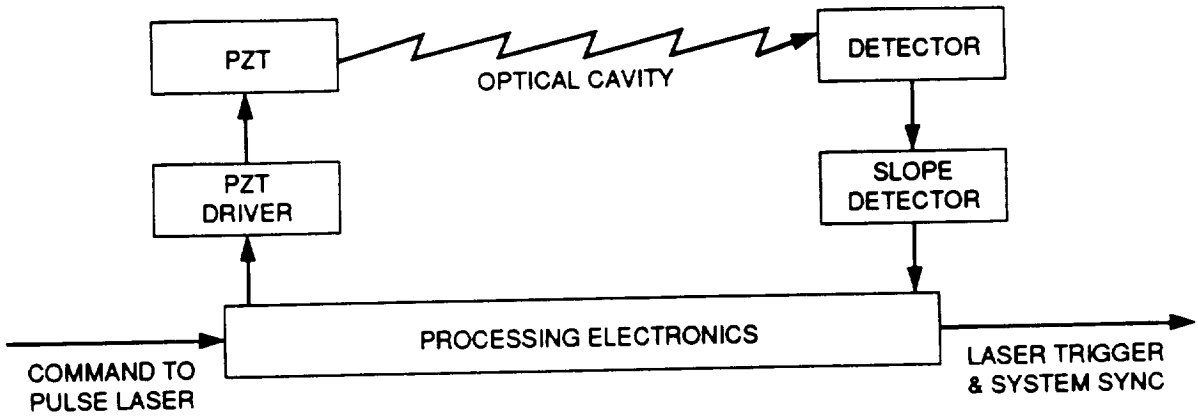

Figure 3-29. Resonator Cavity Matching Control

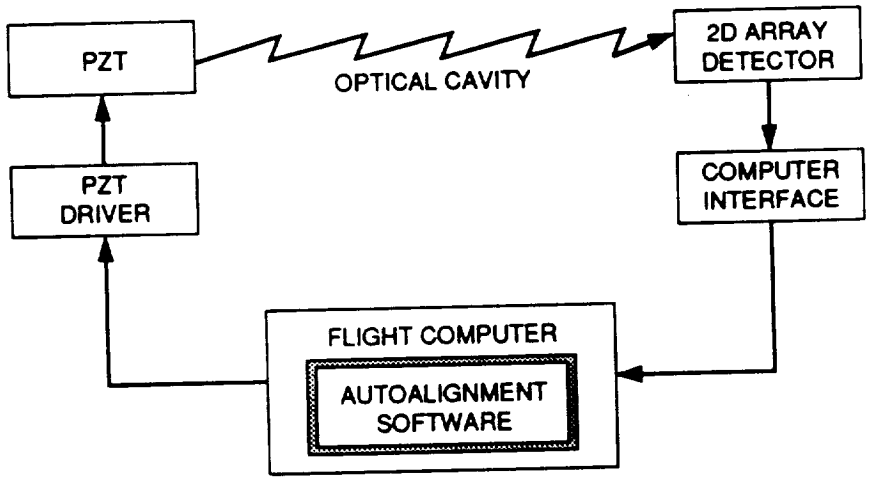

Figure 3-30. Auto-Alignment Functional Diagram

3.3.1.5 Parts Requiring Complex Manufacturing Techniques

Some of the complex components of the space laser device are expected to be similar, if not identical, to those of the Phase II risk reduction laser breadboard. The following breadboard drawings may be used for preliminary specifications:

- Contour machined components
  - Muffler Assembly L23219
  - Cathode Housing LAW23215, LAW23285
  - Preionizer Assembly LAW23250, LAW23236
- Cathode Bar LAW23214
- Shroud Brackets LAW23281
- Contraction Duct LAW23231
- Corona Bar LAW23229
- Support Plates LAW23234.

3.3.1.6 Software Systems

Software required to operate and monitor the transmitter consists of modules designed to handle I/O of signals and commands via the computer interface unit. These modules are implemented for the operating system and in the programming language specified by NASA for the flight computer.

These modules monitor control input bits from on/off sensors, control on/off -- open/close devices, monitor analog signals sensors, and control analog actuators and voltage controlled functions. One module provides the logic needed to undertake steps outlined in the failure mode analysis for those failure modes which cannot be automatically handled by mechanical or electrical switching. Another module implements the algorithm for autoalignment of the transmitter optics. Finally, additional modules perform such functions as data partitioning, communications, and compression as well as flagging and linking of routines.

3.3.1.7 Laser Subsystem Summary

Figure 3-31 summarizes development efforts for the laser subsystem. This summary includes the overall development schedule (A), the required subsystem equipment and implementation/verification plan (B&C), trade studies to establish the baseline (D), and a summary of subsystems risk (E).

A LASER TRANSMITTER PLAN OVERVIEW

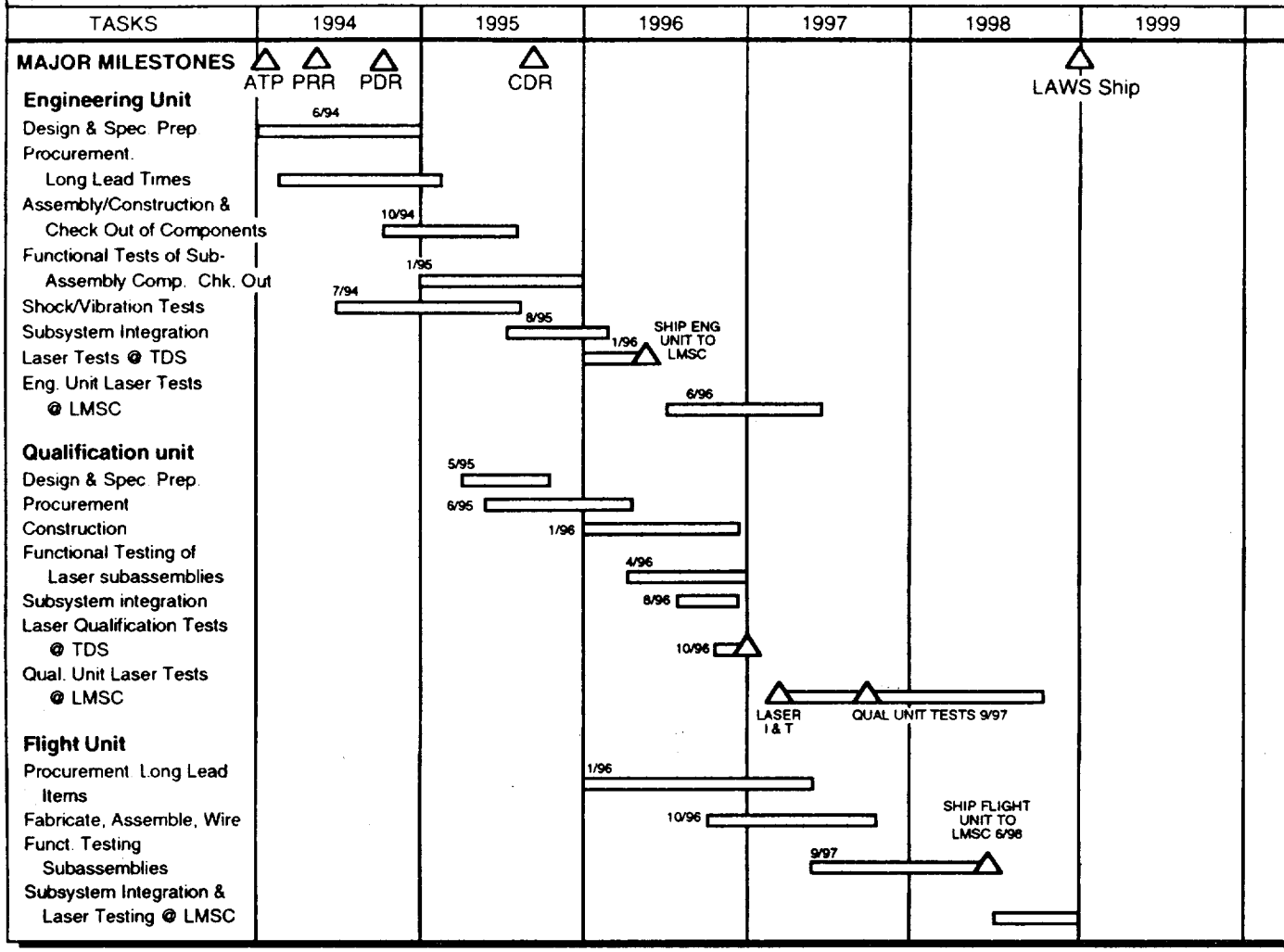

B REQUIRED SUBSYSTEM EQUIPMENT

COMPONENT*	SOURCE	QUANTITY/UNIT	ENG. UNIT	QUAL. UNIT	FLIGHT UNIT**
Pulsed Power Laser	TDS	1	1	1	1
Discharge Cavities	TDS	2	2	2	2
Flow Loop/Fans/Catalyst	TDS/VOP	1/2/2	1/2/2	1/2/2	1/2/2
Pressure Vessel	TDS	1	1	1	1
Pulse Forming Network	TDS	1	1	1	1
Thyratrons	TDS	2	2	2	2
Pulsed Power Supply	ALE	1	1	1	1
Optical Resonator/Bench	TDS/LMSC	1/1	1/1	1/1	1/1
CW Injection Laser	MPB	2	2	2	2
Single Mode PZT Controller	BURLEIGH	1	1	1	1
CW Local Oscillator Laser	MPB	2	2	2	2
Controls and Instrumentation	TDS	1	1	1	1
Alignment Laser and Mechanism	ITEK	1	1	1	1
Laser Thermal Control System	TDS	1	1	1	1

** "S" parts*

*** Engineering unit components used for spares*

F320789-050

E

Fan Failu
Individual
Catalyst C
Thyratron
PFN Cap
Feedback
Mirror Da
Window D

FOLDOUT FRAME

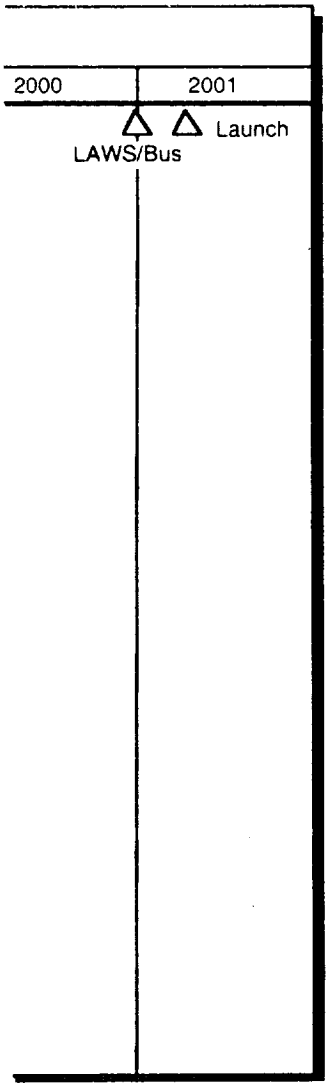

C REQUIREMENT IMPLEMENTATION/VERIFICATION

KEY REQUIREMENT	IMPLEMENTATION	VERIFICATION
Operational Life and Reliability	• 5 yr on orbit • 10^9 Shots	Extended Life Tests • Components to > 10^9 • System to > 3 x 10^8 Design for: Robustness and Key Component Redundancy
Performance	• 9.11 μm ($C^{18}O^2$) • 20 J/Pulse • Single mode pulses • 3 μp FWHM pulse length • <200 kHz CHIRP • 4.67 Hz scan mode } xπ/2 • 10 Hz design mode } (max PRF)	Performance Validation Test • Breadboard • Eng Unit • Qual Unit • Flight Unit
Interfaces and Software Functions	• Flight Processor – Auto alignment SW – Failure handling SW – Data handling SW – Signal & Command SW • Telescope control system • Platform Power Control System • Platform Thermal Control System • Beam Detector System • Gas Handling System	Simulation and test

D PLANNED TRADE STUDIES

TRADE ITEM	BASELINE DESIGN
Discharge Parameters	
• Gas mixture composition	• He : $C^{18}O^2$: N_2 = 3:1:1
• Gas pressure	• 0.625 atm
• Electrodes/Preionizers materials	• Proprietary
• Cavity dimensions/Gain length	• 4.2 x 4 cm/150 cm
• Voltage/Energy Loading	• 35 kV/80 J/L
• Flush factor	• 3.0
Resonator Parameters	
• Magnification	• 2.25
• Scraper geometry	• Square (square vs. circular)
• Cavity reflectivity	• Uniform (uniform vs. graded)
Flow Loop Parameters	
• Catalyst configuration	• Dual in-line Beds, 400 cells/in^2

RISK SUMMARY

RISK ITEM	RISK LEVEL	RISK REDUCTION APPROACH
	Moderate	1. Dual fans provide redundancy; laser can operate on one fan.
ischarge Arc or Preionizer Failure	Moderate	1. Redundant preionizer and associated discharge modules. 2. Operation at lower discharge voltages to reduce probability of arcing and failure
ntamination	Probably Low (not yet established)	1. Catalyst reactivation heaters, flushing of pressure vessel laser gas refill, plus pre-launch clean room and bake out procedures.
ailure	Moderate	1. Backup provides redundancy.
itor Short Circuit	Moderate	1. Isolate faulty capacitor, switch in backup spare.
Mirror PZT Drive Failure	Low	1. Robust design is essential.
age or Contamination	Risk not yet established	1. Robust design and cleanroom and bake out procedures to minimize effects.
mage or Contamination	Risk not yet established	1. As above; also addition of lasing mixture, cope with a small crack.

Figure 3-31. Overview/Summary of the Laser Transmitter Subsystem

3.3.2 Optical Subsystem

3.3.2.1 Optical Subsystem Baseline Design

The LAWS optical subsystem has two major functions. First, it acts as a transmitter in the role of a beam expander, taking the 4 cm output of the 9.11 micron laser and forming a 1.67 m diameter beam which is scanned via a bearing assembly across the Earth's atmosphere. Second, it performs the function of a receiver, acquiring the Doppler shifted scattered energy from the troposphere. The optical subsystem interfaces with the LAWS Laser via the transmitter relay optics and with the LAWS receiver at the tip/tilt mirror, which performs dynamic lag angle compensation.

The optical subsystem functional flow diagram is shown in *Figure 3-32*. The selected baseline design for the telescope is a two-mirror afocal configuration operating with a split field. With a F/1.5 primary mirror, the telescope fits within the current packaging envelope. The transmit optic axis is oriented off-axis by 0.2 deg in object space in order to remove the course lag angle which is due to the telescope scanning in azimuth and the round trip time for each transmitted laser pulse. Compensator optics are required in the transmit path to balance focus error from telescope field curvature. The receive channel is oriented on-axis. Pupil relay optics are required to limit the size of the radiation through the scan bearing over the entire ±0.3 mrad object space field-of-view. The pupil relay also creates a real pupil at which a single tip/tilt mirror can correct for second order dynamic lag angle compensation.

The periscope follower is a two-mirror assembly which rotates synchronously with the telescope in order to fold the receive radiation back on axis. Telescope alignment is monitored by additional active sensors and maintained by actuators controlling the location and orientation of the secondary mirror. The physical characteristics which result from this preliminary baseline design activity are summarized in *Table 3-2*. Other design features include a lightweight system with a 90 percent lightweighted ULE primary mirror, silicon carbide fold optics, and graphite epoxy structures. The low residual wavefront error is due to a low sensitivity design, the alignment maintenance system, and the use of ULE with its virtually zero CTE and variation of CTE.

Details of the primary mirror structure, reaction structure, and metering structure are shown in *Figures 3-33, 3-34, 3-35*, respectively. Light weight is a key feature of each of these designs. Optical component prescription data are tabulated in *Table 3-3*. These are the only nonplanar surfaced elements in the optical subsystem and include the three receive channel relay elements and the two transmit channel compensator elements.

The optical subsystem development schedule is shown in *Figure 3-36 (A)*. The major long lead time items are the ULE blanks for the 1.67 m primary mirror. The first primary requires approximately 9 months to fabricate.

Subassemblies for the various units are listed in *Figure 3-36 (B)*. Key requirements, implementations, and verification approaches are shown in *Figure 3-36 (C)*.

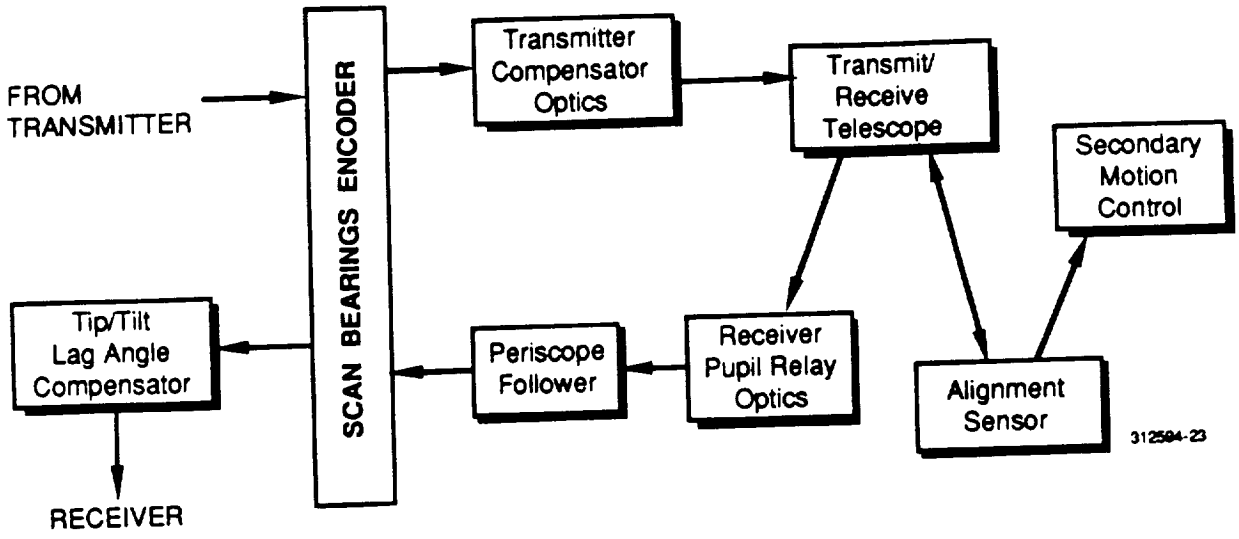

Figure 3-32. Optical Subsystem Functional Flow Diagram

Table 3-2. Optical Design Characteristics

Parameter	Value
Aperture (cm)	167.6
Magnification	41.8x
Primary F-Number	F/1.5
FOV (circular)	Tran.: 13 μrad Rec.: 0.6 mrad
Pri-Sec Spacing (cm)	245.4
Obscuration (area)	<1%
Wavelength (μm)	9.11
Optical Quality (RMS WFE)	Trans.: 0.018 l λ Rec.: 0.003 l λ

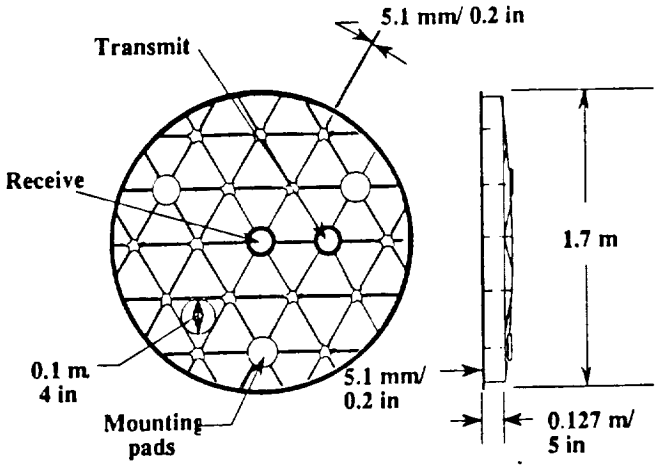

- Superb CTE variation minimizes wavefront errors from temperature soaks
  - 53 °C soak change yields 0.007 rms
- Lightweight mirror design meets weight requirements while maintaining its durability
  - 1.5 m diameter LPMA withstands 18 g's
- Detailed weight estimate (kg)

Facesheet	37
Closure wall	7
Ribs	27
Fillets & Parasitics	4
Total	75

Figure 3-33. Primary Mirror Design

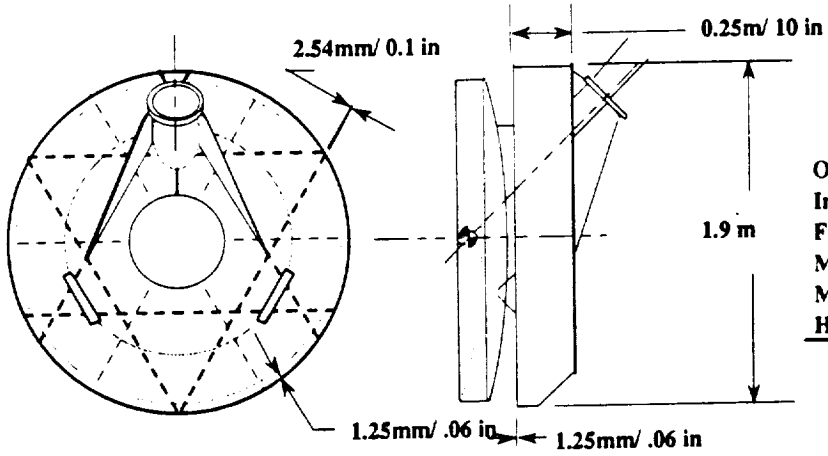

Mass Properties (kg)	
Outer closure ring	4
Inner closure ring	1
Facesheets (front and back)	13
Main ribs	11
Minor ribs	3
Hardware, mounts & clips	3
Total	35

- All graphite epoxy structure
  - Egg crate construction yields high stiffness with a low density
  - G/E coefficient of thermal expansion well matched to that of ULE
- Primary mirror kinematically mounted to structure through three bipods

F312539-tek-13

Figure 3-34. Reaction Structure Design

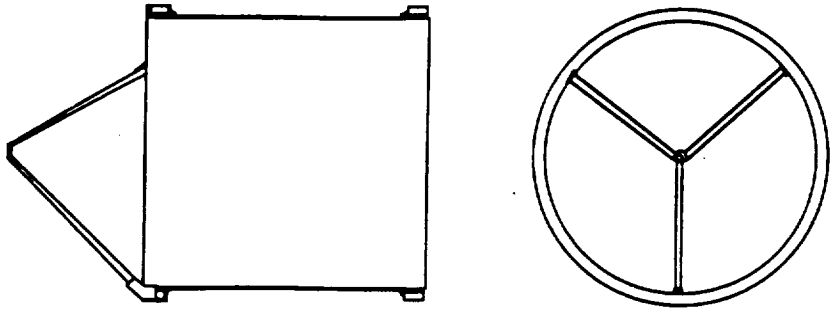

- **All graphite epoxy structures with invar hardware inserts**
- **Weight summary (kg)**

Metering structure	
Reenforced tube	**22.0**
Hardware	**3**
Metering legs	
Legs	**0.5**
Hardware	**1.5**
Secondary mirror assembly	
Mirror	**0.5**
Bezel & hardware	**1.5**
TOTAL	**29.0**

F312539-tek-14

Figure 3-35. Metering Structure Design

Table 3-3. Optical Component Data

Component	Radius	Conic Constant	F-Number	Diameter
Primary	502.920 cc	-1.00000	1.50	167.6
Secondary	12.040 cx	-1.00000	1.50	4.0
Compen 1 (Trans.)	4.382 cc 59.172 cc	t=0.381	—	3.6
Compen 2 (Trans.)	12.656 cc 4.969 cx	t=0.635	—	5.1
Relay 1 (Rec.)	130.176 cx ∞	t=1.270	—	10.9
Relay 2 (Rec.)	6.975 cx 5.630 cc	t=1.270	—	3.8
Relay 3 (Rec.)	53.273 cc 34.724 cx	t=1.270	—	5.1

*Linear units are centimeters

A OPTICAL SUBSYSTEM OVERVIEW

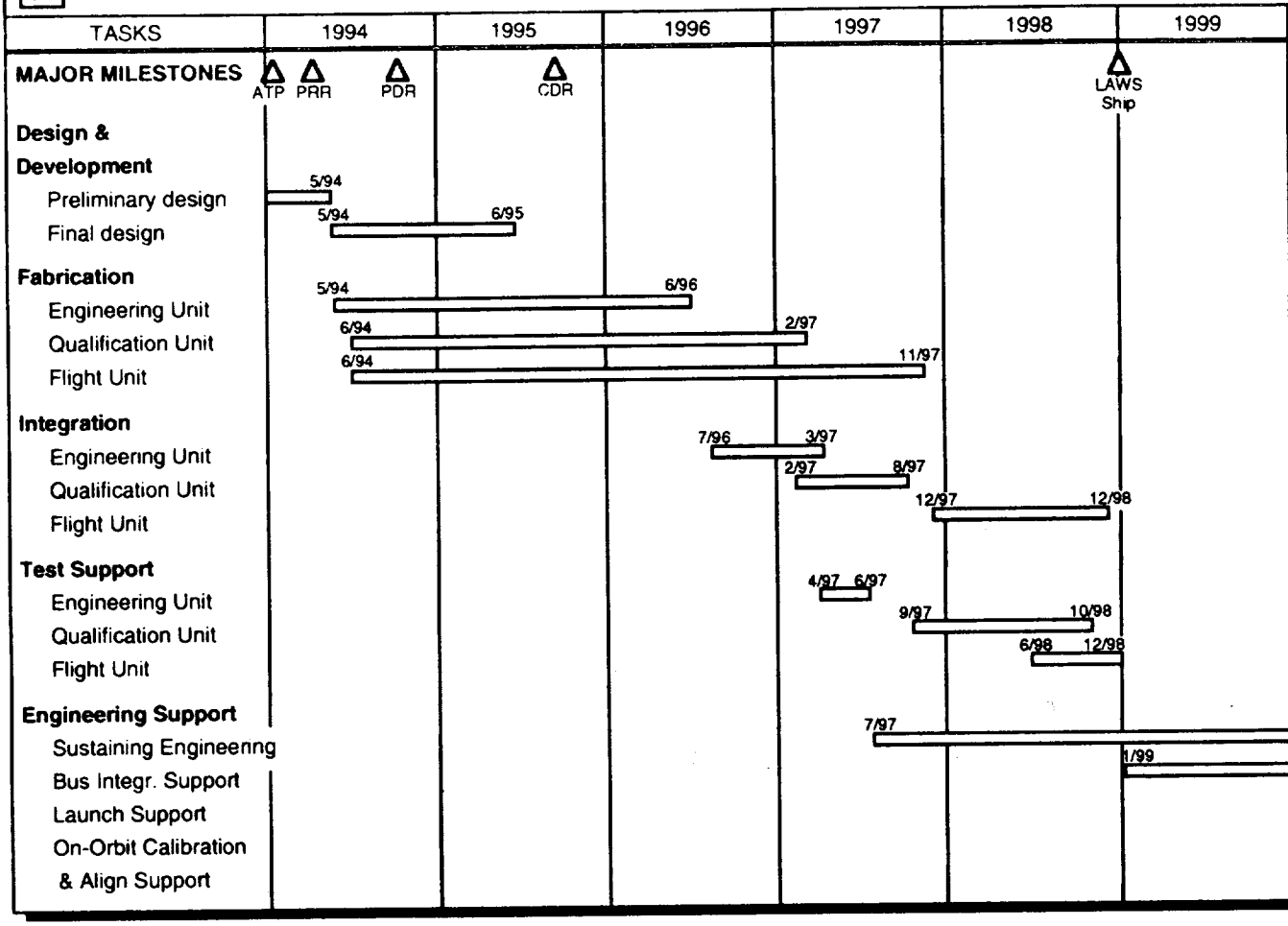

B REQUIRED SUBSYSTEM EQUIPMENT

COMPONENT*	SOURCE	QUANTITY/UNIT	ENGINEERING. UNIT
Primary Mirror Assembly	Litton-Itek Optical Systems	1	1
Secondary Mirror Assembly	Itek	1	1
Metering Structure	Itek	1	1
Reaction Structure	Itek	1	1
Transmit Relay Optics Set	Itek	1	1
Receive Relay Optics Set	Itek	1	1
Fold Optics Set	Itek	1	1
Thermal Control System	Itek	1	1
Azimuth Scanning System	Itek	1	1
Tip/Tilt Mirror	Itek	1	1
Telescope Alignment System	Itek	1	1
Mechanical, Thermal, Electrical, and Optical Interfaces	LMSC	5	5

* "S" Parts
**Engineering unit components used for spares

FOLDOUT FRAME

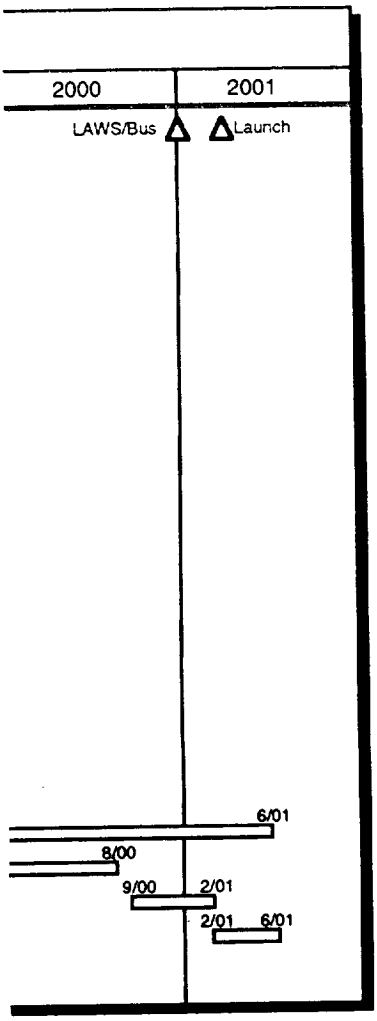

JAL. UNIT	FLIGHT UNIT**
1	1
1	1
1	1
1	1
1	1
1	1
1	1
1	1
1	1
1	1
1	1
1	1
5	5

C REQUIREMENT IMPLEMENTATION/VERIFICATION

KEY REQUIREMENT	IMPLEMENTATION	VERIFICATION
Operational Life	5 years on orbit	Comparison and test
Maximize Heterodyne Efficiency	• Wavefront error ≤ 0.07 waves RMS • Flat field over receive FOV • Obscuration < 3% • Round trip pointing stability ≤ 1.5 μrad • Magnification: 42X	Analysis, simulation, and test
Lag Angle Compensation	• Format: 2 points separated in field by 0.185° • Dynamic tip/tilt mirror	Analysis and simulation

D PLANNED TRADE STUDIES

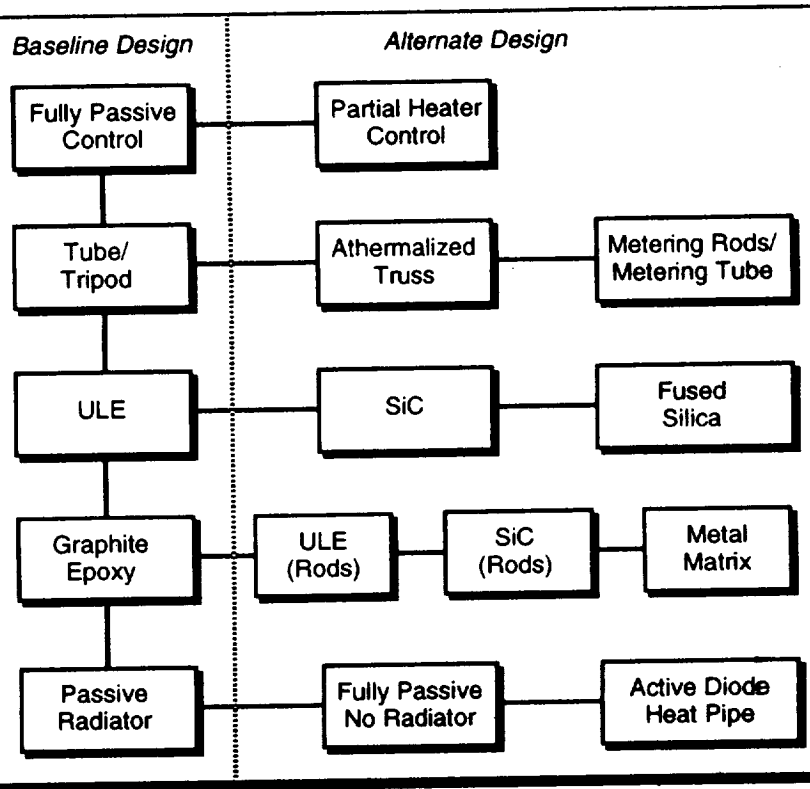

E RISK SUMMARY

RISK ITEM	RISK LEVEL	RISK REDUCTION APPROACH
Motor/Bearing/Encoder	Low	Space qualified and demonstrated unit
Optical Coating Fatigue	Low	Risk reduction testing with LAWS laser breadboard
Telescope Alignment System	Low	Risk reduction testing with alignment system breadboard

F320789-07

Figure 3-36. Overview/Summary of the Optical Subsystem

FOLDOUT FRAME 2

3.3.2.2 Optical Subsystem Alignment System

An active alignment system is required to correct for positional changes due to gravity release when the unit is first placed on orbit and for changes which result from thermally induced contractions and expansions. The latter are relatively slow changes, so high bandwidth responses will not be required. The alignment system provides an error signal to control the secondary mirror position in tilt and despace.

The basic alignment approach is shown in *Figure 3-37*. The concept consists of three major optical paths. The first path is a sample of the transmit beam direction represented by a coaligned laser beam centered in the main transmit beam. This is folded into the integrated alignment sensor (IAS) via a penta fold mirror. The sample from the transmit beam is offset in angle from the receiver axis. This process is used to separate this return from the receiver beams. The transmit beam surrogate is spatially separated and focused onto a CCD detector. This provides the angular coordinates of the beam in primary mirror coordinate space.

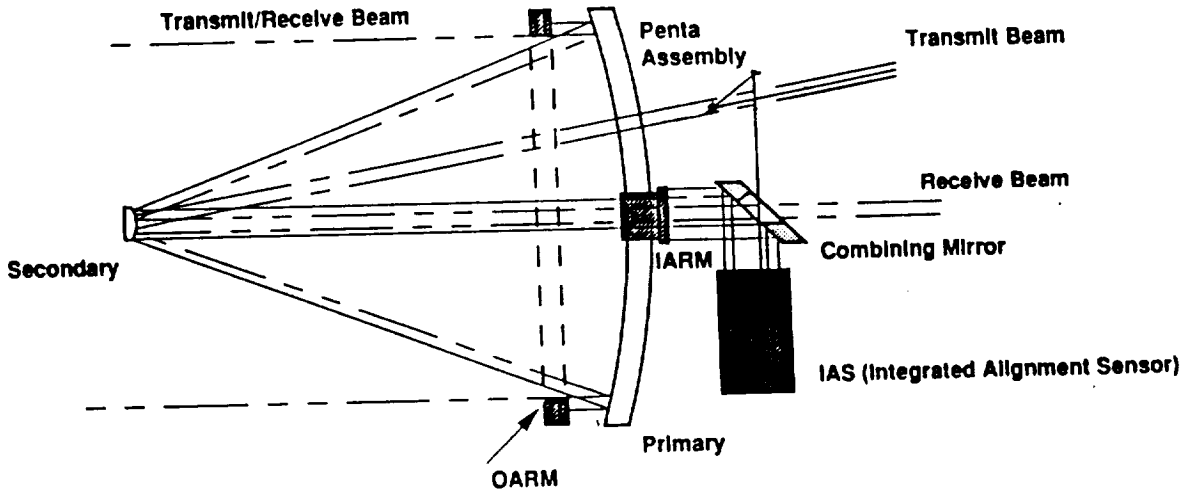

Figure 3-37. Alignment System Concept

The return beam from the input annular reference mirror (IARM) is reflected from a beam divider to provide angular coordinates of the IARM in IAS space. This allows the IAS to move since the measurements are made relative to this measurement. This division of the main beam is made possible by locating the divider at an image of the IARM -- a pupil. The beam which passes through the IARM image provides a measurement of the tilt and defocus of the telescope.

The second path originates from the IAS. The annular collimated beam is folded onto the receiver axis by a combining mirror -- a perforated flat mirror. It then autocollimates off an IARM which is kinematically mounted to the primary mirror assembly. This returns a beam representing the receiver axis coordinate system.

The third beam is formed by allowing a portion of the IAS beam to pass through the IARM. It traverses the optics of the telescope. The beam from the primary (output space) then autocollimates from the output annular reference mirror (OARM). This sample provides both tilt and defocus information of the beam expander.

The alignment is carried out by means of surrogate beams which are co-aligned with the LAWS optic axes. The alignment sequence is as follows:

(1) The transmit beam and transmit reference beam are coaligned
(2) Transmit reference is folded into IAS via a penta fold
(3) The IAS reference is inserted onto the receiver optical axis via the combining mirror
(4) The IAS reference beam is divided at the IARM
(5) Part of the beam is autocollimated off the IARM -- this represents the coordinate system of the primary mirror
(6) The transmitted portion of the beam traverses the telescope to the OARM
(7) The three returns (transmit beam reference, IAS reference, and telescope reference) enter the IAS.

The IAS transmits the alignment data to the flight computer, which then provides signals to the actuators that control the orientation of the secondary mirror.

3.3.2.3 Design Trades and Sensitivity Analyses

Various configurations for the telescope have been evaluated against the requirements. These requirements changed during the course of the system development when the nadir angle specification was changed from variable to fixed. With a fixed nadir angle, the dominant contribution to the lag angle is also fixed. This eliminated the need for some of the flexibility initially considered.

The preliminary trades reduced viable telescope configurations to two candidate options: a two-mirror afocal and a three-mirror afocal system. With the adoption of a fixed nadir angle, a split field telescope was considered the most applicable approach and the inherent design flexibility afforded by the three-mirror was no longer demanded. Wavefront error sensitivities for tilts and displacements were calculated and determined to be comparable. The strongest advantage of the three-mirror system is the existence of a real pupil. With a real pupil, second order lag angle and

other dynamic corrections can be accommodated with a single tip/tilt mirror. However, with additional optics, a real pupil can be created in a two-mirror telescope. This approach allows a reasonable compromise of simplicity while still allowing the very small secondary mirror of the two-mirror design.

The two-mirror afocal design is shown schematically in *Figure 3-38*. The large primary operates at F/1.5, and both mirrors are parabolas. The split field allows the static lag angle due to telescope rotation during the round trip time of the laser pulse to be accommodated. Sensitivities to tilts and displacements have been analyzed for this as well as the three-mirror design. The results of these calculations for the two-mirror system are shown in *Tables 3-4* through *3-7*.

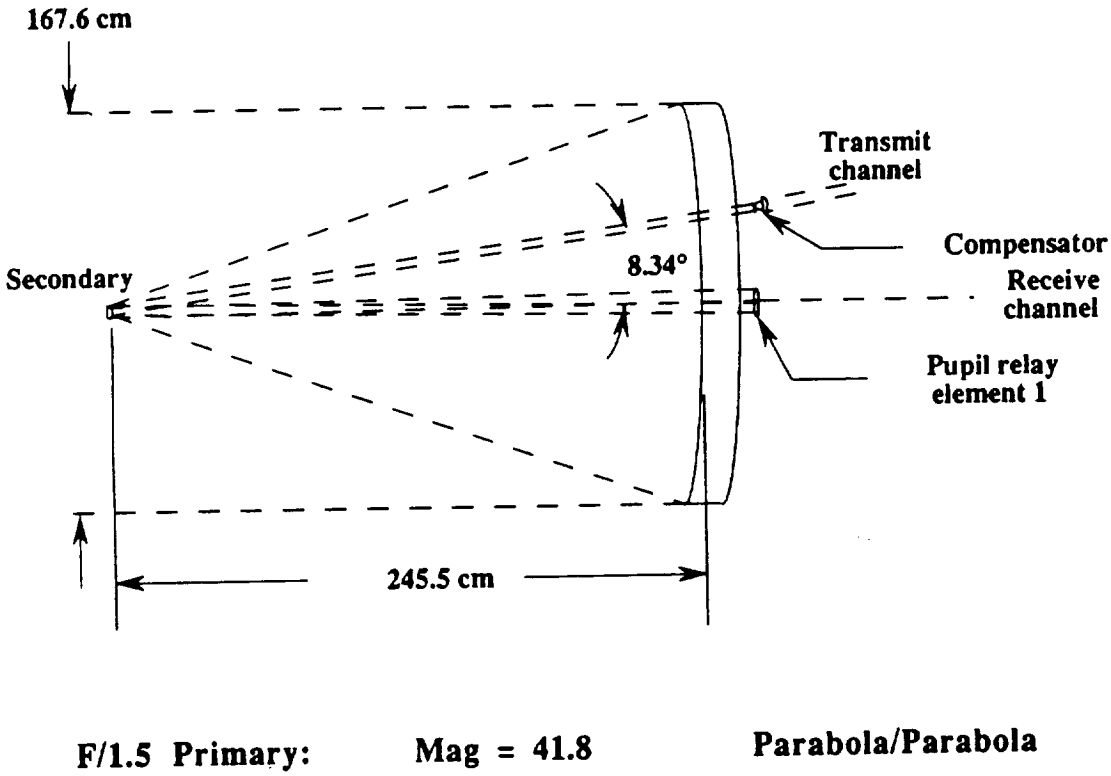

Figure 3-38. Two-Mirror Afocal Split Field Design

Table 3-4. Receiver Channel Wavefront Error (WFE) Sensitivities (Rigid Body Alignment Errors)

Element	Tilt			Displacement		
	Alpha	Beta	Gamma	X	Y	Z
Primary	0.030	0.030	0.000	0.003	0.003	0.044
(W/Refocus)	0.030	0.030	0.000	0.003	0.003	0.000
Secondary	0.001	0.001	0.000	0.003	0.003	0.043
(W/Refocus)	0.001	0.001	0.000	0.003	0.003	0.000
Relay 1	0.000	0.000	0.000	0.000	0.000	0.000
(W/Refocus)	0.000	0.000	0.000	0.000	0.000	0.000
Relay 2	0.000	0.000	0.000	0.000	0.000	0.000
(W/Refocus)	0.000	0.000	0.000	0.000	0.000	0.000
Relay 3	0.000	0.000	0.000	0.000	0.000	0.001
(W/Refocus)	0.000	0.000	0.000	0.000	0.000	0.000

All entries are rms WFE for wavelength = 9.11 μm
Δ X,Y,Z = 0.001 inches (Primary and Secondary)
Δ X,Y = 0.005 inches (Relay 1,2,3)
Δ Z = 0.002 inches (Relay 1,2,3)

Δ Tilt = 0.0001 radians (Primary and Secondary) ⇒
= 0.0010 radians (Relay 1,2,3)

TIR (inches)

PRI	0.0066
SEC	0.0002
REL 1	0.0045
REL 2	0.0015
REL 3	0.0020

Primary Tilt is most sensitive error

Table 3-5. Transmitter Channel WFE Sensitivities (Rigid Body Alignment Errors)

F312511-Kek-22

Element	Tilt			Displacement		
	Alpha	Beta	Gamma	X	Y	Z
Primary	0.013	0.018	0.000	0.005	0.006	0.042
(W/Refocus)	0.011	0.007	0.000	0.004	0.005	0.001
Secondary	0.002	0.003	0.000	0.004	0.005	0.045
(W/Refocus)	0.002	0.003	0.000	0.004	0.004	0.001
Compen 1	0.009	0.009	0.000	0.020	0.022	0.118
(W/Refocus)	0.009	0.009	0.000	0.020	0.020	0.004
Compen 2	0.004	0.004	0.000	0.020	0.021	0.121
(W/Refocus)	0.004	0.004	0.000	0.020	0.020	0.004
Comp 1 & 2	0.002	0.002	0.000	0.000	0.000	0.000
(W/Refocus)	0.002	0.002	0.000	0.000	0.000	0.000

All entries are rms WFE for wavelength = 9.11 μm
Δ X,Y,Z = 0.001 inches (Primary and Secondary)
Δ X,Y = 0.005 inches (Compensator 1 & 2)
Δ Z = 0.002 inches (Compensator 1 & 2)

Δ Tilt = 0.00001 radians (Primary) ⇒
= 0.0001 radians (Secondary)
= 0.0010 radians (Compensator 1 & 2)

Primary Tilt is most sensitive error

TIR (inches)

PRI	0.0066
SEC	0.0002
REL 1	0.0045
REL 2	0.0015
REL 3	0.0020

Table 3-6. Receiver Channel LOS Error Sensitivities (Rigid Body Alignment Errors)

Element	X-Tilt	Y-Tilt	X-Dec	Y-Dec	Z-Dec
Primary	0.199	0.199	-0.010	-0.010	0.00000
Secondary	-0.005	-0.005	0.010	0.010	0.00000
Relay 1	-0.0002	-0.0002	-0.0033	-0.0033	0.00000
Relay 2	-0.0006	-0.0006	-0.0012	-0.0012	0.00000
Relay 3	0.0005	0.0005	0.0045	0.0045	0.0000

Δ X,Y,Z = 0.001 inches (Primary and Secondary)
Δ X,Y = 0.005 inches (Relay 1,2,3)
Δ Z = 0.002 inches (Relay 1,2,3)

F312511-tek-23

Δ Tilt = 0.0001 radians (Primary and Secondary)
= 0.0010 radians (Relay 1,2,3)

- Primary tilt is most sensitive error

Note: LOS displacement in object space (mrad)

Table 3-7. Transmitter Channel LOS Error Sensitivities (Rigid Body Alignment Errors)

Element	X-Tilt	Y-Tilt	X-Dec	Y-Dec	Z-Dec
Primary	-0.020	-0.020	0.010	0.010	0.00003
Secondary	0.005	-0.005	-0.010	-0.010	-0.00080
Relay 1	-0.0010	-0.0010	-0.0555	-0.0555	-0.00036
Relay 2	0.0018	0.0018	0.0550	0.0550	0.00023
Relay 3	0.0113	0.0113	-0.0005	-0.0005	0.00000

F312511-tek-24

Δ X,Y,Z = 0.001 inches (Primary and Secondary)
Δ X,Y = 0.005 inches (Compensator 1 & 2)
Δ Z = 0.002 inches (Compensator 1 & 2)

Δ Tilt = 0.00001 radians (Primary)
= 0.0001 radians (Secondary)
= 0.0010 radians (Compensator 1 & 2)

- Primary tilt is most sensitive error

Note: LOS displacement is object space (mrad)

Table 3-4 lists receiver channel wavefront errors induced by tilts and displacements by the individual optical elements. The relay elements refer to the relay optics which transfer the received beam through the scan bearing and form the real pupil, which is used for second order lag angle correction. Refocus refers to the telescope's ability to adjust secondary-primary mirror spacing for best focus. The optic axis for the telescope is labeled the Z-axis.

Table 3-5 is a tabulation of similar data for the transmitter channel. The two compensator lenses refer to the device which adjusts the curvature of the transmitter beam before it impinges on the secondary mirror. In this table, as before, wavefront error is listed in fractions of the operating wavelength.

Tables 3-6 and 3-7 are tabulations of the effects of tilts and displacements on the lines-of-sight of receiver and transmitter channels, respectively. In *Table 3-7*, relay 1, relay 2, and relay 3 refer to transmitter compensator lens 1, compensator lens 2, and compensator lenses 1 and 2 acting as a unit, respectively.

Other trades were performed to ensure that the optical subsystem meets its requirements and still remains within weight, volume, and power restrictions. A list of the selected baseline approaches and alternates is shown in *Figure 3-36 (D)*. In each case, we selected the baseline design adequate to meet requirements for the lowest weight or power. Ultra low expansion (ULE) glass has been chosen for the material for the primary mirror because it exhibits virtually zero coefficient of thermal expansion (CTE) and a very low variation of the coefficient of thermal expansion within the mirror blank. The low values of CTE and the low variation of CTE help minimize the sensitivity of the optical subsystem to changes in thermal soaks and gradients. Errors related to the non-zero CTE typically result in focus type errors which can be compensated by adjusting the primary to secondary mirror spacing. On the other hand, the variation of CTE within the mirror results in random wavefront errors which cannot be corrected. The results of an analysis of worst case orbital thermal effects on the optical subsystem are tabulated in *Table 3-8*.

An assessment of risk areas is summarized in *Figure 3-36 (E)* along with approaches for risk reduction.

Table 3-8. Orbital Thermal Analysis Summary

	ΔT °C	RMS WFE (WAVES) @λ=9.11 μm	with refocus	LOS Pointing Error (μrad)
Primary mirror				
Gradient	2.5	0.080	0.008	
Soak (ΔCTE)	53.0	0.007	0.007	
Soak (radius of curvature)	53.0	0.080	0.008	
Metering Structure				
Despace	53.0	0.051	0.001	0.006
Decenter (grad)	8.0	0.0005	0.0003	0.9
Decenter (ΔCTE)	53.0	0.001	0.0006	2.0
Tilt (Grad)	8.0	0.003	0.0007	4.9
Tilt (ΔCTE)	53.0	0.006	0.002	10.8

Notes:

- Worse case orbital thermal analysis provides thermal soaks and gradients for each of the major components
- Thermal perturbations used in conjunction with the optical alignment sensitivities, produced from the lens design, to yield the corresponding LOS and wavefront errors.

3.3.3 Receiver/Processor Subsystem

The receiver/processor subsystem baseline is summarized as follows:

- Redundant HgCdTe photovoltaic detector arrays with 52 percent effective quantum efficiency at 100 MHz and 43 percent at 1300 MHz (47.5 percent average)
- Mixing efficiency of 0.33 for uniformly illuminated annular aperture with ratio of inner to outer diameter of 0.44
- Signal aligned on central element of array with exterior elements for alignment monitoring
- Local oscillator beam tailored for central (signal) element for shot noise limited operation with phase front matched to signal beam; spill over to alignment elements
- Redundant Split Stirling Cycle cryogenic coolers to optimize detector operating temperature
- Redundant Split Stirling Cycle cryogenic coolers to optimize preamp operating temperature
- Bias supply and preamplifiers space-qualified versions of standard units
- Automatic gain control for wide dynamic range between aerosol and ground returns
- 10 bit 75 million samples per second analog-to-digital (A/D) converter for adequate wind signal frequency response and dynamic range.

The LAWS receiver/processor subsystem consists of a wide bandwidth photo detector array, active cooling for the photo detector, bias circuitry, preamplifiers, and on-board signal processing electronics. For each of these components, several options were considered. These options will be outlined below, along with the logic for selection of the baseline receiver/processor subsystem components.

Figure 3-39 is the receiver/processor subsystem block diagram, and *Figures 3-40* and *3-41* are views of the physical arrangement. The local oscillator optical source (upper left hand corner of *Figure 3-39*) from the master oscillator is expanded to match the 4 cm diameter of the beam received from the telescope before being focused on the photo detector. The Doppler signal is received from the telescope and optical train, superimposed on the local oscillator, and directed toward and focused on the photo detector array. Cooling is provided for the detectors. Outputs from the detectors are amplified and frequency shifted to the frequency/amplitude range of the A/D converter. The "zero" Doppler (relative to the ground) is set for the center of the 0 to 30 MHz baseband to minimize A/D frequency span requirements. The levels of each channel from the detector array are measured to monitor the received optical signal spot location upon the detector array for optimal alignment. The output of the A/D is buffered and telemetered to the platform data interface.

3.3.3.1 Photo Detector

The LAWS photo detector is a critical element of the overall system. The detector detects the returned signal (Doppler shifted radiation) which is mixed with the local oscillator (LO) radiation at a controlled frequency to produce the Doppler shifted beat signal.

The line-of-sight Doppler signal of the tropospheric winds as measured from the orbiting satellite will vary from $+(2/\lambda)(V_S \pm 1V_W)\text{Sin}\alpha$ to $-(2/\lambda)(V_S \pm 1V_W)\text{ Sin}\alpha$. As the LAWS telescope traverses the conical scan, the satellite velocity either adds to or subtracts from the wind velocity component. For a cone half angle (α) of 45°, a laser wavelength (λ) of 9.11×10^{-6} m, and a satellite velocity (V_S) of 7.5 km/s, this satellite velocity bias varies from approximately 5.3 km/s to -5.3 km/s or $\pm 1.16 \times 10^9$ Hz. (The wind velocity adds only ±15 MHz to this number for 150 kn winds.) Thus, if the detector sees a purely homodyned signal with no LO offset, it must be capable of efficiently detecting signals with a bandwidth of approximately ±1.2 GHz.

Single element detectors have been built and tested with 70 to 80 percent effective quantum efficiency for bandwidths of less than 0.3 GHz, 35 to 45 percent for bandwidths up to 1 GHz, and to 35 percent for bandwidths up to 2 GHz. *Figure 3-42* presents test data. Optical preamplifiers can lead to increasing these efficiencies, as has been demonstrated with low pressure, low bandwidth, optical preamplifiers for low bandwidth requirements. However, for the above GHz bandwidths, the optical preamplifier requires a high pressure, low electrical efficiency design, and is thus not included in this baseline.

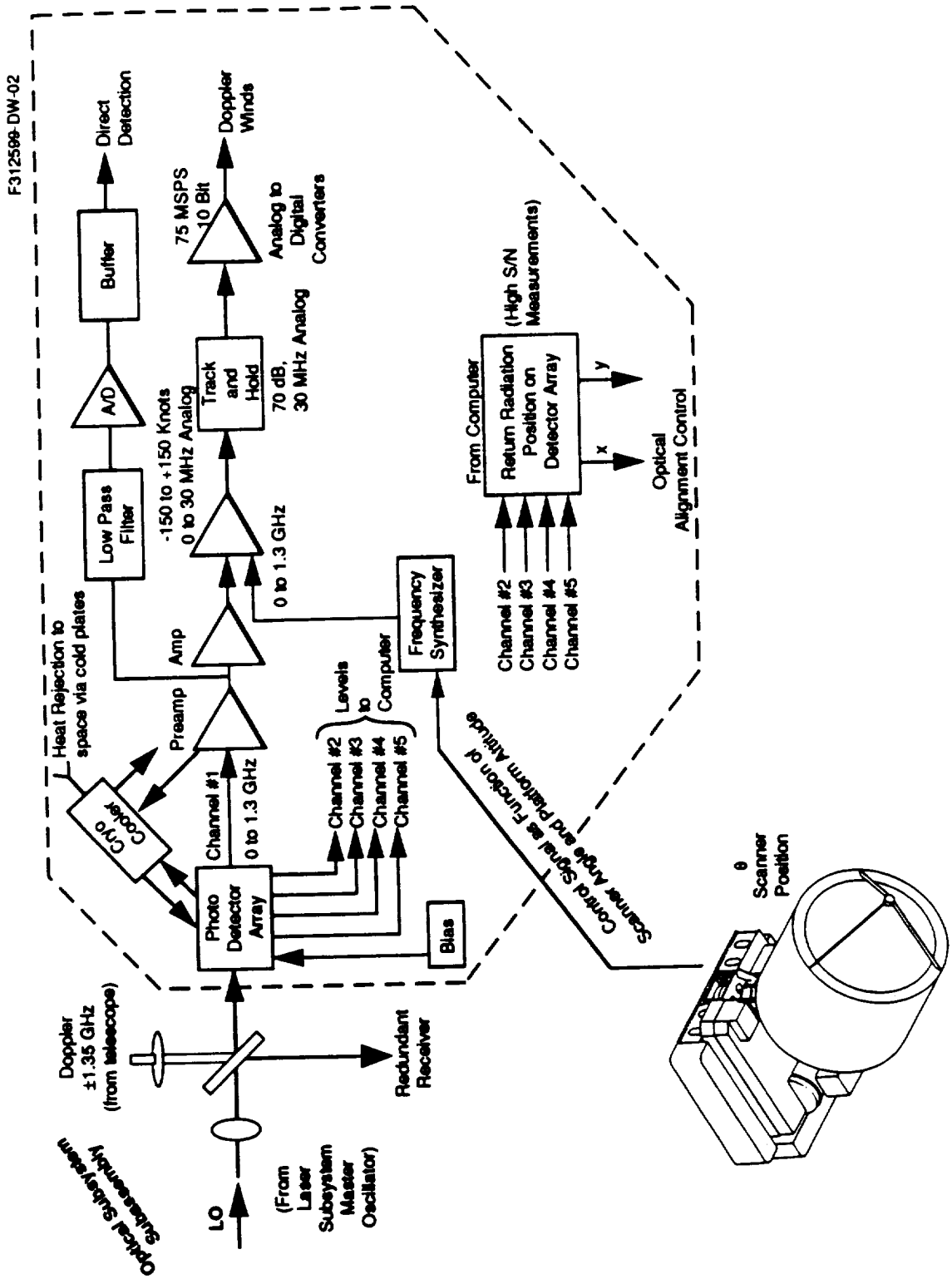

Figure 3-39. LAWS Receiver/Processor Subsystem Block Diagram

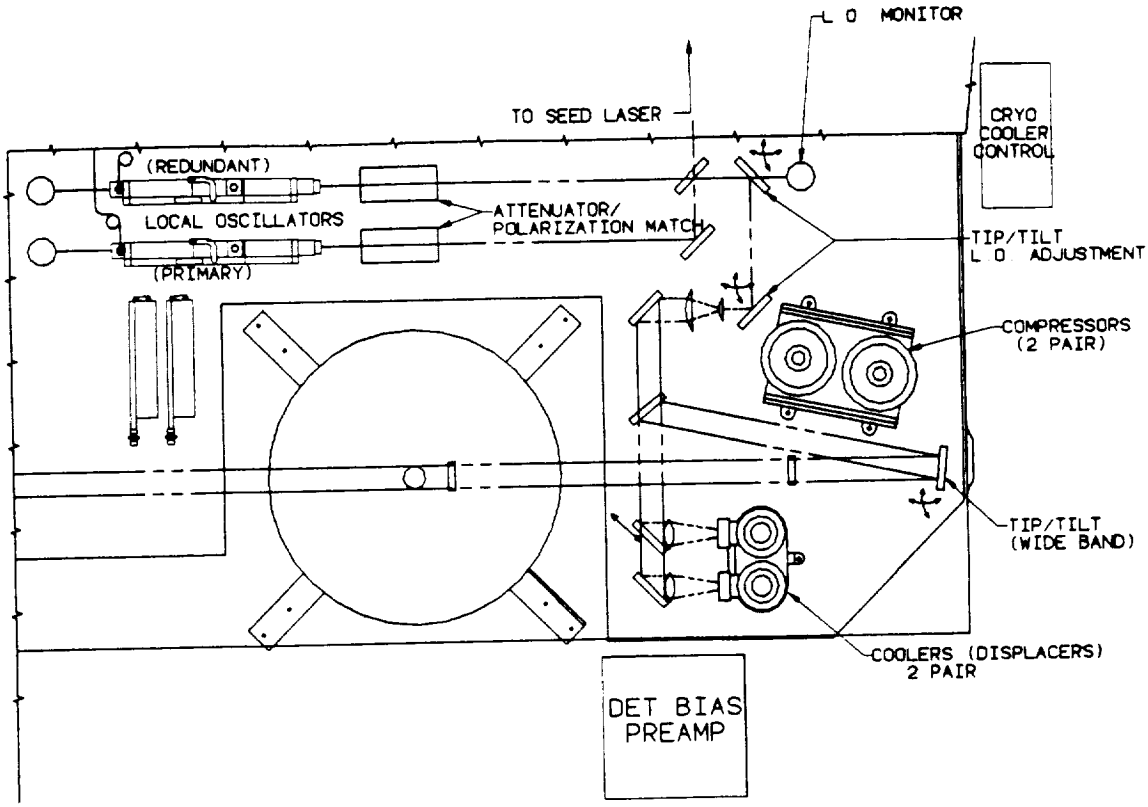

Figure 3-40. Receiver/Processor Layout

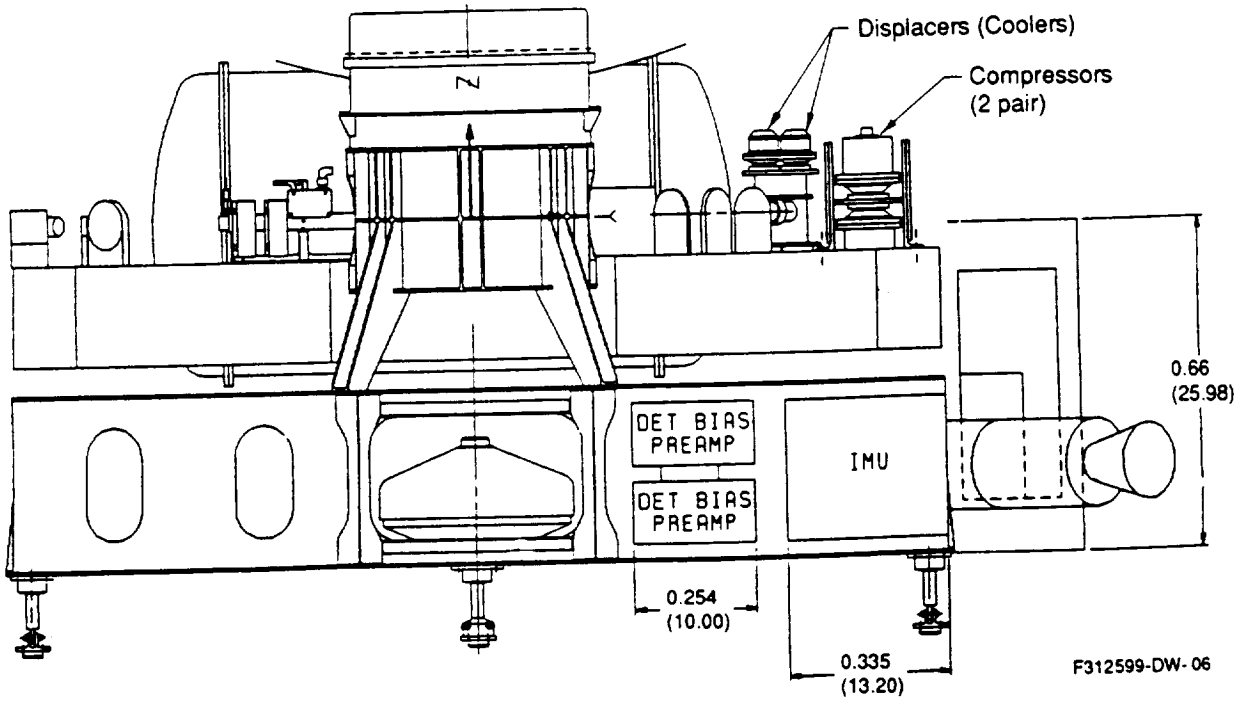

Figure 3-41. Receiver/Processor Components - Side View

Quantum efficiency is stressed here because a 1 dB improvement in receiver efficiency is equivalent to a 26 percent increase in laser energy or telescope aperture area. Potentially the highest quantum efficiency could be achieved via heterodyning with a controllable local oscillator signal, i.e., an LO which can be programmed to provide a known frequency output as a function of conical scanner position to compensate for the gross Doppler shift due to the satellite velocity. The following two methods have been discussed to offset the local oscillator frequency:

- Shift the frequency of the LO laser with cavity length tuning
- Externally modulate the frequency with either an acousto-optical or electro-optical (EO) modulator.

The desired frequency shift of the LO is a controlled +0.9 GHz to -0.9 GHz for the 45 deg cone half angle. The resulting beat signal of the optical signal on the detector would be below ±0.3 GHz. This bandwidth reduction would allow us to maximize detector performance and receiver efficiency. However, it has not been demonstrated as a compact, space qualifiable device, and is thus eliminated from our baseline design.

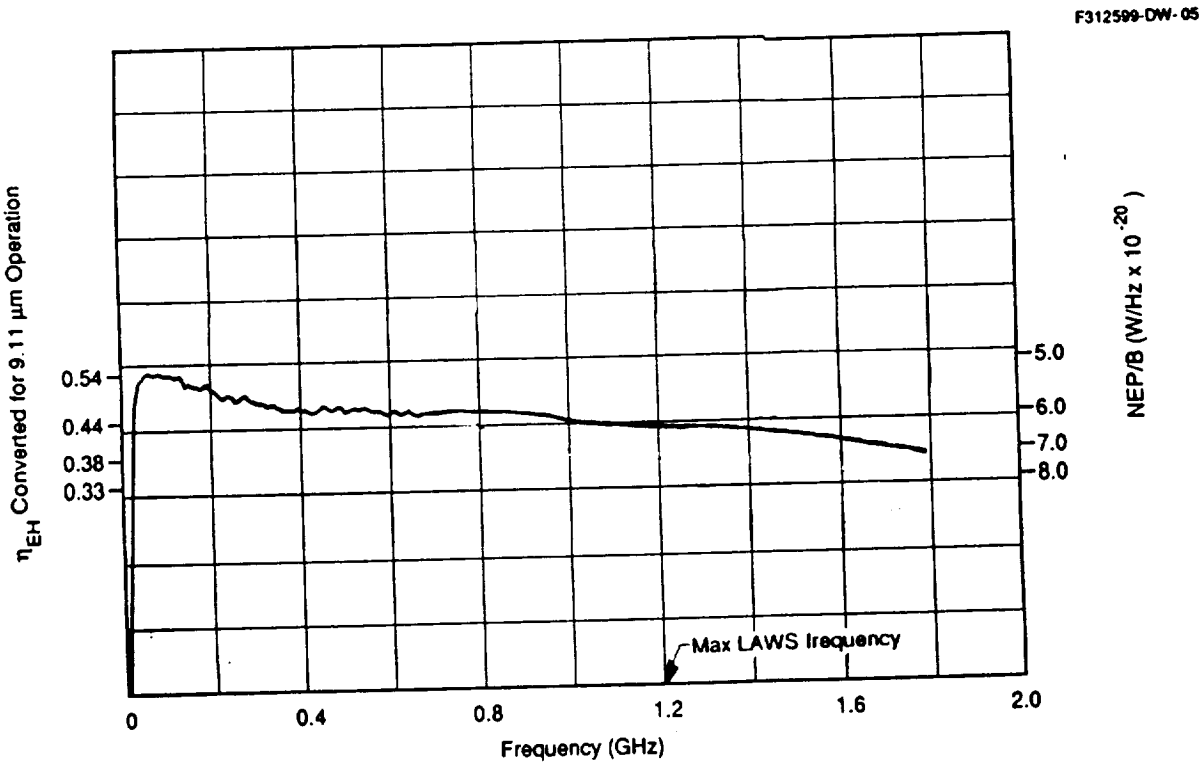

Figure 3-42. Test Data

Thus the LAWS detector baseline configuration requires a high bandwidth detector with a non-shifted LO.

A two dimensional detector array of elements is selected over a single element to simplify system alignment. Matched optics are used to optimize LO distribution upon the detector elements. Typical detector arrays have some losses due to physical (line width) separation between the elements; optimal performance is achieved when the signal is directed to the single signal element. The elements will be physically arranged to allow optical alignment of all received signals upon the central element. Ground returns will be used to aid in this alignment process. Defocusing of the receiver will allow acquisition of the ground returns from non-optimally aligned optics.

3.3.3.2 Detector Cooling

Photo detectors operating in the 9 to 12 μm range have optimum performance when cooled to approximately 77 K. For long-term satellite operation, two types of cooling are potentially available to achieve operation at these temperatures: passive or active.

Passive cooling is practical on satellites for low energy heat loads where free-space look angles are available to the detector cold finger. The cold finger must be kept short in length to minimize heat leaks into the detector which would raise the detector's temperature. The passive cooler is ruled out for LAWS baseline because of the geometries involved, the low polar orbit, and the overall cooling requirements.

The active thermal cooler proposed for many of the other EOS Facility payloads is adequate and is selected for the LAWS baseline. Lifetime of the cooler is a consideration and is being tested/enhanced for these other programs. Vibration is a consideration which is important with the LAWS Instrument. Lockheed/Lucas are developing a very low vibration cryocooler assembly. Care must be taken in designing the mechanical fixtures and providing vibration isolation where required. Views of the cooler arrangement are shown in *Figures 3-43* and *3-44*. A cooler power schematic is shown in LAWS DR-8, *Preliminary Design Document* (LMSC-HSV TR F312594).

3.3.3.3 Bias and Preamplifiers

Bias and preamplifiers for the LAWS receiver are very similar to those used for conventional coherent lidar systems, but the LAWS device must be space-qualified and operates over a very wide dynamic range, with β varying from 10^{-11} to 10^{-6} m^{-1} sr^{-1} (plus speckle) and ground returns varying up to 10^{-2} (plus speckle).

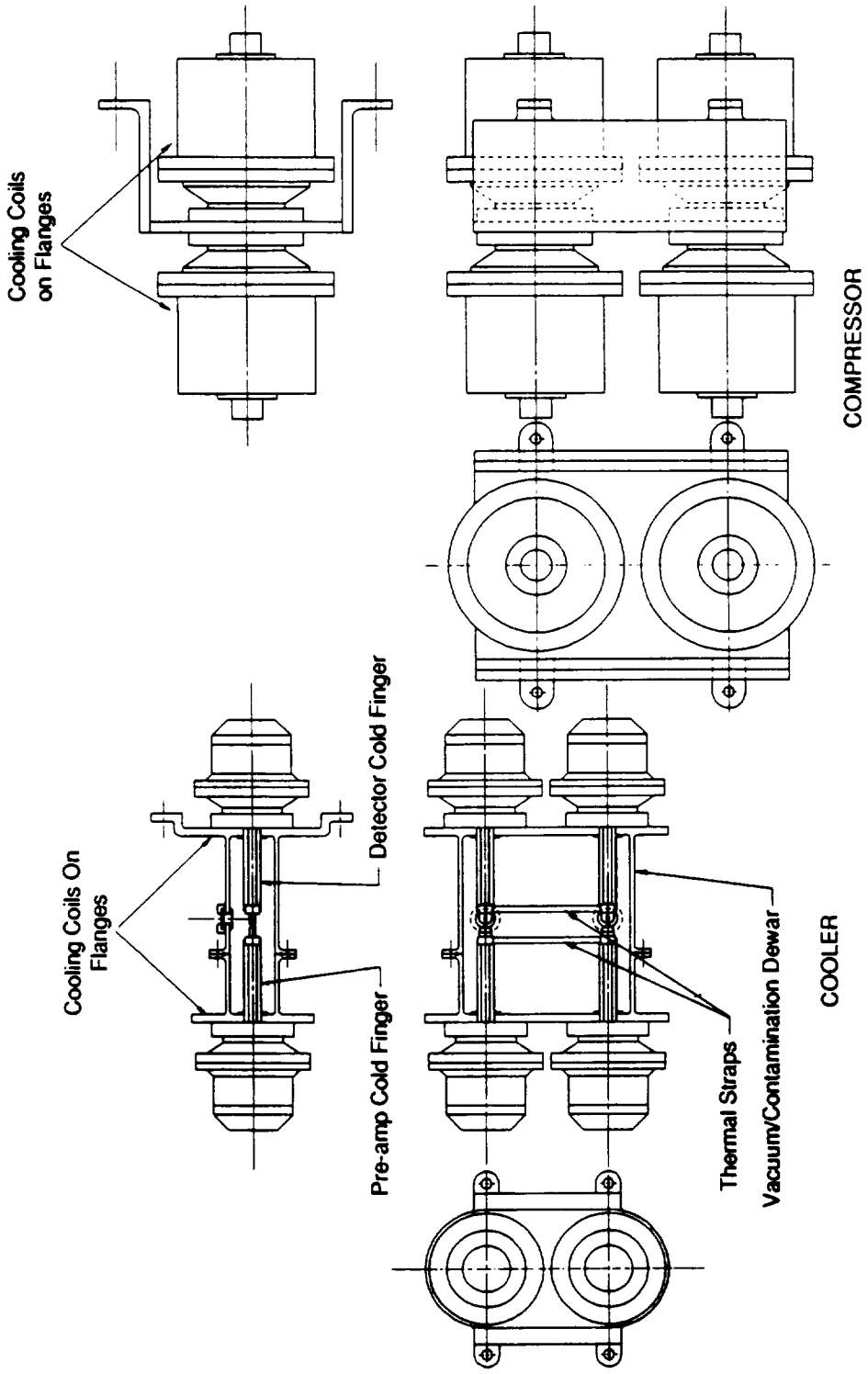

Figure 3-43. Cryocooler Concept

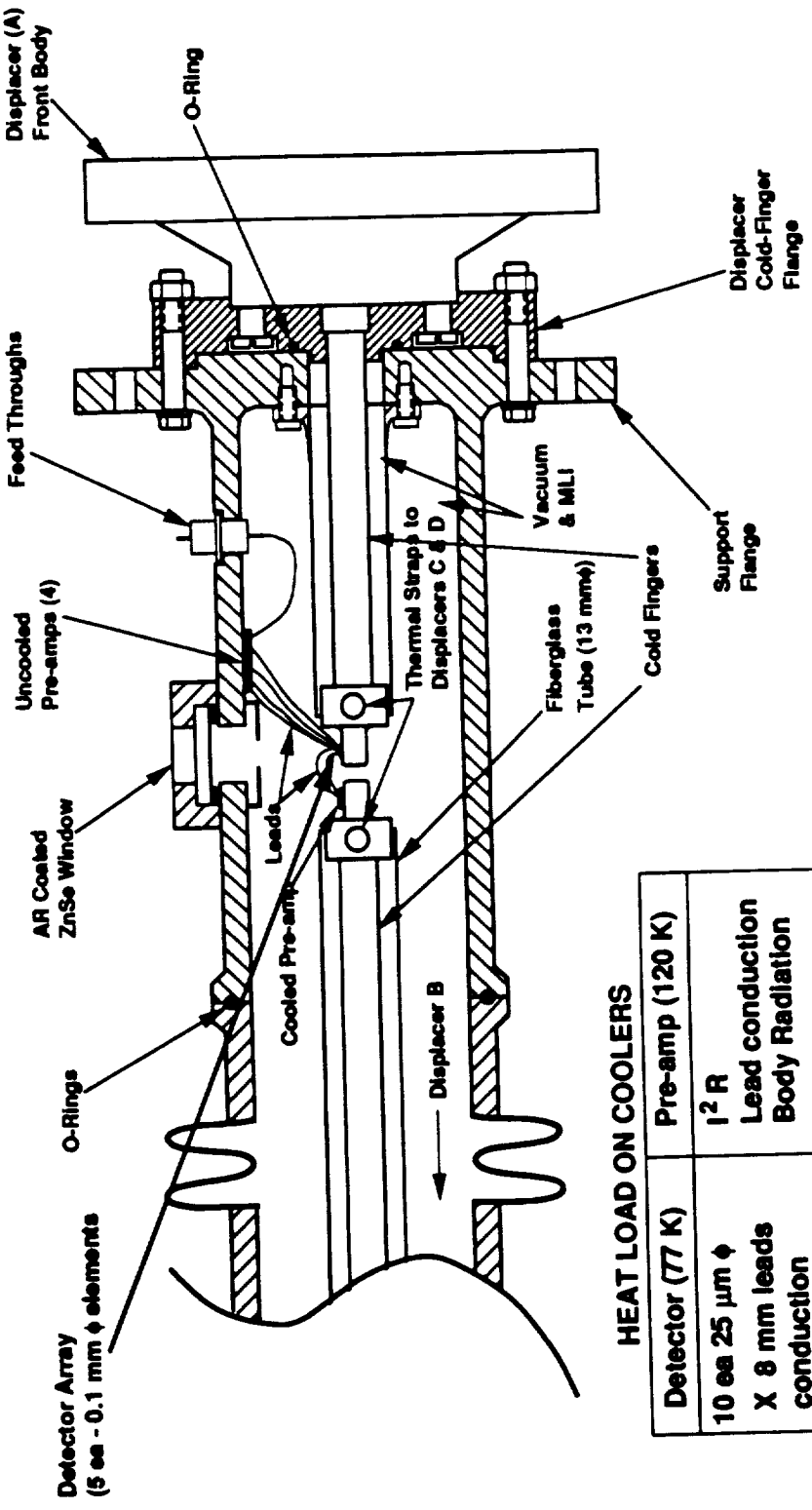

HEAT LOAD ON COOLERS		
Detector (77 K)	Pre-amp (120 K)	
10 ea 25 μm ϕ X 8 mm leads conduction • Window Radiation • Body Radiation • 0.005 W LO • I^2R	I^2R Lead conduction Body Radiation	
Estimate 0.05 W		Estimate 0.5 W

Figure 3-44. Vacuum Dewar with Cold Fingers, Detectors, and Pre-Amps

To provide this wide dynamic range and incorporate very low noise preamplifiers, an electronic switch (cooled with a 0.1 dB noise factor) is used in the signal channel to (1) switch between preamplifier frequency ranges and (2) switch in a shunt when the preamplifiers become saturated. The preamplifiers -- cooled only where required -- are switched between frequency spans as a function of scanner azimuth angle. If saturation occurs over 50 ns, the shunt is switched in (gallium arsenide preamplifiers recover in this time) and Earth returns are measured with unsaturated amplifiers. Shorter saturations due to speckle do not activate the switch. Actions of the switch are monitored and entered into the data stream for subsequent amplitude data processing.

Less concern about preamplifier noise is applied to the outlying alignment detectors. Wide dynamic range is also a requirement. Thus the signal is split prior to the first preamplifier, with the low level signals receiving 30 dB more gain than the higher level signals. A less than 3 dB loss is incurred in this split. A single preamplifier is used to span the entire frequency range, with less stringent control of preamplifier noise than for the signal channel. Knowledge of scanner azimuth angle and satellite velocity are again used to reduce the A/D conversion frequency requirement to a modest 3 MHz bandwidth. A/D output is fed to the computer, where sum and difference alignment computations are made.

3.3.3.4 Signal Processor

The signal processor receives the preamplified signal from the preamplifiers, provides gain to the signal appropriately for input into the A/D converter, and performs any required additional on-board signal processing. A signal amplitude detector (i.e., a track and hold and narrow band A/D) is required for each detector element for alignment purposes under conditions of strong returns. For baseline configuration, a frequency synthesizer is used to convert the 0 to 1.2 GHz signal into a 0 to 30 MHz signal analog bandwidth. The 0 to 30 MHz allows measurement of line-of-sight wind velocities from -150 to +150 kn or over any selected 300 kn span (e.g., from -50 to +250 kn).

Discussions by the Science Team have revealed a potential requirement for real time wind velocity (frequency spectra) data to be downlinked directly from the LAWS Platform. To meet this requirement, an optional on-board FFT processor is offered. To provide $\pm$100 kn winds with 1 m/s resolution (0.2 MHz), a 512 point FFT processor is selected for 256 point frequency resolution. This will be a miniaturized version of the unit we have operating in the laboratory today.

3.3.3.5 Summary

Figure 3-45 provides an overview of the receiver/processor subsystem development, including schedule, component quantities, requirement, implementation and verification, planned trade studies, and risks.

A RECEIVER / PROCESSOR PLAN OVERVIEW

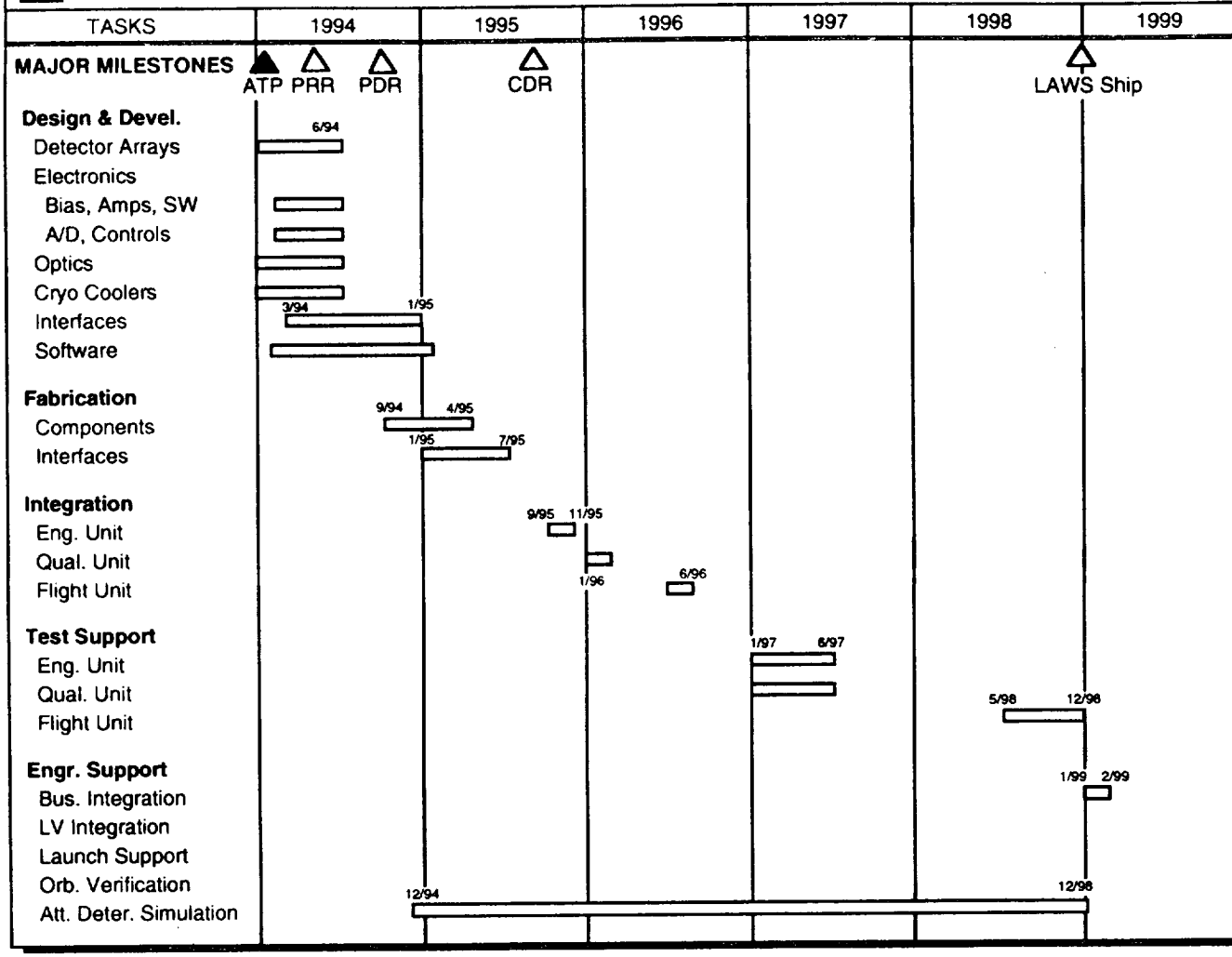

B REQUIRED SUBSYSTEM EQUIPMENT

COMPONENT*	SOURCE	QUANTITY/UNIT	ENG. UNIT	QUAL. UN
Detector Array	RP 1	2	2	2
Support Optics	RP 2	1 set	1 set	1 set
Support Electronics				
Bias ckt, Amps	RP3	1 set	1 set	1 set
A/D Conv., Controls	RP4	2 sets	2 sets	2 sets
Cryo Cooler Assembly	LMSC	4	4	4
Cables	LMSC	2 sets	2	2

** "S" parts*
*** Engineering unit components used for spares*

FOLDOUT FRAME

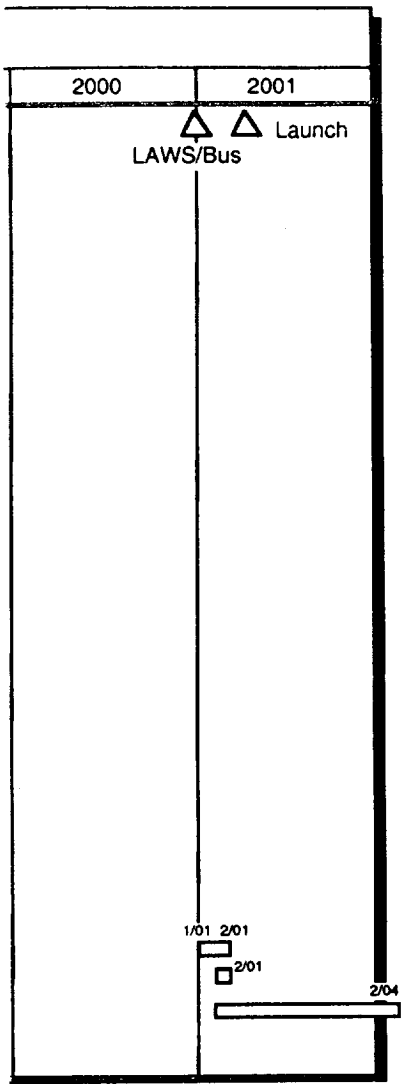

C REQUIREMENT IMPLEMENTATION/VERIFICATION

KEY REQUIREMENT	IMPLEMENTATION	VERIFICATION
Operational Life	• 5 yr on orbit • No single point fail	Comparison and test Analysis and test
Performance	• A/C quantum effect • Closed loop tracking • Acceptable aging • Temperature control • Data handling/control	Measurement Analysis, measurement and simulation Measurement, analysis, comparison Measurement and analysis Simulation
Interfaces and Software Functions	• Ground return alignment • Automated gain control • Data digitization & storage • System performance monitor	Simulation and test

D PLANNED TRADE STUDIES

TRADE ITEM	BASELINE DESIGN
Cooled vs. uncooled Amps	Cooled where noise figure is improved
Number of pre-amps for signal detector	Baseline is four switched pre-amps
Redundant vs. nonredundant	Redundant detectors and coolers
Adjustable focus vs. fixed miniscus lens	Adjustable focus
Dual tip-tilt vs. single for L.O. adjustment	Dual
Number of array elements	Four alignment plus central

E RISK SUMMARY

RISK ITEM	RISK LEVEL	RISK REDUCTION APPROACH
Detector Failure	Moderate	1. Produce several batches of detectors and perform accelerated aging tests. 2. Design with redundant detectors.
Loss of S/N from misalignment	Moderate/Low	1. Design for graceful S/N loss from misalignment. 2. Design for low BW on orbit alignment correction.
Cooler failure	Low	1. Lockheed developing/qualifying under EOS-A contracts.

F PERFORMANCE ENHANCEMENT TOOLS

ITEM	POTENTIAL ENHANCEMENT
Detector A/C quantum efficiency	Perform 18 to 30 month development/test effort; anticipate 30 to 60 % performance improvement.

	FLIGHT UNIT**
	2
	1 set
	1 set
	2 sets
	4
	2

F320789-01

Figure 3-45. Overview/Summary of the LAWS Receiver/Processor Subsystem

FOLDOUT FRAME 2

3.3.4 Structures and Mechanical Subsystem

This section describes key analyses, trades, and verification plans for the LAWS structures and mechanical subsystem (SMS). (The thermal control system, which is part of the structures and mechanical subsystem, is discussed in paragraph 3.3.6.) The major structural elements of the SMS are the base platform, the telescope mounting pedestal, the optical bench, and the telescope structure. The SMS mechanism is the telescope motor/bearings with V-band caging device for off-loading the bearings during ascent.

The base structure design is structural edge beams with internal cross beams covered by top and bottom face sheets. All components are constructed from graphite epoxy for light weight, high strength, and low thermal coefficient of expansion. Three kinematic mounts provide the structural interface between the LAWS Instrument and the spacecraft. All components are sized for the launch loads with the prescribed safety factors.

The base structure is the mounting platform for the laser, telescope, and majority of other subsystem components. The subsystem components are mounted around the perimeter on the edge beams. The location is based on thermal requirements to take maximum advantage of passive heating or cooling.

The optical bench is attached to the base structure by three kinematic mounts. The optical bench is a honeycomb structure with face sheets, and is made of graphite epoxy material for minimum distortions and light weight. The seed laser, local oscillator, detectors, and all relay optical system elements are mounted on the bench.

3.3.4.1 Requirements and Design Margins

The SMS baseline design was developed by combining directly specified requirements and derived requirements from the spacecraft, telescope, and optics system levels to their respective structure and mechanical subsystems. A summary of key SMS requirements and respective verification methods is given in *Figure 3-46 (B)*.

3.3.4.2 Analyses and Trade Studies

NASTRAN structural math models were developed to perform deformation, stress, and modal analyses. Preliminary sizing of the structural components was based on these analyses for stiffness and launch loads. Modes, frequencies, and structural response to the launch loads and to the laser pulses were determined and the structure sized for these load environments.

A STRUCTURES & MECHANICAL DDT&E PLAN OVERVIEW

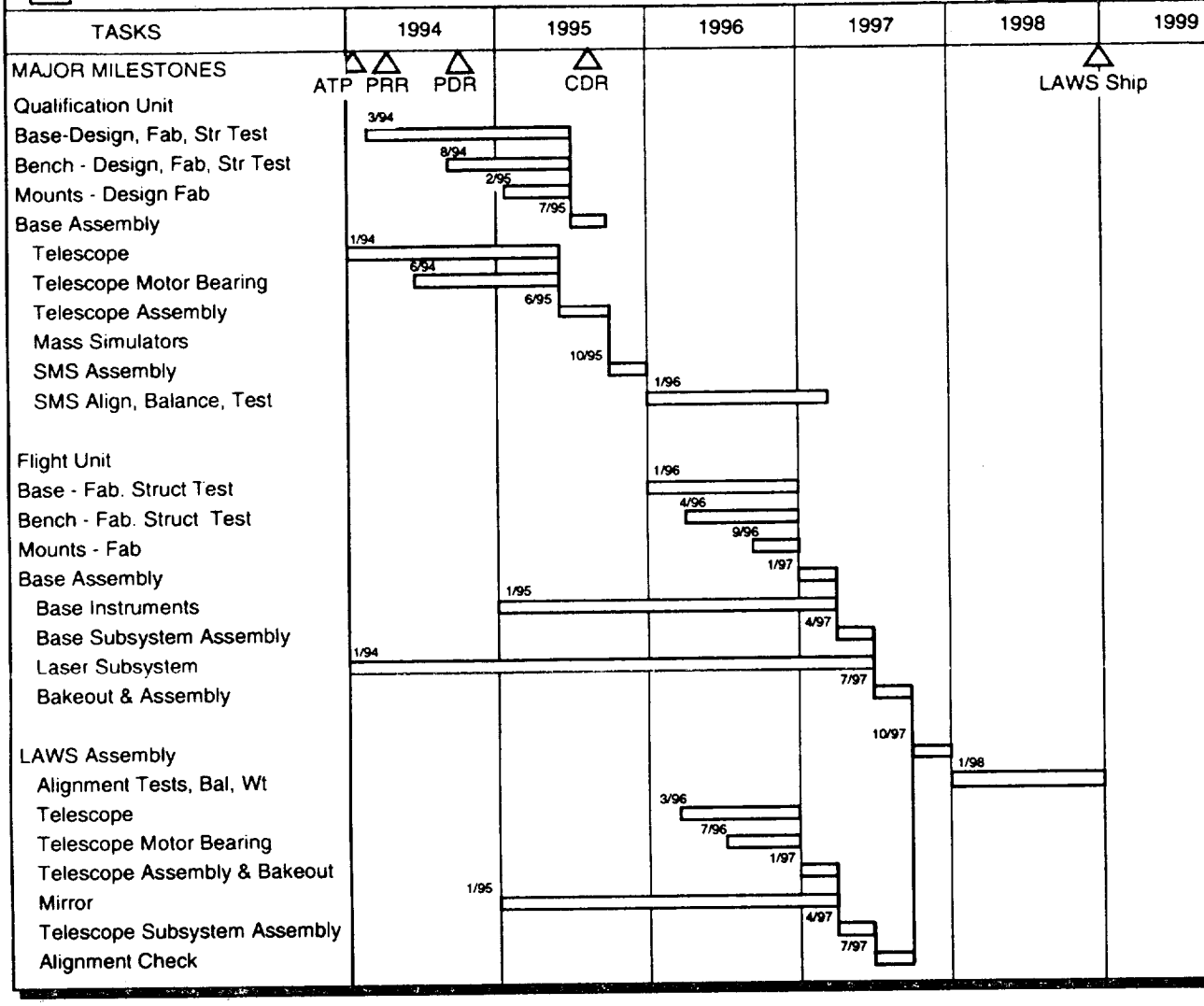

B SMS REQUIREMENTS/VERIFICATION

KEY REQUIREMENT	IMPLEMENTATION
Launch Vehicle Interface • Shroud Envelope • Interface Loads	Designed to meet envelope for max ascent loads
Contamination	Contamination shield material selection
Strength/Dynamic Characteristics	Designed for positive margins with adequate factors of safety & inert structural frequency/stiffness requirement
Operational Life	Motor bearing design
Redundancy Management	Redundant motor bearings
Allignment/Stability • Telescope Rotation • Laser Pulse • Thermal Deflections • On Orbit Dynamics • IG/OG Distortion	 Telescope dynamically balanced Structure stiffness/shock mounts Thermal covers/control Structural stiffness design Structural stiffness design

ATTITUDE D

FOLDOUT FRAME

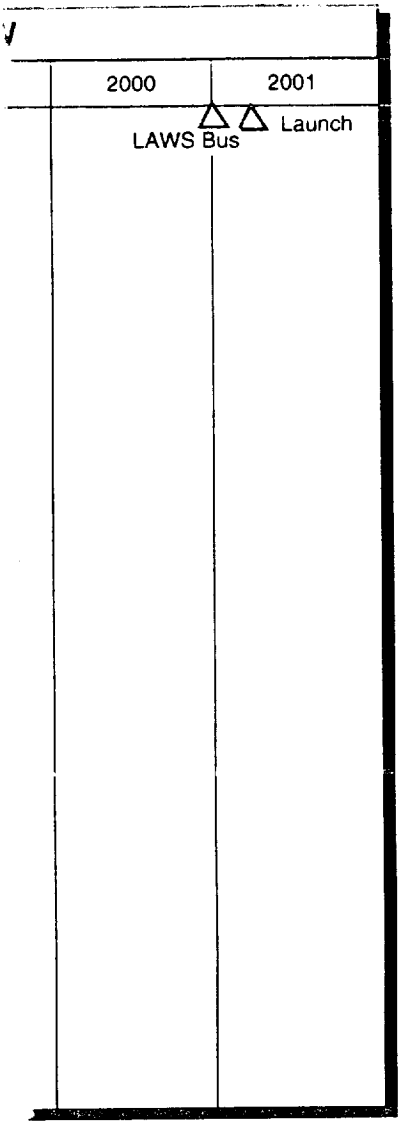

C DESIGN ANALYSES & TRADE STUDIES

ITEM	ANALYSES
Optical Bench*	To determine weight/stiffness/strength optimum for Honeycomb or multiple truss core
Base Structure*	To determine weight/stiffness/strength optimum for GE member size and layup
Telescope Pedestal	To determineweight/stiffness/strength optimum for material trade and design
Laser Mounts*	To determine laser pulse effects on telescope pointing
SMS*	To determine sensitivity of telescope imbalance on telescope attitude & optics alignment
SMS	To determine the effect of gravitational field alignment at on orbit conditions
SMS	To determine changing structural design effects on dynamic modes & natural frequencies (thereby, attitude control)
SMS	To determine space platform effects on attitude control
SMS	To determine thermal distortion effects on attitude control and optics alignment

*Ongoing analyses begun in Phase B.

D PLANNED TRADE STUDIES

TRADE ITEM	BASELINE DESIGN
Telescope Support Pedestal	Titanium vs. Graphite Epoxy
Optical Bench Core	Honeycomb vs. Multiple Truss
Base Thickness	Thick, Thin, Medium (completed)

	VERIFICATION
	Test & Analysis
	Test & Analysis
	Test & Analysis
	Test & Analysis
	Test
	Test
	Test & Analysis
	Test & Analysis
	Test & Analysis
	Test & Analysis

TERMINATION SUBSYSTEM

E SMS VERIFICATION SUMMARY

	Functional	Static	Modal	Random Vib.	Thermal Vac	Acoustic UCB	Pyroshock
SMA Qualification Structure w/Mechanism	X	X	Q	Q	Q	Q	Q
SMS Flight Structure	X	X	A	A	A	A	A

X = Same Levels Qual/Flight
Q = Qualification Test Levels*
A = Acceptance Test Levels*
* = Levels Per Mil-Std-1540B

312594-MT-FO

Figure 3-46. Overview/Summary of the Structures and Mechanical Subsystem (1 of 2)

FOLDOUT FRAME

F DYNAMIC TEST PLAN/FEATURES

- Free-Free Modal Test
- Measure dynamic stiffness of spacecraft interface via impedance test
- Combine results of these two tests to produce fixed base mode shapes and natural frequenc
  - Test article suspended by air bearings
  - All suspension system modes below 2 Hz
  - Pure random excitation
  - -50 + acceleration measurements
  - Modal curve fitting techniques extract mode shapes, natural frequencies, and modal

G RISK SUMMARY

RISK ITEM	RISK LEVEL	RISK REDUCTION APPROACH
Structural Assembly Failures	Low	– Large strength margins
		– Early identification and control of fracture critical items
Motor/Bearing Failure	Low	– Redundant motor wiring
		– Similarity with other flight proven units
SMS Attitude Control Failure	Low/Med	– Dynamic analyses with respect to space platform pertur
		– High rev dynamic balance of telescope
		– Deflection analyses supported by tests
Optics Alignment Failure	Low/Med	– Thermal deflection analyses and testing
		– Dynamic analyses with respect to space platform pertur

H REQUIRED SUBSYSTEM EQUIPMENT

COMPONENT	SOURCE	HERITAGE	FLT	QUAL	MO
Base	LMSC	New	1	1	
Bench	LMSC	New	1	1	
Telescope Mount	Vendor	New	1	1	
Motor Bearing	Vendor	Modified Flight Proven	1	1	
Telescope	Vendor	New	1	1	
Mirror	Vendor	New	1	0	
Test Hardware:					
Mass Simulators	LMSC	New		1 ea	
Test Fixture	LMSC	New		1	

FOLDOUT FRAME

I PLANNED SMS ANALYSES

ANALYSIS TYPE	ALL SMS EQUIPMENT	ALL SMS STRUCTURES	SMS MECHANISMS
Strength	X		
Dynamics		X	
Thermal	X		
Mass Properties	X		
Producibility	X		
Life Cycle Cost	X		
FMEA	X		
Reliability	X		
Venting	X		
Stress Controls			X
Performance			X
Math Model Verification		X	

312594-MT-FO-2 of 2

J PHASE B STRESS/DYNAMICS MODEL

Equipment packages are reproduced as point masses (not plotted).

454 Grids
1034 Elements

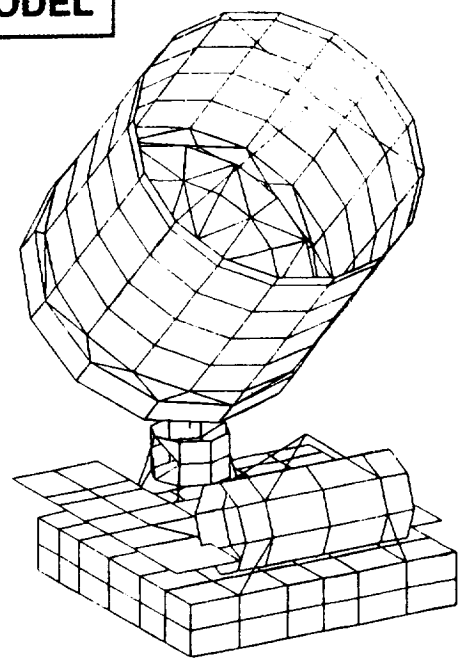

Figure 3-46. Overview/Summary of the Structures and Mechanical Subsystem (2 of 2)

FOLDOUT FRAME 2

The thick/thin base trade study is complete and results included in the 0.34 m thick baseline design. This study is presented in detail in Lockheed Engineering Memorandum LMSC-HSV EM F312479, 22 April 91.

Key planned design analyses and trade studies for Phase C/D are given in *Figure 3-46 (C)*. These studies will complete the studies initiated in Phase II for SMS optimization. The analyses in Phase II are discussed in paragraph 3.3.4.8. A trade study summary is given in *Figure 3-46 (D)*.

3.3.4.3 Flow Network/Schedule

The schedule for major SMS DDT&E activities, shown in *Figure 3-46 (A)*, includes efforts directed at risk reduction and a natural flow and integration of hardware consistent with specified program milestones.

3.3.4.4 Verification Process

A summary of the verification approach for major SMS components is given in *Figure 3-46 (E)*. Qualification and acceptance test levels are in accordance with MIL-STD-1540B. A pyroshock test is required for the telescope motor bearing decaging device. A functional test is required for all subsystems after each environmental test for both qualification and flight units. Static tests on base and bench are performed to verify calculated structural stiffness (the math models) and to verify manufacturing/design integrity. Corrections required due to these tests (performed soon after fabrication) will have minimal schedule impact and ensure compliance with critical performance requirements.

The dynamic test plan and features are given in *Figure 3-46 (F)*. These tests will further verify the math model, provide a basis for the coupled load analysis, and qualify/accept the respective units per MIL-STD-1540B.

3.3.4.5 Risk Reduction

All elements of the SMS will be analyzed for high risk identification. Each major assembly of the SMS has appropriate risk reduction actions defined. *Figure 3-46 (G)* summarizes SMS risk reduction. The motor bearing mechanism considered will be similar to a flight proven model. The base and bench structures will be both statically and dynamically tested and modeled.

3.3.4.6 Equipment Summary

SMS hardware to be produced during Phase C/D is categorized in *Figure 3-46 (H)*.

3.3.4.7 Planned SMS Analyses

Key planned SMS analyses are summarized in *Figure 3-46 (I)*. Strength, dynamics, thermal deflection, and stability analyses will be made with a continuously updated math model. This model will incorporate design changes and will be verified by qualification static, dynamic, and weight measurements. The Phase II math model is shown in *Figure 3-46 (J)*.

3.3.4.8 Phase II SMS Analysis Summary

Five SMS analyses were initiated in Phase II and will be ongoing as the LAWS design matures and more accurate data are incorporated. These analyses will be discussed in the following paragraphs.

The LAWS SMS platform thickness trade study has been completed and is documented in LMSC-HSV EM F312479.

The current modes and frequencies summary for free and constrained conditions is presented in *Table 3-9*. Typical mode shapes are given in *Figure 3-47*. These data are a result of the latest mass and motor bearing stiffness data. Current caged and uncaged effective stiffness are almost equal, which means that constrained on orbit and constrained lift-off modes are very similar.

Interface reaction loads and key deflections under launch and staging conditions are given in *Tables 3-10* and *3-11*. These data result from worst case static plus dynamic design load factors obtained from the Titan IV User's Handbook. Maximum lateral loading occurs at liftoff, while maximum axial loading occurs at stage 1 burnout. The telescope deflections reflect the latest motorbearing caged stiffness.

Table 3-9. LAWS Natural Frequencies and Mode Shapes Telescope Motor Bearing Supported (Caged)

MODE DESCRIPTION	FREE-FREE		CONSTRAINED	
(PRIMARY MOTION)	MODE	FREQUENCY (Hz)	MODE	FREQUENCY (Hz)
Rigid body modes	1-6	Approximately 0.0	NA	NA
Telescope pitch (X rotation)	8	19.17	1	13.0
Telescope yaw (Z rotation)	7	14.97	2	13.8
Telescope roll (Y rotation)	–	–	3	14.6
Laser Y translation	–	–	4	23.3
Laser roll (Y rotation)	9	24.62	5	24.4
Telescope sun shield breathing	10	30.2	6	34.6
Optical bench warp	11	37.31	7	37.2
Base/bench warp	12	39.27	8	40.2
Telescope sun shield ringing	–	–	9	42.5

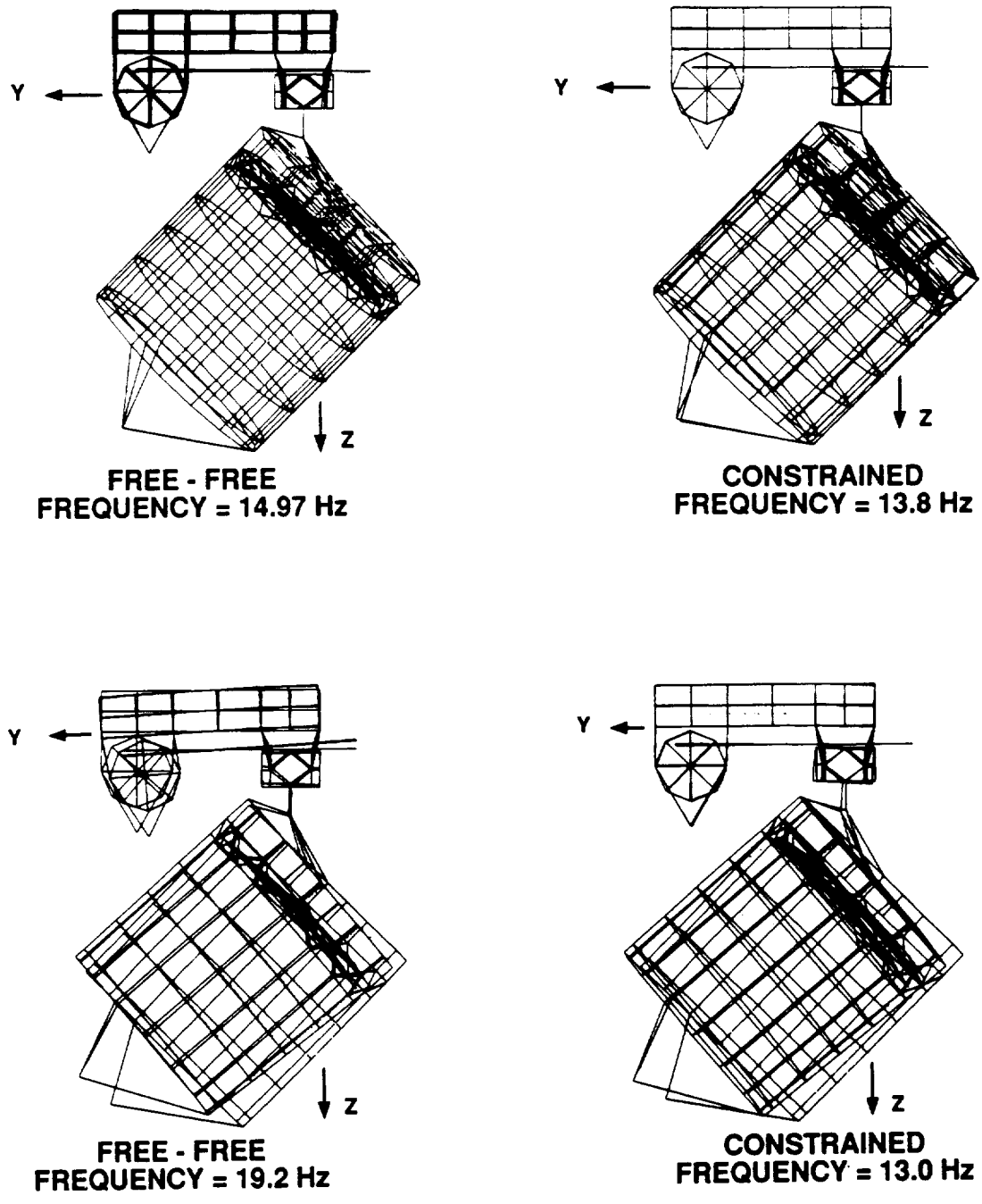

Figure 3-47. Typical Mode Shapes

Table 3-10. Interface Reaction Loads

REACTIONS (Newtons)						
LOAD*	A		B		C	
	Ry	Rz	Ry	Rz	Rx	Rz
3.5 g Lateral (X)	-1.57E+4	1.12E+4	1.57E+4	-1.12E+4	-2.81E+4	-9.65E-1
3.5 g Lateral (Y)	-1.53E+4	-6.62E+3	-1.30E+4	-6.58E+3	-5.49E-5	1.32E+4
6.5 g Axial (Z)	4.2E+1	-1.95E+4	1.60E+2	-1.52E+4	9.20E-5	-1.79E+4

*Loads as shown are "worst case" (static + dynamic) design load factors obtained from the Titan IV User's Handbook. Maximum lateral loading occurs at lift-off while max axial loading occurs at stage 1 burnout.

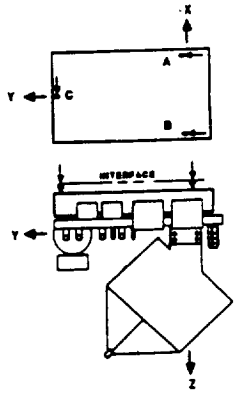

F312584-MT-03

Table 3-11. Static Deflections

LOAD	LOCATION	DISPLACEMENT (M)
3.5 Gx	Secondary Mirror	6.45E-3 (X)
3.5 Gx	Spin Bearing CG	1.33E-3 (X)
3.5 Gx	Laser Power Supply	3.06E-3 (X)
3.5 Gx	Optical Bench (Detector)	1.17E-3 (X)
3.5 Gy	Secondary Mirror	9.74E-3 (Y)
3.5 Gy	Spin Bearing CG	1.01E-3 (Y)
3.5 Gy	Laser Power Supply	5.25E-3 (Y)
3.5 Gy	Optical Bench (Detector)	2.99E-4 (Y)
6.5 Gz	Secondary Mirror	1.03E-3 (Z)
6.5 Gz	Spin Bearing CG	8.48E-4 (Z)
6.5 Gz	Laser Power Supply	1.69E-3 (Z)
6.5 Gz	Optical Bench (Detector)	9.06E-4 (Z)

F312584-MT-04

The laser pulse analysis was performed to ensure that the acoustic shock of laser firing does not propagate through the structure and disturb the operation or performance of the LAWS Instrument. The analysis also ensures that the firing frequency of the laser does not couple with a natural frequency of the structure to produce instability. The following assumptions are made:

- One percent of discharge (2 J) goes to acoustic impulse
- Load profile is sinusoidal over 0.1 ms
- Laser fires every 62.5 ms (16 Hz)
- Transient model was run for 2 s (32 laser firings).

The following conclusions were reached:

- Steady state response is reached within 1 s
- Maximum deflection at detector = ± 0.12 μm
  at telescope = ± 0.08 μm
- Maximum rotation at detector = ± 1 μrad
  at telescope CG = ±0.15 μrad
- No coupling of lower modes with laser firing frequency.

Transient response plots are given in *Figures 3-48* through *3-51*. This analysis will be continued with continued laser mounting definition and enclosure design.

A study was made to determine the sensitivity of static and dynamic telescope balance to its attitude stability. The results are as follows (assuming 188 kg mass rotating at 8.3 rpm as shown in *Figure 3-52*):

- For static imbalance only: 0.116 μrad/m (or 0.116 μrad telescope deflection for one mm CG off axis of rotation); the variation from x direction to y direction is 34 percent
- For dynamic imbalance only: 1.5 μrad/N•m with x/y direction variation of 2 percent.

Note: As modeled, with no provisions for dynamic balancing, the telescope exerted 5.26 N•m moment at 8.3 rpm.

We concluded that, since telescope attitude budget is 50 μrad per resolution, telescope balance is not as critical as anticipated. However, design and testing to minimize imbalance loads will be undertaken.

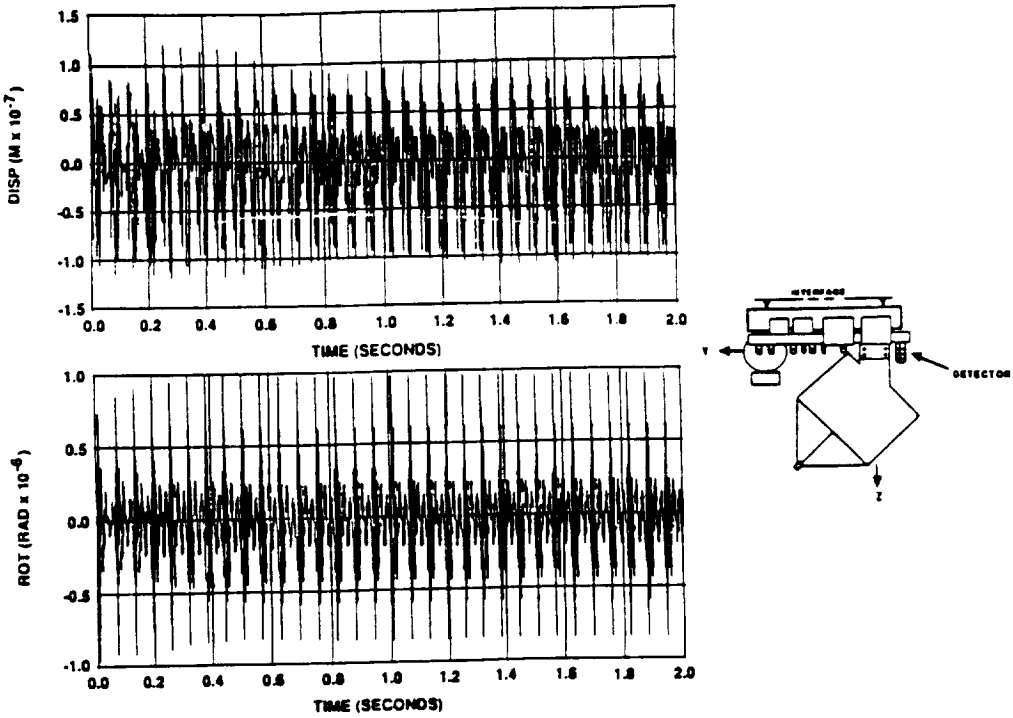

Figure 3-48. Transient Response at Detector Due to Laser Firing Acoustic Shock

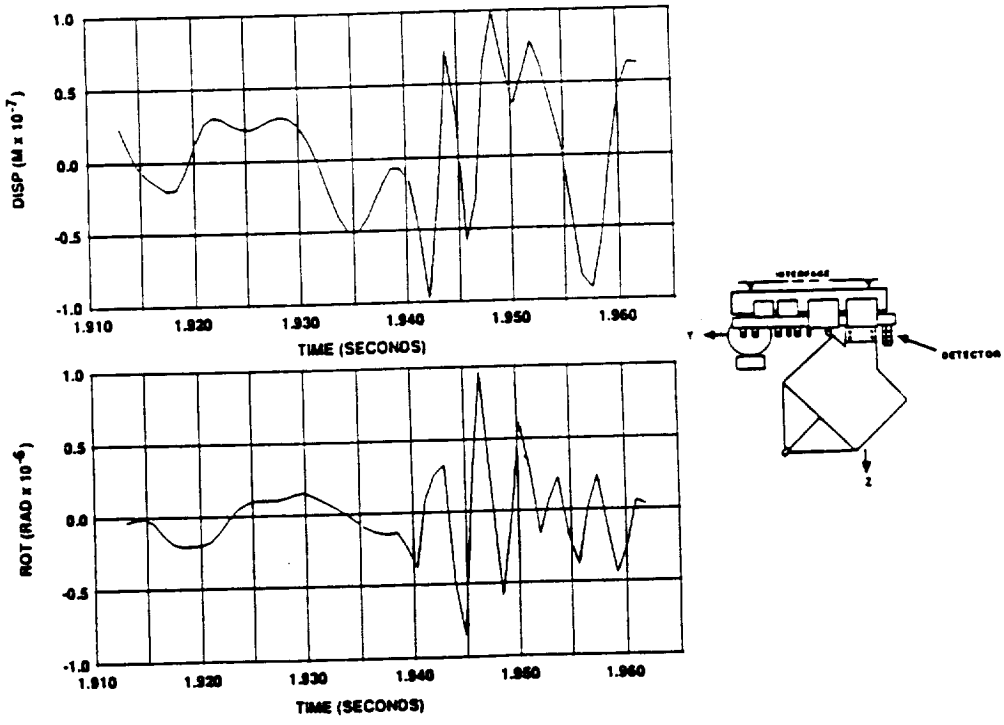

Figure 3-49. Transient Response at Detector Due to Laser Firing Acoustic Shock

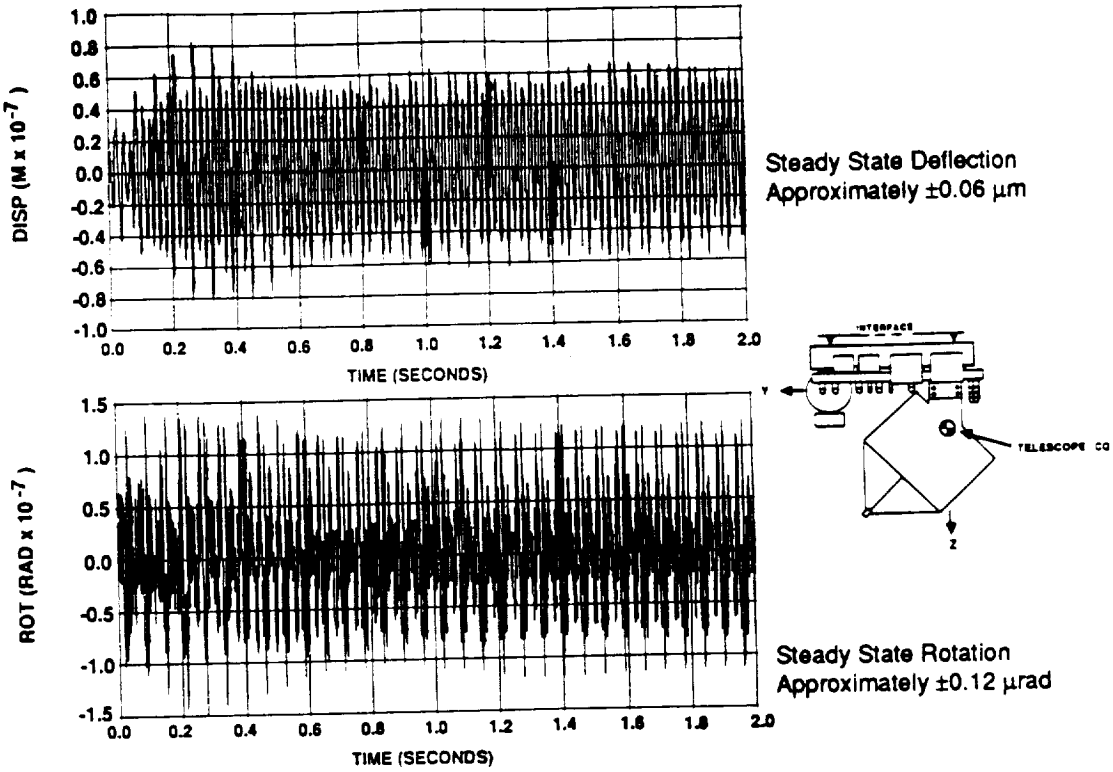

Figure 3-50. Transient Response at Telescope CG Due to Laser Firing Acoustic Shock

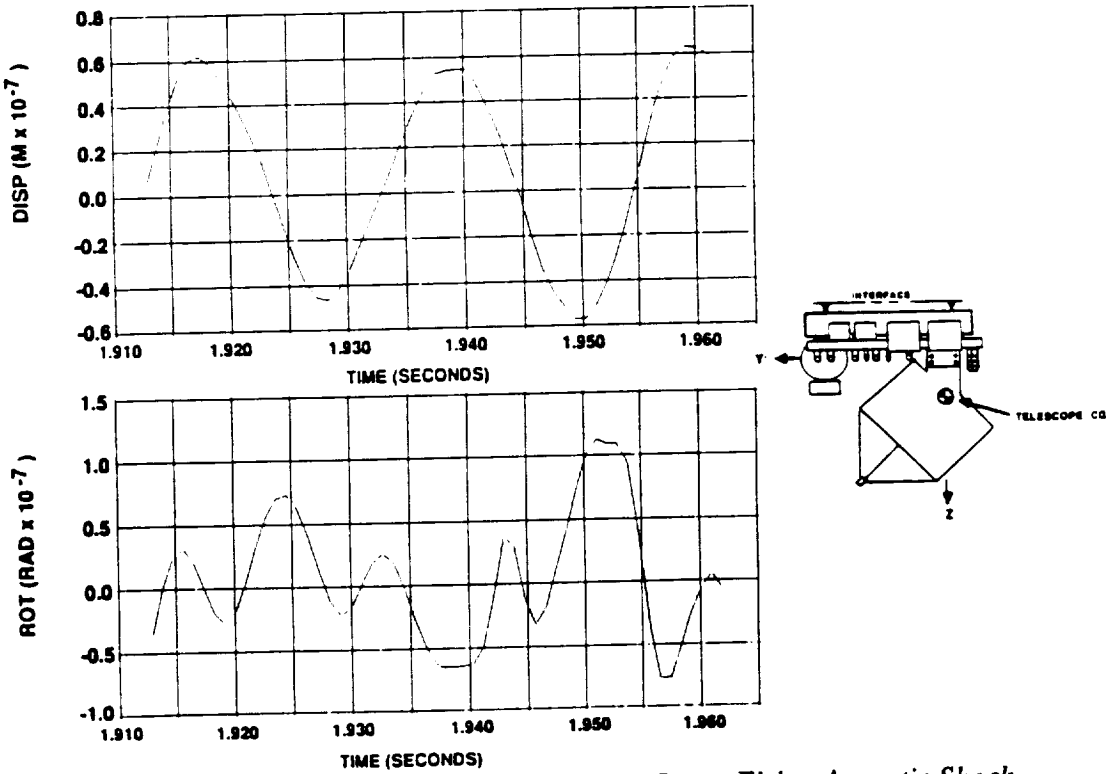

Figure 3-51. Transient Response at Telescope CG Due to Laser Firing Acoustic Shock

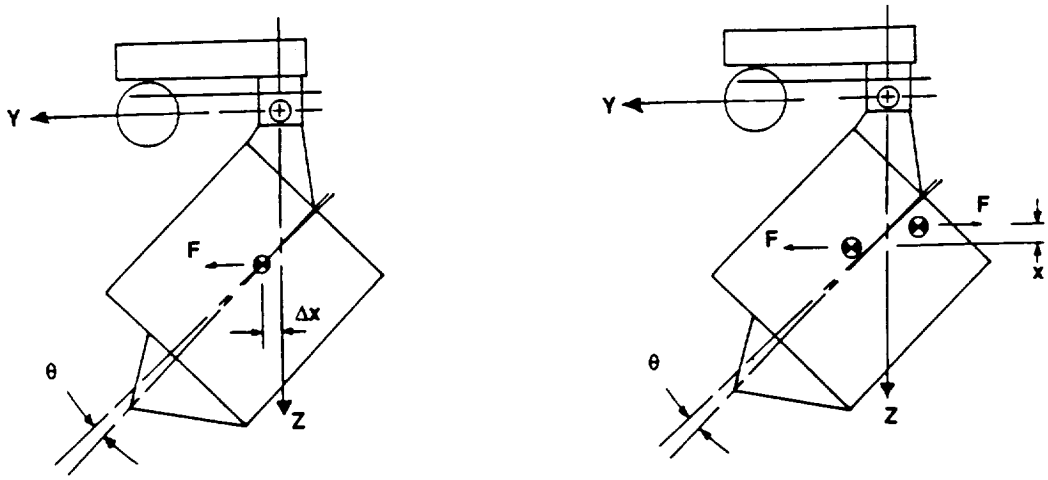

- Due to telescope/base deflection with respect to space platform
- For 188 kg mass rotating at 8.3 rpm

STATIC IMBALANCE

SENSITIVITY:

95.98 μrad/m off axis of rotation
(or .096 μrad/mm CG off axis)
Variation X to Y direction = 34%

DYNAMIC IMBALANCE

SENSITIVITY:

1.5 μrad/N•m of dynamic imbalance
(as modeled telescope has 5.26 N•m dynamic imbalance)
Variation X to Y direction = 2%

Figure 3-52. LAWS Telescope Attitude/Balance Sensitivity

3.3.5 Attitude Determination, Scan Control, and Lag Angle Compensation

3.3.5.1 Introduction

The successful operation of the LAWS Instrument dictates that attitude knowledge, attitude accuracy, and transmit-receive alignment be controlled/maintained within acceptable limits.

Attitude knowledge is maintained by the onboard attitude determination subsystem, which determines the LOS of each outgoing laser pulse. An accurate accounting of this parameter is required in order to permit the resolution of the orbital and Earth rotation velocity components along the LOS of the laser pulse. These velocity components must then be removed from the measured LOS velocity in order to determine the true wind velocity.

The attitude accuracy involves the control of space platform attitude and scanner position such that the desired shot placement results.

The transmit-receive alignment involves control of the receiver LOS such that it is properly oriented in space and with respect to time when the returned energy arrives at the LAWS Instrument. This control requires compensation for scanner motion, space platform motion, and

C-2

misalignment and jitter of the Instrument structure due to disturbance forces and thermal influences. The requirements for each of these parameters are presented in *Table 3-12.*

Table 3-12. Critical LAWS Attitude Pointing and Stabilization Requirements

CATEGORY	DEFINITION	PARAMETER AFFECTED	MAJOR ERROR CONTRIBUTORS	REQ'MT
Transmit-receive angular misalignment (Jitter)	Misalignment between transmit LOS when laser is fired and receiver LOS when backscattered energy returns 5 ms later	S/N	• Platform jitter • Telescope C.G. offset & bearing wobble • Lag compensation errors • Laser disturbance • Static misalignment	3 μrad one sigma
Attitude knowledge error	The error in determining the LOS of the outgoing laser energy	LOS velocity measurement error	• Attitude reference (IRU) unit errors • Structural flexibility • Scanner bearing runout • Static misalignment	100 μrad per axis one sigma
Attitude control	The difference in the actual and desired attitude of the LAWS Instrument	Shot placement	• Platform attitude error • LAWS attitude knowledge error	8 mrad per axis one sigma

F312594-RJ-10

3.3.5.2 Overview of Design and Design Drivers

In order to meet the requirements for attitude/pointing described in *Table 3-12*, provision is made for control of five elements:

- Attitude control accuracy
- Attitude determination
- Lag compensation
- Platform jitter compensation
- Transmit-receive alignment.

Attitude control accuracy is determined by space platform attitude accuracy and LAWS Instrument attitude knowledge. The requirement is 8 mrad per axis. Since the LAWS Instrument attitude knowledge accuracy is 100 μrad per axis and the quoted EOS-B accuracy is 50 arc-s (~250 μrad) per axis, this requirement is met.

The implementation of the four remaining attitude control elements and the primary design drivers is summarized in *Table 3-13.* A schematic representation of the implementation illustrating the primary hardware and computational interfaces is shown in *Figure 3-53.* In this figure, the software element for the transmit-receive alignment is combined with the lag angle compensation element since both functions are mechanized by action of the tilt-tip mirror. Scan control consists of determining a scan rate which will satisfy a combination of shot placement and static lag compensation requirements. The scanner drive control will then maintain the constant scan speed

within the required tolerance. The body-fixed Star Trackers and IMU are mounted on and part of the LAWS Instrument and form the heart of the attitude determination system.

Table 3-13. Features of Attitude Control Preliminary Design

ATTITUDE CONTROL CATEGORY	PRELIMINARY DESIGN METHODOLOGY/FEATURES	PRIMARY DESIGN DRIVER OR JUSTIFICATION
Attitude Determination	Dedicated inertial reference unit and star trackers.	Space platform attitude reference output not accurate enough to satisfy velocity accuracy requirement.
Lag Compensation	• Static – Optics has fixed angular offset between transmit & receive. • Dynamic – Programmed motion of tilt-tip mirror.	Scan and orbital motions can be predicted with sufficient accuracy for this implementation.
Platform Jitter Compensation	Passive techniques are used. Included are mechanical design including use of isolators and dampers.	Active systems require sensing and actuating bandwidths that extend the state of the art.
Transmit-Receive Alignment	Low bandwidth active control using the multi-element detector as sensor and tilt-tip mirror as corrector.	A closed loop system is necessary to maintain the S/N at maximum.

F312584-RJ-01

3.3.5.3 Attitude Determination

The implementation of the attitude determination function is driven directly by the allowable errors in the measured LOS velocity due to errors in the attitude knowledge. The budget for the LOS velocity error due to uncertainty in the LOS of the output pulse is presented in *Figure 3-54* and is approximately 100 μrad per axis, as previously stated. Of this total, 63.7 μrad (corresponding to an LOS velocity measurement error of 0.42 m/s) is budgeted for the Instrument attitude reference. This requirement is met by locating an attitude reference at the LAWS Instrument.

Figure 3-55 shows a functional diagram of the preliminary design for the LAWS attitude determination. Included are an IMU and two Star Tracker units. Software is provided to implement a strapdown attitude reference with the gyro readings and to provide compensation for attitude reference drift. The scanner encoder output is then utilized to determine the estimated output pulse LOS in inertial space. In addition, the position in orbit resolves the LOS in Earth-fixed space permitting the determination in applicable coordinates such as latitude and longitude of the illuminated area. This information is time tagged to correspond to each laser pulse such that the location of the returns may also be catalogued, along with the LOS data.

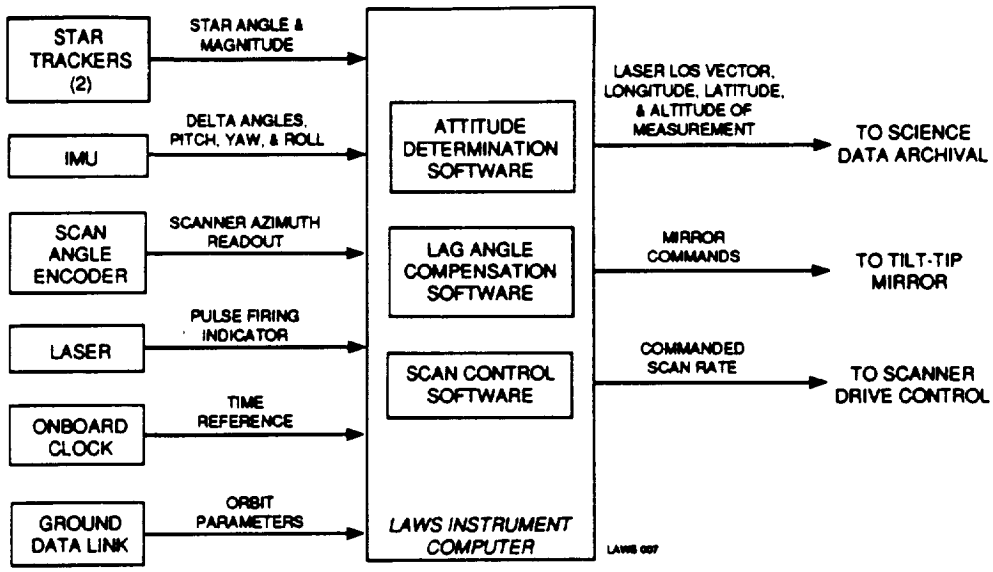

Figure 3-53. Attitude Determination, Scan Control, and Lag Compensation Implementation

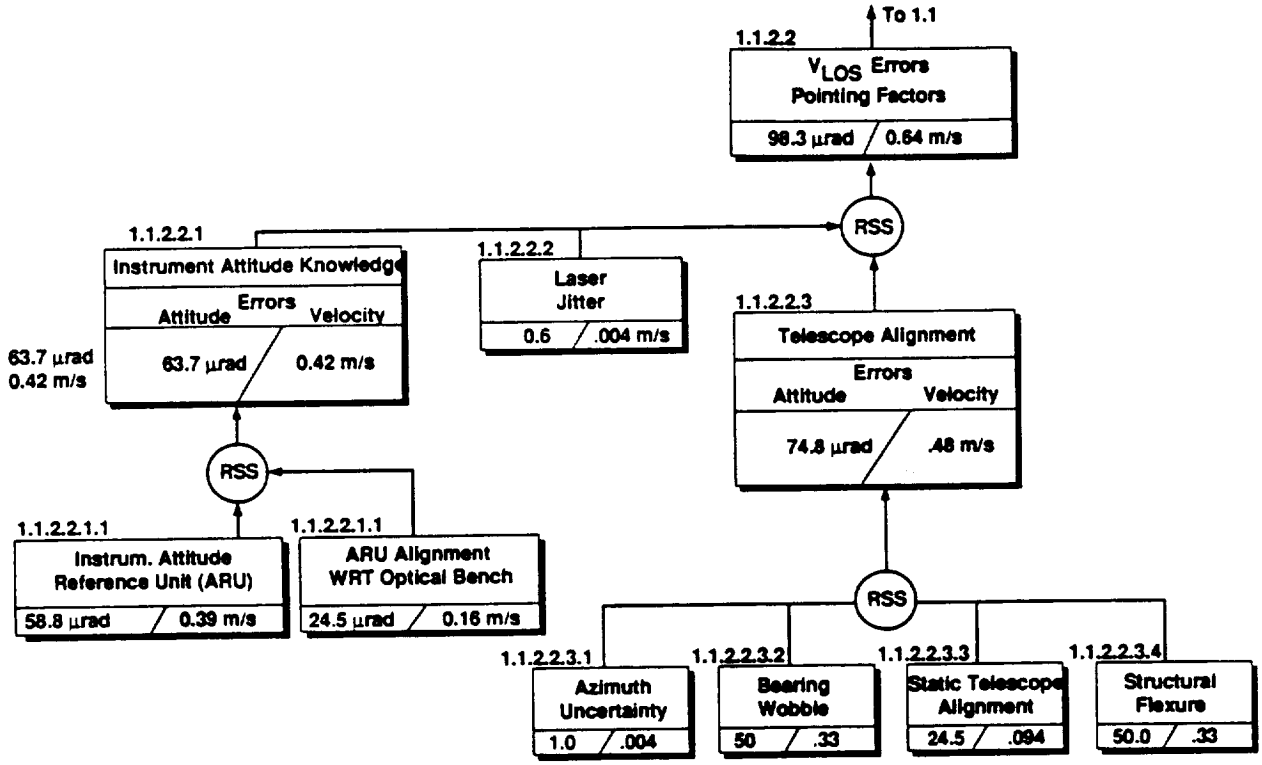

Figure 3-54. V_{LOS} Pointing Factor Errors

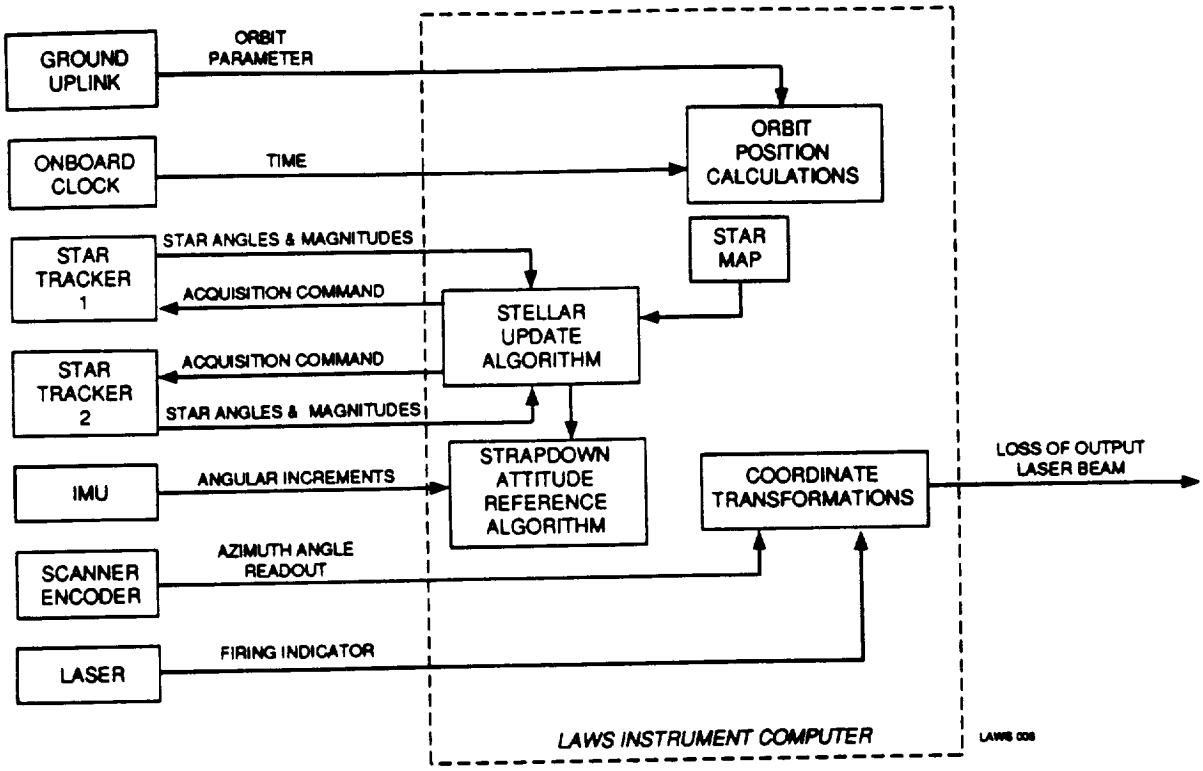

Figure 3-55. Attitude Determination Functional Diagram

A schematic of the IMU and Star Tracker mounting with respect to the Instrument system is shown in *Figure 3-56*. As shown, the Star Trackers view the celestial sphere in a plane normal to nadir and toward the cold side of the sun-synchronous orbit. The area that the Star Trackers will view (for an 8 deg field of view) during an orbit is also shown in *Figure 3-56*.

The event shown is for a typical day approximately three months after launch. Due to orbital precession, the right ascension will cycle through 360 deg in one year. The bounds of the declination angles that the Star Trackers will view remain essentially constant throughout the yearly cycle. An analysis of the star field appearing within the star tracker field of view indicates that at least ten Star Tracker updates per orbit are practical. The proposed Star Tracker units can acquire stars as dim as +6 magnitude.

A trade of permissible IMU drift rate uncertainty vs. scale factor error for 5 and 10 Star Tracker updates per orbit are shown in *Figure 3-57*. For the case of 10 updates orbit and Star Tracker error of 5 arc-s, an IMU with drift rate uncertainty less than 0.01 deg/hr and scale factor error less than 75 PPM is satisfactory. The IMU and Star Tracker design specifications are summarized in *Figure 3-58*.

The specifications for the attitude reference are indicated in *Figure 3-59*. The IMU and Star Tracker will be procured, and interfaces (brackets, cables, etc.) will be built or procured by Lockheed.

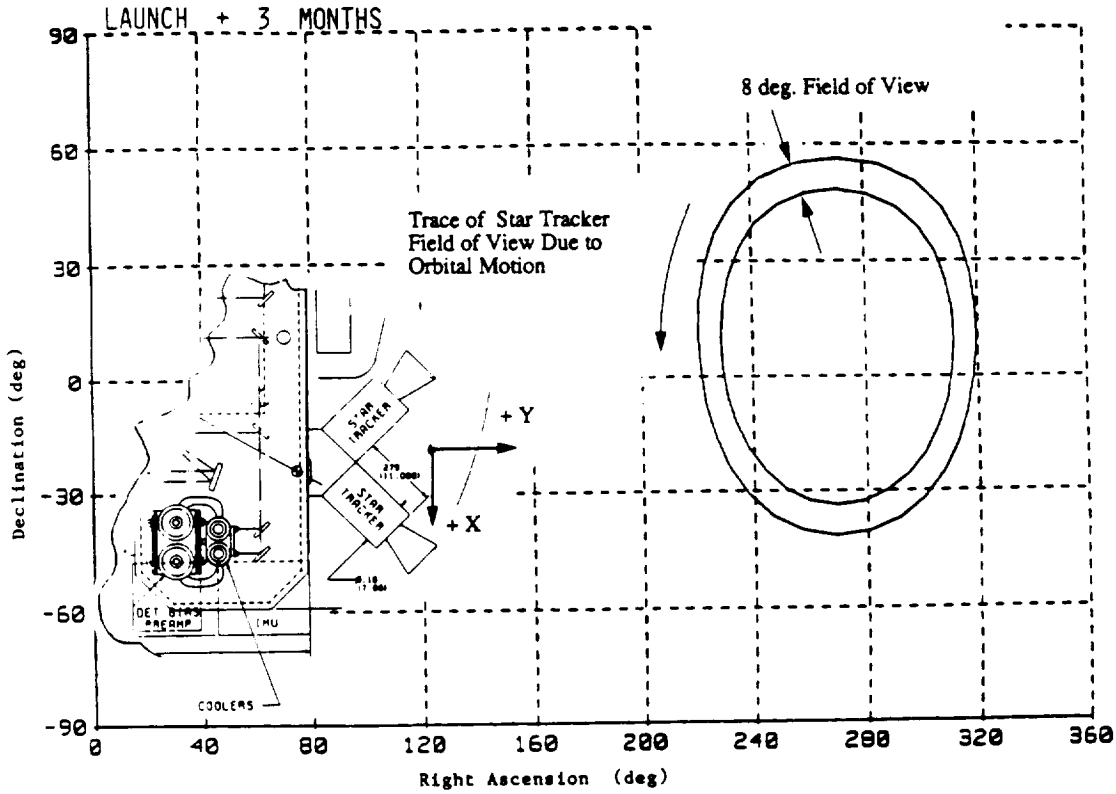

Figure 3-56. Star Tracker View Traced Out Over an Orbital Period

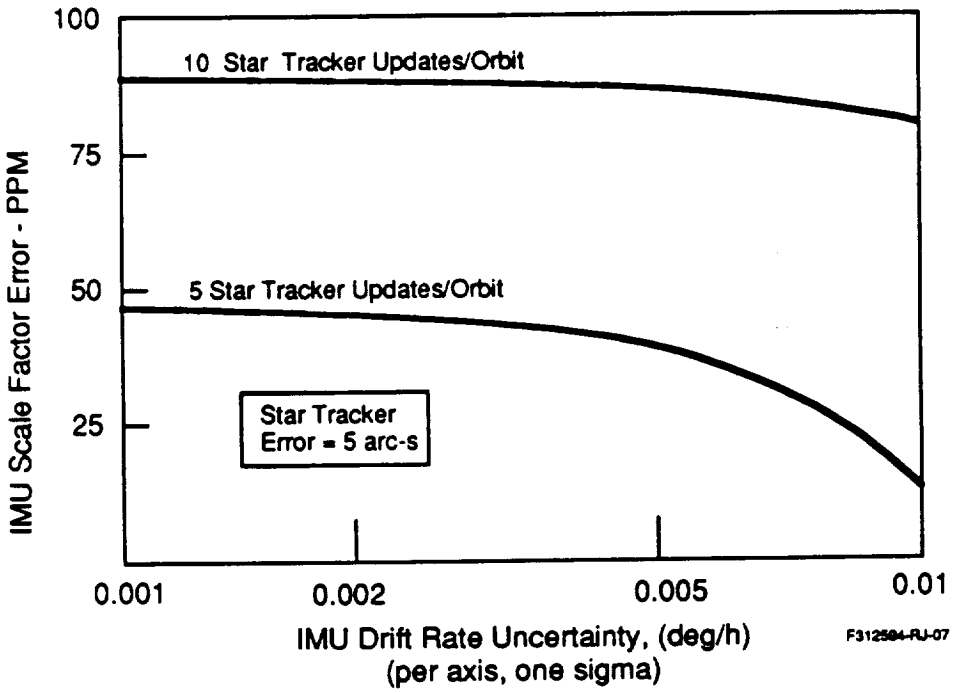

Figure 3-57. Attitude Determination Hardware Performance Tradeoff

IMU	• Drift Rate Uncertainty: < 0.01 deg/h • Scale Factor Error: < 75 PPM
Star Tracker	• FOV ≥ 8° x 8° Error ≤ 5 arc-s Sensitivity = +6 magnitude

F312594-RJ-08

Figure 3-58. Preliminary Hardware Specifications for Attitude Determination

COMPONENT	QUANTITY	WEIGHT	VOLUME	POWER
IMU	1	17 kg 37.5 lb	33 cm x 30 cm x 28 cm (13 " x12 " x 11")	22.5 W
Star Tracker	2	8.2 kg ea 18 lb ea	18 cm dia x 30 cm long (7" dia x 12" long)	12 W ea

COMPONENT*	SOURCE	QUANTITY/UNIT	ENG. UNIT	QUAL. UNIT	FLT UNIT**
Inertial Measurement Unit	AD1	1	1	1	1
Star Tracker	AD2	2	2	2	2
Mechanical Interface	LMSC	3	3	3	3
Cables	LMSC	6	6	6	6

F312594-RJ-02

* "S" Parts
**Engineering Unit Components Used for Spares

Figure 3-59. Summary of Components for Attitude Determination Preliminary Design

3.3.5.4 Lag Angle Compensation and Transmit-Receive Alignment

Lag compensation is performed to account for motions of the LAWS Instrument during the interval between transmit and receive (approximately 5 ms for a 525 km orbit). These motions arise from scanner motion (approximately 6 rpm) and orbital motion (nadir tracking). The required compensation angle consists of a static or bias component and a much smaller dynamic component. Included are also components along and normal to the direction of scan. Typical static and dynamic lag angle components for a 525 km orbit and 6 rpm scan are approximately 2300 μrad and 90 μrad, respectively.

The static lag compensation is implemented by a fixed angular offset between the transmit and receive optics. The implementation of the dynamic lag compensation is shown in *Figure 3-60*. The dynamic lag compensation is accomplished by slewing of the tilt-tip mirror located on the optical bench. The lag compensation commands due to scanner motion and the compensation for orbital motion are combined vectorially to form the final slewing commands as shown. Adjustments in the static lag angle are necessary to correct for orbital altitude variations resulting from orbit decay and reboost. This adjustment is accommodated through onboard hardware/software by periodic resetting of the tilt-tip mirror "zero" position.

The lag compensation is open loop in that it accounts for transmit-receive LOS differences due to known motions only, e.g., scan and orbital motions. Two other sources of transmit-receive LOS error are also of concern. The first of these sources is platform jitter. The two options considered as solutions were active and passive compensation. Active control consists of sensing jitter motion and compensating with a high bandwidth gimballed mirror in the receive optical path. Passive control consists of utilizing isolating mounts and damping where applicable to attenuate space platform jitter disturbances. The passive technique was selected for the preliminary design. The trades illustrated in *Table 3-14* were the basis of this selection. The primary disadvantages of the active approach are the large bandwidths anticipated for sensors and actuators (estimated to be on the order of 1 kHz).

The locations of isolators, if required, are anticipated between the space platform and LAWS base to attenuate the platform jitter. The characteristics of the isolators are dependent on the power spectral density of the platform jitter. The error due to platform jitter is budgeted at 0.7 μrad (see *Figure 3-61*). Acceptable power spectral density boundaries for residual platform jitter at the LAWS Instrument have been determined. These boundaries are shown in *Figure 3-62*. Evaluation of space platform jitter characteristics (when available) will permit the evaluation of the need for isolators and the required isolator characteristics.

A second source of transmit receive alignment error is the misalignment due to zero-g and thermal cycling. These misalignments will be monitored during orbital flight and corrected using the multi-element detector and the tilt-tip mirror capability.

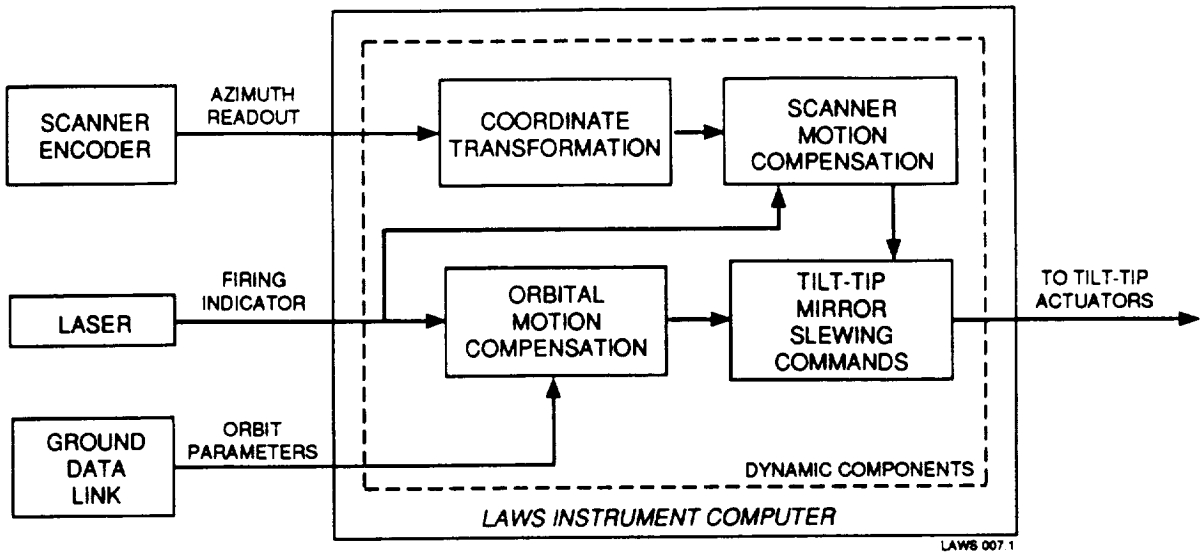

Figure 3-60. Lag Compensation Functional Diagram

Table 3-14. Active vs. Passive Control of Platform and LAWS Jitter

CATEGORY	ACTIVE*	PASSIVE**
Within State-of-the-Art?	No; high bandwidth sensors and actuators	Yes
Weight	Lightest	Heavier
Risk	Higher	Lower
Reliability	Lower	Higher
Cost	Higher	Lower
Selection		✔

F312584-RJ-03

* Jitter measured by sensors and corrected by gimballed mirror
**Structural design, dampers, and isolators used

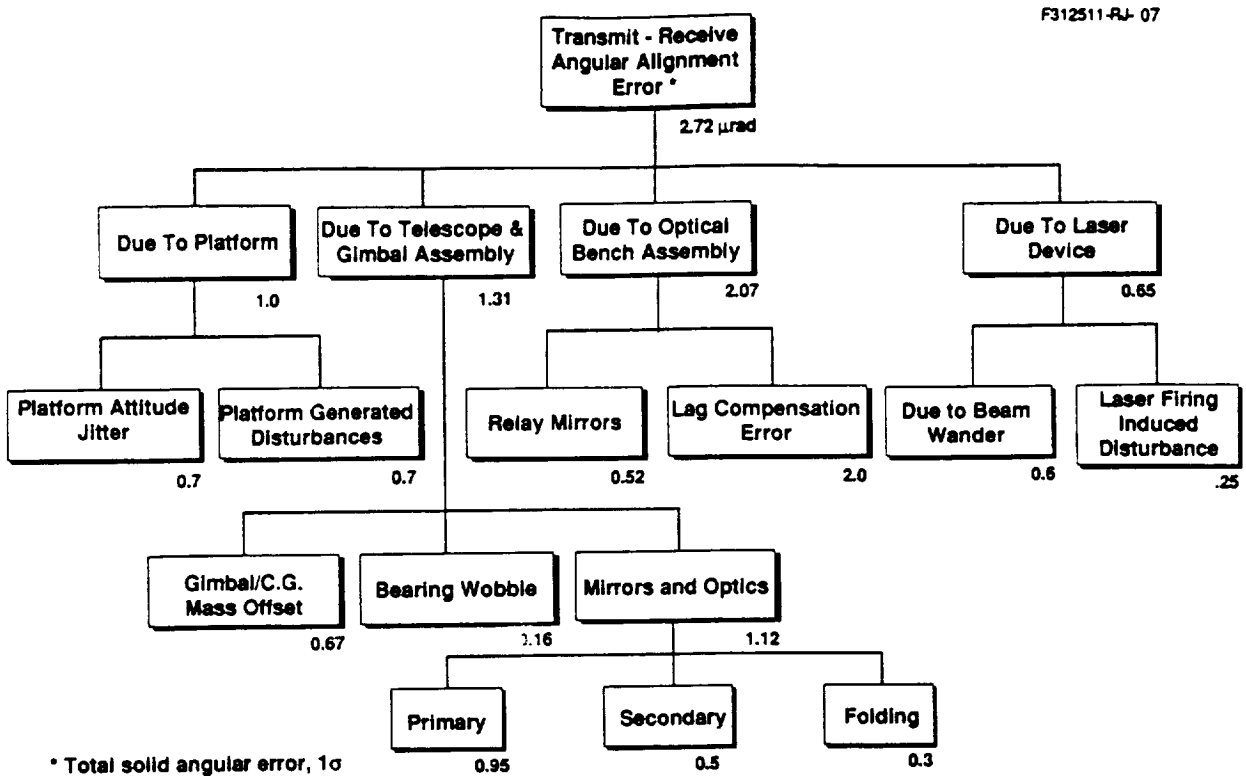

Figure 3-61. Transmit-Receive Error Budget Tree

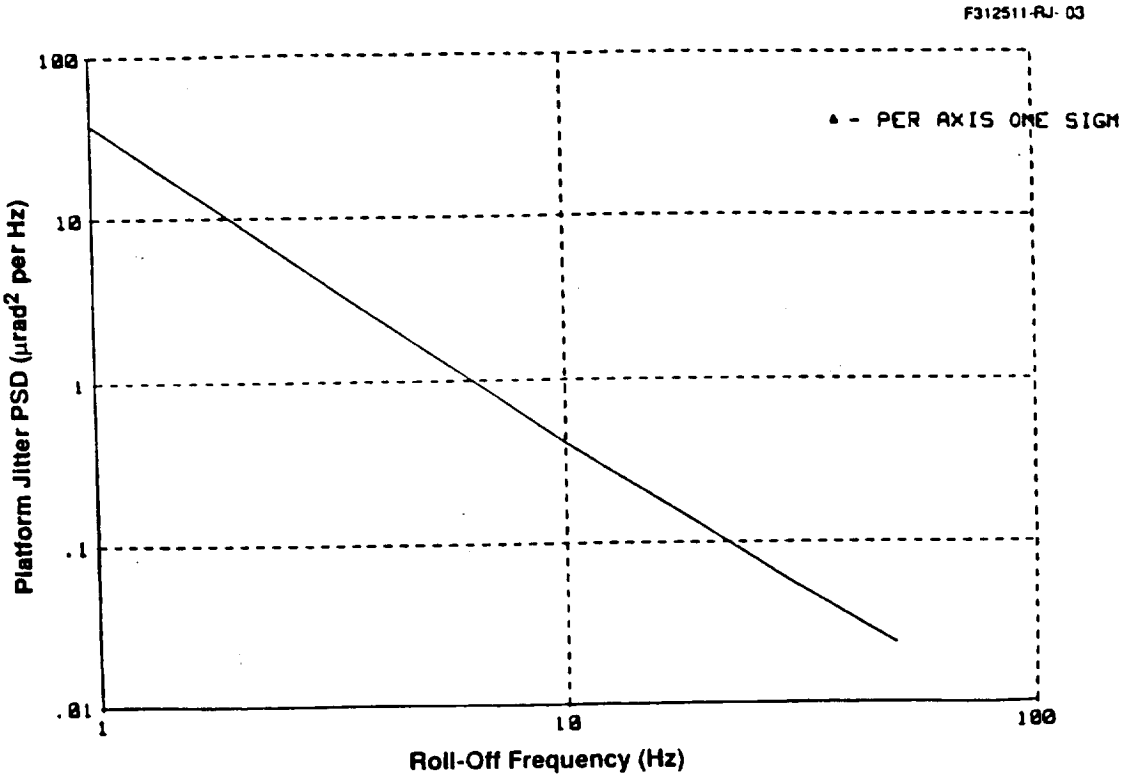

Figure 3-62. Acceptable Boundary for Platform Attitude Jitter PSD

3.3.5.5 Scan Control

The scan control is described above. The implementation consists of selecting a commanded scan rate which is optimized for shot placement. The scanner is commanded to rotate at a constant rate for a given orbit. The regulation of scan rate is critical to the proper operation of lag compensation. Based on the allocation of 2.0 μrad for lag compensation error (see *Figure 3-61*), the speed should be regulated to within 0.0055 rpm. This represents a speed regulation of 0.09 percent for a 6 rpm scan rate.

3.3.5.6 Software

The software modules required for the attitude determination, lag compensation, and scan control functions consist of that software required to interface with the various hardware units including commands and readouts where applicable. Other functions include algorithms required for attitude reference propagation, coordinate transformations, and compensation for the various lag angle phenomena.

3.3.5.7 Structural Dynamics and Component Math Models

General

Math models are maintained for all major components associated with attitude pointing, attitude determination, and attitude stabilization of the LAWS Instrument. The significant parameters include dynamic characteristics, frequency response, performance, error models, etc.

Structural/Dynamic Models

The structural design refinement process of Phase C/D will require periodic dynamic analyses using an updated model. Modes and minimum natural frequencies will be considered with respect to attitude control error budget for structures and mechanisms.

A telescope dynamic balance study will determine the sensitivity of both static and dynamic imbalance on telescope attitude and optics alignment. This study will use the model to determine the degree of accuracy required in balancing the telescope about its axis of rotation. The structural/dynamics model also will be used to determine the effect of space platform perturbances on attitude control.

The accuracy of the mathematical model used in these analyses will be verified by the static and modal structural tests.

3.3.5.8 Simulations

A computer simulation will be used for partial verification of the attitude pointing, attitude determination, and attitude stabilization concept, performance, hardware component parameter, and software algorithms.

The simulation will be based on existing 6-DOF models where possible and will incorporate the rigid and flexible body dynamics of the LAWS Instrument. It will also account for disturbance forces and orbital effects and will be based on the component math models discussed above.

3.3.5.9 Stability Analysis

In Phase C/D, models of all closed loop systems will be maintained and periodically updated. Stability analyses will be performed to verify that response characteristics are adequate and that stability margins are within accepted limits for orbital space pointing/stabilization systems.

Typical stability analyses to be performed are illustrated by the baseline preliminary design for the transmit-receive alignment loop shown in *Figure 3-63*. Analyses will be utilized to verify that gain margins of 6 to 10 dB and phase margins on the order of 25 to 30 deg are achieved.

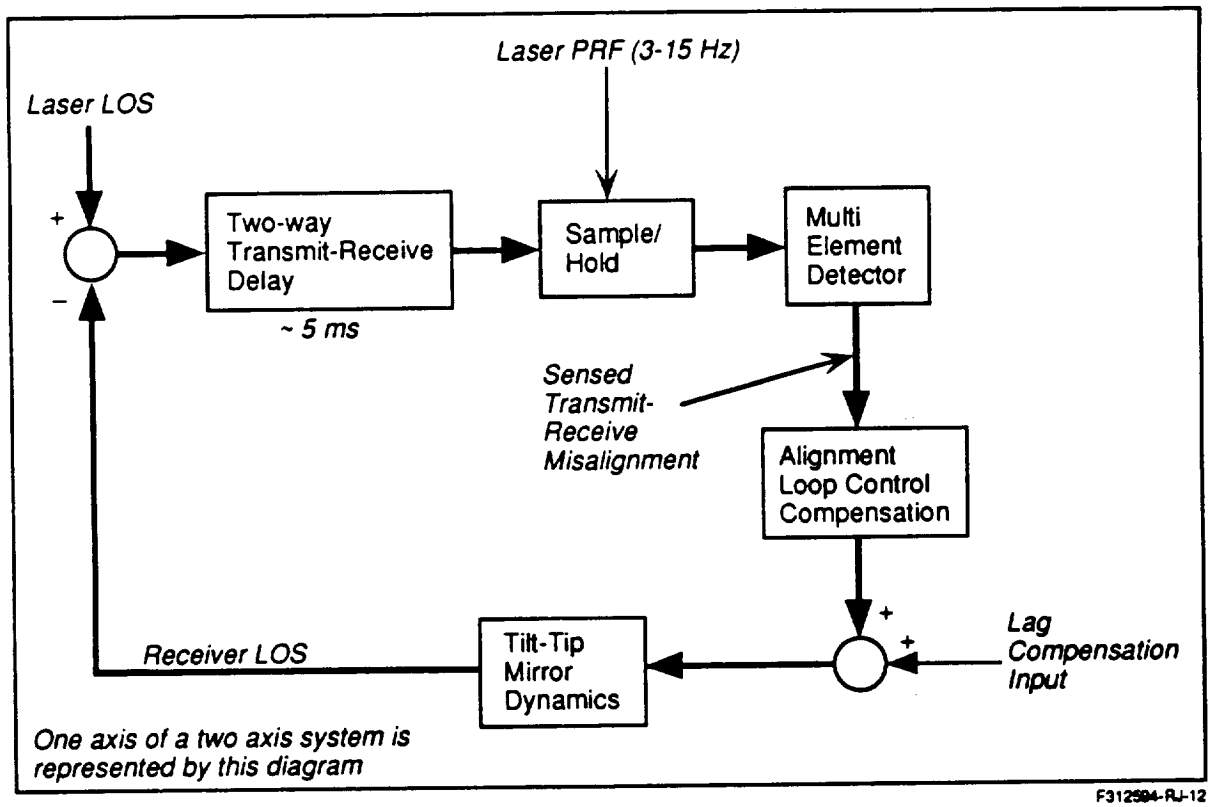

Figure 3-63. Alignment Loop Representation for Stability Analysis

3.3.5.10 Mode Definition and Description

Various modes will be provided for power up/down, checkout, initialization, and nominal on-orbit operation of the attitude determination, lag compensation, scanner, and alignment operations. These modes will be under the control of the LAWS Instrument computer with appropriate ground inhibit/override and status monitoring as per TBD requirement.

3.3.5.11 Summary

Figure 3-64 outlines the program plan, equipment list, verification approach, planned trade studies, and risk reduction plan for the attitude determination subsystem.

3.3.6 Thermal Control Subsystem

This section discusses the LAWS thermal control subsystem (TCS). First, the design requirements in the form of thermal loads and timelines are presented and explained. Next the designs of the active (fluid loop) subsystem and the passive (radiation cooled) subsystem are discussed. These subsystems are shown to meet all of the stated requirements. Finally an overview chart is shown for the combined TCS.

3.3.6.1 Design Loads and Conditions

Table 3-15 summarizes the LAWS thermal loads to be dissipated by the TCS. Electrical power is also shown. The basic requirement is that the LAWS Instrument will not exceed an orbital average power of 2200 W.

Each component which uses power and generates heat is shown. These components are further broken down into variable power thermal load and constant power thermal load groups. These loads are also broken down into survey mode, 4.61 Hz average PRF, and design mode, 10.0 Hz average PRF. Maximum allowable temperature for each component is also given.

As seen in *Table 3-15*, the total variable thermal loads are 1444 W and 3133 W for the survey and design modes, respectively. The total constant load is 569 for both operating modes. The total variable plus constant loads are 2013 W and 3702 W for the survey and design modes, respectively. The thermal load is less than the electrical load because some of the energy is dissipated by other means, for example that which goes out in the laser beam. Environmental thermal loads (i.e., solar UV, albedo, and Earth IR) are not included in the values in *Table 3-15* because most of these components are either under the thermal cover or on the cold side of LAWS. These components are assumed to be mounted on thermal isolators to prevent heat transfer to the base.

A ATTITUDE DETERMINATION PLAN OVERVIEW

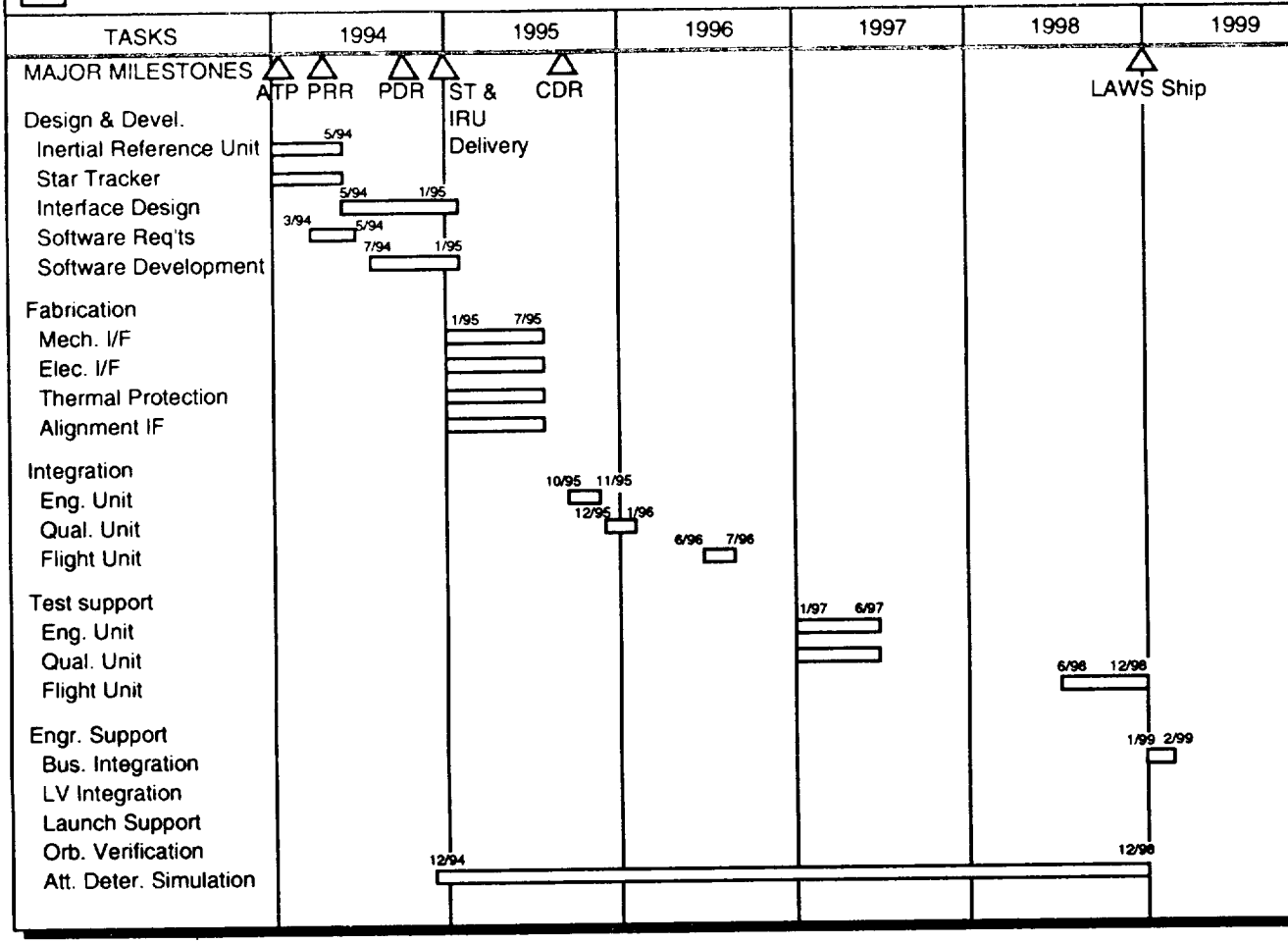

B REQUIRED SUBSYSTEM EQUIPMENT

COMPONENT*	SOURCE	QUANTITY/UNIT	ENG. UNIT	QUAL. U
Inertial Reference Unit	AD1	1	1	1
Star Tracker	AD2	2	2	2
Mechanical Interface	LMSC	3	3	3
Cables	LMSC	6	6	6

* "S" Parts
**Engineering Unit Components Used for Spares

FOLDOUT FRAME

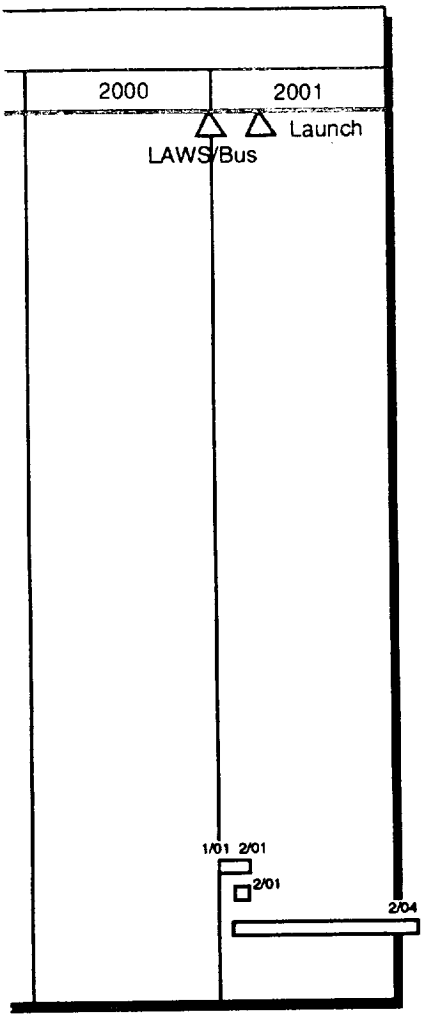

C REQUIREMENT IMPLEMENTATION/VERIFICATION

KEY REQUIREMENT	IMPLEMENTATION	VERIFICATION
Operational Life	5 yr on Orbit	Comparison and Test
Performance	• Attitude Knowledge: 100 μrad/Axis, One Sigma • Receive Transmit Align: 3 μrad/Axis, One Sigma • Pointing Accuracy: 8 mrad/Axis, One Sigma	Analysis and Simulation
Interfaces and Software Functions	• IRU Attitude Update • Star Tracker Update • Lag Compensation • Receive-Transmit Alignment Loop	Simulation and Test

D PLANNED TRADE STUDIES

TRADE ITEM	BASELINE DESIGN
No. of Star Updates Per Orbit vs. IRU Performance	10 Updates/Orbit, Scale Factor Error < 75 PPM, Gyro Drift Rate Uncertainty < 0.01 deg/hr
On Orbit Recalibration Procedures for Attitude Determination	Use Hard Target Return to Recalibrate LOS of Outgoing Laser Beam
Methodology of Compensating for Space Platform Jitter; Active vs. Passive	Passive; Use Isolators Between Base Assembly and Optical Bench as Required *(Need Goddard to Supply Jitter PSD of Space Platform)*

IIT	FIT UNIT**
	1
	2
	3
	6

312594-RJ-FO

E RISK SUMMARY

RISK ITEM	RISK LEVEL	RISK REDUCTION APPROACH
IRU Failure	Low	Space Qualified and Demonstrated Unit with Built-in Double Redundancy for Each Attitude Axis
Star Tracker Failure	Low	Space Qualified and Demonstrated Unit
Misalignment Due to Zero g and Launch	Moderate	Develop Methodology to Recalibrate Using Hard Target Returns

Figure 3-64. Overview/Summary of the Attitude Determination Subsystem

FOLDOUT FRAME 2

Table 3-15. LAWS Electrical/Thermal Load Summary

Component	Maximum Operation Temp °C	Electrical Power, W		Thermal Load, W		Central System Heat Rejection, W		Passive System Heat Rejection, W	
		4.61 Hz Ref PRF	10 Hz Avg PRF	4.61 Hz Ref PRF (Survey Mode)	10 Hz Avg PRF (Design Mode)	4.61 Hz Ref PRF (Survey Mode)	10 Hz Avg PRF (Design Mode)	4.61 Hz Ref PRF (Survey Mode)	10 Hz Avg PRF (Design Mode)
Variable Power/Thermal Load									
Laser									
Power Supply	40	1537	3333	384	833	384	833	–	–
Laser Energy Loading	27	–	–	1060	2300	1060	2300	–	–
Total Variable Load		1537	3333	1444	3133	1444	3133	–	–
Constant Power/Thermal Load									
Laser									
Laser Fans	40	40	40	40	40	40	40	–	–
Thyratron Filament/ Reservoir	50	135	135	135	135	135	135	–	–
Local Oscillator								–	–
Power Supply	40	30	30	8	8	8	8	–	–
Energy Loading	20	–	–	22	22	22	22	–	–
Seed Laser									
Power Supply	40	100	100	27	27	27	27	–	–
Energy Loading	20	–	–	73	73	73	73	–	–
Receiver									
Det Bias/Preamp	20	10	10	10	10	–	–	10	10
Cryocoolers	20	50	50	50	50	50	50	–	–
Electronics	40	20	20	20	20	–	–	20	20
Optics									
Azimuth Drive	40	30	30	30	30	30	30	–	–
Moment Compensator	40	15	15	15	15	15	15	–	–
Telescope Thermal Control	20	40*	40*						
Electrical									
Power Distribution	40	10	10	10	10	–	–	10	10
Thermal									
Thermal Control	40	66	66	66	66	66	66	–	–
Comm. and Data Handling									
Flight Computer	40	15	15	15	15	–	–	15	15
Attitude and Position Ref									
IMU	50	23	23	23	23	–	–	23	23
Star Tracker	50	25	25	25	25	–	–	25	25
Total Constant Load		609	609	569	569	466	466	103	103
Total: Variable + Constant Load		2146	3942	2013	3702	1910	3599	103	103

F312594-33

**Required for heaters on mirrors and telescope, therefore not included in thermal load*

Figure 3-65 shows a typical power and thermal load timeline or schedule for one orbital period. The shot frequency is managed to yield an orbital average power consumption of 2200 W. The shots are scheduled to prevent overlap along the ground track as the orbit approaches and passes over the poles. This reduced frequency conserves energy which can then be used in operating at the 10 Hz design mode for some time without exceeding the 2200 W orbital average limit. In this case, 879 seconds of design mode operation were obtained. The orbital conditions used for this case are also shown in *Figure 3-65*. Again, note the difference in the electrical and thermal loads.

The life expectancy requirement for the LAWS TCS is from 5 to 7 years operation in orbit without maintenance.

The following orbital parameters are planned for LAWS:

- Sun synchronous orbit
- Orbital altitude = 525 km
- Orbit inclination = 97.497 deg
- 6:00 a.m. (14 hr GMT) launch due south from Vandenberg AFB.

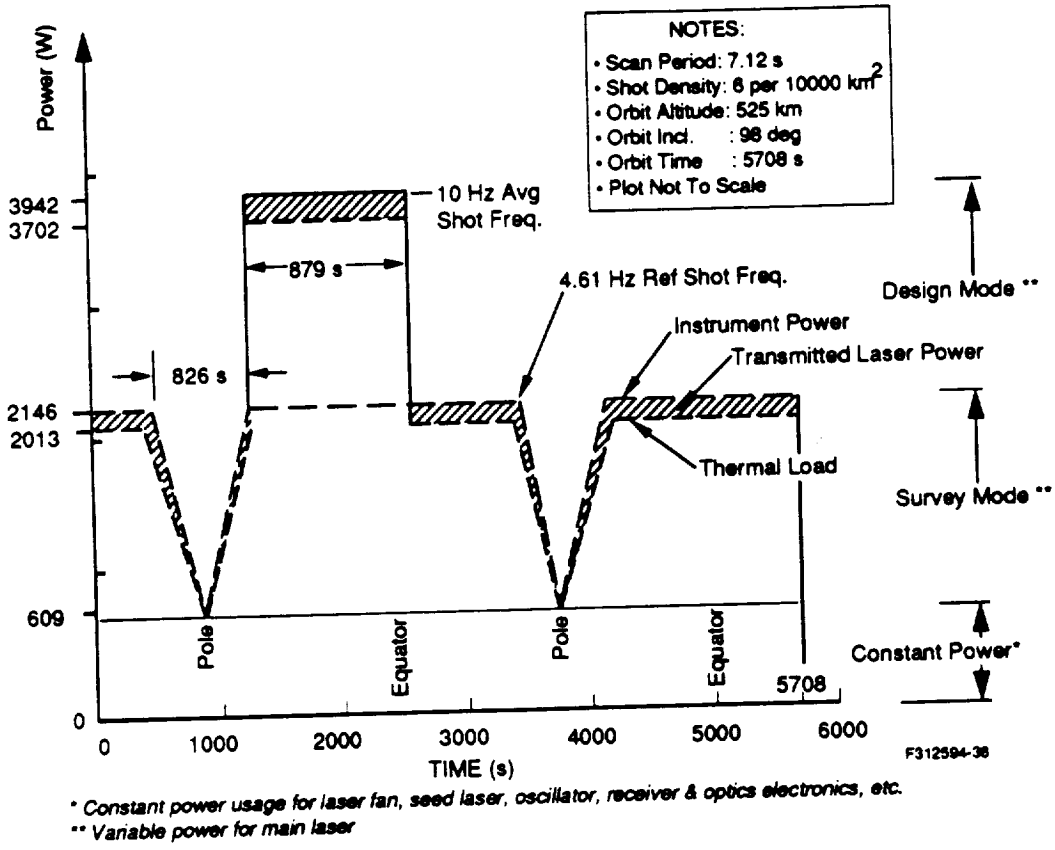

Figure 3-65. LAWS Power and Thermal Load Schedule

These conditions yield an annual beta angle range of approximately 59 to 90 deg. These two beta angles were used as upper and lower limits in the passive system design. This orbit results in an occultation period (i.e., not full sunlight for the entire orbit), which gives the percent time in the sun for each day of the year. This percentage ranges from 77 to 100 percent. Both the power system and the TCS were designed to accommodate these conditions.

3.3.6.2 Design Approach

The design approach used for the LAWS TCS is to dissipate as much waste heat passively (i.e., by radiation to space) as possible. However, many of the larger loads, particularly the laser gas cooling, have to be taken out by using a convective heat exchanger. This then dictates the use of an active pumped coolant loop system. *Table 3-15* shows which components are cooled actively and which are cooled passively.

3.3.6.2.1 Active Thermal Control System Description

Figure 3-66 is a schematic of the LAWS active TCS. A two-stage centrifugal pump is used to flow the coolant through all components to be cooled and then through two 1,000 W coldplates which are mounted back-to-back with the spacecraft central system coldplates. The coolant being used is a 30/70 ethylene-glycol/water mixture with a freezing point of approximately -18 °C (0 °F).

Following the flow path of *Figure 3-66*, after the coolant leaves the coldplates it begins its circuit to pick up heat, going first through the components to be maintained at the lower allowable temperature and then proceeding to the higher allowable temperature components. The cryocooler compressor and expander thermal/mechanical mounting flanges are cooled first, then the seed lasers and local oscillators. A flow divider device then splits the flow into two equal parts which flow in parallel through the laser gas convective heat exchangers. The flow then combines into a single line and cools the laser power supply and laser fan motors. Vibration isolation loops are provided between the optical bench and laser components to reduce vibration transmission from the laser pulses.

The coolant then flows through the seed laser and local oscillator power supplies, the azimuth drive motor, the momentum compensator motor, and back to the pump. Filters are provided before the flow enters the pumps, the pump check valves, the diverter valves, the pump bypass valve, and the flow dividers to prevent contamination from interfering with their operation.

Figure 3-67 is a schematic of the LAWS coolant pump package. This package contains two redundant pumps. Only one pump runs at a time. Check valves prevent backflow through the non-operating pump. Each of the pumps is capable of meeting the stated life expectancy requirement. This provides a factor of 2 margin on pump life.

The pumps chosen are existing space qualified pumps which have been used on the Space Shuttle Orbiter TCS for a number of years.

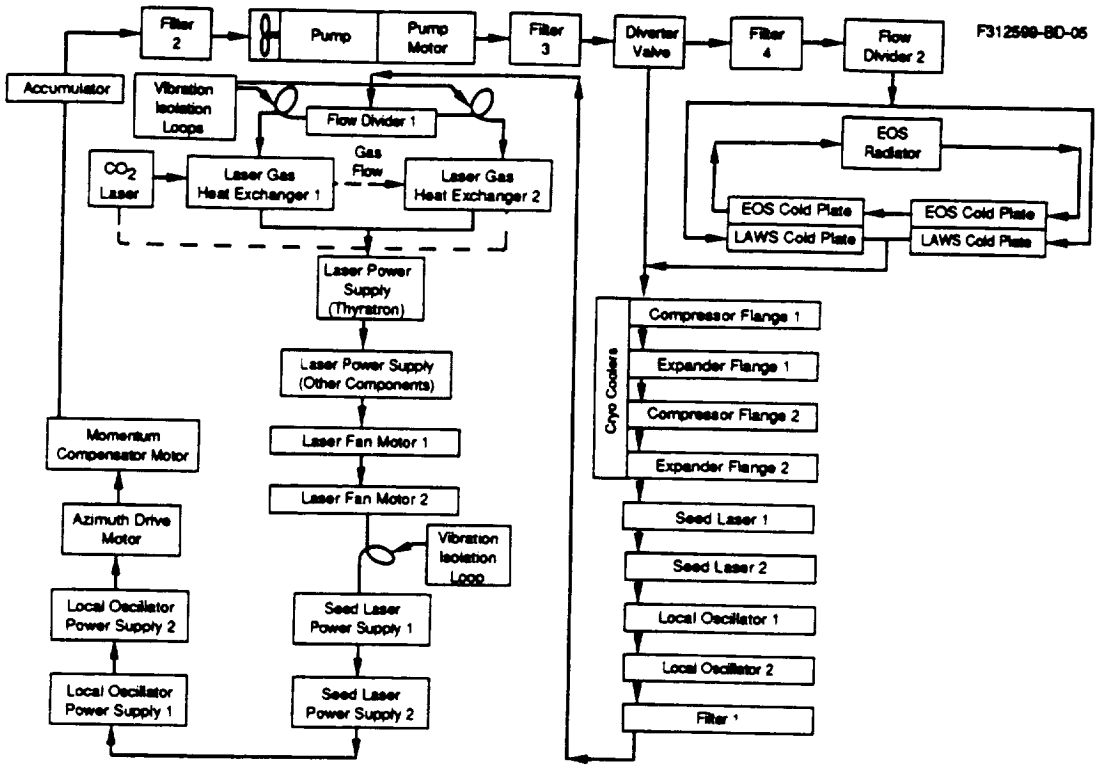

Figure 3-66. LAWS Active TCS Schematic

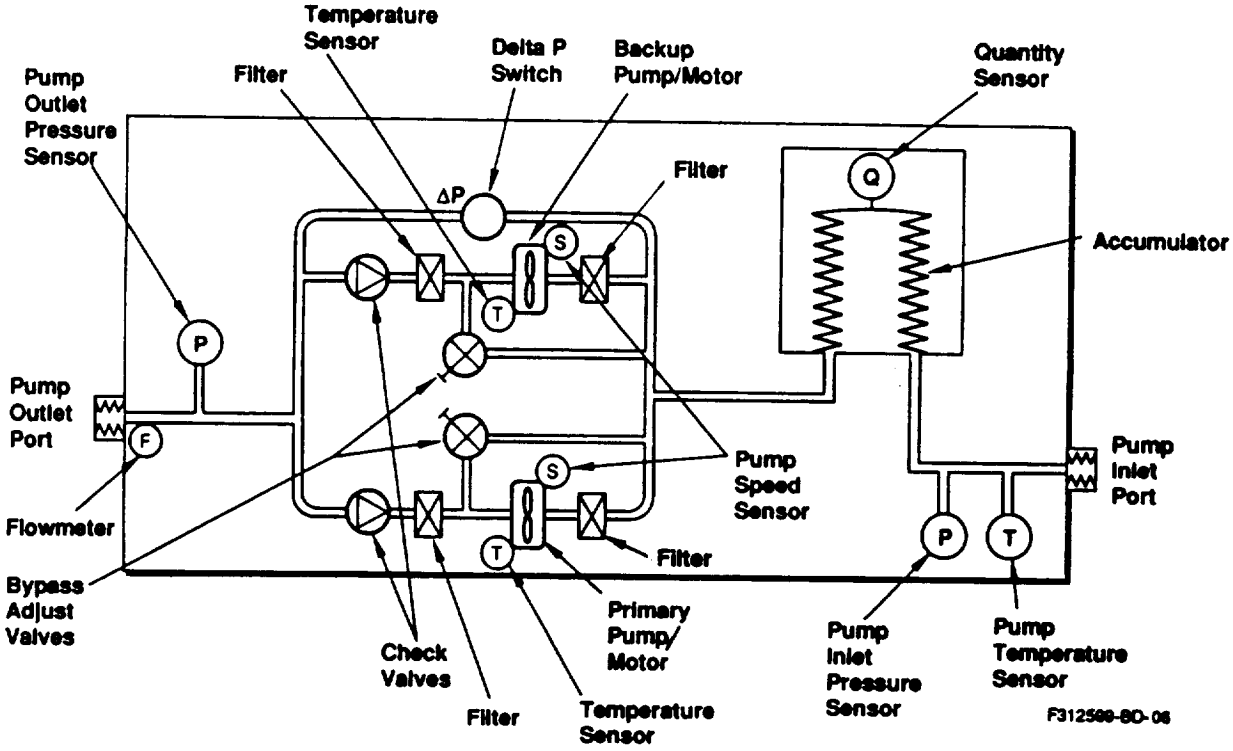

Figure 3-67. LAWS Coolant Pump Package Schematic

Table 3-16 shows the coolant temperatures which result as the active TCS cools each of the LAWS components. Inlet and outlet temperatures are shown and compared to allowable values for both survey mode and design mode operation. The flow rate used is 238 kg/hr, (1 GPM, 524 lb/hr). The flow passes through all components in the order shown on the layout of *Figure 3-68* and then dumps the heat to the platform coldplates. It then returns to the original 15 °C temperature. Comparison of these temperatures shows they are within the allowable limits.

Table 3-16. Results, LAWS Active TCS Coolant Temperatures

	SURVEY MODE					DESIGN MODE				
COMPONENT	Q DOT WATTS	T IN DEG C	DT DEG C	T OUT DEG C	T ALLOWABLE DEG C	Q DOT WATTS	T IN DEG C	DT DEG C	T OUT DEG C	T ALLOWABLE DEG C
CRYOCOOLERS										
#1 COMP FLANGE	22	15.00	0.10	15.10	20	22	15.00	0.10	15.10	20
#1 EXPANDER FLANGE	3	15.10	0.01	15.12	20	3	15.10	0.01	15.12	20
#2 COMP FLANGE	22	15.12	0.10	15.22	20	22	15.12	0.10	15.22	20
#2 EXPANDER FLANGE	3	15.22	0.01	15.23	20	3	15.22	0.01	15.23	20
SEED LASER #1	36.5	15.23	0.17	15.40	20	36.5	15.23	0.17	15.40	20
SEED LASER #2	36.5	15.40	0.17	15.57	20	36.5	15.40	0.17	15.57	20
LOCAL OSCILLATOR #1	11	15.57	0.05	15.62	20	11	15.57	0.05	15.62	20
LOCAL OSCILLATOR #2	11	15.62	0.05	15.67	20	11	15.62	0.05	15.67	20
FILTER NO 1	0	15.67	0.00	15.67	40	0	15.67	0.00	15.67	40
FLOW DIVIDER #1	0	15.67	0.00	15.67	40	0	15.67	0.00	15.67	40
LASER GAS HT EX 1,2	1060	15.67	4.93	20.61	27	2300	15.67	10.70	26.38	27
LASER POWER SUPPLY	519	20.61	2.42	23.02	40	968	26.38	4.51	30.88	40
LASER FAN MOTOR #1	20	23.02	0.09	23.12	40	20	30.88	0.09	30.98	40
LASER FAN MOTOR #2	20	23.12	0.09	23.21	40	20	30.98	0.09	31.07	40
SEED LASER PR SUPP #1	13.5	23.21	0.06	23.27	40	13.5	31.07	0.06	31.13	40
SEED LASER PR SUPP #2	13.5	23.27	0.06	23.34	40	13.5	31.13	0.06	31.20	40
LOCAL OSCIL POW S #1	4	23.34	0.02	23.35	40	4	31.20	0.02	31.22	40
LOCAL OSCIL POW S #2	4	23.35	0.02	23.37	40	4	31.22	0.02	31.23	40
AZMUTH DRIVE MOTOR	30	23.37	0.14	23.51	40	30	31.23	0.14	31.37	40
MOM COMPENSATOR MOTOR	15	23.51	0.07	23.58	40	15	31.37	0.07	31.44	40
FILTER NO 2	0	23.58	0.00	23.58	40	0	31.44	0.00	31.44	40
PUMP	0	23.58	0.00	23.58	40	0	31.44	0.00	31.44	40
PUMP MOTOR	66	23.58	0.31	23.89	40	66	31.44	0.31	31.75	40
FILTER NO 3	0	23.89	0.00	23.89	40	0	31.75	0.00	31.75	40
DIVERTER VALVE	0	23.89	0.00	23.89	40	0	31.75	0.00	31.75	40
FILTER NO 3	0	23.89	0.00	23.89	40	0	31.75	0.00	31.75	40
FLOW DIVIDER #2	0	23.89	0.00	23.89	40	0	31.75	0.00	31.75	40
	1910					3599				
LAWS/EOS C PLATES 1,2	-1910	23.89	-8.89	15.00		-3599	31.75	-16.75	15.00	

NOTES:

1. Ethylene glycol/water (30/70)
2. Mass flow rate, 238 kg/hr (534 lb/hr) = 1 gpm
3. CP = 0.778 Cal/g-K, (0.778 Btu/lbm °R)
4. Density = 1.04 g/cm3 (65.4 lb/ft3)
5. All temperatures within allowable limits

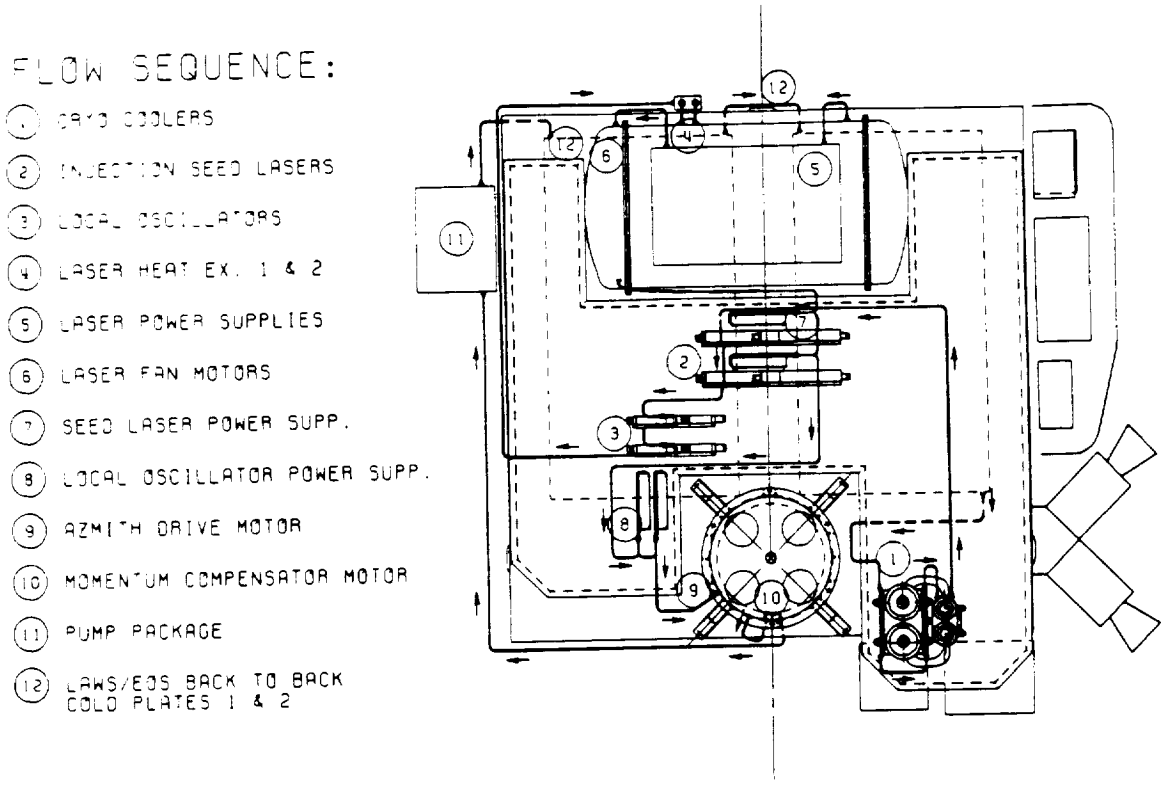

Figure 3-68. Coolant Line Layout

3.3.6.2.2 Passive Thermal Control System Description

On-orbit thermal control for the LAWS Instrument is achieved by a hybrid form of thermal control system. An active fluid loop as described above is used to transport the heat from high powered components such as the main laser, oscillator, seed laser, and azimuth drive. The heat is transferred through interfacing coldplates to be rejected to space via EOS central thermal bus radiators. Heat is also rejected passively by radiation from external surfaces of all components with an adequate field-of-view to space. Components are placed on the LAWS Platform such that, in combination with conventional passive thermal techniques augmented with electrical heaters, they are controlled effectively to within their allowable temperature limits during operational and non-operational (survival) modes. Passive thermal control is achieved by use of multilayer insulation (MLI), thermal coatings and tapes, thermal covers, and thermal isolation materials. The passive TCS is based on HST TCS design with a wide application of low α/ε atomic oxygen resistant Ag FOSR (Flexible Optical Solar Reflector: Teflon with vapor deposited silver) designed for a 15 yr lifetime.

The planned baselined orbit for LAWS is a sun-synchronous orbit, with a 6:00 a.m. launch due south from Vandenberg AFB, attaining an attitude of 525 km with an orbit inclination of 97.497 deg. This results in the orbit beta angle varying between 59 and 90 deg and an occultation period for some 100 days of the yearly cycle that begins when the beta angle becomes less than 68 deg.

The planned attitude for the LAWS Instrument is with its X-axis in the velocity vector, i.e., with the telescope leading. The combination of attitude and sun-synchronous orbit results in one side (-Y side) always toward the sun. Therefore, this configuration is used to position the receiver electronics, flight computer, power distribution unit, cryocooler controller, and Star Trackers on the cold side, facing deep space, since these components generate a significant amount of heat (see *Table 3-15*). These components, with the exception of the Star Trackers, are effectively controlled with a lightweight thermal cover with a combination of thermal coatings inside and outside. The Star Trackers require a thermal coating of SiOx on vapor deposited aluminized Kapton taped on them for maintaining design allowable temperatures. The IMU and detector bias and preamps are positioned on the +X side of the Platform. The pump package, which is inherently self-cooling, is positioned on the hot (-Y) side since it is part of the active fluid loop central bus heat rejection system. The pump package is protected from freezing in case of active system shutdown by being placed on the hot side of the Platform. The passively controlled components discussed are shown in *Figure 3-69* with their designed thermal coatings/covers.

The telescope is also passively controlled using Al teflon tape. Surfaces along the optical path are painted black. Varying total absorbed orbital fluxes as the telescope resolves were considered in the TCS design and evaluation of required thermal coatings. This is depicted in *Figure 3-70*. A similar telescope assembly was also evaluated for the downsized 5 J laser. The primary mirror diameter is approximately half that for the 20 J laser. The mirror, made of Corning ULE material, was analyzed to predict temperature gradients along the surface. This was necessary for thermal stress and deformation evaluation and to study the effect on optical performance.

The graphite epoxy base structure on which the laser is mounted, the graphite epoxy honeycomb structure for the optical bench, and the telescope mount are anticipated to be covered with MLI to reduce temperature gradient and structural distortion within these structures. Al FOSR is applied over the environmental/thermal cover for the optical bench. Although a temperature gradient can be expected on the cover, it is a nonstructural part and is maintained cold with the low α/ε coating so it can be used as a contamination collector for the optics mounted on the optical bench and under this cover.

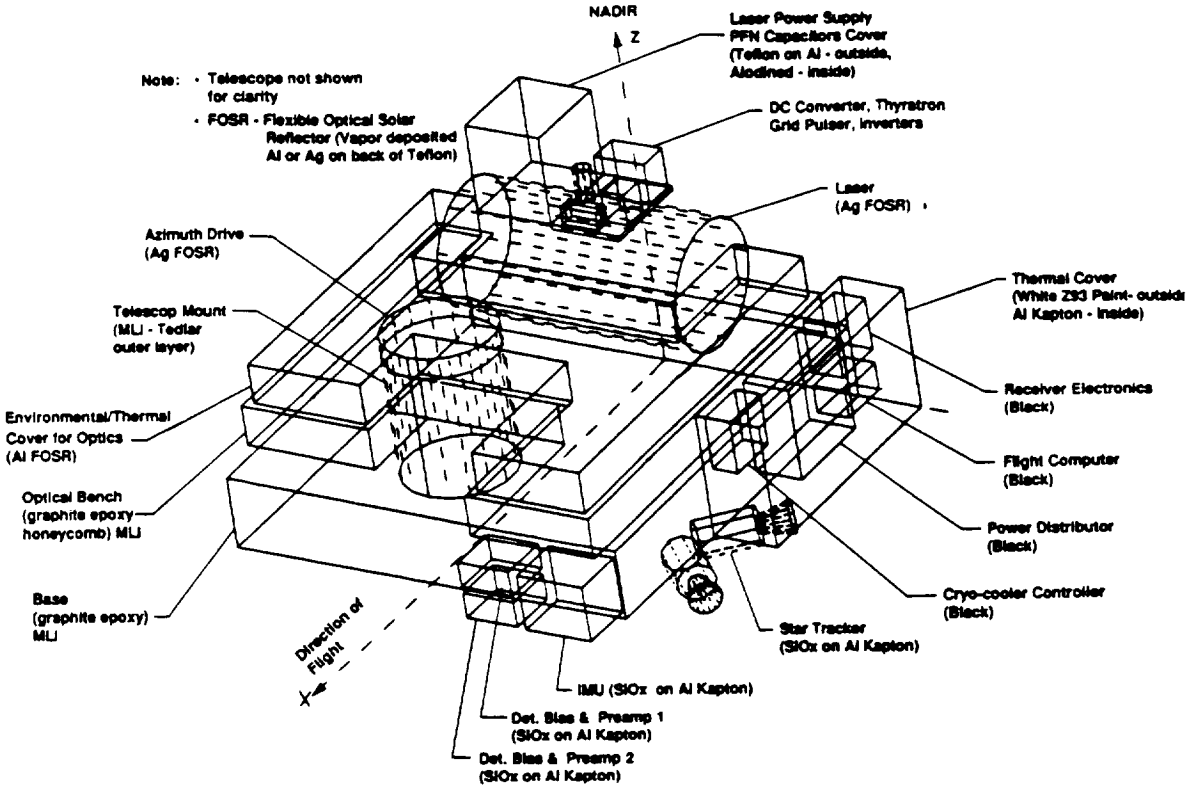

Figure 3-69. Thermal Radiation Model Plot of LAWS Instrument Showing Passive TCS Surface Coatings

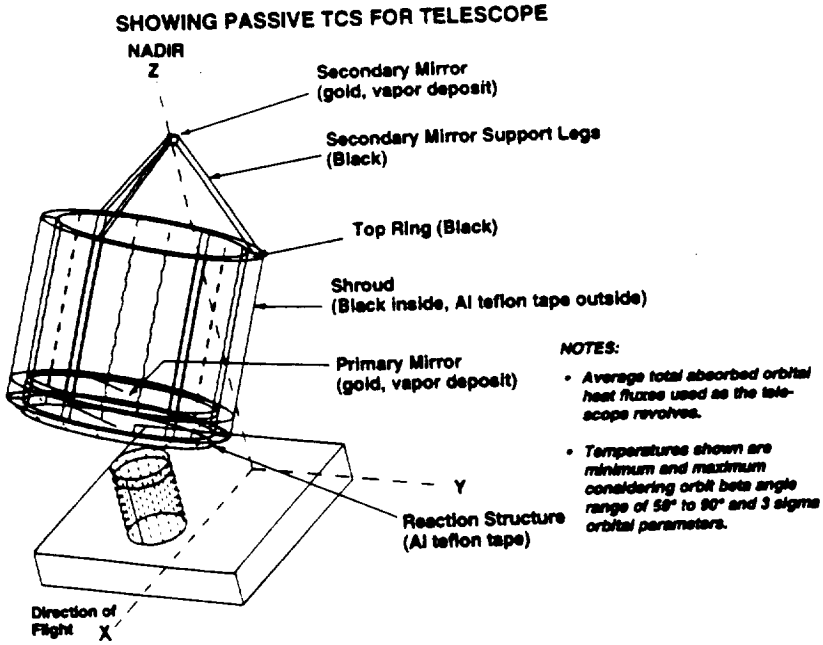

Figure 3-70. Thermal Radiation Model Plot of LAWS Instrument Telescope Showing Passive TCS

The laser power supply is mounted on the laser tank, which in turn is mounted on the base structure. Acoustical/electrical induced vibrations are isolated from the optical bench, which is mounted on kinematic mounts attached to the base. Active cooling is required for the high internal heating components such as the thyratron and dc-dc converter of the power supply. To reduce the active cooling load, these components are placed on a coldplate with their surfaces exposed to space. The relatively low internal heating PFN capacitors are controlled by using a small cover coated with aluminized teflon (see *Figure 3-69*).

The passive TCS design philosophy has been to perform analysis for a hot design case using +3 sigma orbital environment, end-of-life optical properties, minimum altitude, minimum MLI effectiveness, and maximum component duty cycles for the range of β angles expected. Maximum component temperatures are maintained well below their upper operational allowable temperatures. Then the cold design case with -3 sigma fluxes, maximum altitude, beginning-of-life optical properties, maximum MLI effectiveness, and minimum component duty cycles is performed for the range of β angles to ensure that component responses are above their lower operational limit.

By using a worst case combination of fluxes, optical properties, MLI effectiveness, duty cycles, and β angles, a good TCS design margin is provided. Heaters, when designed for the telescope, are sized with a 50 percent margin at minimum bus voltage to ensure adequate capability. MLI design will incorporate net spacers to obtain better performance. The number of layers and net spacers will be based on thermal-vat (TV) tests, and the blankets will be baked out separately or after installation to minimize contamination. TCS requirements are verified by analysis, component level TV tests, and LAWS systems TV tests.

3.3.6.3 Laws Thermal Control Subsystem Overview

Figure 3-71 shows an overview of the LAWS TCS. Part A shows the schedule from January 1994 through launch in 2001. The first nine quarters are used for preliminary and detailed design after one quarter of finalizing requirements. We propose to start pump life testing at the very beginning of this schedule and continue throughout the design and qualification period. Two pumps are expected to be sufficient to meet the 5 to 7 year LAWS life requirement. However, design "scars" will be provided so that additional pumps can be added to the pump package if required as a result of these life tests. Up to four pumps can be easily used in the existing design package.

Functional and development tests are planned at both the component and integrated levels. These will provide inputs directly to the design. Passive and active testing will be conducted separately at first, and then these systems will be combined for continued integrated testing. Both component level and integrated testing will be conducted on both the qualification and flight hardware. Thermal support will be provided for LAWS-to-bus integration and checkout and for bus-to-vehicle integration.

A THERMAL CONTROL SUBSYSTEM DEVELOPMENT, TEST AND EVALUATION PLAN OVERVIEW

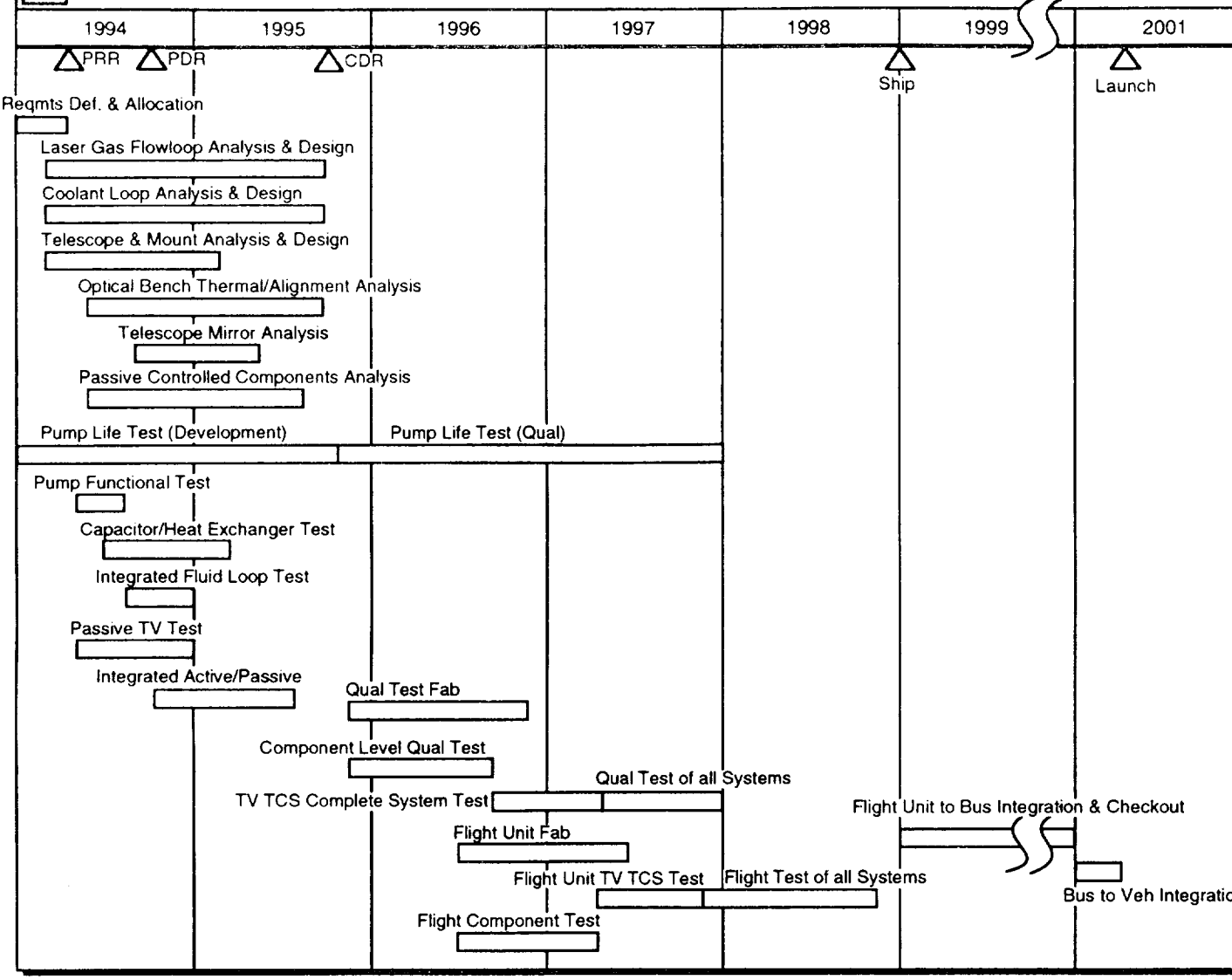

B REQUIRED THERMAL CONTROL SUBSYSTEM EQUIPMENT

COMPONENT	SOURCE	MATURITY/HERITAGE	LIFE TESTING	ENGINEERING MODEL	QUAL UNIT	FLIGHT UNIT	SPARES
Pump Package	Supplier 1	Space Qual/Space Lab	1	1	1	1	1
Pumps	Supplier 1	Space Qual/Space Lab	3				1
Cold Plates	TBD	Same as EOS		2	2	2	
Diverter Valves/Controllers	Supplier 1	Space Qual/Shuttle	1	1	1	1	1
Heat Exchangers	TBD	Modified/Breadboard		2	2	2	2
Ag FOSR	Supplier 2	Off the Shelf/HST		TBD	TBD	TBD	
MLI	Supplier 2	Off the Shelf/HST		TBD	TBD	TBD	
Heaters, Kapton	Supplier 3	Off the Shelf/HST		TBD	TBD	TBD	

FOLDOUT FRAME

C TCS REQUIREMENT IMPLEMENTATION/ VERIFICATION

KEY REQUIREMENTS	IMPLEMENTATION	VERIFICATION
1. Maintain laser gas temp at all PRF	Convective heat exchanger within active cooling loop	Analysis, test
2. Five year life on active cooling system	Redundant pumps	Life test
3. Maintain temp limits of components for all mission phases	Active cooling and passive Ag FOSR outer surfaces, MLI	Analysis, TVT
4 Control of thermally sensitive optical bench, telescope & mirror/ supports	Controlled by FOSR, heaters, ULE optics, gold coatings	Analysis, TVT
5. Minimize contamination of optics	Optical bench thermal cover as contamination collector and spatial separation of fluid lines from optics	Analysis, TVT
6. Design for 5 year atomic oxygen environment	Teflon Ag FOSR, $\Delta\alpha$ = 0.012 per year based on flight data	Analysis, LDEF data
7. Decouple optics from orbit environment	Thermal covers, Ag FOSR outer surfaces, low α/ε external, thermal isolators	Analysis, TVT
8. No single point failure	Redundant pumps, valves heater systems	Analysis
9. Maintain hardware and components above survival temperatures	Safe mode developed with heaters/thermostats to maintain component above lower survival limits	Analysis
10. Maintain struct temp gradients and changes to meet pointing requirem"ts	Thermal cover, Ag FOSR and heater system	Analysis, TVT

D TCS TRADE STUDIES AND ANALYSIS

1. Position of passively controlled avionics components on the base.
2. Compact convective heat exchanger versus back-to-back cold plates for EOS/LAWS active thermal control interface.
3. Pumped loop versus heat pipe active TCS.
4. Redundant loops versus single loop with redundant pumps for active TCS.
5. Existing space qualified pump packages versus new development long life pumps.
6. Passive versus active cooling of main laser power supply.

E TCS RISK REDUCTION SUMMARY

RISK	LEVEL	RISK REDUCTION APPROACH
1. Five year pump life	High	Life testing & redundant pumps
2. Five year valve life	Med	Cyclic testing
3. Five year life of other TCS compon.	Low	Stable materials
4. Contamination due to outgassing	Low	Material selection, bakeout & design
5. Contamination due to coolant leaks	Low	Use of brazed joints and leak containment devices
6. Contamination due to biological growth in coolant	Low	Sterilization system

F VERIFICATION SUMMARY

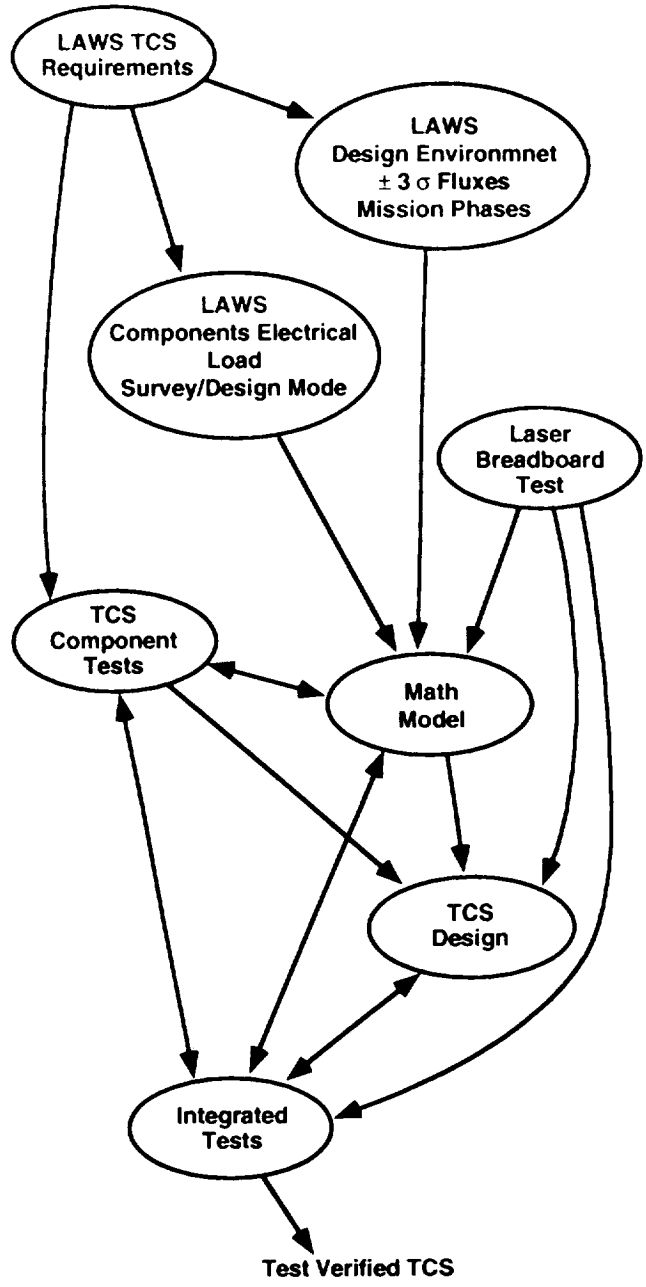

G DESIGN MARGINS AND GROWTH

1. Using hot and cold design cases with 3σ fluxes
2. Range of equipment duty cycles and MLI/thermal coating performance
3. Heaters sized 1.5X required at minimum bus voltage
4. Controlling to levels well within requirements
5. 2.0 x pump life
6. Redundant pump controller and power circuits
7. Redundant heaters & heater thermostats

312594-11

Figure 3-71. Overview/Summary of the LAWS Thermal Control System

FOLDOUT FRAME

Figure 3-71 (B) shows the major TCS components, the intended source, the maturity/heritage and quantities of each component required for life testing, engineering units, qualification units, flight units, and spares. The suppliers selected are all well qualified with a wealth of experience in their particular areas. The maturity/heritage for these components shows either already qualified or off-the-shelf availability. Heritage derives from the Shuttle, HST, and Space Lab or EOS.

Figure 3-71 (C) identifies the steps or design features incorporated to implement the key requirements planned for verification of each requirement. Part D summarizes some of the trades and analyses either completed, planned, or on-going.

Figure 3-71 (E) shows the TCS risk reduction summary. Pump-life risk is minimized by actual life testing in our labs to verify the pump performance. Design scars will be left in order to incorporate the number of pumps needed to meet the 5 to 7 year life required with a factor of 2 margin. At present, it is felt that two redundant pumps meet this goal. If not, additional pumps will be added as required.

Figure 3-71 (F) shows the logic to be used during the process of the LAWS program to produce a verified design/subsystem. Part G shows the design margin, again showing the planned factor of 2 on pump life.

3.3.7 Electrical Power Subsystem

3.3.7.1 Overview

The block diagram of the LAWS power distribution system (PDS) is shown in *Figure 3-72*. The spacecraft's two 120 Vdc (GIIS-specified) power buses are labeled Platform +120 Vdc bus 1 and Platform +120 Vdc bus 2 in *Figure 3-72*. The PDS derives two redundant 28 Vdc power buses from the spacecraft's two 120 Vdc power buses. Each of the two buses are capable of supplying all power required by the LAWS Instrument. Since both buses are active simultaneously, each bus supplies half of the LAWS power load. For clarity, the redundancy of individual components in the PDS is not shown. The PDS supplies 120 Vdc to the transmit laser and 28 Vdc to the other LAWS subsystems. Only power distribution to the transmit laser, computer, and receiver is shown. Power distribution to other LAWS subsystems is similar.

In *Figure 3-72*, circuit breaker 1 and circuit breaker 2 protect the spacecraft 120 Vdc power bus from faults in the LAWS system. Circuit breakers 3 and 4 protect the PDS dc/dc converters from faults occurring in the individual LAWS subsystems. These circuit breakers are remotely resettable. If a circuit breaker trips, it can be reclosed by commands from the flight computer or spacecraft. Commands and health and status monitors pertaining to the PDS are discussed in later sections.

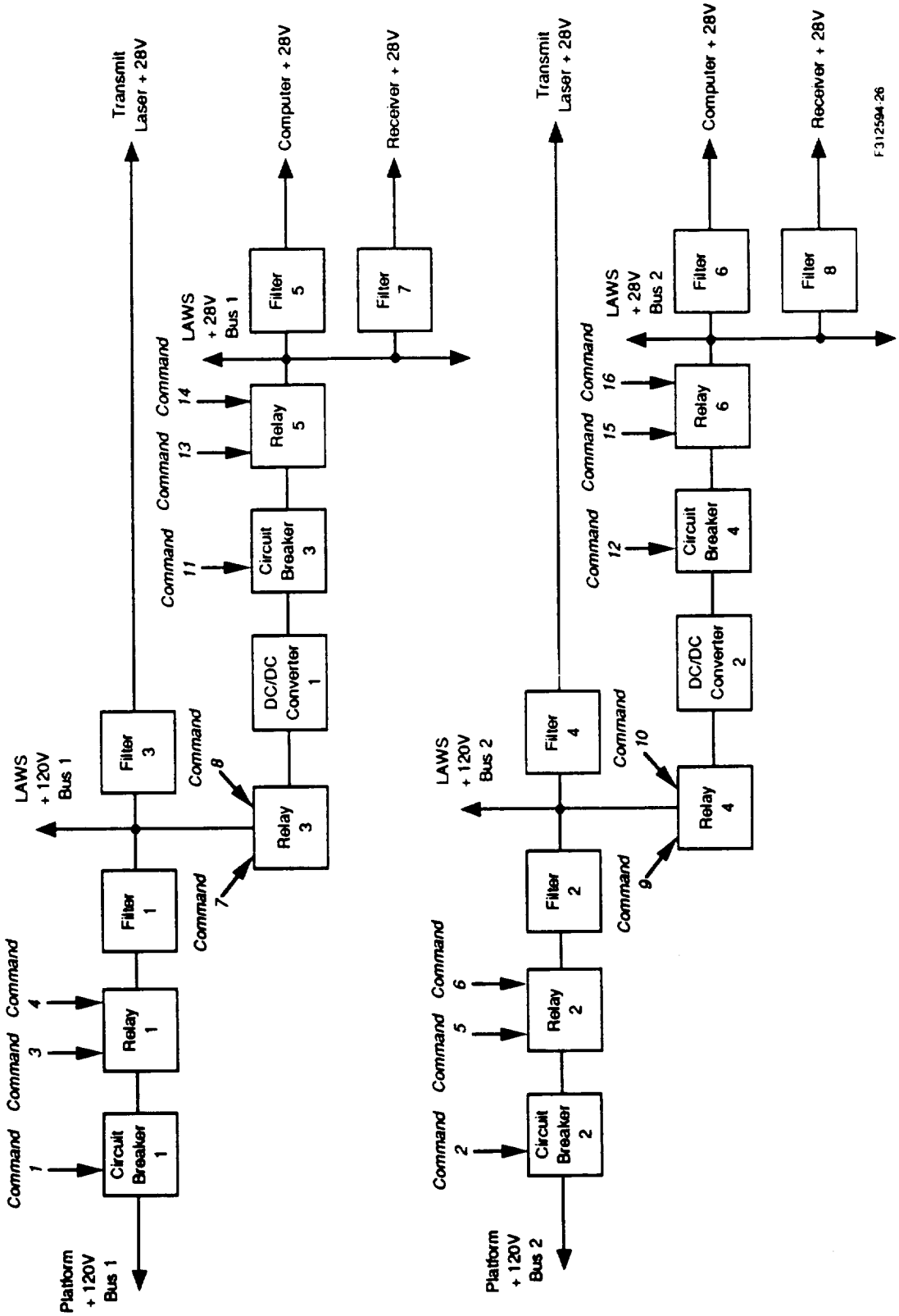

Figure 3-72. LAWS PDS (Commands Indicated)

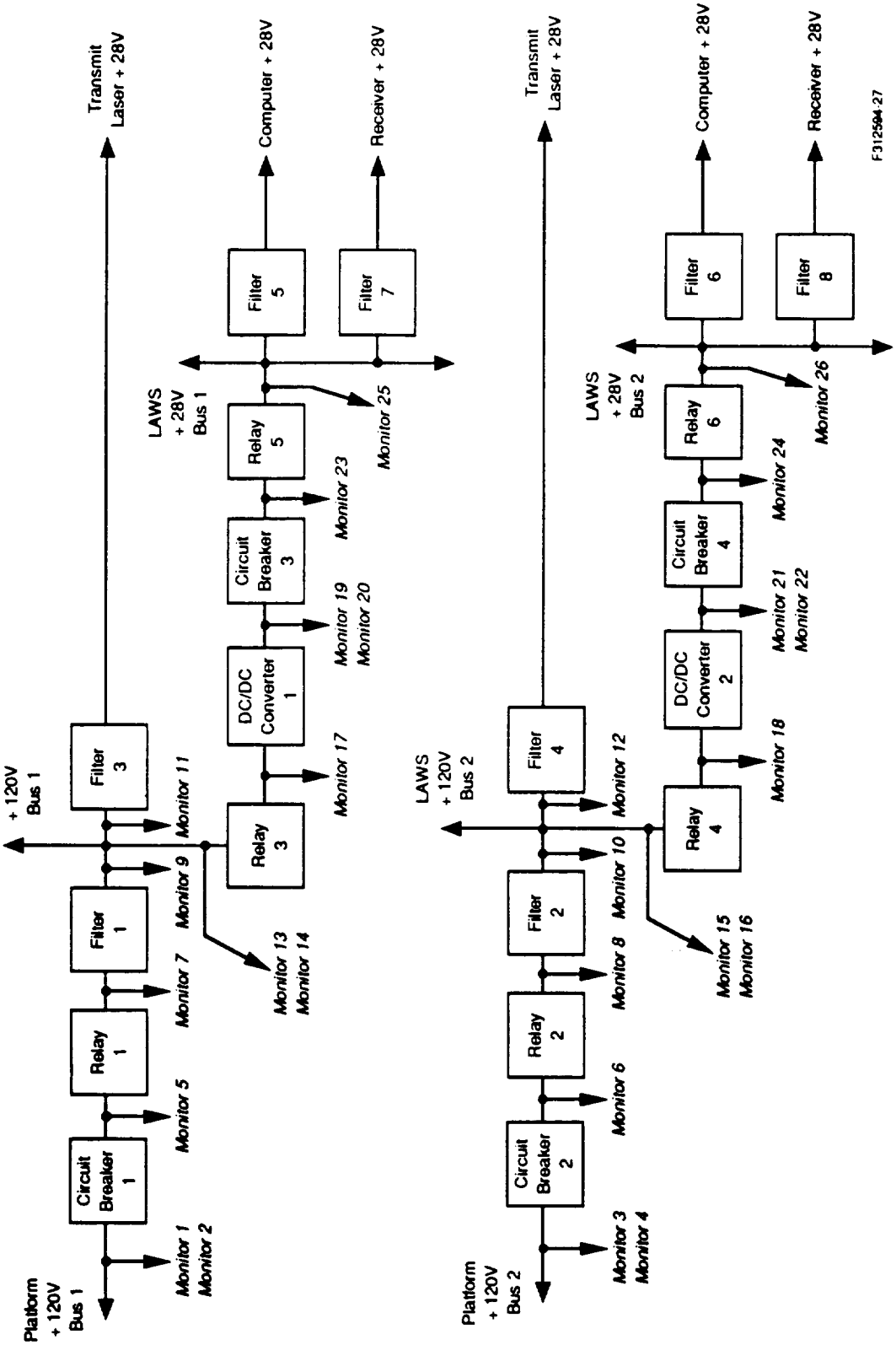

Figure 3-72. LAWS PDS (Monitors Indicated)

Relay 1 and relay 2 disconnect the LAWS Instrument from the spacecraft's 120 Vdc bus. If the spacecraft 120 Vdc bus 1 is utilized, relay 1 is closed. If the spacecraft's 120 Vdc bus 2 is used, relay 2 is closed. Relays 3 and 4 disconnect the converters from the +120 Vdc power buses. The dc/dc converters convert the 120 Vdc buses to two redundant 28 Vdc power buses. Relays 5 and 6 disconnect the 28 Vdc power buses from the LAWS subsystems. All relays in the figure are the latching type.

The spacecraft's 120 Vdc power buses are filtered by filters 1 and 2. In addition, the 28 Vdc power to the individual subsystems is filtered at the PDS output connectors.

3.3.7.2 Commands & Monitors

Location of the commands is shown in *Figure 3-72 (1 of 2)*. The command labeled 1 closes circuit breaker 1 if the breaker trips. Commands 3 and 4 open relay 1 and close relay 1, respectively. The commands are summarized in *Table 3-17*.

Figure 3-72 (2 of 2) shows the monitors in the PDS. The monitors in the PDS are used to monitor the PDS status and isolate PDS faults. Monitors 2, 4, 14, 16, 20, and 22 are current monitors. All others monitors are voltage monitors. Monitors 1 and 5 are used to monitor the voltages at the points where they are located and to determine the status (open or closed) of circuit breaker 1.

3.3.7.3 Redundancy

The individual circuit breakers and relays shown in *Figure 3-72* represent four circuit breakers and four relays. Placing two relays in series protects against a short circuit failure. Placing two relays in parallel protects against an open circuit failure. For example if relay A does not close, the path can be closed by closing relays C and D. Thus, the configuration functions if any one relay becomes stuck closed or open.

3.3.7.4 Cabling

Cabling for the LAWS system is shown in *Figure 4-73* of DR-8. The cables are summarized in *Table 4-19* of DR-8. Power cables from the PDS to the individual LAWS subsystems and data cables from the computer to the LAWS subsystems are included.

3.3.7.5 EMI/EMC

The generation and control of electromagnetic radiation have been considered in the overall design of the LAWS system and in the design, fabrication, and testing of the laser breadboard. The generation of short (i.e., a few μs) energy pulses used to power the laser, if not properly isolated and shielded, provides a relatively high energy source of EMI. In designing the laser, we considered the control of this specific radiation source. Control of EMI is required to prevent contamination of laser cavity match electronic controls as well as overall LAWS Instrument and platform operations.

Table 3-17. PDS Commands

Command	Description
1	Recloses circuit breaker 1
2	Recloses circuit breaker 2
3	Opens relay 1
4	Closes relay 1
5	Opens relay 2
6	Closes relay 2
7	Opens relay 3
8	Closes relay 3
9	Opens relay 4
10	Closes relay 4
11	Recloses circuit breaker 3
12	Recloses circuit breaker 4
13	Opens relay 5
14	Closes relay 5
15	Opens relay 6
16	Closes relay 6

3.3.7.6 Subsystem Summary

Figure 3-73 provides a summary of the electrical power subsystem development.

A ELECTRICAL POWER DISTRIBUTION SUBSYSTEM OVI

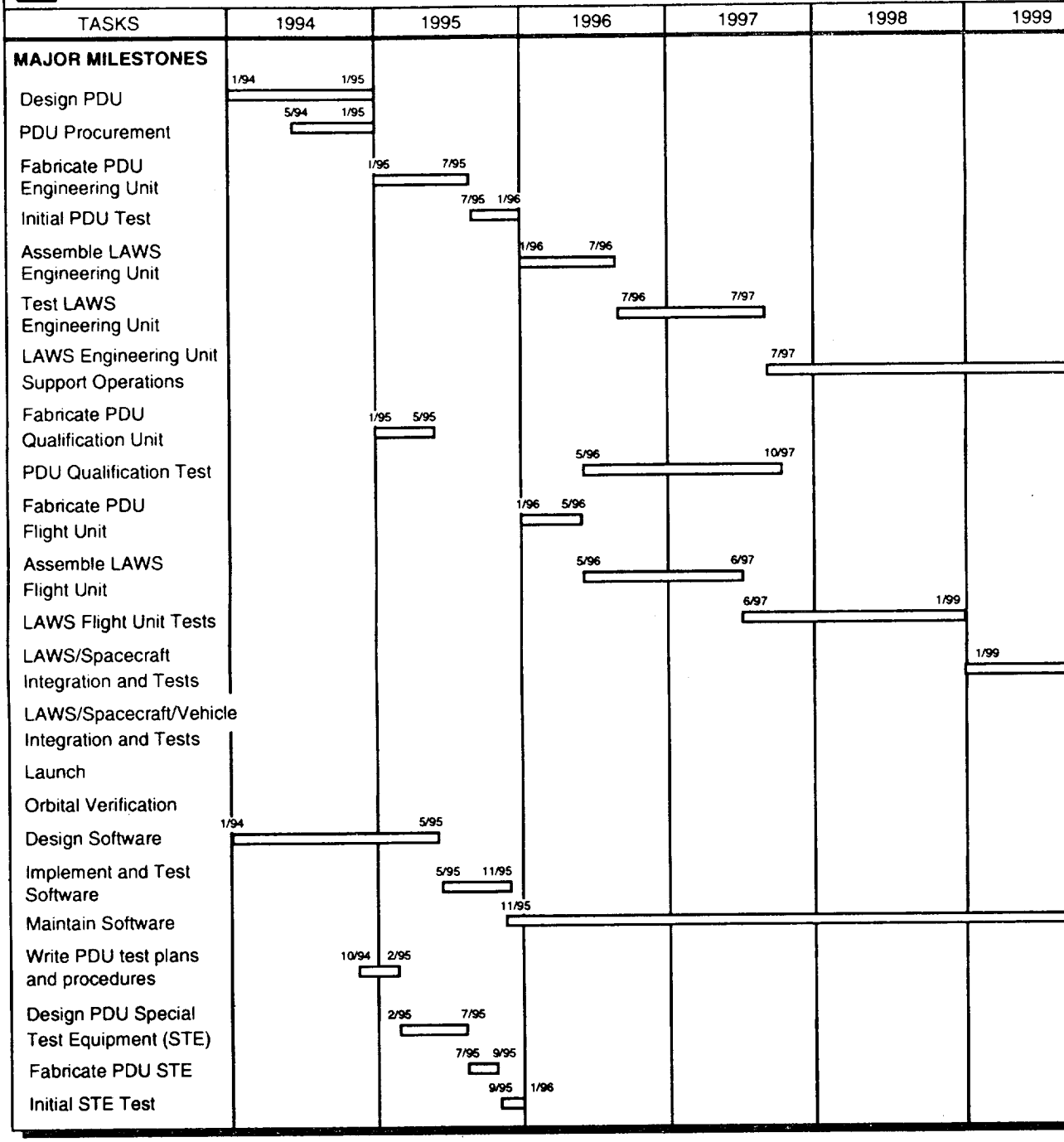

B REQUIRED SUBSYSTEM EQUIPMENT

COMPONENT	SOURCE	MATURITY/HERITAGE	MOCKUPS	ENGINEERING
Power Distribution Unit	LMSC	Modified/HST	1	1
Cables	LMSC	Modified/HST	28	28

FOLDOUT FRAME

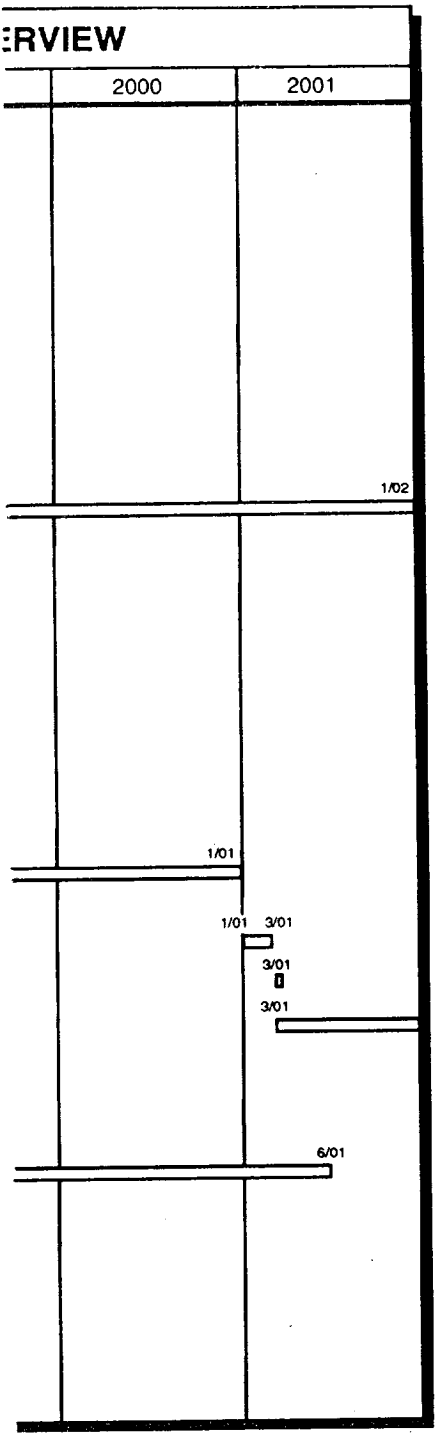

NIT	QUAL. UNIT	FLIGHT UNIT
	1	1
	28	28

F320789-02

C REQUIREMENT IMPLEMENTATION/VERIFICATION

KEY REQUIREMENT	IMPLEMENTATION	VERIFICATION
28 V ± TBD Vdc	dc/dc Converter output voltage = TBD Vdc	A/T
TBD W of power	dc/dc Converter output voltage = TBD W	A/T
Energy storage	Batteries	A/T
Circuit protection	Remotely resettable circuit breakers	A/T
Redundancy	Multiple parallel components in power path; two redundant isolated power busses	A/T

D PLANNED TRADE STUDIES

Distributed vs. centralized power distribution units

E RISK SUMMARY

RISK ITEM	RISK LEVEL	RISK REDUCTION APPROACH
PDU Failure	Low	Space qualified parts, redundancy, system testing

F VERIFICATION SUMMARY

Acceptance, development, and verification testing per MIL-STD-1540

G SI ACCOMMODATION

Standard power control and distribution interface

H DESIGN MARGIN AND GROWTH

Multiple power buses rated for 20% growth in loads

Figure 3-73. Overview/Summary of the Electrical Power Subsystem

FOLDOUT FRAME 2

3.3.8 Command and Data Management Subsystem

The C&DM subsystem baseline design is summarized as follows:

- Hardware implementation
  - Flight computer
  - Communication links
  - Star Trackers
  - Inertial reference unit
- Software modules
  - System management
  - Shot management
  - Communication management.

The flight computer, applying associated software, provides autonomous direction to the LAWS Instrument, controlling when the laser is to be fired to achieve measurements for selected wind components. The flight computer also receives and executes commands from the spacecraft via the BDU and exercises stored math models to compute the time associated with the telescope pointing angles for the laser pulses. Star Trackers (2) are located on the LAWS Instrument baseplate. Outputs from these Star Trackers to the LAWS Instrument are managed by the attitude and position determination elements of this subsystem. The command and data transceiver assembles and transfers data from the LAWS Instrument to the spacecraft for transmission via data relay satellites as depicted in *Figure 3-74*.

All communications with the LAWS Instrument, to and from the spacecraft, and with the NASA control centers are directed through the LAWS C&DM subsystem via the BDU. The few interfaces not controlled by this subsystem are related to the LAWS spacecraft electrical, thermal, and mechanical interfaces. These interfaces, however, are monitored and reported by the health and status instrumentation sensors.

The flight computer controls laser shot management firing commands, computes orbital Platform position location, collects telescope line-of-sight azimuth angle values for each laser shot, provides short time storage of wind data for transmission to the spacecraft data management system and formatting of data into CCSDS format, and performs other command and data management functions.

Decisions for flight hardware and software (command, communication, and control of the system) based on requirements analysis and definition of the associated functions to be implemented and their interrelationships have been completed. The C&DM subsystem encompasses all functions associated with system control, data processing, and communication control. The system operation concept described above shows how this subsystem provides the control and communication management. This subsystem controls system operation and communicates data and commands (see *Figure 3-74* for the location of these functions in the system functional hierarchy).

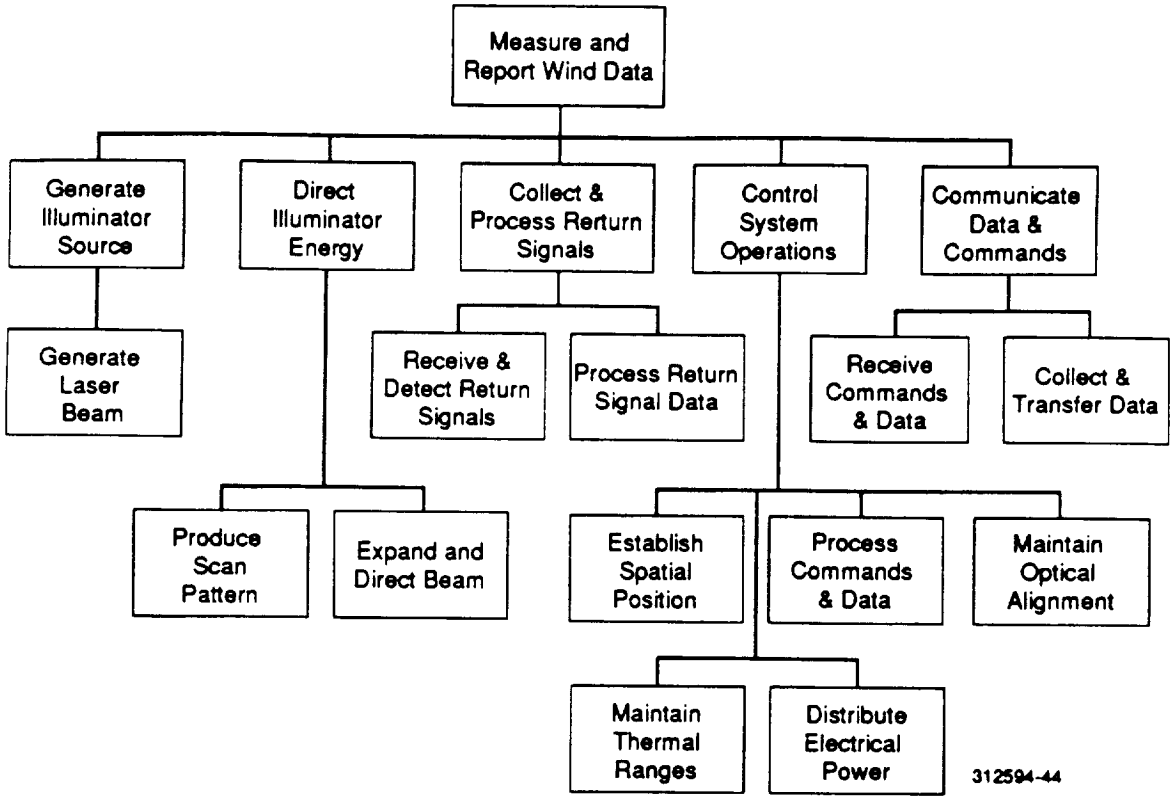

Figure 3-74. LAWS Functional Hierarchy

3.3.8.1 Requirements Analysis

The following system requirements govern this subsystem design:

1. Provide continuous on-board operation
2. Provide a control system
3. Employ shot management to conserve laser life and obtain optimal measurements of the wind vector components
4. Monitor and report Instrument health and status
5. Report measured wind data in Level 0 format
6. Append Platform ephemeris data, ground calibration data, and time to level 0 to create Level 1A data
7. Perform calibration and alignment checks
8. Accept commands from BDU
9. Provide safing control.

Requirement 1 dictates that the LAWS operation be in real-time. Requirement 2 is an all encompassing requirement that says a separate and distinct control must be provided. Requirement 3 is based on analysis conducted in Phase 1. Requirements 4 through 8 are derived from analysis of the "LAWS Data System Preliminary Requirements Review," dated 6 December 1989. The creation of level 1A data is included as an option. Requirement 9 is applicable for all EOS Platform operations.

3.3.8.2 Flight Software Definition

Figure 3-75 identifies the functions to satisfy the operations of the LAWS system and meet the system requirements as identified. These functions have been classified as related to system management, shot management, and communication management. All system management functions are associated with control and implementation of the system operations. Shot management controls the laser pulse operation. Attitude/position determination is a function that supports shot management. It provides Instrument attitude and position data required to correctly fire the laser for a given beam location during a telescope scan. The timing of each laser pulse is derived from logic based determination of attitude, time position in space, and position in the scan. Communication management is concerned with communication between the LAWS Instrument and its host Platform and between the LAWS hardware components. All communications (i.e., commands received from or data transmitted to the ground) to and from the ground station are assumed to be handled by the host Platform. Therefore, the LAWS design communication interface between the Instrument and host Platform is through the BDU.

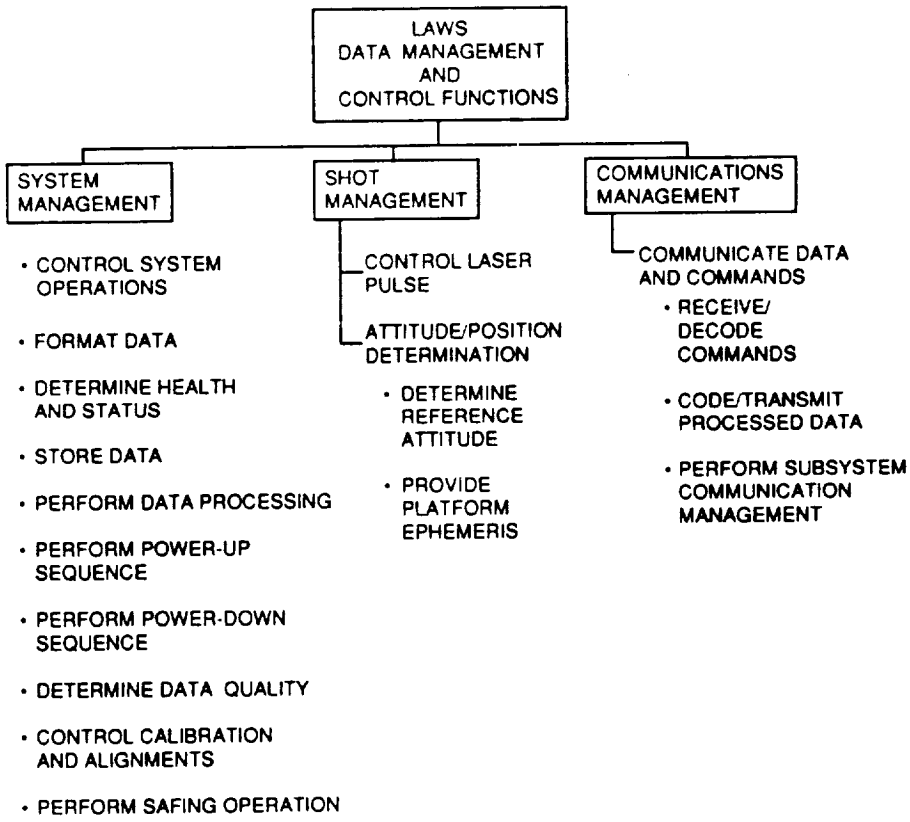

Figure 3-75. LAWS Flight Data Management Functional Hierarchy

3.3.8.2.1 Control of/and Data Flow from Subsystems

Both hardware and software are required to implement the functions identified in *Figure 3-75*. *Figures 3-74* and *3-76* present the LAWS Instrument from a top level systems viewpoint and show the first level of allocations to the hardware components. *Figure 3-76* also indicates the overall flow of signals through the Instrument.

3.3.8.2.2 Flight Computer Functions

The flight computer implements all functions associated with system management, shot management, and communication management. The actual functional implementation is via the flight software identified in *Figure 3-77*. It is assumed the flight software will be a single configuration end item. As shown in *Figure 3-77*, the flight software configuration end item consists of three subelements: the system management module, shot management module, and communication management module. Brief descriptions of these major modules and their submodules are given below.

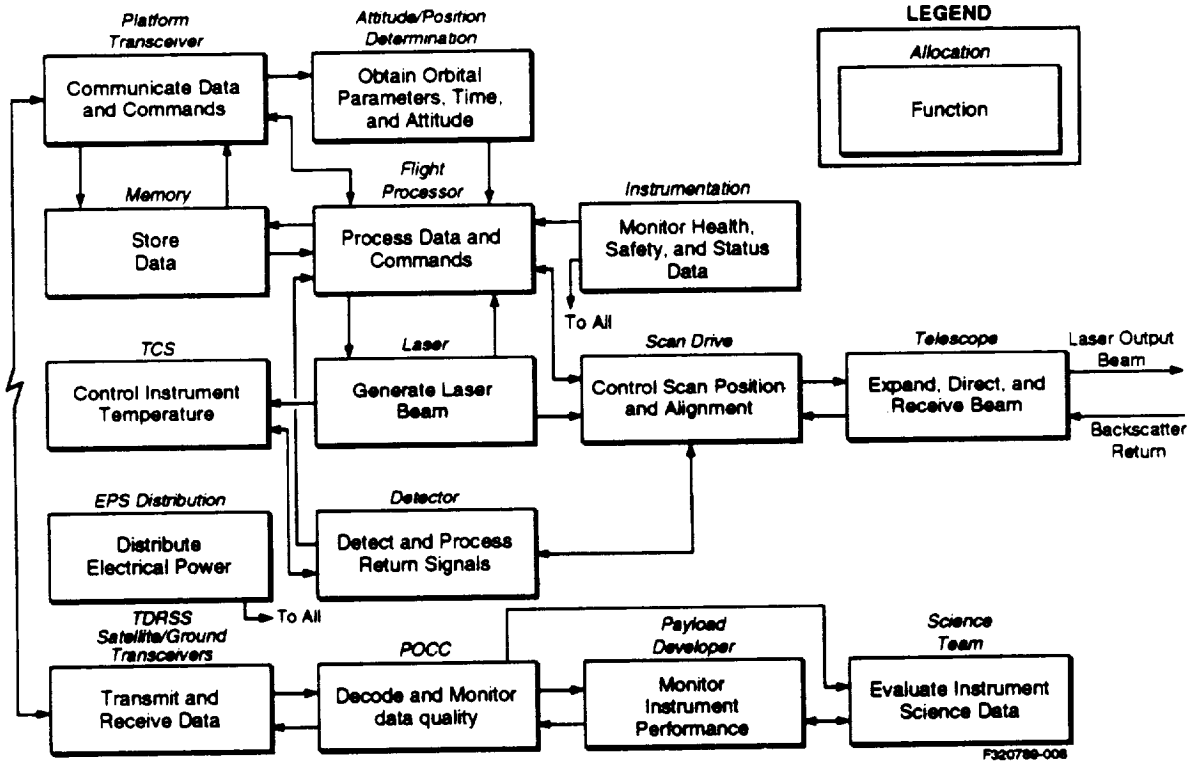

Figure 3-76. LAWS System Functional Flow Diagram

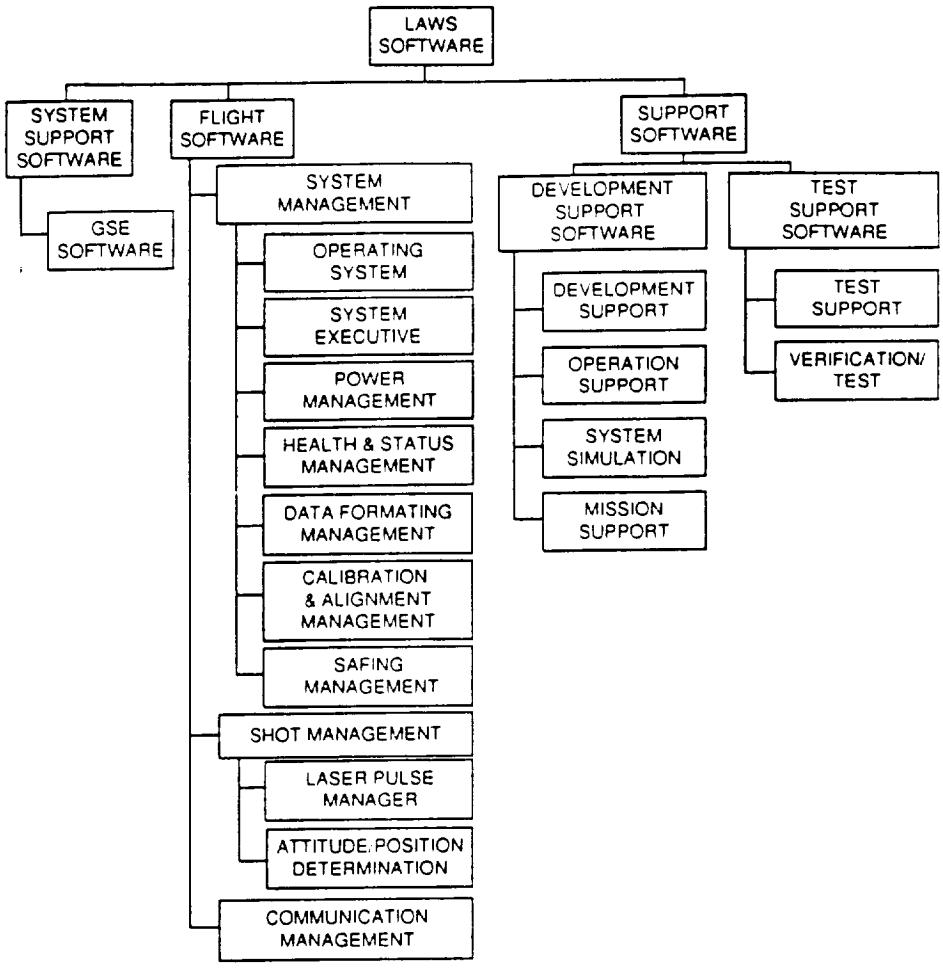

Figure 3-77. LAWS Software Tree

System Management Module. The system management module provides the overall control for operation of the LAWS Instrument. This module is activated at system start-up and operates continuously until the Instrument is powered down. The clock provides the system time. Provisions are included to update the time from either the host Platform or the ground. The time accuracy is currently TBD. Data storage is provided to store system control parameters and Platform ephemeris, and to temporarily store ancillary data and processed data.

System Executive. This module is the system real-time monitor and schedules the activation of other modules to execute the appropriate function. The system executive module accepts ground commands for Instrument status determination. A status message is generated for transmission to the ground receiving station.

Power Management. This module has two functions: (1) initiate and manage the Instrument power-up sequence, and (2) initiate and manage the Instrument power-down sequence.

The modules execute via a preprogrammed sequence for each mode (i.e., power up or power down). When power up is complete, a ready status flag is generated to indicate that the Instrument

is ready for operation. During the Instrument deployment operation, this module manages all operations required to deploy the LAWS Instrument (i.e., the telescope). It also manages locking the telescope in position for reboost.

Safing Management. This module initiates and controls operations required to bring the LAWS to a condition compatible with the Platform requirements.

Health and Status Management. This module maintains the current health and status of the LAWS Instrument. It executes in a background mode on a predefined schedule and polls hardware component status sensors to determine the operational status of each component.

Data Formatting Management. This function generates two data strings: Level 0 data and Level 1A data. All data strings are encoded with the proper "hand shaking" for transmission. Level 0 data includes all Instrument data, which are the digitized data stream, Instrument performance data, and status information. The status information to the Level 0 data is a status indicator. The status indicator denotes routinely and upon command.

Calibration and Alignment Management. This module initiates and controls calibration and alignment checks performed by various hardware elements. Lag angle compensation (tip-tilt) is performed under this function.

Attitude/Position Determination. This module provides the current attitude and position. The reference attitude is obtained from the attitude and position determination system. The Platform ephemeris is obtained from the host Platform and stored for use. The telescope azimuth angle is obtained from the beam scanner assembly.

Laser Pulse Manager. This module contains the logic to compute the timing sequence necessary to correctly generate a laser pulse at the appropriate times.

3.3.8.3 Other LAWS Software

Figure 3-77 identifies three categories of software required for the LAWS Instrument: system support software, flight software, and support software. Flight software is discussed above. System support software includes GSE software. GSE software is any software that will be developed for the GSE. Support software includes any software required to support development of the flight, GSE, or support mission operations. Development support software is primarily the set of case tools used in design of the flight software. Operations support are data bases and software used in Instrument performance evaluation. System simulation is any software used in simulating the Instrument operations. Mission support software is any software developed by the prime contractor to support mission operations. Test support software includes all software used to checkout and verify the flight and GSE software.

3.3.8.4 LAWS Computer Hardware

The computer subsystem will be sized from a detailed analysis of the required computational, interface, and storage functions. Interface functions are delineated above. The computational functional requirement is sensitive to shot management and on board alignment functions. The computer memory requirement is dependent upon the above stated requirements to acquire and store data from such sources as the ephemeris and to reformat from Level 0 to 1A. (This function could be performed on the ground.) If the option selected by the LAWS team is to broadcast frequency spectra data direct from the Platform, the storage requirement could increase significantly. If the LAWS Instrument instead of the Platform is required to provide data storage for down link to EOS facilities, the data storage requirement increases from fractions of a second to several minutes.

The selection of a candidate flight processor was driven not only by computational criteria but also by environmental data. The GIIS Section 11.2, "Flight Environments," was used to provide baseline orbital environments. Previous programs have indicated that the requirements for radiation hardening, single event upset, and single event latchup can be the more important drivers in selecting a flight computer. For this reason, it was desirable to find a previously flown or soon to be flown computer. The unit understudy will fly on an MIT experiment before LAWS. A different generation was flown by LMSC on a Shuttle experiment. It is modular in form and can be configured to meet the LAWS requirements. It has the following features:

- Modular based microcomputer
- Incorporation of fault tolerant and fault recovery circuits
- Radiation harness
  - Total dose
    $> 10^6$ rads SI
    $> 10^{14}$ neutrons/cm^2
  - Transient
    10^9 rads/s functional
    10^{12} rads/s survival
  - SEU
    $< 10^{-10}$ errors/bit/day
  - Latchup immune
- High reliability with "S" level parts.

The operating temperature is -55 to 70 °C or -175 to 70 °C with the use of thermofoil electric heaters. The design accommodates a vibration environment of 30 g's rms in a vacuum of 1E-8 torr.

Special test equipment will be purchased from the manufacturer to support integration and test tasks.

3.3.8.5 Command and Data Management Subsystem Summary

Figure 3-78 provides a summary/overview of the C&DM subsystem development, including a top-level schedule, study and verification plans, risk identification, and related planning information.

3.4 VERIFICATION (TEST & EVALUATION)

3.4.1 Development Test Plans

A complete test program for the NASA LAWS Instrument hardware and software includes plans for development, qualification, acceptance, and prelaunch testing. NASA scientists, assisted by members of the Science Team and Lockheed operations engineers, will also develop plans for tests to be conducted after the LAWS satellite is launched and operating in space.

Development tests have been conducted during the breadboard laser development phase to aid in the selection of suitable materials, components, and assemblies for use in building the operating laser. Additional tests will be performed to validate the use of other materials, hardware components, and assemblies as new tests are performed during the Phase II Extension period.

Development test plans will also be prepared to validate the design of components, assemblies, and software modules developed during the CD Phase. The purpose of these tests is to ensure that the hardware components and software modules produced by these designs meet the qualification test limits imposed by MIL-STD-1540B and perform the measurement functions required by the LAWS Instrument CEI Specification.

3.4.2 Qualification Test Plans

Test plans will be prepared and conducted in Lockheed owned and operated test facilities to demonstrate that the LAWS Instrument hardware and software fully meet the qualification test margins imposed by the requirements of the NASA approved LAWS Instrument CEI Specification and MIL-STD-1540B. The sequence of tests to be conducted is shown in *Figure 3-79*. Component qualification tests will be conducted to verify that components and assemblies, built in accordance with the approved LAWS Instrument design, can withstand the rigors of qualification tests as individual elements.

A C&DM REQUIREMENTS/VERIFICATION

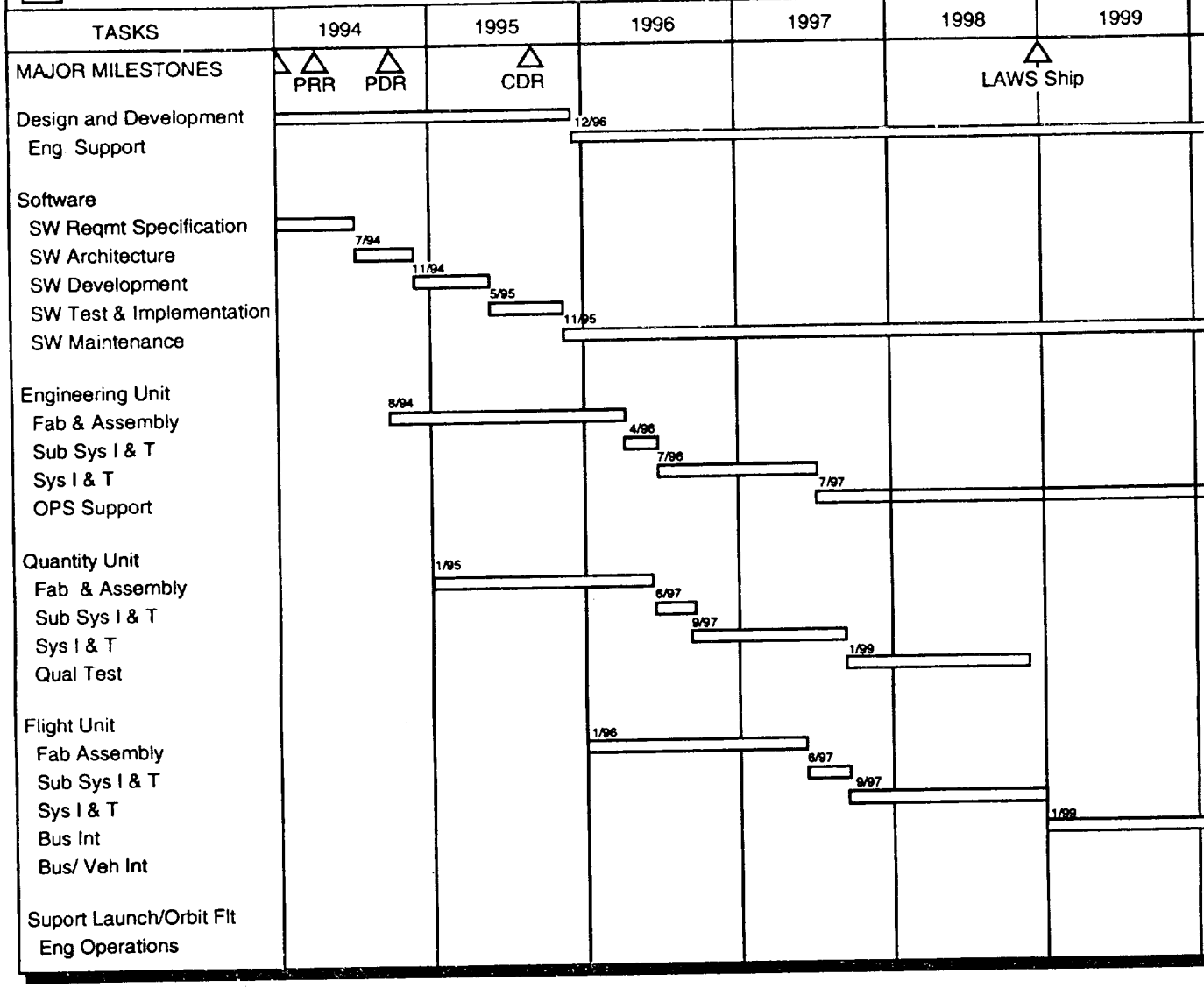

B REQUIRED COMMAND AND DATA MANAGEMENT SYSTEM EQUIPME

Component	Source	Maturity/heritage	Bread-boards*	Development Units
Flight processor	NASA	Modified NASA/ESs		2
Observatory bus interface unit			0	2
Oscillator	Lockheed	Modified HSI	0	0
So Atlantic anomaly detector		Modified/HEAO-2	0	1

*Number of cards to be bread boarded

FOLDOUT FRAME

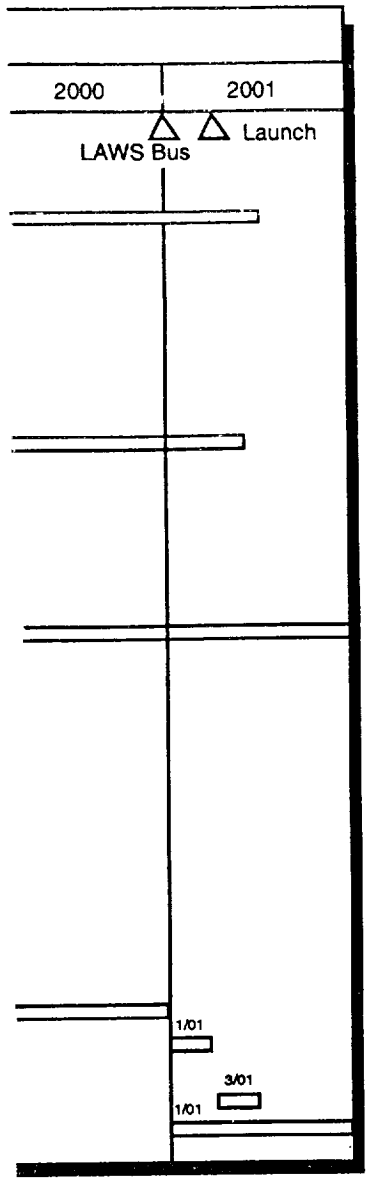

T	
light Units	Spares
1	1
1	
2	1
2	0

C REQUIREMENTS IMPLEMENTATION/ VERIFICATION

Requirement	Implementation	Verification
Merge ENG and SCI data	FP, BDU	T, S
Selectable fixed and programmable telemetry formats	FP	T
Command decoding with error detection	FP	T
Digital processing with 100% margin	FP	A, I
Timing accurate to 10^{-9} in 24 hr, time coding to within 100 µsec of UTC	FP, BDU Oscillator	A, S
High energy protect	MCU, OBS BDU, SAAD	T, A

*A = Analysis/simulation, I = inspection, S = Similarity, T = test

D PLANNED TRADE STUDIES

Structured vs. object oriented tech.
ADA vs C language

E RISK SUMMARY

Risk Item	Risk Level	Risk Reduction Approach
Command processing	Low	Utilize existing designs as applicable. Engineering Specialist (ES) to monitor process flow.
TLM format and rates	Low	Utilize existing formats as available, provide hardwired contingency format. ES to monitor process flow.
Computer processes	Medium	New S/W design – ES to evaluate HW/SW design.
Subsystem integration	Low	Identified hardware/ software test facility. Critical path monitored by ES. Assure QA surveillance of parts used.
Safe mode control	Medium	Minor modification to existing design. ES to monitor standard process flow.

F VERIFICATION SUMMARY

Development tests

FP development test

Purpose: establish functional FP operation

Equip required: development unit, MCU development cards, test equipment

Integrated avionics test

Purpose: establish functional CDMS operation of the MCU with BIUs via the serial bus

Equip required: tested MCU dev unit, a tested OBS BIU development unit, a tested SI BIU development unit, a non-flight-item oscillator, a vehicle systems simulator, and the MCU test equipment

Environment: ambient

SAAD development test

Purpose: establish functional SAAD operation

Equip required: SAAD dev unit and standard digital test equipment

Environment: ambient

Qualification/acceptance tests

On units shown above

Purpose: individual equipment qualification

Equipment required: per unit as shown above

Environment: ambient, thermal vacuum, thermal cycle, vibration, and EMI

G SCIENCE INSTRUMENT ACCOMMODATION PLAN

South Atlantic anomaly detector provides warning to instruments based on software selectable thresholds.

Safe mode power control commands backup primary science instrument power switching system.

H DESIGN MARGINS AND GROWTH

Processor sized to ensure 100% margin in worst case: average processor margin is 240%

Memory sized to ensure 100% margin in worst case; average margin provided is 260%

Serial bus provide 320% margin at 1 MHz

Bus design allows for additional BIUs

BIU design allows command and telemetry to be added in discrete increments by adding appropriate cards

Modular design allows the incorporation of new technologies

Figure 3-78. Overview/Summary of the Command and Data Management Subsystem

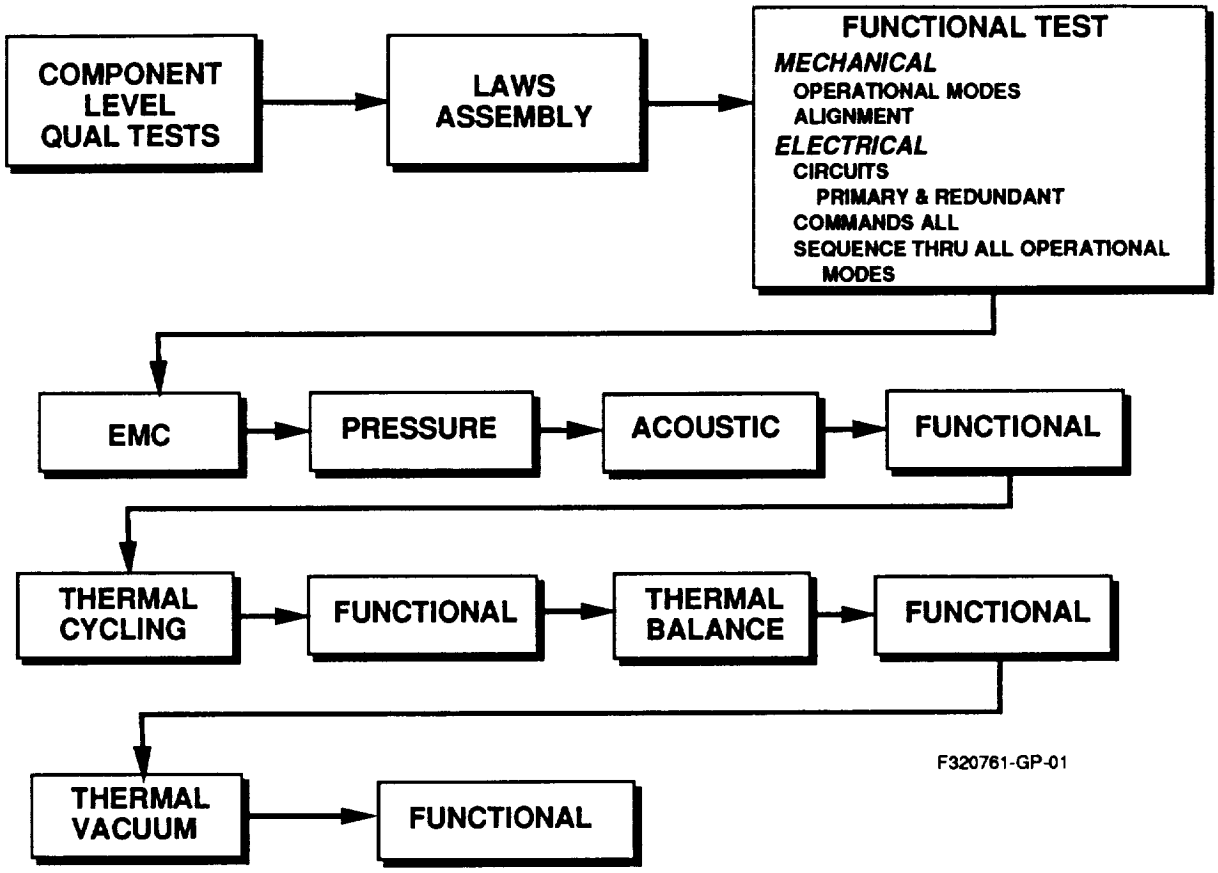

Figure 3-79. Vehicle Qualification Tests

After all of the components have been tested as shown in *Figure 3-80*, and have satisfactorily met the component qualification level test criteria, the components and assemblies will be assembled into a complete LAWS Instrument qualification test assembly. This assembly will be mechanically and optically aligned and functionally tested before formal qualification tests proceed. These functional tests will be repeated after scheduled test sequences are completed to verify that the test results show no degraded performance characteristics due to stresses imposed by the qualification tests.

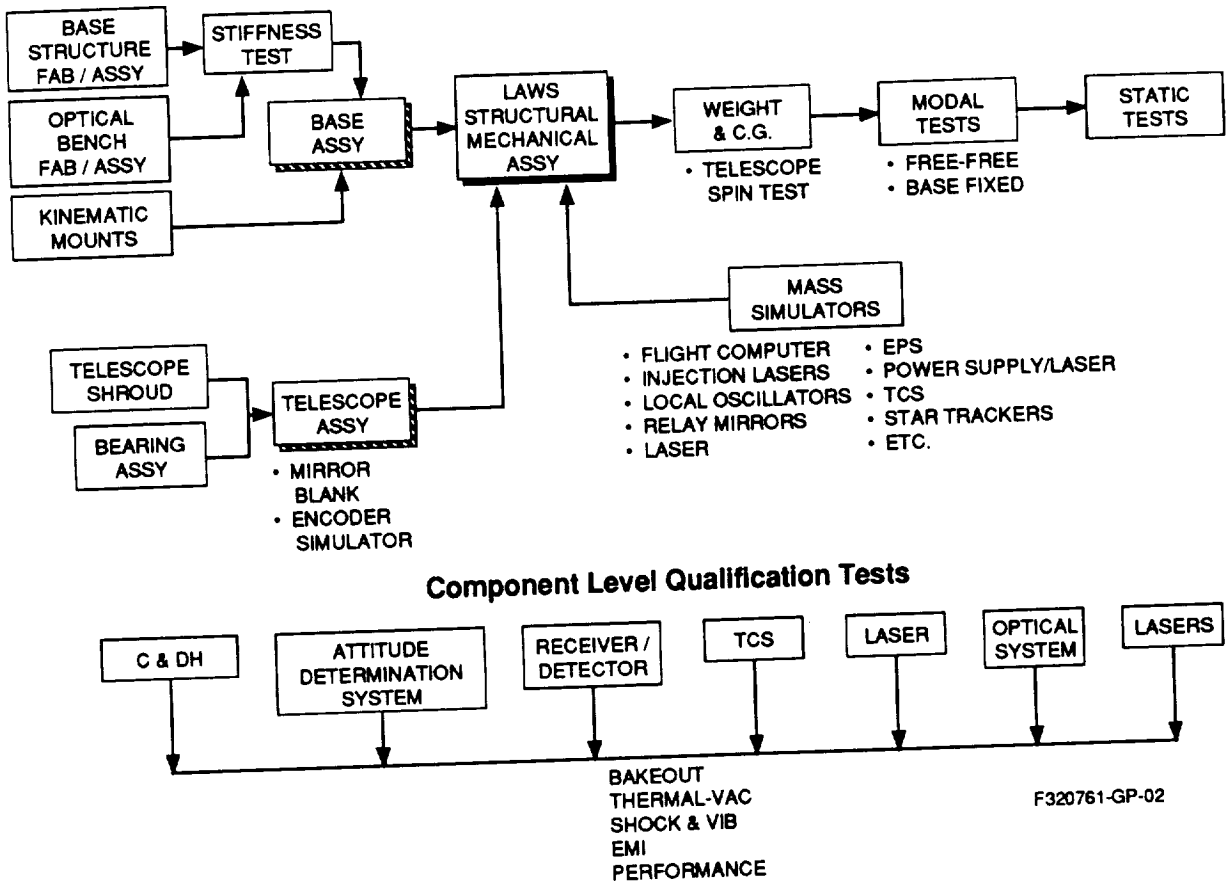

Figure 3-80. Component Qualification Tests

3.4.3 Acceptance Test Plans

Acceptance tests will be conducted on the LAWS Instrument flight hardware, as shown in *Figure 3-81*, to demonstrate the flight-worthiness of the Instrument hardware and software.

These tests will rigorously exercise all flight software controlled sequences and computations, as well as the electrical and mechanical operations. All functions to be performed in space by the Instrument or the space platform will be duplicated to simulate all Instrument operations as closely as possible in a one-g environment. Test plans, prepared in accordance with MIL-STD-1540B, will be presented to NASA for concurrence and approval before the Flight Acceptance Tests are conducted. Records of these tests will be collected for comparison with data collected when the Instrument is integrated with the Space Platform.

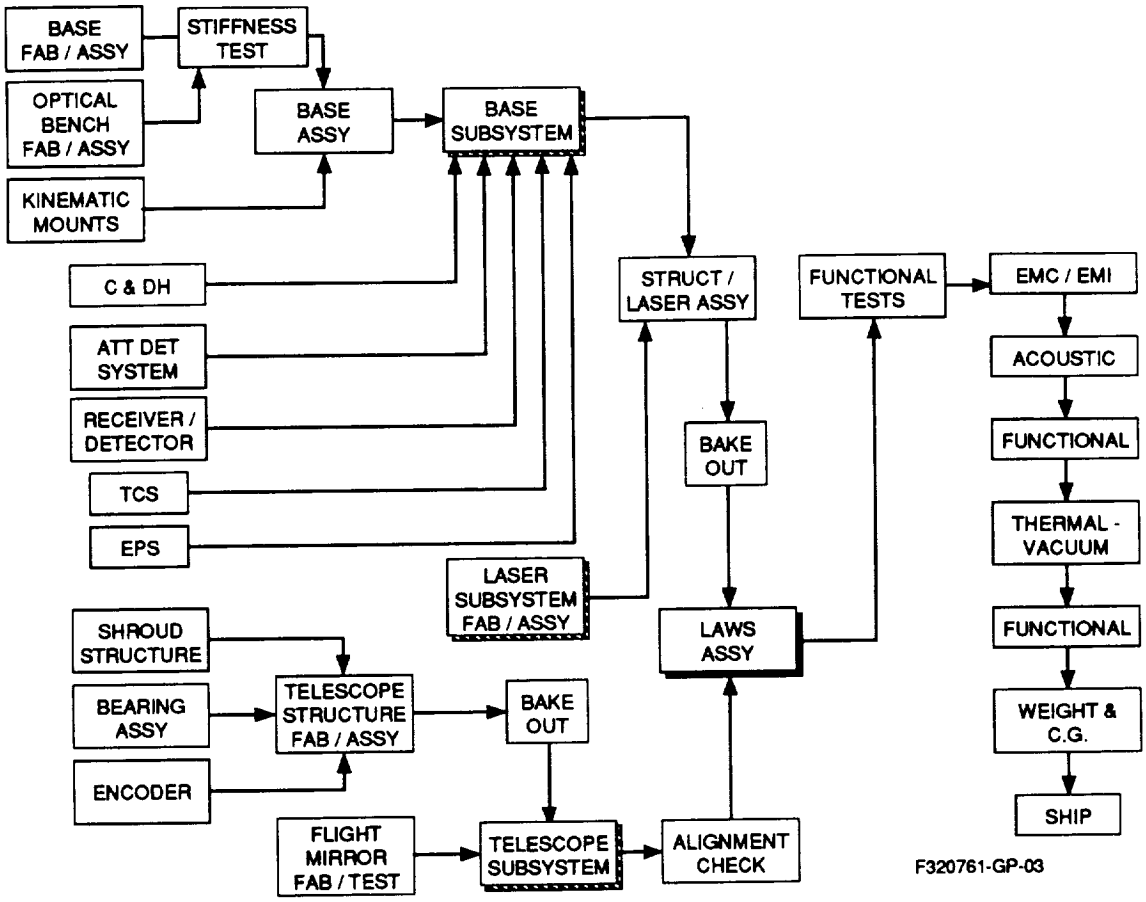

Figure 3-81. Flight Unit Acceptance Tests

3.4.4 Prelaunch Validation Test Plans

Test data, resulting from tests conducted on both the Space Platform and the LAWS Instrument, will be closely examined for interconnection compatibility before the two are physically and electrically interconnected. The planned test sequence will progressively verify all physical clearances for the operational modes before powered drive sequences are initiated.

Every operational command sequence will be exercised and data transfer links will be operated as they will be operated in space. Remotely commanded optical and mechanical alignment of the LAWS Instrument will be tested and calibrated. All health and status sensors and transducer circuits will be checked for validity and calibration. Software self-test sequences will be tested and verified.

Launch stowage conditions will be checked, and the programmed sequence required to begin the operation of the Instrument in space, after the satellite orbit has been established, will be verified. The Instrument stowage and recovery operation required for the reboost operation will also be verified.

3.4.5 Documentation

Test procedures will be prepared for all tests to be conducted to prepare the NASA LAWS Instrument for launch and operation in space. These tests will document component development, qualification, acceptance, prelaunch validation, and software tests.

A Contamination Control Plan will be prepared to control the accumulation of particulant and non-volatile residue contamination on Instrument flight critical surfaces during fabrication, assembly, test, integration, launch, and operation in space. A Safety Plan will be prepared to assure the safe operation of the Instrument during all test operations.

3.5 OPERATION REQUIREMENTS AND SCENARIOS

The EOS GIIS defines the mission phases and the EOS Platform modes of operation. The services provided to the experiments during each mode of operation are discussed in the EOS GIIS. The primary operating constraints of the LAWS Instrument are driven by the services provided by the EOS Platform in each operating mode. *Table 3-18* shows each mission phase, platform mode, platform supplied support (LAWS constraints), LAWS mode, LAWS activities, and LAWS support requirements. Two platform modes of operation are not included: boost-deboost mode and orbit adjust mode. It is assumed that during these phases the LAWS Instrument will enter into the survival mode.

3.6 PERFORMANCE ANALYSIS

There are two aspects of LAWS performance: signal-to-noise ratio (SNR) performance and scanning performance.

SNR Performance. *Figure 3-82* shows the SNR equation used to evaluate LAWS Instrument performance. The equation is narrowband SNR. The rationale for selection of telescope diameter and laser pulse energy is presented in Section 3.2. Given these selections, the primary effect of system design on SNR performance is contained in the optical efficiency. *Figure 3-83* shows how the elements which contribute to optic efficiency are built up into the overall optic efficiency. The contributors to transmit and receive optics efficiences are clearly identified. The derivation of the receiver-related elements (i.e., mixing efficiency and effective quantum efficiency) are discussed in Section 3.3.3.

Scanning Performance. Scanning performance is controlled by the scanning requirements and by the limitations on power to the Instrument. In the following paragraphs,the first discussion is related to scanning performance during the portion of the year when the orbit is not occultated.

Table 3-18. Operating Modes, Mission Phases, and Support Requirements (1 of 2)

Mission Phase	Platform Mode	Platform Supplied Support (Constraints)	LAWS Mode	LAWS Activities	LAWS Support Requirements
1.0 Prelaunch	Ground test	Power low rate telemetry Low rate commanding	Final checkout mode	1. Final subsystem checkout: • Instruments configured to power "off" • Mirrors "caged" • Survival heaters "on" • Confirm communication link between LAWS computer and EOS computer • Power-off LAWS computer	Requirement: 1. Power: TBD W 2. Telemetry link 3. Command link
2.0 Launch/Ascent 3.0 Orbit Acquisition Initialization	Launch mode Acquisition mode	None 1. Power to heaters 2. Essential S-band telemetry 3. Essential preprogramed commands	Launch mode Acquisition mode	None 1. Establish communication link between LAWS computer and EOS computer 2. Supply power to survival heaters	1. Power: TBD W 2. Command link 3. Telemetry link
4.0 Orbit Acquisition	Standby mode	1. Power to support non-science activities 2. Low rate telemetry support	Orbit acquisition mode	1. Power-up LAWS subsystems 2. Begin preprogrammed turn-on sequence for LAWS Instrument 3. Spin-up telescope and momentum compensator 4. Begin conditioning of catalyst 5. Begin preprogrammed verification activities	1. Power: 609 W 2. Low rate telemetry link 3. Low rate commanding link
5.0 Operational Initialization	Standby	1. Complete activation of observatory 2. Complete checkout of all observatory functions and systems	Verification mode	1. Complete orbital verification of LAWS Instrument 2. Establish high data rate transfer link 3. Establish command transfer link 4. Internal alignments 5. Internal calibrations	1. Power: ~2.2 kW average/ orbit 2. Low and high rate telemetry link 3. Low rate commanding link 4. Command transfer link

Table 3-18. Operating Modes, Mission Phases, and Support Requirements (2 of 2)

Mission Phase	Platform Mode	Platform Supplied Support (Constraint	LAWS Mode	LAWS Activities	LAWS Support Requirements
6.0 Operational	Science mode	1. Fine attitude control 2. High rate data handling (storage and transfer) 3. Full electrical power 4. Centralized thermal control	Survey mode	1. Laser PFR 4.63 - 7.27 Hz 2. Continue internal alignments & calibration as required 3. LAWS Instrument fully operational	1. Power: ~2.2 kW average/ orbit 2. Low and high rate telemetry links 3. Data storage: Max: ~8.5 E +9 bits/2 orbits
			Design mode	1. Laser PFR 10 - 15.7 Hz 2 & 3 see above	
			Stand-by mode	1. Laser PFR = 0	1. Power: 609 kW 2. Low rate telemetry 3. Low rate commanding
	Safe mode	1. Survival heater power only	Safe mode	Preprogrammed ordered shutdown of LAWS Instrument to be completed in TBD minutes after platform initiation	1. Power: TBD survival heaters only
	Survival mode	1. Low rate commanding 2. Low rate telemetry 3. Essential power	Survival mode	1. Preprogrammed ordered shutdown nonessential systems	1. Power: TBD 2. Low telemetry 3. Low rate command
7.0 Disposal			Disposal	1. All systems shutdown and secured for controlled reentry	1. Power: TBD* 2. Low rate commanding* *Needed until verification of orderly shutdown and systems secured

$$SNR = \frac{1}{h\upsilon}\ \frac{\pi D^2}{4R^2}\ J\ \frac{c\tau}{2}\ \beta\ \frac{[\text{Absorption Effects}]}{[\text{Turbulence Effects}]}\ [\text{Efficiencies}]$$

Where:

$h\upsilon$ = Photon Energy = 2.18E - 20 J (for 9.11 μm)

$\frac{\pi D^2}{4}$ = Aperture Area

J = Pulse Energy

$\frac{c\tau}{2}$ = Pulse Half Length (for Distributed Target)

R = Range to Target

β = Backscatter Coefficient (Given)

Absorption Effects (Given)

Turbulence Effects (Small Number at these Ranges)

η = Combined Efficiencies

For LAWS

$\eta = \eta$ Transmit Optics $\cdot\ \eta$ Receiver Optics $\cdot\ \eta$ Heterodyne Efficiency $\cdot\ \eta$ Effective Quantum Efficiency

312500-32

Reference: EB23/W. Jones, November 1990, Modification for Turbulence to D. Emmitt's October 1990 memo.

Figure 3-82. Signal-to-Noise Ratio Equation Used to Evaluate LAWS Instrument Performance

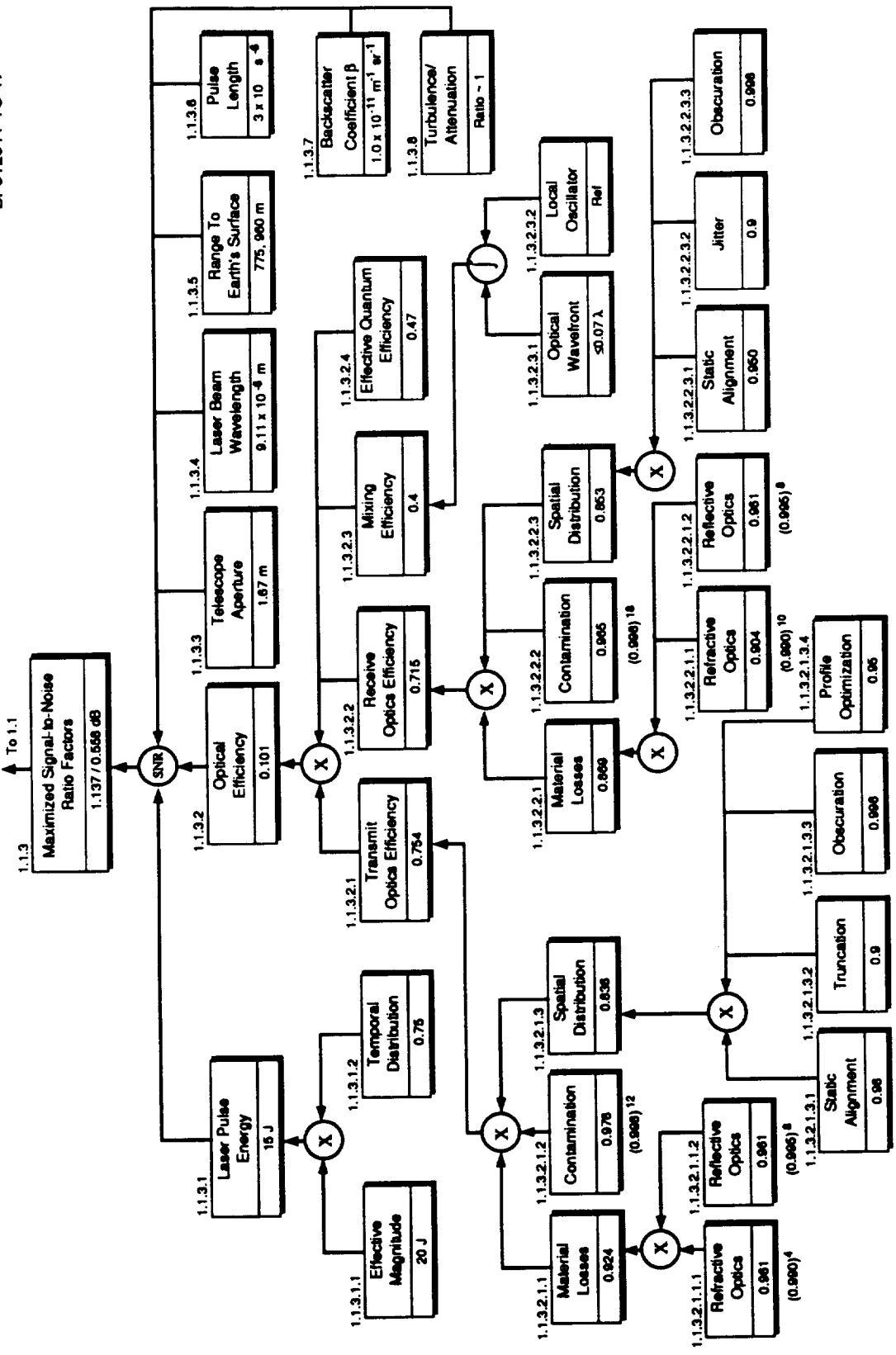

Figure 3-83. Contributing Factors for Maximized Signal-to-Noise Ratio

Survey Mode. The basic scanning mode is the survey mode, which requires three shot pairs per 100 km by 100 km grid square, with the grid aligned along the satellite ground track. In order to give a good distribution of shots throughout each grid square, the scan rate has been selected to give two scans per 100 km of ground track at the satellite altitude of 525 km. This results in a scan rate of 8.43 rpm or 7.12 s per scan. The shot schedule was then selected to give a uniform distribution of shots in the lateral direction. *Figure 3-84* shows the shot pattern for the survey mode. The first scan for each grid square makes shots at 50, 117, 183, 250, 317, 383, 450, and 517 km from the satellite ground track. The second scan for each grid square makes shots at lateral distances of 17, 83, 150, 217, 283, 350, 417, 483, and 55 km from the satellite ground track. The figure shows that each shot has a ground track of approximately 24 km for measurements from 20 km altitude to the earth's surface. For each 100 km of ground track for the survey mode, the instrument takes 66 shots in 14.24 s, resulting in an average pulse repetition frequency (PRF) of 44.63 Hz. The maximum PRF is 7.27 Hz for forward and aft shots near the satellite ground track.

Design Mode. The design mode requires a scan-average PRF of 10 Hz. For a uniform distribution of shots across the swath, a maximum PRF of 15.7 Hz would be required, requiring a maximum power of 5844 W. *Figure 3-85* shows a limitation of 4800 W during the non-occultation period. Therefore, the power limitation of 4800 W imposes a non-uniform distribution of shots across the swath. The design mode has been selected to operate at a PRF of 12.57 Hz (maximum achievable with 4800 W of power) in the center portion of the scan and to provide uniform distribution of shots in the outer portion of the scan so that the overall average PRF is 10 Hz. This produces a shot density of 10.4 shots per grid at the center of the swath and a shot density of 13.1 shots per grid at the edges of the swath. *Figure 3-86* shows the times and lateral distances at which shots are made for a half scan.

Operation During Occultation Portion of the Year. *Table 3-19* summarizes LAWS scanning performance constrained by available power. As discussed above, scanning performance during the days when occulation does not occur are shown. For the days in which occulation occurs, the survey mode is not contrained during darkness, and some design mode operation is possible. *Figure 3-85* shows the maximum available power during daylight during days in which occultation occurs. During operation in light, the survey mode is constrained as shown in the table, and design mode operation is not possible.

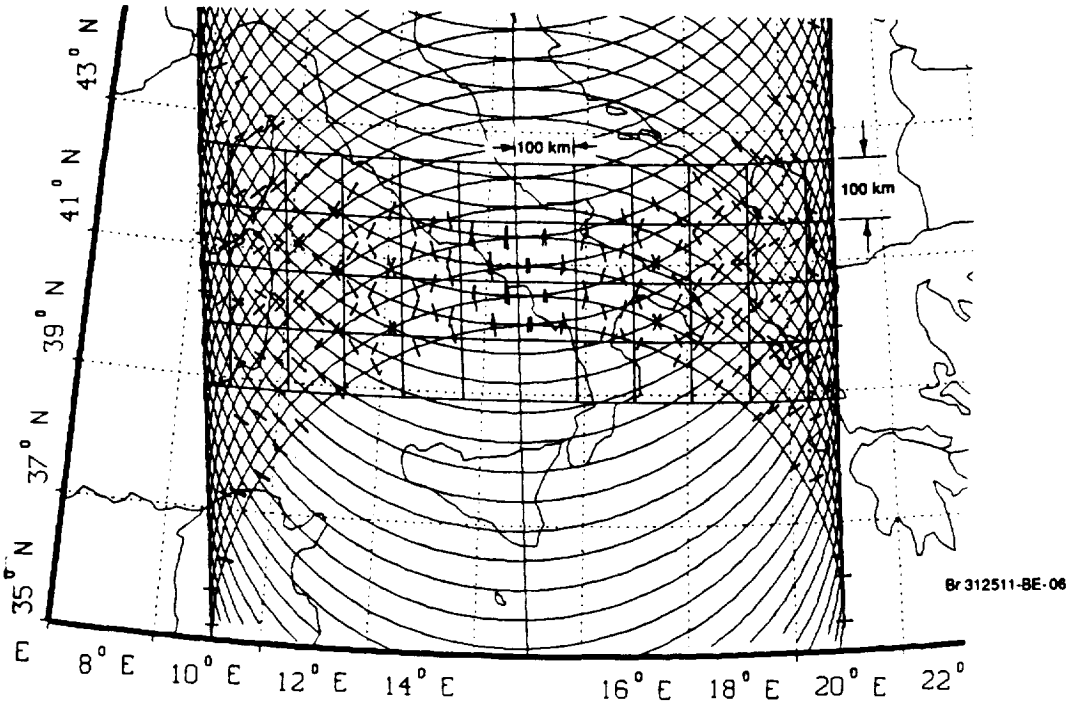

Figure 3-84. Survey Mode Shot Pattern Showing Forward Looking and Aft Looking Shots

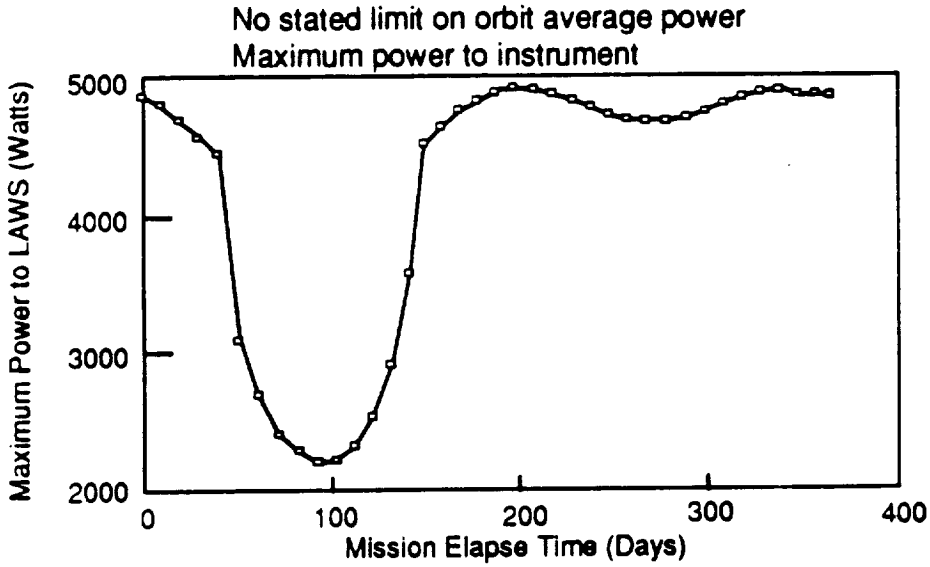

Figure 3-85. Maximum Power Available for LAWS Experiment, Sun Synchronous Orbit, 0600 Descending Node Crossing

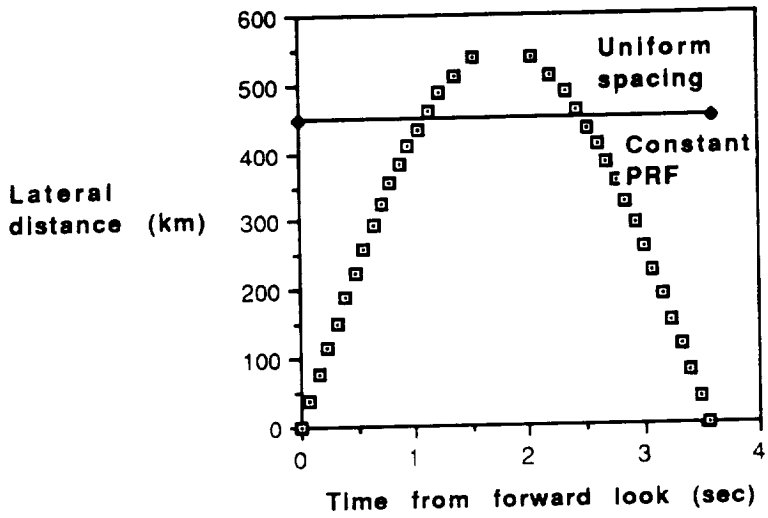

Figure 3-86. Shot Schedule for Design Mode with Instrument Power Limited to 4800 W

Table 3-19. LAWS Operational Characteristics Constrained by Available Power

	Non-occultation		Occultation (≈100 days)			
			Dark		Light	
	Survey	Design	Survey	Design	Survey	Design
Maximum Instantaneous Power Available (watts) note (1)	4800	4800	6497	6497	2200	Not Possible
Scan Average Power (watts)	2146	3924	2146	3924	1920	
Maximum Instantaneous Power (watts)	3022	4800 note (2)	3022	5844	2200 note (3)	
Heat Rejection Rate (watts)	2013	3702	2013	3702	1995	
Orbit Average Heat Rejection with No Design Mode (watts)	1722		1722		1703	
Orbit Average Heat Rejection with 1615 sec Design Mode (watts)	2200		2200	note (4)	2185	
Orbit Energy Balance						
Time per orbit (hrs)	1 59		0 36		1 23	
Avail at LAWS (watt-hrs) (assumes 4800 watts in sun)	Not constrained by orbit energy balance	Not constrained by orbit energy balance	0		5904	
Used for LAWS (watt-hrs)			773		2362	
Avail for Storage (watt-hrs)			0		2504 note (5)	
Used from storage (watt-hrs)			773			
(amp hrs @ 26.8 volts)			28.8			
Battery storage cap (amp hrs)			130			
Charge Current (amps)			-80		23.4	

Notes
(1) Maximum instantaneous power defined by "bowl" chart
(2) For uniform distribution of shot across swath, max. power is 5844 watts. Max. available power imposes non-uniform distribution of shots across swath. Average PRF of 10 Hz required for design mode is met
(3) For uniform distribution of shots across swath, max. power is 3022 watts. Max. available power imposes non-uniform distribution of shots across swath. Shot density is 3.9 shots/grid at center of swath and 6 shots/grid at edges of swath
(4) Orbit energy balance is defined by survey mode during occultation. Some design mode operation is possible.
(5) Efficiency of solar to battery to load process is 0.707 that of direct solar to load process.

Section 4
WORK BREAKDOWN STRUCTURE

Figure 4-1 provides the top-level work breakdown structure for the LAWS Instrument. A complete WBS depicting hardware and software to be developed and produced, services to be performed, and data to be submitted during the Phase C/D contract is provided in Volume III of this final report and separately as DR-5. These documents provide a WBS tree to the required levels, a WBS index, and a WBS dictionary.

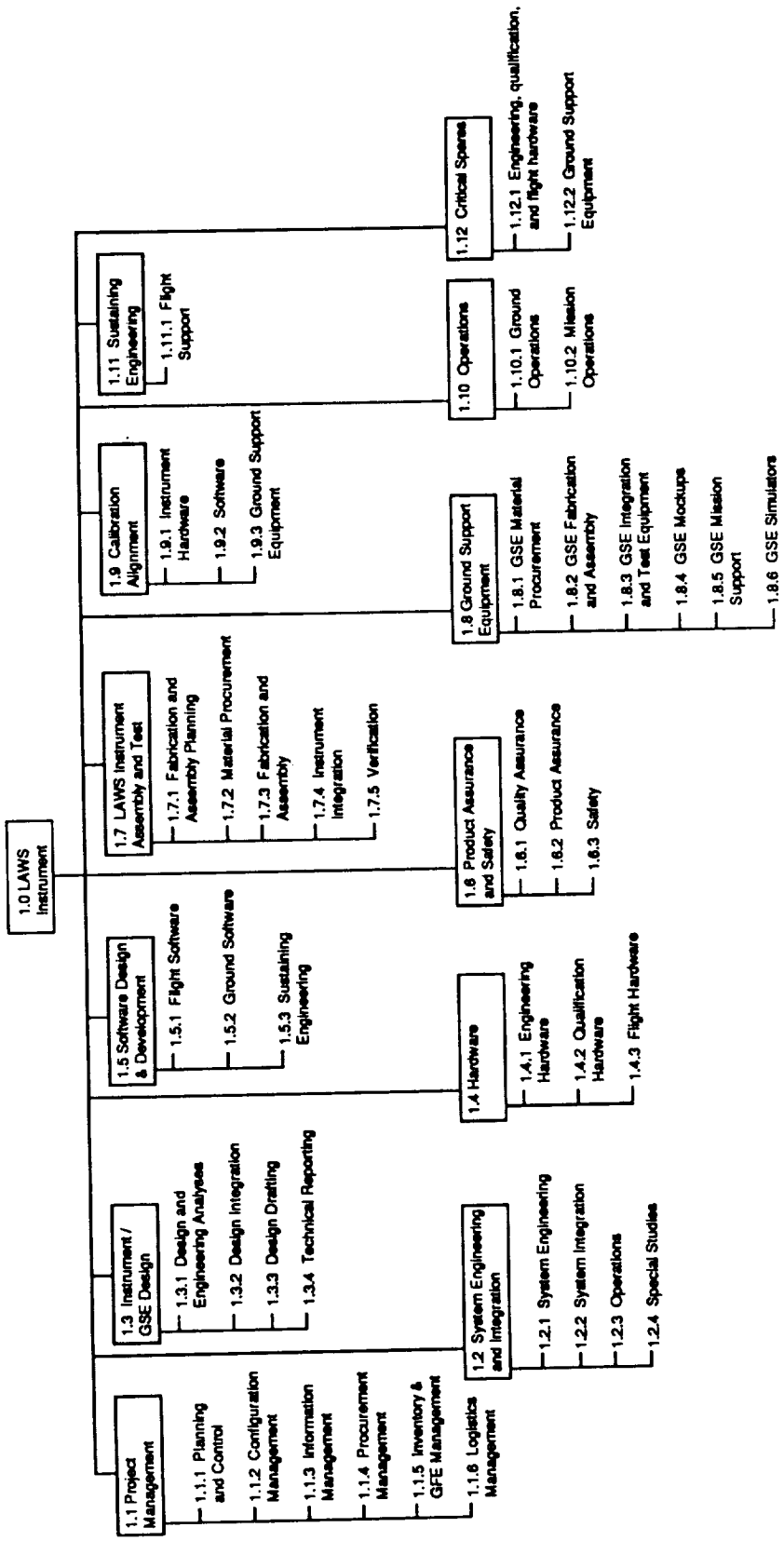

Figure 4-1. WBS 1.0 LAWS Instrument

Section 5
ENVIRONMENTAL ANALYSIS

This section briefly identifies LAWS program suggested actions and alternatives, and their environmental effects.

5.1 ACTIONS AND THEIR ALTERNATIVES

The LAWS Instrument will be transported into low Earth orbit via an Atlas IIAS. This LAWS Instrument will not be returned to Earth for any reason other than burn-up during its de-orbit to Earth.

During the orbital mission, a small quantity of benign gases will occasionally be vented to exoatmosphere. These gases include helium, nitrogen, and carbon dioxide. No other viable alternatives to this program have been identified at this time.

5.2 ENVIRONMENTAL IMPACT OF THE ACTIONS AND THEIR ALTERNATIVES

For the issue of this document, possible areas of concern will be identified, and initial analysis performed.

5.2.1 Prelaunch Phase

During the manufacture, assembly, verification, transportation, and launch integration of the LAWS Instrument, care will be taken that no environmentally harmful substance is used or generated by LMSC or its subcontractors. The ony currently identified environmental concern is the possible health hazard related to the ground testing of the laser subsystem. This issue is resolved by proper protection and procedures.

5.2.2 Launch Phase

No environmental effects due to the LAWS mission payload, carried into orbit by an Atlas IIAS launch vehicle, have been identified. A possible concern is the possibility of a crash or accident during launch through the atmosphere. It is possible that a small amount of benign gas material (CO_2, helium, and nitrogen) contained in the laser subsystem is released. We have concluded that this is not an environmental issue.

5.2.3 On-Orbit Operations Phase

Other than (1) normal outgassing of the LAWS Instrument components in the low Earth orbit environment, and (2) occasional release of the benign gas material (CO_2, helium, and nitrogen) used in the laser subsystem, the LAWS payload will appear to the environment as a passive, non-interacting object.

The use of a laser system raises the concern of eye and skin safety. The effects of lasers on human eyes and skin have been investigated extensively, and industrial standards for the safe use of lasers have been established. Maximum permissible energy (MPE) loading due to the operations of different types of lasers are documented in ANSIZ136.1-1986.

An analysis of the space operation of the proposed LAWS laser indicates that there is no eye or skin safety concern.

5.2.4 De-Orbit Reentry

The LAWS Instrument is designed to stay on orbit for a five-year mission life. There is no plan to return the LAWS Instrument to Earth, so there would be no environmental impact for its Earth return. At the end of the mission, the LAWS Instrument together with the space platform will be de-orbited and reenter the Earth's atmosphere. The aerodynamic heating of the reentry will break up the LAWS Instrument and burn the majority of its components. The only hardware that could pose a danger as reentry debris is the 1.67 m diameter primary mirror of the telescope. Considerations in designing and material selection will enhance the break-up and burn-up of the LAWS Instrument. Controlled reentry maneuvering will restrict the dispersion of reentry debris to an unpopulated region of the Earth. Analysis will be performed to investigate the reentry integrity of the LAWS Instrument. Mission analysis will also be performed to predict the scattering footprint of the reentry debris. Results of these analyses will be reported in an update to this document.

The only other concern during reentry is the possible release into the atmosphere of a small column of benign gas material (CO_2, helium, and nitrogen) contained in the laser subsystem. This release is not an environmental issue.

5.3 AREAS OF CONTROVERSY

At this time no areas of controversy have been identified.

5.4 ISSUES REMAINING TO BE RESOLVED

Two issues remain to be resolved:

- Dispersion of reentry debris during the end-of-life de-orbit reentry of LAWS Instrument in the atmosphere
- Eye and skin safety during ground testing of LAWS Instrument.

5.5 CONCLUSION

At this time, LAWS is viewed as an environmentally passive object in low Earth orbit. As such, no major environmental concerns have been identified. During the design phase of the program, this issue will continue to be analyzed and this report updated for further reviews.

No requirement for an environmental impact statement has been found at this time.

Section 6

LASER BREADBOARD

6.1 REQUIREMENTS

A specification for the laser breadboard was developed jointly by LMSC and TDS using MSFC laser requirements integrated with LAWS system requirements as a baseline. This functional specification, included as an appendix to this report, includes such parameters as repetition rate, output energy, maximum energy in gain switch spike and tail, maximum frequency chirp over pulse length, minimal extraction efficiency, mode purity, beam quality, physical envelope, and other performance indicators.

6.2 DESIGN

The laser breadboard design was developed to duplicate the requirements of the LAWS laser flight unit with respect to the resonator, flow control, catalytic operation, cavity/pressure vessel size and output parameters: energy - 15 to 20 J/pulse, repetition rate - 20 Hz, lifetime, and pulse fidelity parameters. Since the pulse forming network (PFN) and energy storage devices offered less of a challenge to the state-of-the-art, commercial/laboratory grade devices were used to perform these functions with plans to upgrade these assemblies with space traceable, reduced volume hardware downstream in the program.

Figures 6-1 and *6-2* depict schematics of the laser breadboard layout including control and diagnostic instrumentation. Instrumentation is depicted for monitoring alignment, frequency variation as a function of time, pulse power out as a function of time (pulse energy), mode purity, output pulse spatial profile, laser line, and other pertinent laser performance characteristics.

Figure 6-3 presents the flow for checkout and integration of the pulse power subsystem from component test through the subsystem testing. Likewise, *Figure 6-4* depicts the integration and testing of the flow loop/discharge/pulse power units into an assembly. In *Figure 6-5*, the components are first tested for the resonator and injection assemblies; next they are assembled and tested as subassemblies; finally they are brought together and tested as an integrated assembly. *Table 6-1* lists components of the laboratory support equipment used to support the LAWS laser breadboard tests.

Figure 6-6 presents end and side views of the LAWS laser breadboard. The power supply PFN is located beneath the optical bench which supports the resonator optics and test instrumentation. The power supply/PFN can be rolled under the bench or removed for diagnostics. Care was taken in designing the breadboard to control ground loops and associated electromagnetic interference. *Figure 6-7* depicts the ground plane arrangement used for the breadboard.

Figure 6-8 provides an overview of the test schedule for the LAWS laser breadboard. Fifteen months were expended from the go-ahead to TDS to develop the laser breadboard until first light was extracted from the laser.

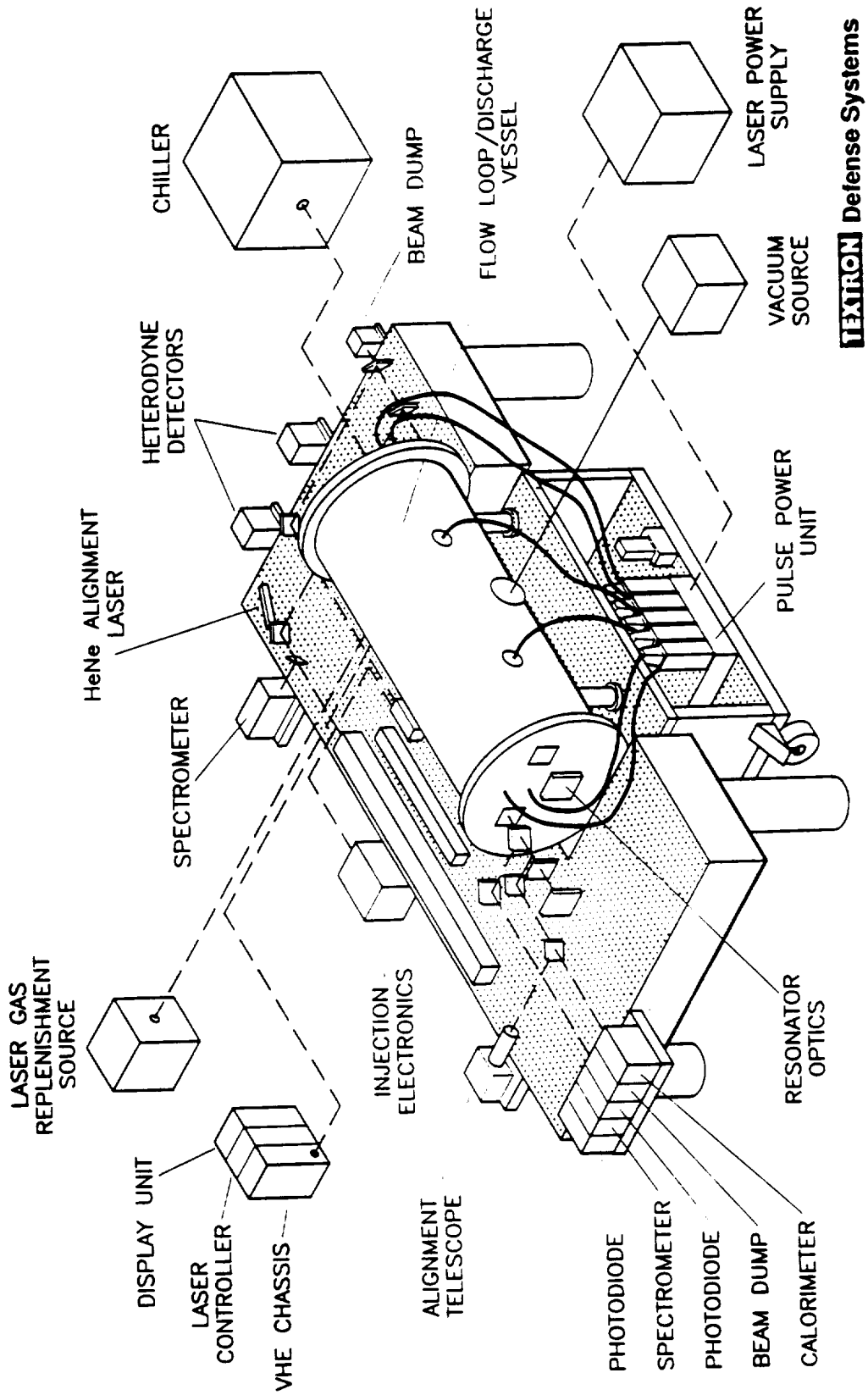

Figure 6-1. Breadboard Test Configuration

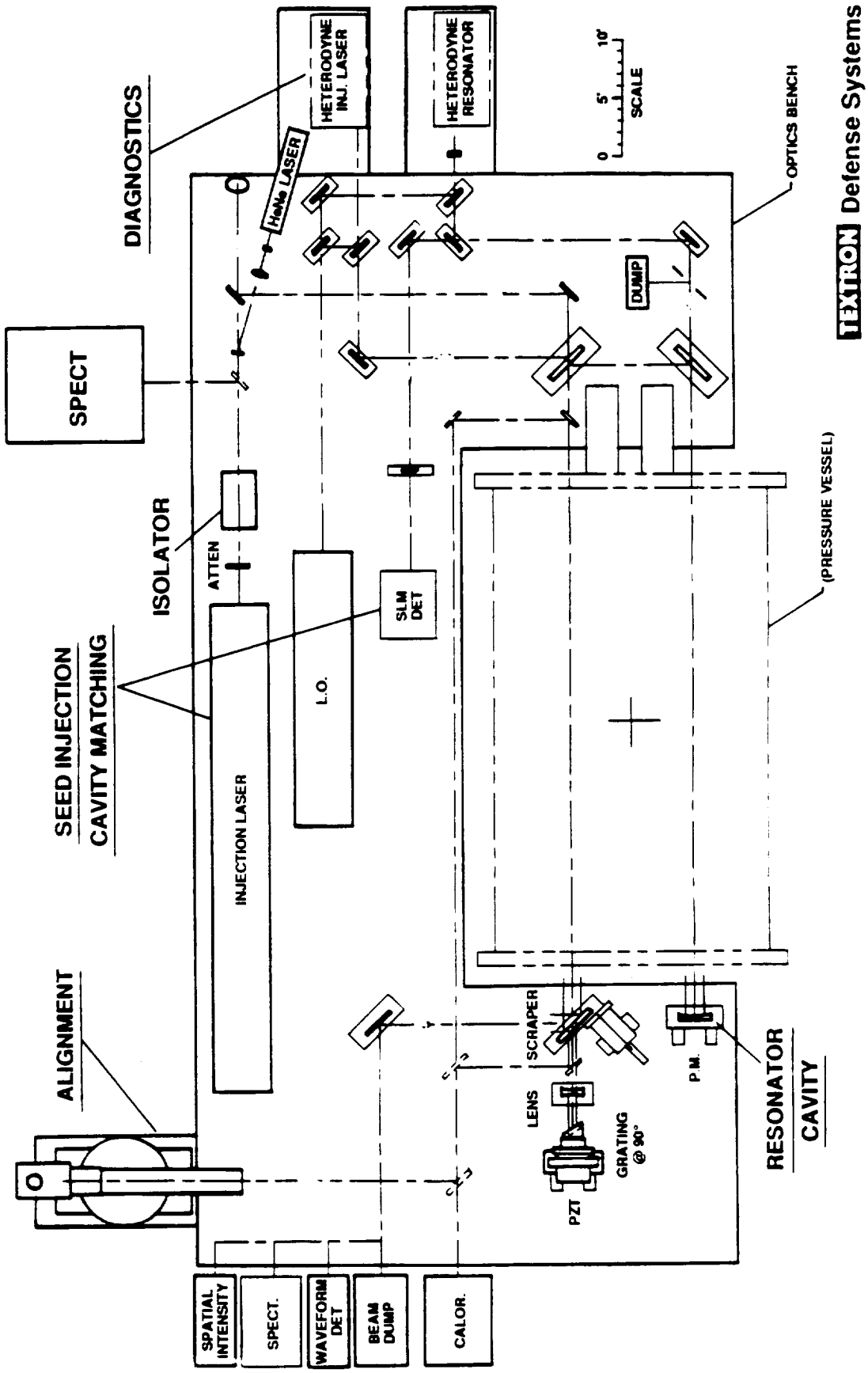

Figure 6-2. Breadboard Test Configuration/Resonator Layout

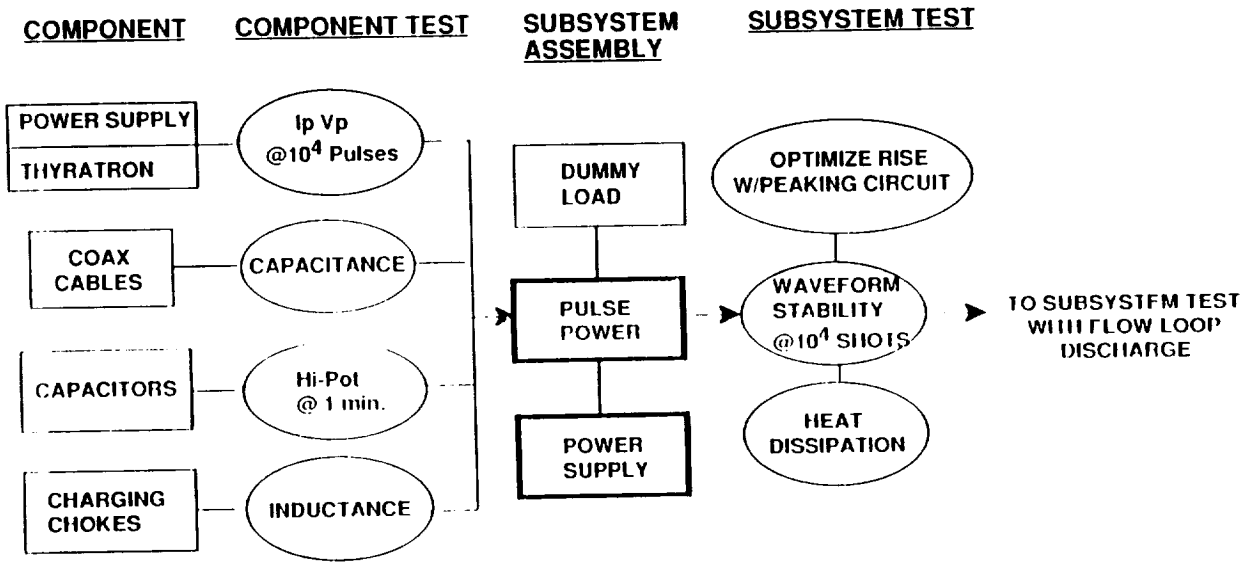

Figure 6-3. Pulse Power System Integration and Checkout

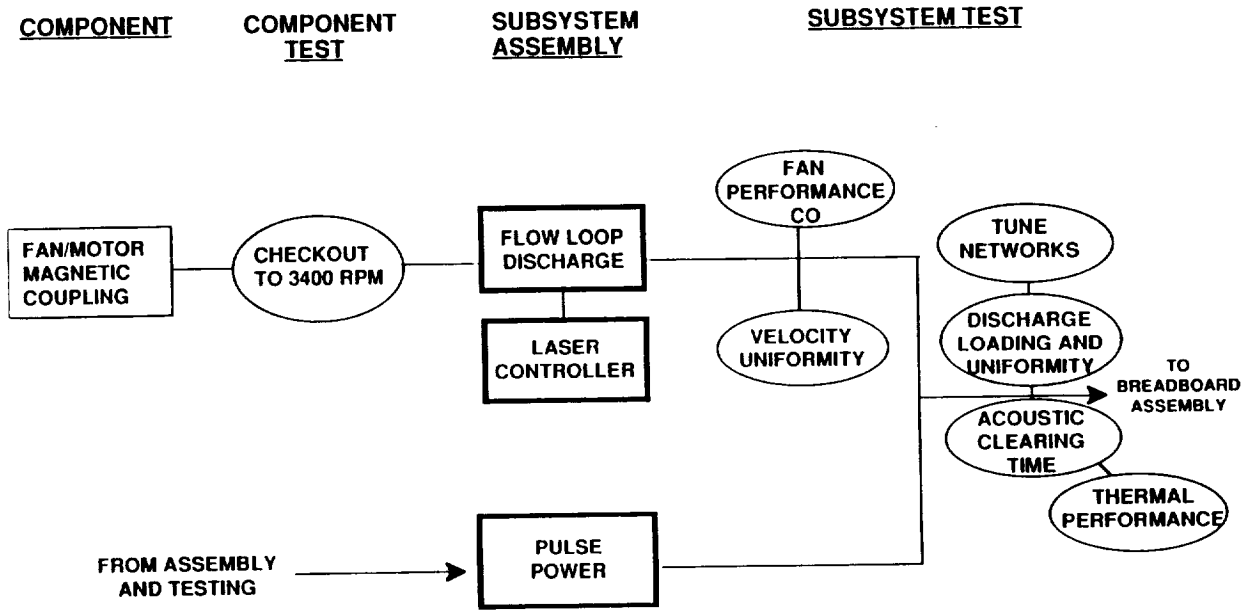

Figure 6-4. Integration and Checkout of Flow Loop/Discharge/Pulse Power Units

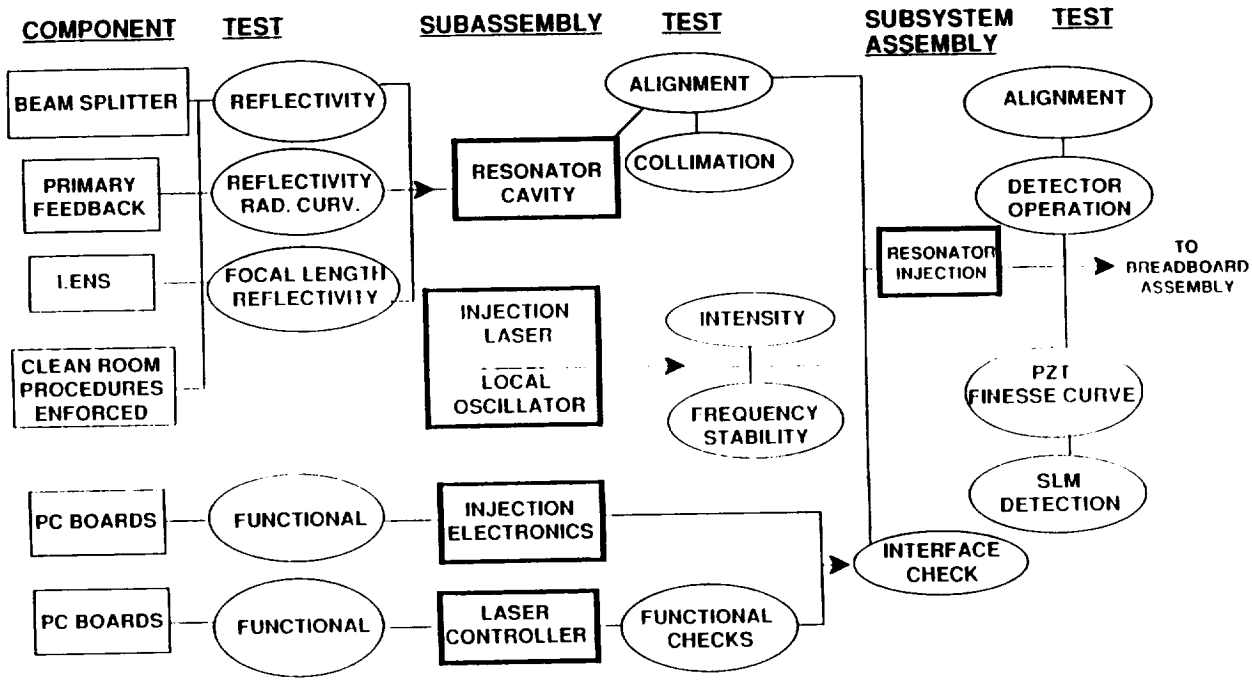

Figure 6-5. Integration Plan for Resonator/Injection Assemblies

Table 6-1. Laboratory Support Equipment

Laser Flow & Gas Control

Gas Chromatography
Mass Spectrometer
Spectrum Analyzer
Cooler 16 kW, E.I. # 39343
Vacuum Pump & Valves
Gas Bottles, Gages
Vac/Press Pump System

Data Acquisition

Oscilloscope, Lecroy #9400 (2)
Oscilloscope, Textronix #251051
Oscilloscope, Textronix #2430
Visicorder # 1858
Visicorder # 1508B
Pulse Generator, Datapulse
Rack 19" x 22" x 5'

Output Diagnostics

Detectors
Lens
Beam Splitter (3)
Fold Mirrors (3)
Attenuators (2)
Calorimeter
Spatial Filter
Spectrometer
Detector, Waveform
Beam Dump
Kinematic Bases
Optical Mounts

Alignment

HeNe Laser
Alignment Telescope
Dichroic
Laser Mount
Fold Mirror
Optical Mounts

Power Supply

HVPS Ale # 153L (2)
Current Transformer, Pearson #310&301(2)
Current Transformer, Pearson #410
H.V. Probe Tex #6015
Cap Divider, Pearson #V305A
Rack 19" x 22" x 5'

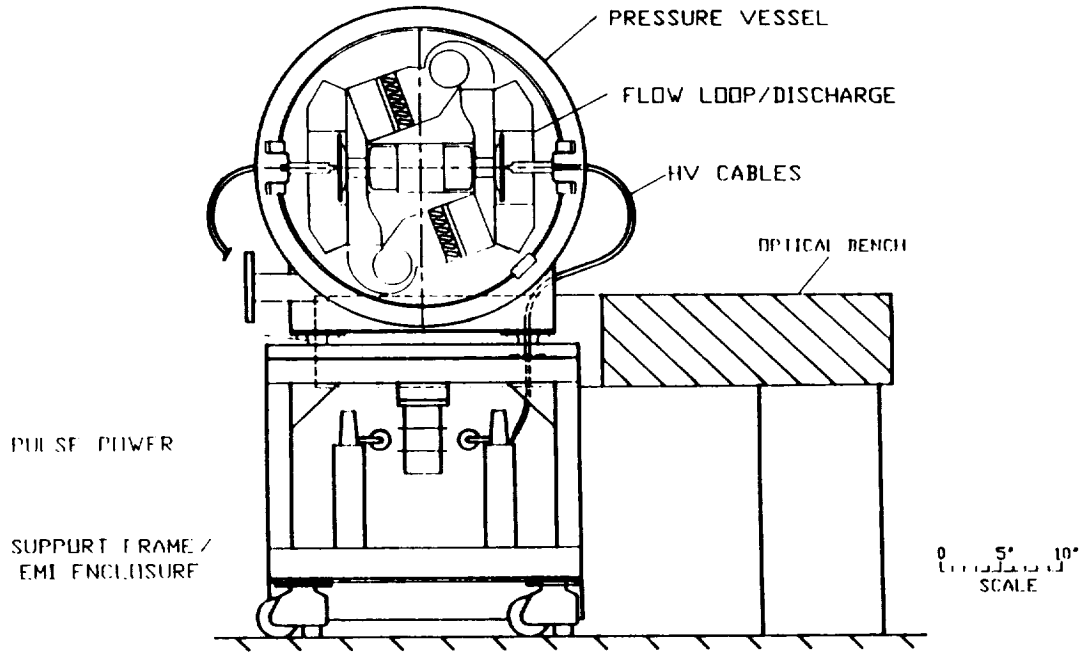

Figure 6-6. Integrated LAWS Laser Breadboard (1 of 2)

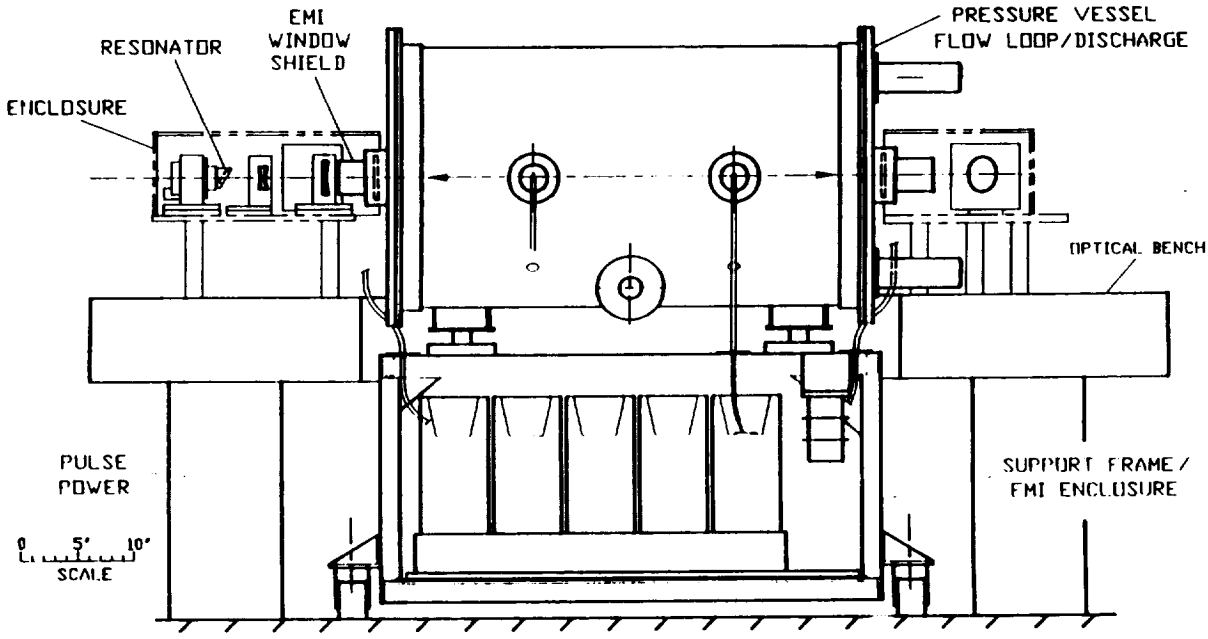

Figure 6-6. Integrated LAWS Laser Breadboard (2 of 2)

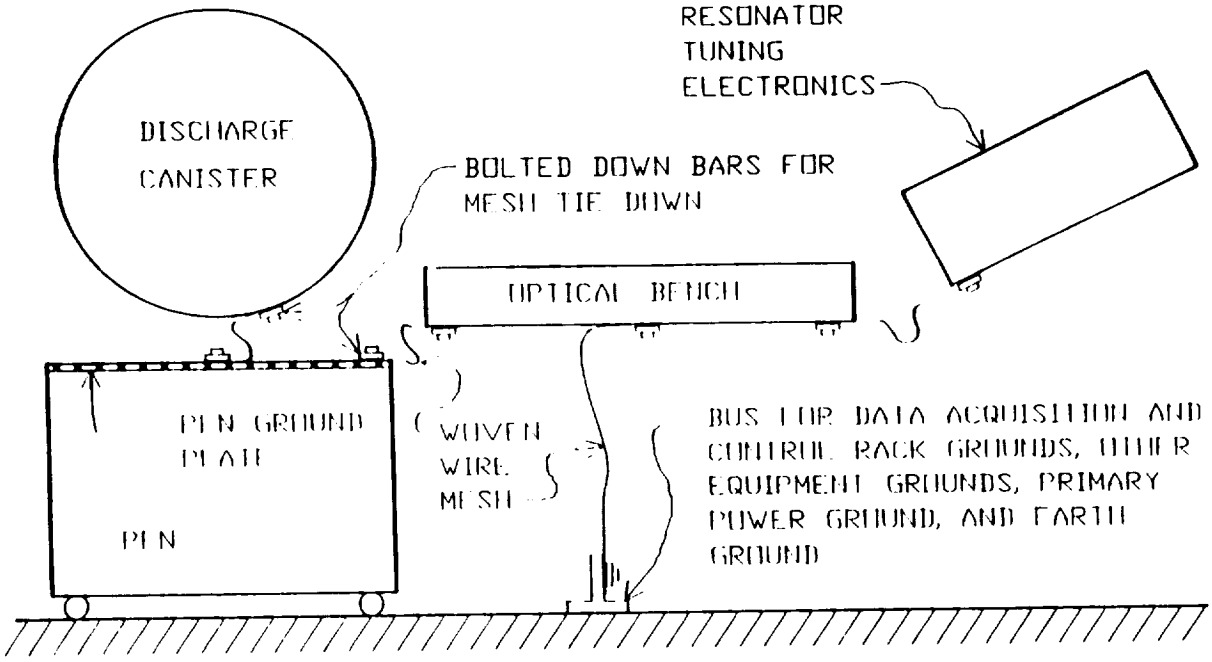

Figure 6-7. System Ground Plane

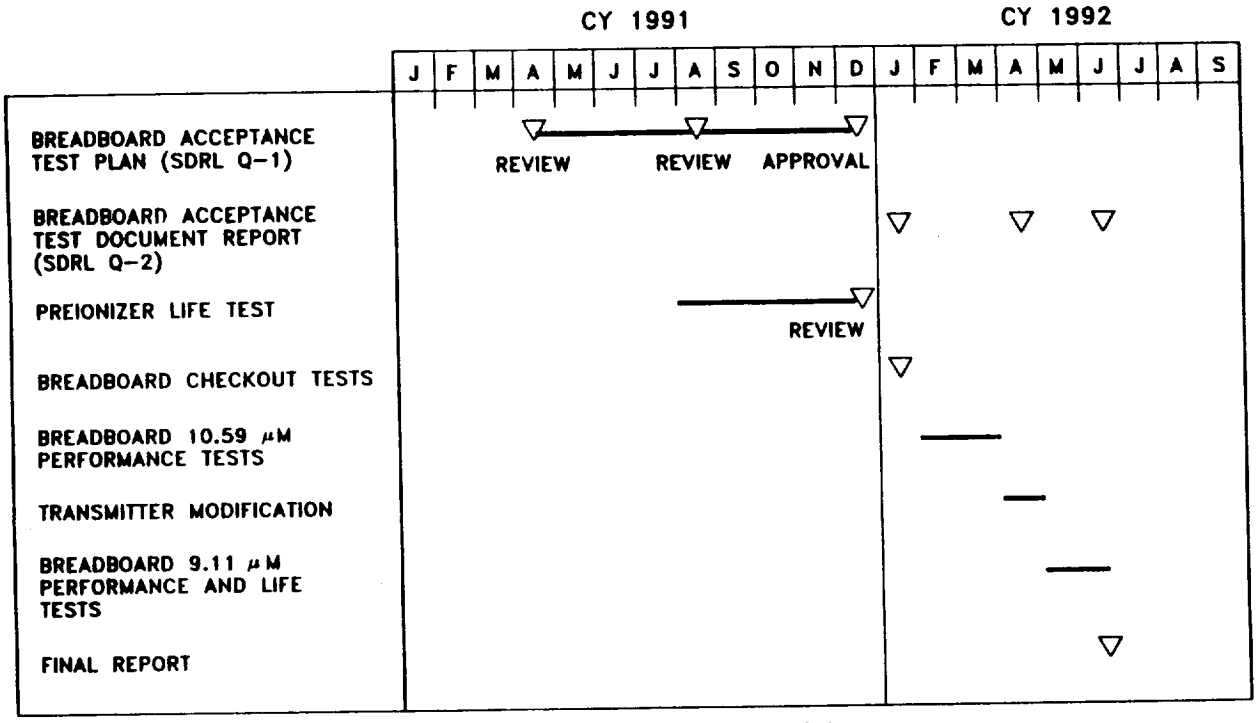

Figure 6-8. Test Plan Schedule

6.3 TEST RESULTS

The LAWS breadboard laser was developed and tested for LMSC. The primary objective of the breadboard tests was to demonstrate acceptable performance parameters for the laser in normal and isotopic CO_2 gas mixtures. The other objective was to conduct life tests to determine component and system reliability.

Tests were carried out at the Textron Defense Systems facility in Everett, Massachusetts, in accordance with the LAWS Laser Breadboard (1) Statement of Work, (2) Functional Specification, and (3) Acceptance Test Plan.

6.3.1 Test Sequence

Acceptance tests were carried out in the sequence described in the Breadboard Acceptance Test Plan referenced above. In general, performance measurements were conducted first in normal CO_2 mixtures at the specified 10 Hz prf and 10.6 μm wavelength. This was followed by life test in the same at an accelerated prf of 20 Hz.

The breadboard system was then modified for operation at 9.11 μm wavelength in isotopic CO_2 (oxygen-18) mixture. These tests were limited because of lack of availability of sufficient isotopic gas and because the catalyst could not be labeled with oxygen-18 prior to the tests because of very long lead times for acquisition of the labeling gas.

6.3.2 Test Facility

The laser breadboard was assembled and tested in a designated area at the TDS-Everett facility. Special care was taken to separate the assembly and checkout of the resonator and the flow loop subsystems to avoid possible contamination of the optical components. *Figure 6-9* shows a photograph of the system during the acceptance tests.

6.3.3 Results

This section describes the results from the acceptance tests conducted between 23 April 1992 and 2 July 1992. The procedures for conducting these tests were described in detail in the Acceptance Test Plan referred to earlier and will not be repeated here.

6.3.3.1 Performance Tests at 10.6 μm

Acceptance tests were performed at 10 Hz in $^{12}C\ ^{16}O_2$ mixtures to evaluate the laser transmitter. The test parameters measured are summarized below.

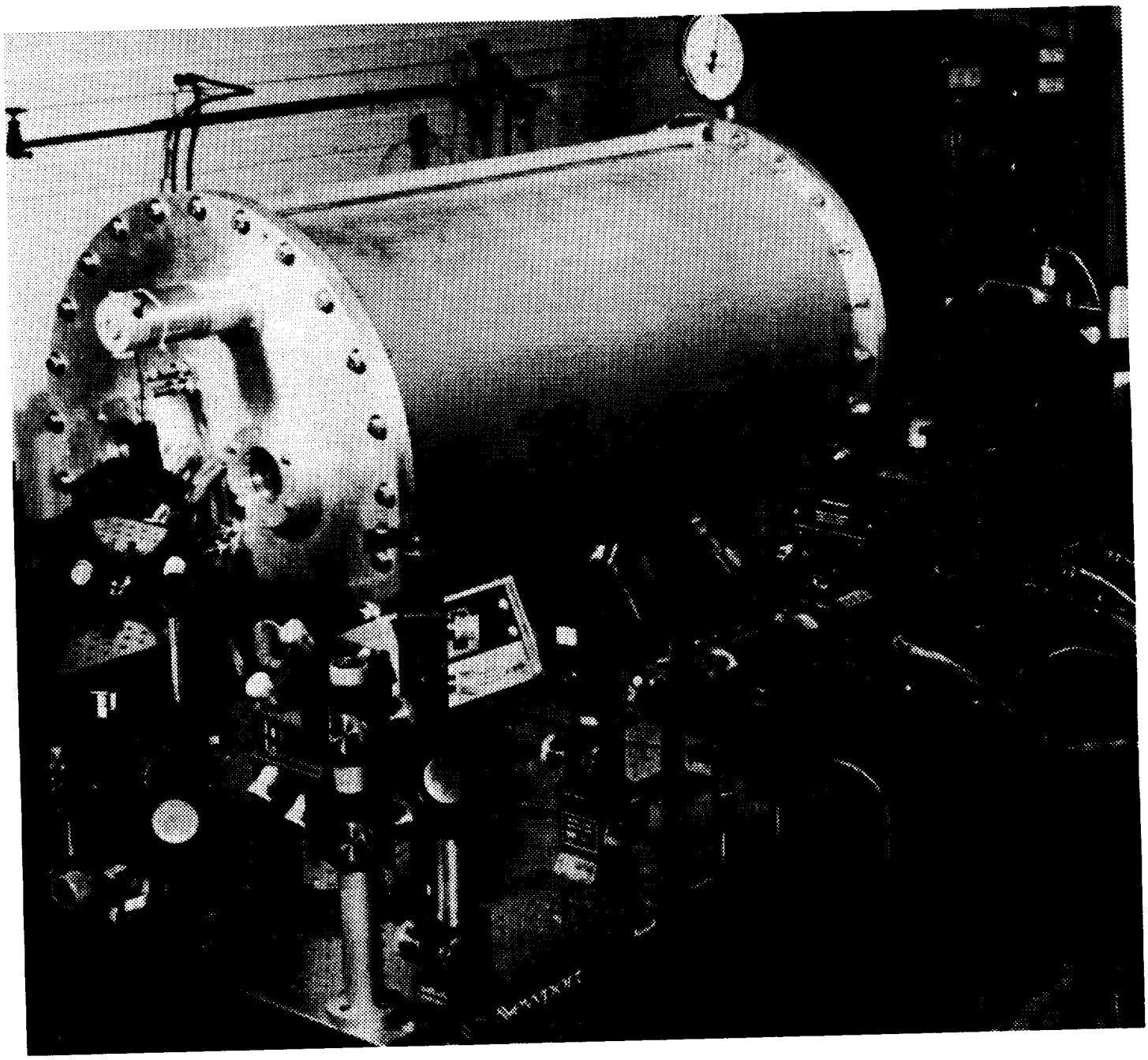

Figure 6-9. Laser Breadboard System

Average Pulse Energy

Pulse energy was measured at the output of the laser with a Scientech 360401 laser power meter under two pressure conditions and several energy loadings as listed in *Figure 6-10*. The tests were conducted in the specified 3:1:1 ($He:CO_2:N_2$) gas mixture. Also plotted in the figure are results of the TDS performance prediction code. Two different pump pulse times are depicted: 4.5 μs for the lower energy levels, and 3.75 μs at the higher levels. Although energy loadings have not yet been extended to the design point, over 19 J/pulse are projected at the design point.

Pulse Shape

A photon-drag detector was used to obtain output pulse temporal characteristics as shown in *Figure 6-11*. The pulse width (FWHM) is 3.6 μs and the output decays to 10 percent of peak within 2 pulse widths, and to very nearly 0 in 3 pulse widths. (Note turn on at +1/5 major division.) This figure depicts several seconds of data at 10 Hz prf, indicating highly stable pulse-to-pulse operation.

Intrapulse Chirp

Intrapulse chirp was monitored by recording the heterodyne beat signal against an offset local oscillator and performing a Fast Fourier Transform (FFT) of the recorded data. *Figures 6-12* and *6-13* are typical examples of these measurements. These figures are a composite of three traces: (1) the lower trace is the beat signal in the time domain at 1 μs/horizontal division; (2) the fine grain central trace is the FFT at 5 MHz/horizontal division and 10 dB/vertical division; and (3) the more coarse central trace is the expanded FFT at 200 kHz/horizontal division and 5 dB/vertical division.

In the example case in *Figure 6-12*, half (3 dB) of the pulse energy spectrum lies within ±55 kHz. In the example case in *Figure 6-13*, half (3 dB) of the pulse energy spectrum lies within ±82 kHz. Likewise, for each of the example cases, three-quarters of the pulse energy spectrum lies within ±120 kHz and ±127 kHz, respectively. These measurements have been made without an attempt to fully optimize the laser pulse forming network (PFN) impedance match. As the energy of the laser is increased toward 20 J/pulse, spectral frequency spread within the pulse is expected to increase. However, with adjustment of the PFN, the chirp at 15 to 20 J/pulse is expected to remain within specification.

Energy Output Repeatability

Repeatability of the output energy was measured under repped mode at 10 Hz. Under normal operating conditions, the laser was activated every morning. From a cold start, the energy meter immediately displays 7 J/pulse. After a 30 minute warm up period, the energy meter levels off at 6.6 J/pulse and remains at that level throughout the test period. During testing over several days with a single gas fill (500,000 pulses), no energy degradation was observed.

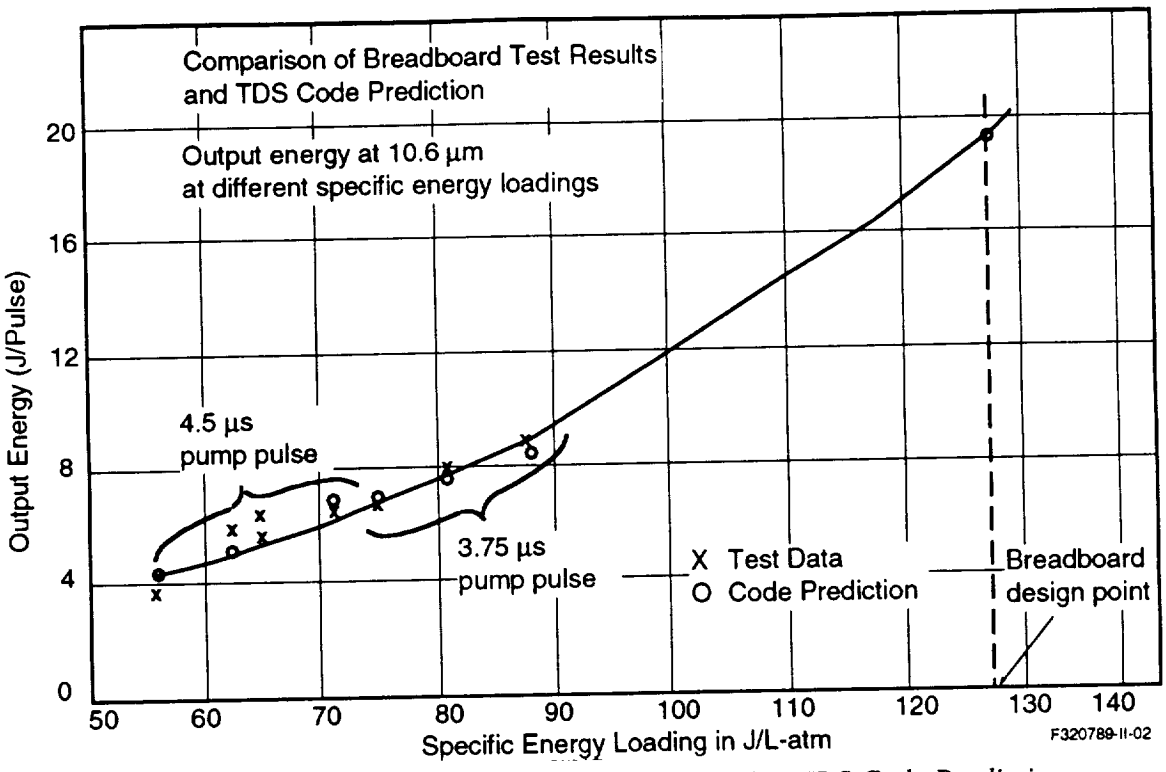

Figure 6-10. Breadboard Test Results Compared to TDS Code Predictions

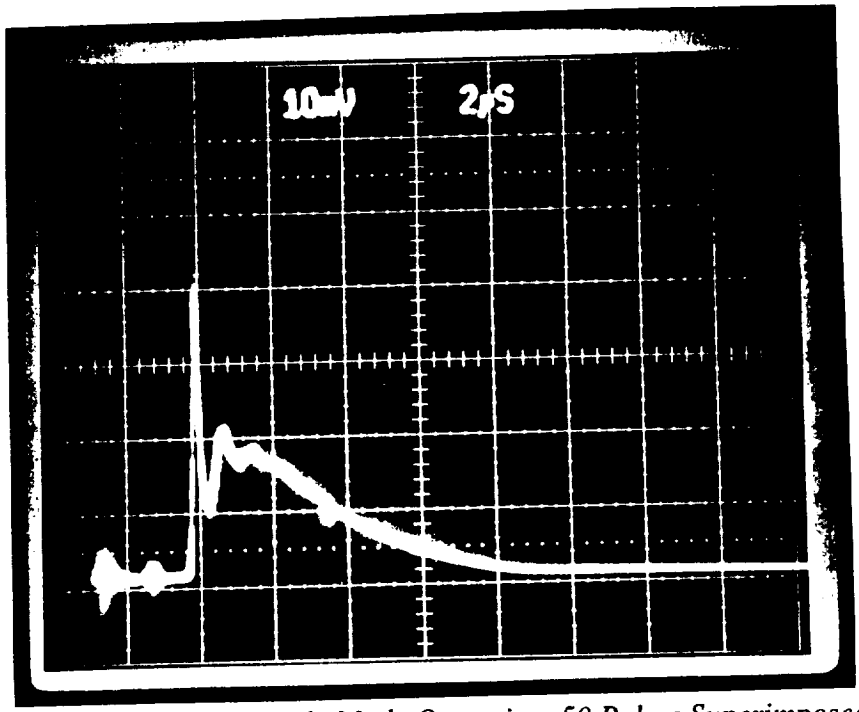

Figure 6-11. 10 Hz Single Mode Operation, 50 Pulses Superimposed

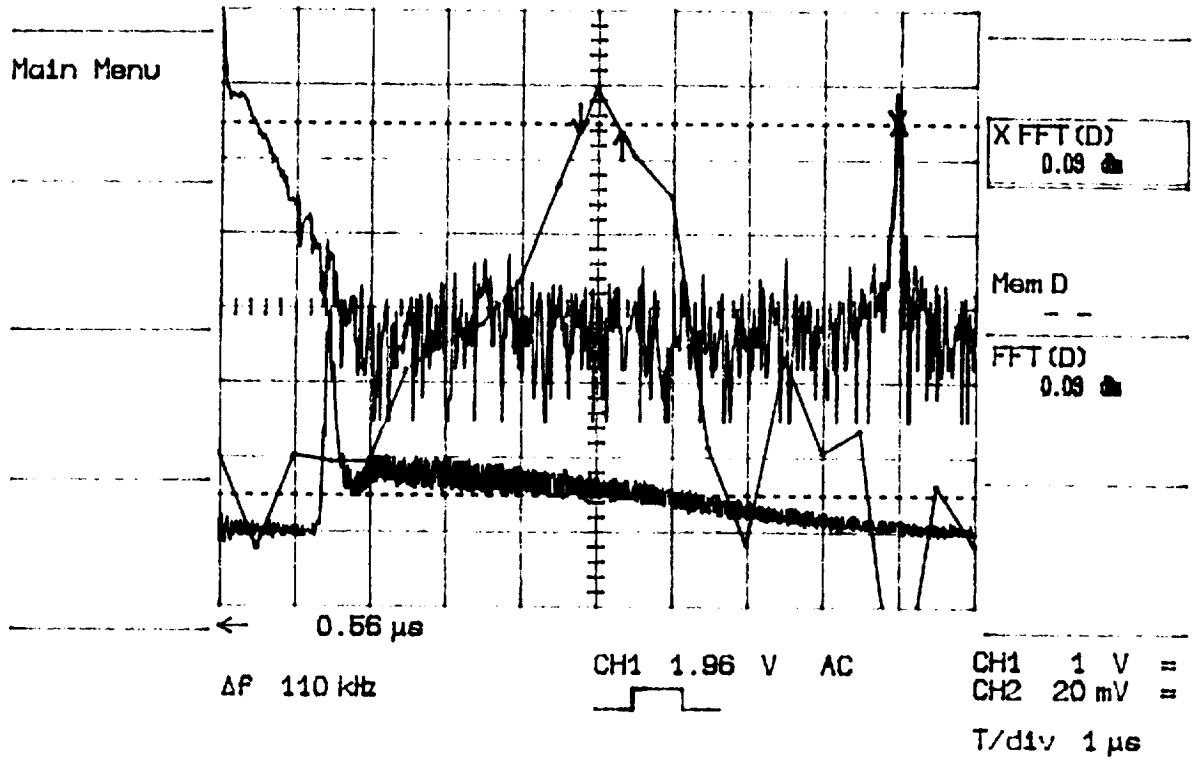

Figure 6-12. Chirp Measurement from Fast-Fourier Transform, Example Measurement A

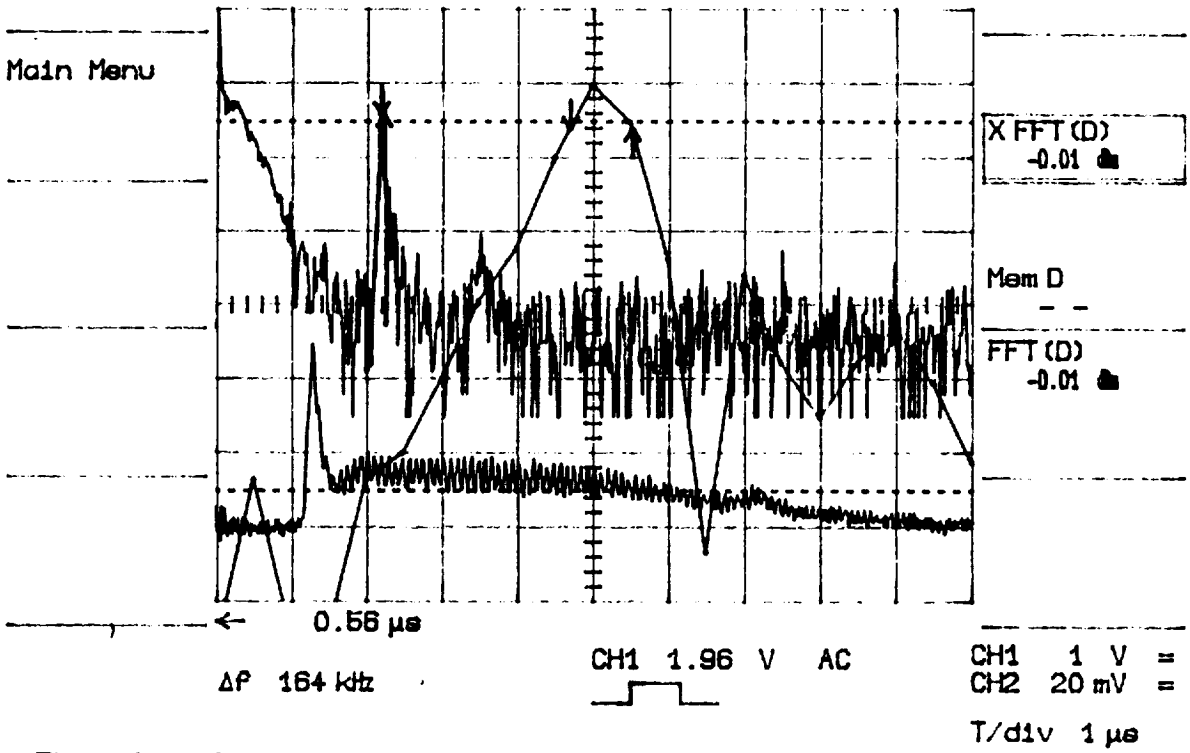

Figure 6-13. Chirp Measurement from Fast-Fourier Transform, Example Measurement B

Beam Jitter

Beam jitter was measured by relaying the far-field spot onto a strip of burn paper attached to the rim of a rotating cylinder with a fixed 0.5 mm wire cross-hair in front of the cylinder, as shown in *Figure 6-14.* The beam jitter angle was below our 80 μrad measurement resolution.

Laser Efficiency Measurement

The laser efficiency, defined as the ratio of near-field laser energy to the electrical energy stored in the PFN, was calculated at three different operating points using the laser output energy and PFN charging voltage measurements:

- 5.8 percent @ 54 J/L-Atm
- 6.4 percent @ 73 J/L-Atm
- 7.4 percent @ 88 J/L-Atm*.

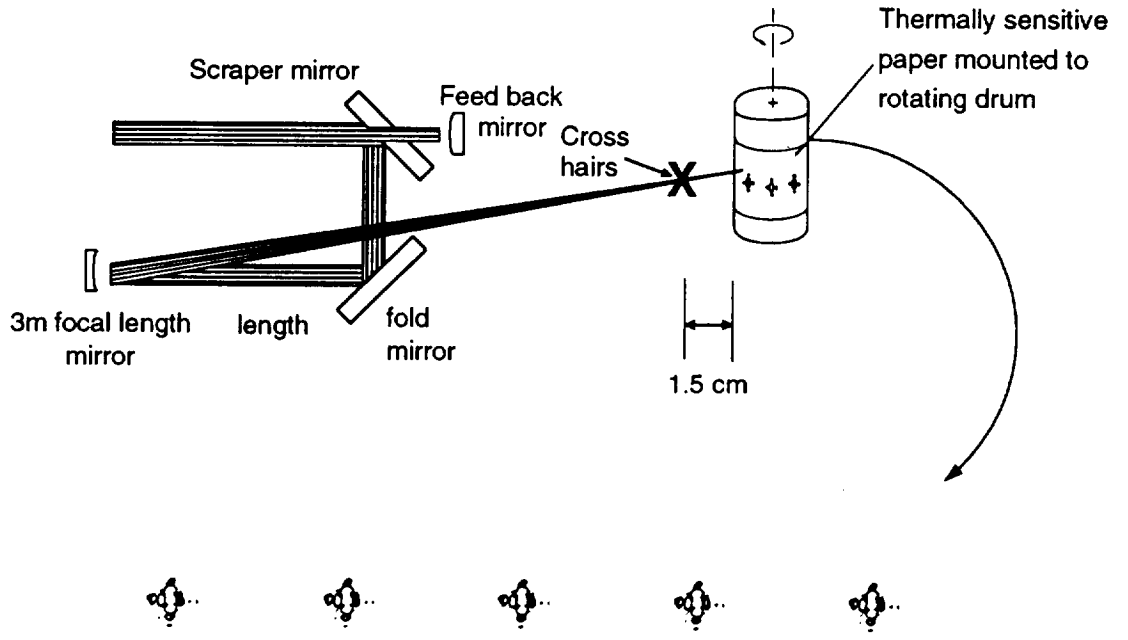

Figure 6-14. Beam Jitter from Pulse-to-Pulse: Much Less Than Our 80 μm Measurement Resolution

* This 7.4 percent efficiency was increased to 10 percent on an ID program subsequent to the initial measurements above using the same hardware (see Appendix B).

The extraction efficiency, which is more strictly defined as the ratio of energy output to the energy deposited in the discharge, is higher than the displayed ratio. Further, it is obvious from the values above that the efficiency continues to increase as the energy loading approaches the design point (~ 120 J/1-atm).

6.3.3.2 Life Tests

Life testing was carried out in oxygen-16 based mixture to one million pulses. The parameters measured are summarized below. There were no major component failures. Most of the shots were accumulated at 10 Hz. 6,000 shots were accumulated at 20 Hz to demonstrate capability of the breadboard to operate at the accelerated prf.

Average Power

The following average power readings were obtained at several different prfs:

- 52 W @ 10 Hz
- 63 W @ 12.5 Hz
- 73 W @ 15 Hz
- 100 W @ 20 Hz.

Figure 6-15 depicts pulse energy for a single pulse as monitored by the Scientech joule meter.

Discharge Voltage and Current

The voltage and current waveforms are shown in *Figure 6-16*, which is a representative shot taken at a PFN charge voltage of 22 kV at 320 Torr gas pressure. As can be seen from the voltage (upper trace), there is a mismatch between the PFN impedance and the discharge impedance resulting in post-pulse reflections. The match improves as the design point is approached. Improvement of this match will improve laser efficiency as well.

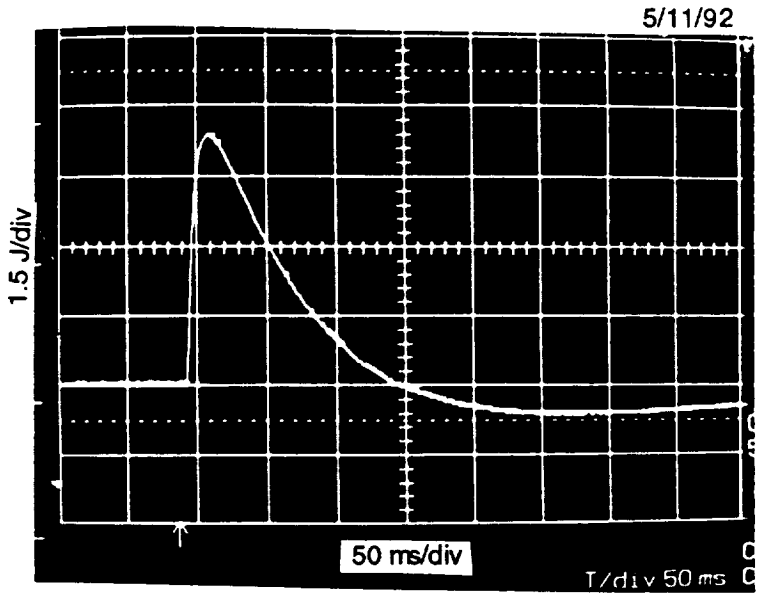

Figure 6-15. Single Pulse Energy Monitored by Scientech Joule Meter

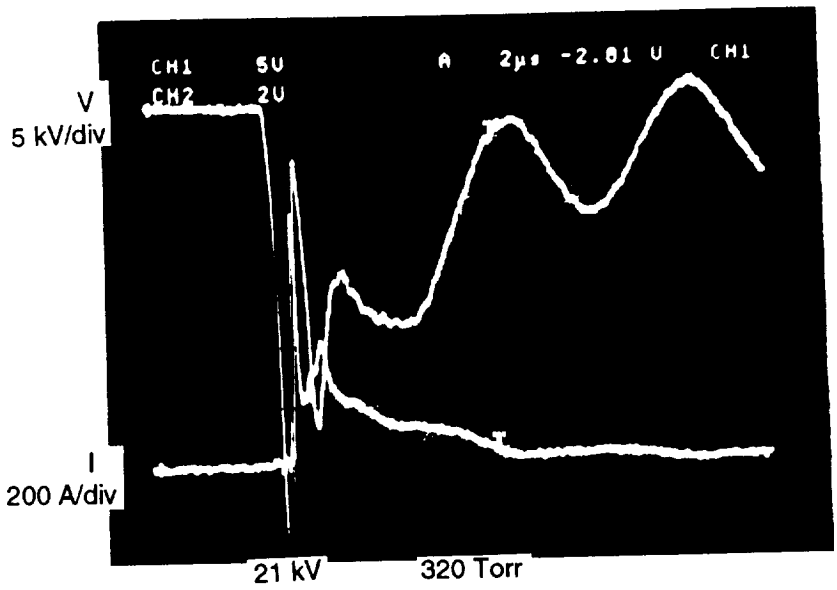

Figure 6-16. Typical Discharge Current and Voltage Waveforms

6.3.3.3 Performance at 9.11 µm

The selection of wavelength for LAWS involved consideration of both atmospheric transmission and back scattering properties of aerosols in air. According to the LAWS Science Team, the recommended wavelength is 9.11 µm. Since the R-branch of the 00°1-02°0 mode of $^{12}C\ ^{18}O_2$ has a relatively strong transition at a wave number of 1097.15 cm^{-1} (9.1145 µm), the ideal gas mixture for LAWS transmitter laser will contain isotopic $^{12}C\ ^{18}O_2$ as the active molecule.

Kinetic information for radiative transitions of the 00°1-(10°0, 02°0) (I,II) bands of isotopic species of $^{12}C\ ^{18}O_2$ was obtained and analyzed by different authors (references 1 through 3). However, previous gain and extraction measurements were mostly made under low-pressure continuous wave (cw) pumping conditions. Since wind sensing Doppler Lidar requires a pulsed coherent laser output, additional data regarding the collisional deactivation rate of upper laser level as well as temperature dependence of the rate constant were needed to construct and validate a reliable model to predict and optimize the performance of a candidate laser.

Design/Validation Experiment

A single-pulse, closed volume, UV-preionized, self-sustained discharge in the isotopic laser mixture was used to determine the kinetic characteristics of the gain media. The discharge test section had a 1.22 x 4.2 x 20 cm^3 volume and a gain length of 3 x 20 cm since three passes of the probe beam were made. A simple two-mirror stable resonator was built to study the laser energy extraction. A concave copper mirror with radius curvature of 16.8 m and a flat output coupler were used to construct the resonator, which produces a 1.2 x 1.2 cm^2 multimode square output beam. The following gases were used: He (Liquid Carbonics, 99.99 percent), N_2 (Liquid

Carbonics, 99.998 percent), and $^{12}C^{18}O_2$, the $^{18}O_2$ isotopic content of which was better than 95 percent (Isotec, Inc.). *Figure 6-17* shows the layout of the experimental setup. All test parameters used to determine the kinetic data are listed in *Table 6-2*. The measured decay rates of gain under various gas mixtures and pressures are shown in *Figure 6-18*. The unamplified probe signal Io was determined by chopping a grating tunable CW laser beam (MPB CO_2 Laser Model GN-802-GGS). The laser output power (TEMoo mode pattern) at 9.11 μm of the $^{12}C^{18}O_2$ line was 9 W. The beam was 7.1 mm in diameter. The amplified probe signal I was detected by using a Cd-Hg-Te detector and recorded on a Tektronix 7104 oscilloscope. The small signal gain coefficient g_o was calculated by using the expression exp (g_oL) = I/Io, where L is the effective length of the discharge region. The measured gain was found to vary within 10 percent from shot to shot. One gas fill lasted approximately 40 to 50 shots without significant change of output. The energy extraction was measured by a power meter (Gentec Joule meter) with two different output couplers (12 percent and 40 percent). The mixture composition and the pumping energy, which in turn determine the temperature of laser gas, affect the overall decay rate of gain.

Applying multiple regression analysis (reference 4) to the measured decay rates, a set of deactivation rate constants is determined, given in *Figure 6-19*.

A summary of (001) vibration relaxation rate constants is given in *Table 6-3*. Since no gas temperature information was reported in reference 3, a direct comparison with our measurements was made at room temperature (300 K). Good agreement was obtained for the rate constant of $K_{CO2\text{-}CO2}$, but significant discrepancy occurred at $K_{He\text{-}CO2}$. The known $^{12}C^{16}O_2$ relaxation rate constants for $^{12}C^{16}O_2$ gas mixture (reference 5) are also listed in *Table 6-3* . Both $K_{N2\text{-}CO2}$ and $K_{CO2\text{-}CO2}$ for $^{12}C^{18}O_2$ have much higher deactivation rates than $^{12}C^{16}O_2$. The new rate constants were subsequently incorporated into the kinetic code to enable prediction of performance of an isotopic $^{12}C^{18}O_2$ laser. *Figure 6-20* shows a comparison of code predictions with the experimental data for the performance of an isotopic $^{12}C^{18}O_2$ laser. More specifically, *Figure 6-20* shows a comparison of code predictions with the experimental data for temporal variation of gain. Comparison of energy extraction measurements with code predictions is shown in *Figure 6-21*. Good agreement is evident in both plots.

Performance Tests of LAWS Breadboard

The resonator was modified for 9.11 μm operation through insertion of a grating in the cavity and subsequent tuning for the 9.11 wavelength. The laser head was filled with a CO_2:N_2:He mixture, with the CO_2 being the rare $^{12}C^{18}O_2$. No preconditioning was performed with $^{18}O_2$ as would be required for long term, full performance operation, because of the unavailability of $^{18}O_2$ due to the long lead time for the gas. (The isotopic preconditioning gas is scheduled for delivery over the next six months at 50 L per month.) More than 8 x 10^3 discharge shots were recorded with the mixture. The initial few shots were monitored with a spectrum analyzer at 9.21 μm; however, after grating adjustment, the 9.11 μm wavelength was achieved on the third shot and maintained through the tests. As these tests were limited in nature, additional testing is desirable to fully characterize the laser performance at 9.11 μm when a full supply of both the $^{12}C^{18}O_2$ and $^{18}O_2$ become available. Model results, validated experimentally as discussed earlier in this section, verify that 14.6 J at 9.11 μm are achievable with the current breadboard design with a 1:1:3 mixture and 0.625 atmospheric pressure.

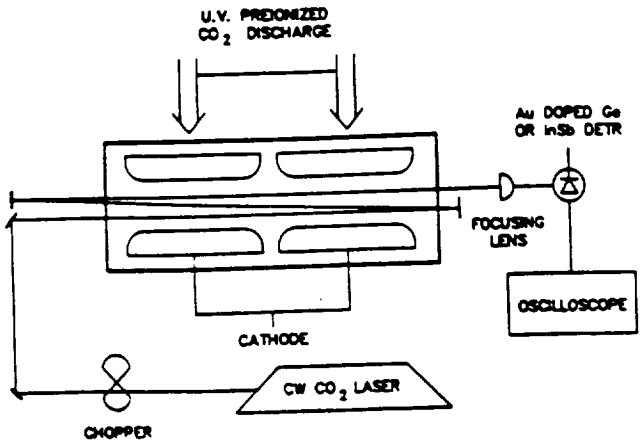

Figure 6-17. Schematic Diagram of Experimental Apparatus

Table 6-2. Test Parameters

- **Small-signal gain and energy extraction measurements**
  - **Energy Loading** — **40 J/L - 180 J/L**
  - **Gas Pressure** — **150 TORR - 600 TORR**
  - **Gas Temperature** — **300°K - 440°K**
  - **Gas Mixture**

He	N_2	CO_2
0	1	1
0	2	1
1	1	1
2	1	1

He	N_2	CO_2
3	2	1
3	1	1
2	3	1
3	3	1

  - **Output Coupler** — **12%, 40%**
  - **Gain Length** — **60 cm (Double)**

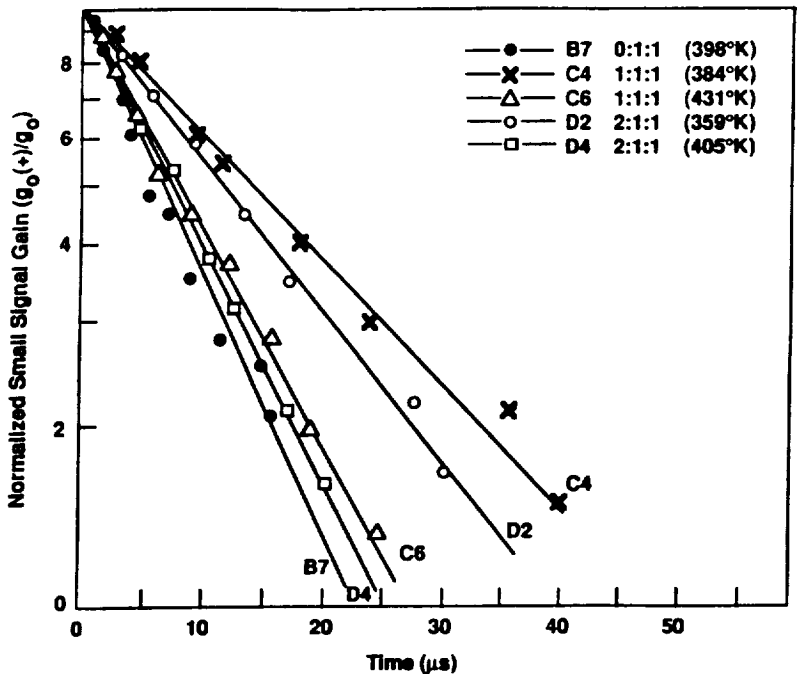

Figure 6-18. Decay Rate of Small Signal Gain

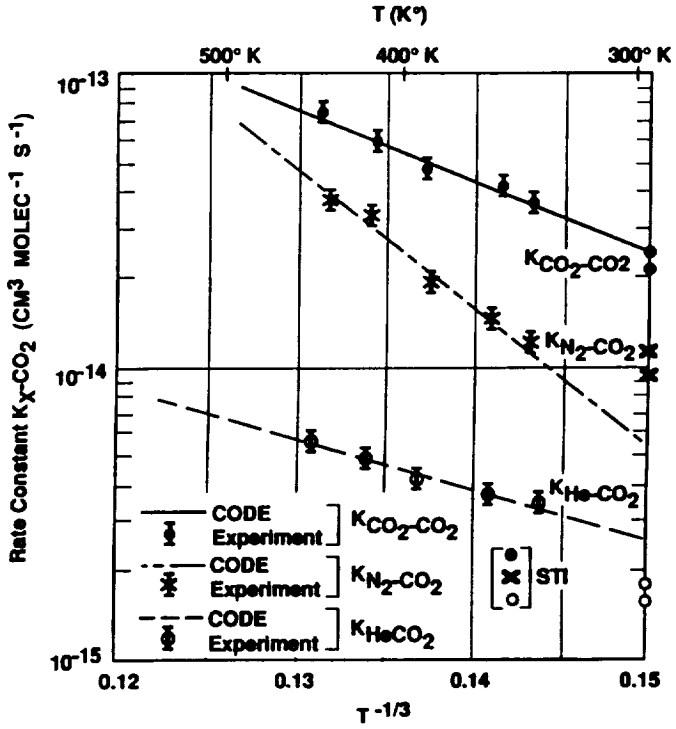

Figure 6-19. Deactivation Rate Constant on Temperature

Table 6-3. Summary of (001) Vibrational Relaxation Rate Constants

GAS TEMPERATURE	$K_{He} \cdot CO_2$ ($TORR^{-1}\ S^{-1}$)	$K_{N2} \cdot CO_2$ ($TORR^{-1}\ S^{-1}$)	$K_{CO2} \cdot CO_2$ ($TORR^{-1}\ S^{-1}$)
340°K	106 ± 10	384 ± 20	1192 ± 101 (MEASURED)
390°K	128 ± 12	649 ± 50	1852 ± 120 (MEASURED)
440°K	170 ± 15	1147 ± 100	2380 ± 200 (MEASURED)
300°K	80.5	212.1	815.6 (Interpolated)
300°K	54.8	354.6	773.7 (STI)
300°K	85	106	350 ($^{12}C^{16}O_2$)

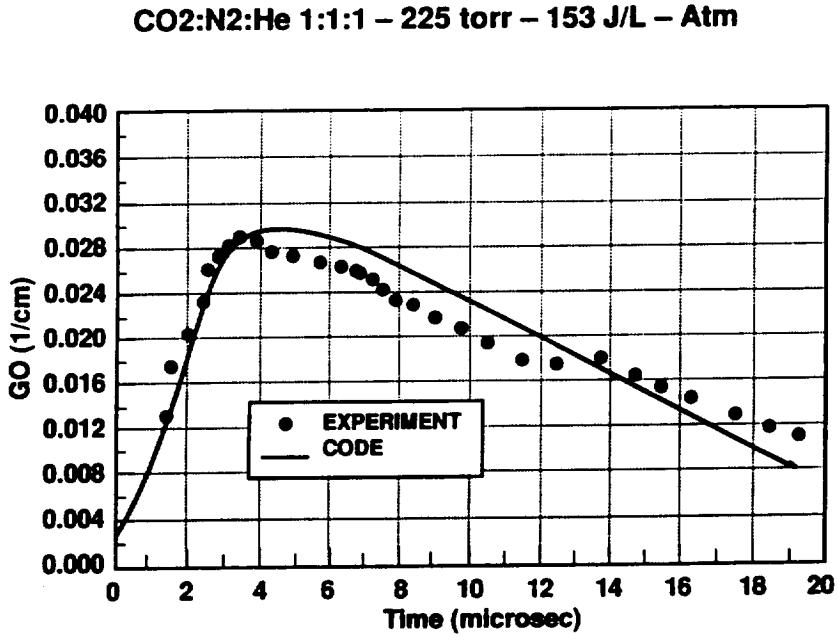

Figure 6-20. Temporal Variation of Gain: Comparison of Experimental Data to Code Prediction

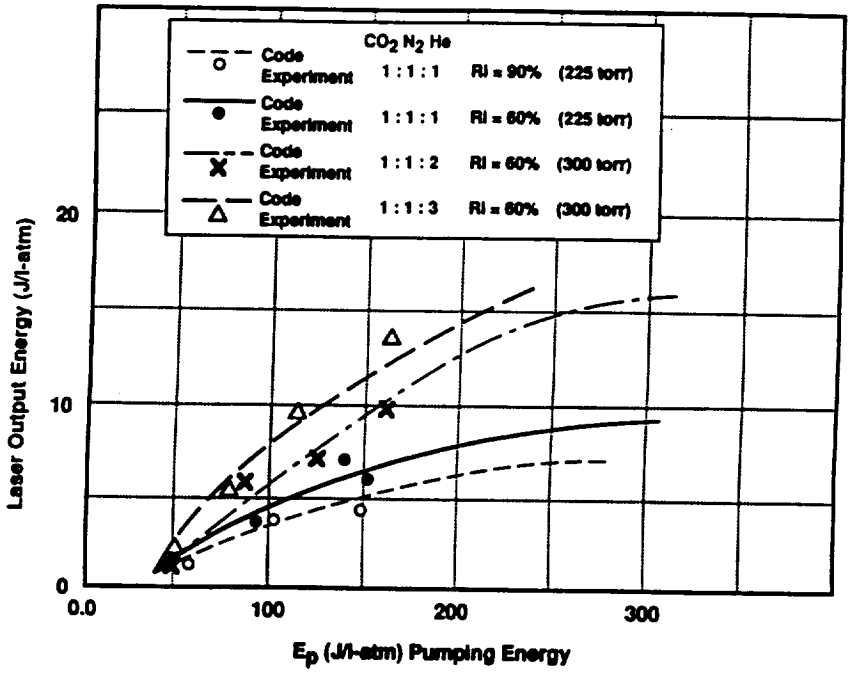

Figure 6-21. Energy Extraction Data for ^{12}C $^{18}O_2$ Mixture

Figure 6-22 depicts a single mode (transverse and longitudinal) pulse at 9.11 μm. Injection seeding with the 9.11 μm seed laser was used to maintain single mode operation for the 9.11 μm tests.

Figure 6-23 depicts the current pulse from the PFN and the heterodyne beat signal for these 9.11 μm tests as the laser output is beat against the local oscillator. The 2.2 μs delay between initiation of the current pulse and the laser output is apparent in the figure. The same low chirp performance of the laser operating at 9.11 is expected as was measured at 10.6 μm (*Figure 6-12*). In additional tests the detector output must be digitized and analyzed (as depicted in *Figure 6-13*) to further validate the chirp characteristics in extended testing.

Figure 6-24 depicts the current/voltage (I/V) pulse out of the PFN (into the laser). The ringing displayed in the figure is again indicative of a non-ideal impedance match between the laser and the PFN. Laser efficiency improvement is achievable with a better impedance match.

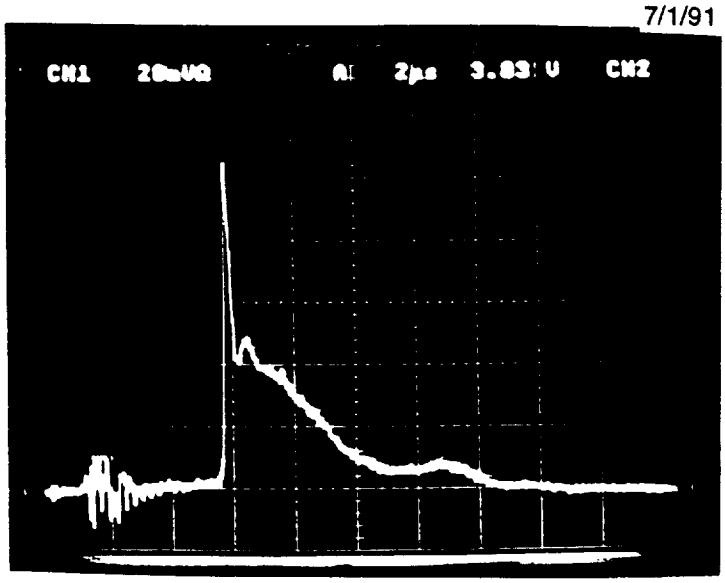

Figure 6-22. Single Mode (L&T) Pulse at 9.11 μm

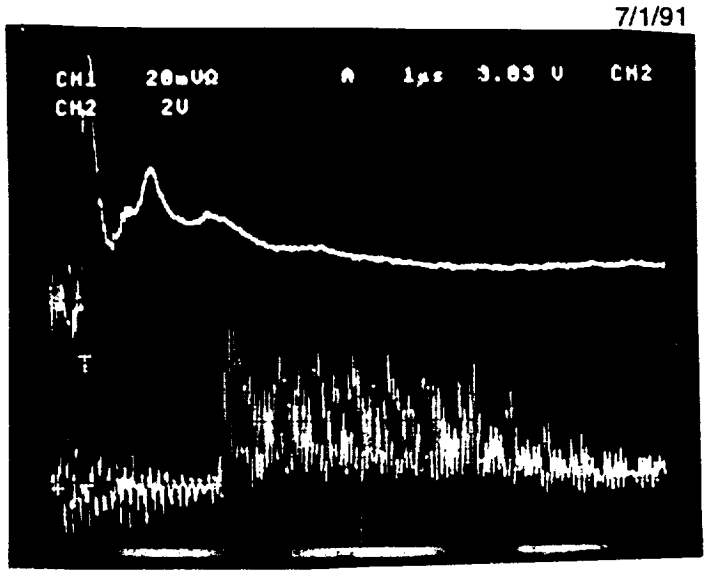

Figure 6-23. Heterodyne Beat Signal at 19 kV

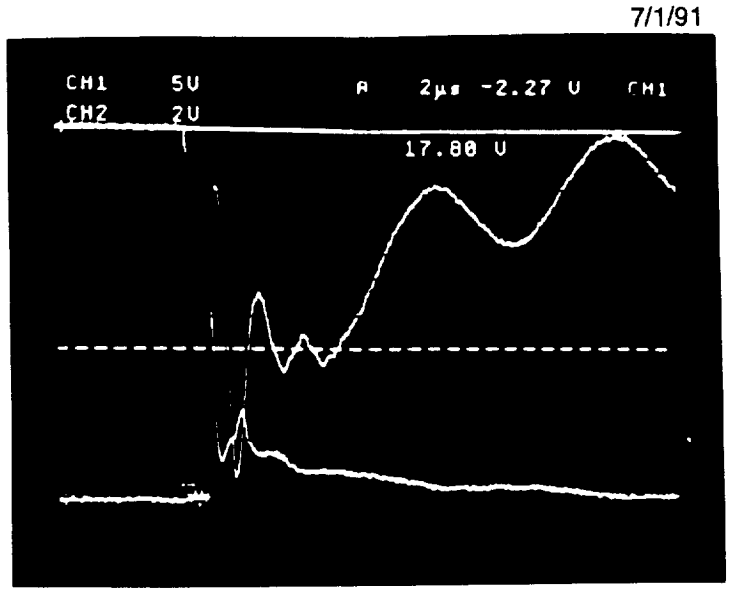

Figure 24. Current Voltage Pulse from Pulse Forming Network

References

1. Freed, L. E., Freed, C., and O'Donnell, R. G., IEEG Journal of Quantum Electronics, QE-18, 1229 (1982).

2. Starovoitov, V. S., Et. Al., Journal of Quantum Spec. Radiat., Transfer 41, No. 2, 153 (1989).

3. Fisher, C. H., Et. Al., Final Report GL-TR-89-0292, Geo. Lab., Hanscom AFB, Massachusetts.

4. Jeong, K. M., Et. Al., Journal of Physical Chemistry, Vol. 93, No. 3, 1145 (1989).

5. Witteman, W. J., "The CO_2 Laser," Springer-Verlag (1986).

Section 7
CONTAMINATION ANALYSIS

7.1 SURFACE CONTAMINANTS PARAMETERS

To analyze the effects of surface contaminants on the transmission of laser intensity through the optical elements, it is assumed that a loss factor due to surface contaminants, α_i, can be specified for each optical element. Depending on the number of surfaces, n_i, of the optical element, the efficiency of transmission of each element can be defined as

$$\eta_i = (1 - \alpha_i)^{n_i} \tag{7-1}$$

The total efficiency of the optical train due to surface contaminants can thus be obtained as

$$\eta = \prod_{i=1}^{N} \eta_i = \prod_{i=1}^{N} (1 - \alpha_i)^{n_i} \tag{7-2}$$

Here N equals the total number of optical elements.

The LAWS Instrument has the following optical train.

The transmitting optics has 7 elements including 6 mirrors and one doublet, giving a total of 8 surfaces. The receiving optics has 15 elements, including 11 mirrors, three lenses, and one window, giving a total of 18 surfaces. A list of all optical elements and the approximate angles of incidence is given in *Table 7-1*.

By assuming a constant loss factor for all the optical elements, total transmission efficiency can be obtained. *Table 7-2* gives the results for several assumed values of α_i. It can be seen that in order to keep total efficiency above 90 percent, average loss factors cannot exceed 0.3 percent.

Surface contaminants can be divided into particulates and molecular, and their effects on optical system performance can be treated separately.

Under ideal situations, molecular deposition of surfaces can be assumed to be uniform. The effects resulting from this molecular deposition are changes in total transmissivity and reflectivity. Loss of reflectivity due to deposition of common spacecraft outgas sources has been measured by Woods, et.al. (AEDC-TR-87-8), and results are given in terms of complex index of reflections. The optical system performance can thus be calculated knowing the thickness of the molecular deposition. In real situations, however, the molecular deposition could be quite nonuniform. In this case, measurements are needed to obtain actual degradation in optical properties. We use either the transmissivity or the reflectivity degradation at the required wavelength as a measure of the contamination effects from molecular species.

Table 7-1. LAWS Optical Elements

Element	Type	Surface	Angle (deg)
Transmitting Optics			
1	Primary Mirror	1	90
2	Secondary Mirror	1	90
3	Doublet	2	90
4	Mirror	1	67.5
5	Mirror	1	45
6	Fixed Mirror	1	45
7	Mirror	1	45
Receiver Optics			
1	Primary Mirror	1	90
2	Secondary Mirror	1	90
3	Mirror	1	67.5
4	Mirror	1	45
5	EL1	2	90
6	Driven Mirror	1	45
7	Driven Mirror	1	45
8	Fixed Mirror	1	45
9	EL2	2	90
10	EL3	2	90
11	Mirror	1	~80
12	Mirror	1	~60
13	Mirror	1	~20
14	Mirror	1	~45
15	Window	1	90

Table 7-2. Total Transmission Efficiency for Several Loss Factors

Loss Factor α_i(%)	Individual Efficiency η_i	Total Transmission Efficiency
0.1	0.999	0.9743
0.2	0.998	0.9493
0.5	0.995	0.8778
1.0	0.99	0.7700
2.0	0.98	0.5914
5.0	0.95	0.2635
10.0	0.90	0.0646

The effect due to particulate contaminants is expressed in terms of obscuration ratio (O.R.). This parameter defines the percent of actual area of the optical surface blocked by the particulates, and can be measured directly. The preferred method of measurements is the imaging method. Other methods which can be used include solvent wash and particle counting, tape lifting from fallout witness samples.

The relationship between the O.R. and optical system performance degradation has been the subject of investigation. Dependence of transmissivity loss on the wavelength and particle size distribution needs to be established. Scattering effects may also be of importance. At present, we are only concerned with the loss of signal.

7.2 CONTAMINATION BUDGETS

To ensure the performance of the LAWS subsystems from excessive degradation due to contamination, contamination budgets will be used to guide the establishment of contamination control requirements. The contamination parameters identified in the previous section will be used, and each will be given a total not-to-exceed limit. An analysis of the flow of hardware from cleaning/assembly through integration/launch to the end of mission will be performed. By analyzing the activities of all mission phases, a contamination budget can be established. Using this budget as a guideline, contamination control requirements for the different phases of the program can be defined. With proper planning and control, the state of cleanliness of the system can thus be maintained.

Experience from previous space flight indicates that the largest particulate contamination accumulation comes from acoustic testing and during launch phase of the mission. The largest contribution of molecular contaminants comes from thermal vacuum testing and during launch and

early phase of orbital operations. Hardware design and operations control will be used to reduce contamination buildup during those critical periods.

Since it is unrealistic to try to maintain all optical elements at the same level of cleanliness, it is our intent to keep internal optics at a higher cleanliness level than the exposed optics. Thus we plan to address the contamination requirements for the primary and secondary mirrors differently than those for internal optics. Measurements of cleanliness of the exposed elements will be used as a verification of contamination control.

Typical contamination budgets for molecular and particulate contaminants for the Hubble Space Telescope (HST) are given in *Figures 7-1* and *7-2*.

A plan to conduct measurements of surface contamination accumulation at different phases of the mission will be established. This plan shall include the method of measurement, the data type, the frequency of measurement, the analysis to be performed, and the pass-fail criteria. Direct measurement of the critical surface is the preferred method, supplemental with indirect measurement data from environmental monitoring. Contingency measures will be used if the measured contaminant level exceeds allocated budget.

Tentative contamination budgets for particulate and molecular contaminants for LAWS primary and secondary mirrors are given in *Tables 7-3* and *7-4*. These budget allocations will be updated as more data from measurements and/or analysis become available.

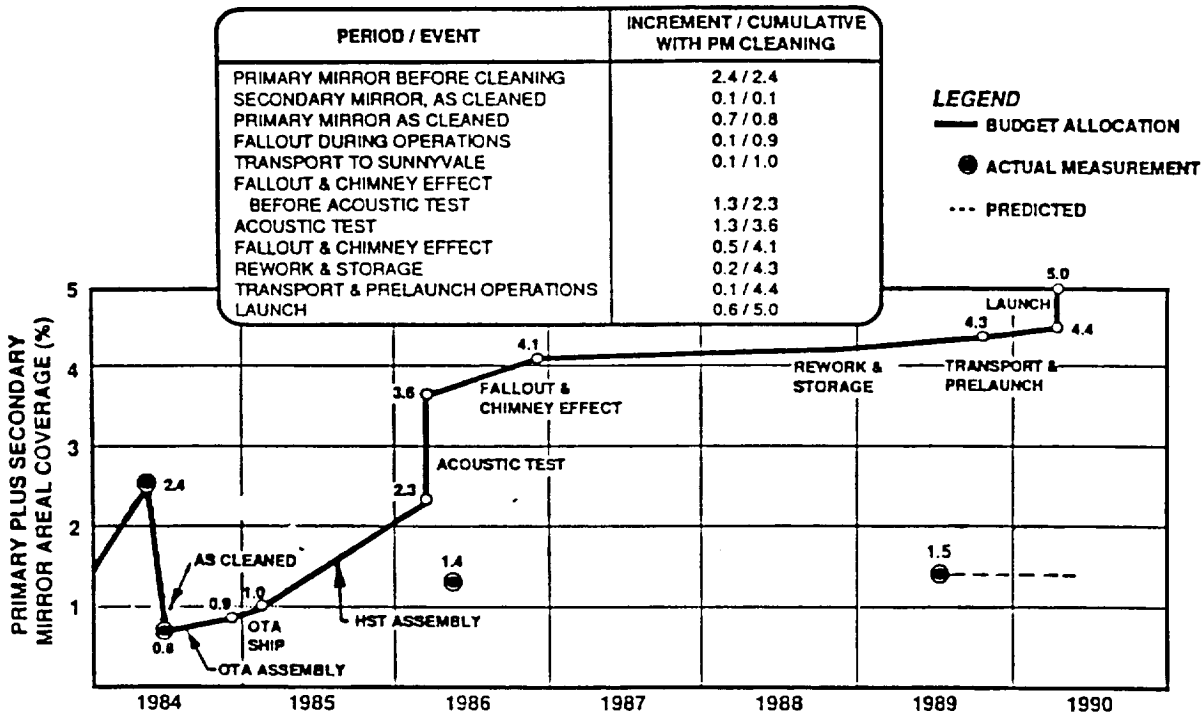

Figure 7-1. Typical Particulate Contamination Budget Allocation

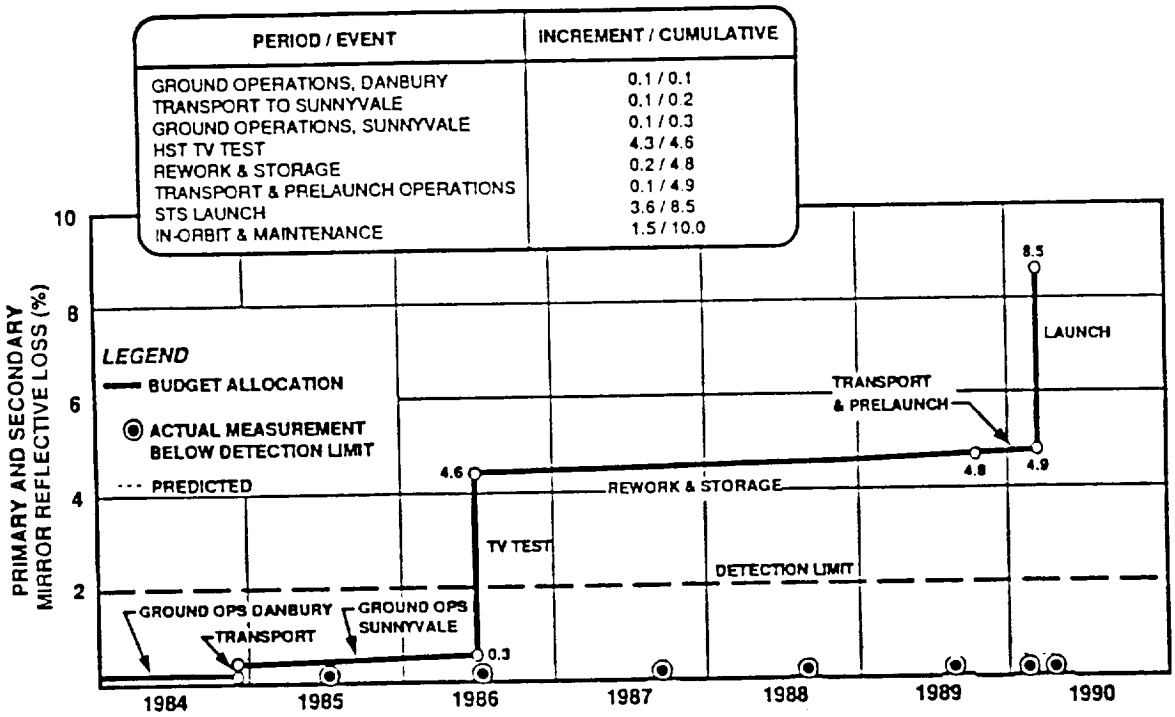

Figure 7-2. Typical Molecular Contamination Budget Allocation

Table 7-3. Tentative Particulate Contamination Budget

Operation Phase	% Obscuration Increment/cum.
Primary Mirror Cleaning	0.1/0.1
Secondary Mirror Cleaning	0.1/0.2
Fallout during Operations at Itek	0.1/0.3
Transport to Huntsville	0.1/0.4
Fallout Prior to Acoustic Test	1.0/1.4
Acoustic Test	1.0/2.4
Fallout Prior to Shipping	0.2/2.6
Transport to Launch Site	0.05/2.65
Prelaunch Operations	0.05/2.7
Launch/Deployment	0.7/3.4
Orbital Operations	0.1/3.5
Total Particulate Budget	3.5%

Table 7-4. Tentative Molecular Contamination Budget

Operation Phase	% Reflectivity Loss Increment/cum.
Ground Operations, Itek	0.1/0.1
Transport to Huntsville	0.1/0.2
Ground Operations Huntsville	0.1/0.3
LAWS TV Test	2.0/2.3
Storage	0.1/2.4
Transportation to Launch Site	0.05/2.45
Prelaunch Operations	0.05/2.5
Launch/Deployment	1.5/4.0
On-orbit Operations	1.0/5.0
Total Molecular Budget	5%

7.3 CONTAMINATION SOURCES AND DEGRADATION EFFECTS

7.3.1 Particulate Contaminants

Sensor performance degradation can be caused by limiting optical throughput, scattering of off-axis radiation due to particle clouds, and enhancement of mirror scattering reflectance (i.e., the bi-directional reflectance distribution function measurements) due to surface particulate contaminants. Major sources of particulate contamination are

- Airborne particulates settling on hardware surfaces during manufacturing, assembly, and test operations
- Paint overspray, insulation shreds, clothing fibers, and other human induced substances
- Particles generated from launch vehicle and payload enclosure material and redistributed during ascent
- Particles dispersed by opening of payload enclosure and deployment of appendages (solar arrays, radiators, antennas, etc.)
- Redistribution of particles trapped in internal surfaces and in crevices of the instrument
- Materials released on-orbit by space vehicle, including products from upper stage, reaction control system (RCS), attitude control system, and orbit transfer rocket firing.

7.3.2 Molecular Contaminants

Deposition of outgassed products on LAWS optical mirrors, optical sensors, and critical optical surfaces may cause performance degradation (e.g., reflectance change). The contaminant sources are

- Lubricants, leaks, and exposed organics from which volatile condensables may emanate and be transferred to critical surfaces
- Volatile condensable materials in the environment to which contamination sensitive critical surfaces may be exposed
- Orbital molecular cloud generated from space vehicle and payload operations
- Molecular flux returning to critical surfaces due to collision with ambient species or among outgas molecules
- Interaction of spacecraft material with space environment, such as atomic oxygen, UV, high energy particles, and space debris.

7.3.3 Contamination Analysis

Contamination studies are needed in support of the LAWS contamination control effort. These analyses identify effects due to various contamination sources which contribute to the contamination budget during various phases of the LAWS mission. These analyses shall include but not be limited to the following:

- Studies to predict outgassing effects from LAWS materials on critical optics
- Studies concerning the redistribution of particulates and their effect on primary mirror obscuration.

The basis of the LAWS contamination control plan shall be derived from the LAWS contamination analyses and shall indirectly be responsible for the LAWS contamination control requirements.

7.4 CONTAMINATION PREVENTION AND CONTAINMENT SCHEME

To achieve the contamination control requirement and to ensure that the contamination budget allocation will not be exceeded, a series of activities will be initiated. A contamination control plan will be developed which identifies the necessary steps to follow during the various phases of the program. It shall include the requirements for manufacturing, cleaning, verification, monitoring, personnel training, and material selection.

7.4.1 Design Considerations

To maintain cleanliness of the optical elements after the initial cleaning and assembly, a contamination enclosure is used to protect the optical train from external environments. It is designed so that contamination accumulations on the optical trains are minimized during testing, launch, and on-orbit operations. With this reduced degradation of the majority of internal optical elements, it is possible to allocate higher contamination budgets for the external optics, mainly the telescope primary and the secondary mirrors, which are exposed to the elements.

Partitions will be used to isolate internal optical elements from potential contamination sources, thus reducing direct depositions during on-orbit activities. Venting paths are designed to avoid transport of contaminants toward critical optical elements. Materials selection guidelines will

be established and followed, and the optical bench and the environmental cover will be thermal vacuum baked out to reduce the amount of material outgas on orbit.

Other design features may be implemented as needed as a result of tradeoff studies and sensitivity analysis which identifies major contributors to the contamination budget. The use of purge gas and the use of an aperture opening cover are among the designs to be studied.

7.4.2 Personnel Training

Since the main source of contamination during ground operations is through human beings, it is critical to reduce the generation and transfer of ground contaminants during manufacturing, testing, and integration. A program will be initiated to train personnel working on the LAWS program on the contamination control requirements.

7.4.3 Operational Constraints/Guidelines

As a result of contamination analysis, constraints shall be established for orbital operations to reduce the possibility of contaminating the critical LAWS external surfaces. As an example, the analysis of contaminant transport during reboost phases will be used to establish constraints and procedures during such operations.

7.4.4 Contingency Measures

Contamination levels for the critical surfaces will be monitored at scheduled intervals during ground operations. The monitored level of contaminants will be compared with the contamination budget. If the measurements indicate the possibility of exceeding budget, contingency measures will be initiated. Such corrective measures shall include the identification of contamination sources, the effect due to the contaminations, suggested corrective actions, and verification of the success of the corrective actions. A revised contamination budget shall be established taking into consideration the results of all these actions.

7.5 CONTAMINATION ANALYSIS

Once the LAWS Instrument is integrated with the spacecraft, installed in the launch vehicle and ready for launch, the chance for further contamination monitoring and cleaning diminishes. However, activities that follow will add contaminants to the ones already accumulated on the critical surfaces. Analyses are used to establish the estimated contamination budget during the launch/deployment, orbital verification, and on-orbit operations, including reboost phases of the mission. *Table 7-5* lists the critical surfaces, their contamination concerns, and the transport mechanism involved. Corresponding analysis will be needed to obtain level of contamination accumulated on the critical surfaces. Some of the omission phase contamination concerns will be discussed in the following sections.

Table 7-5. LAWS Contamination Evaluations

Critical Surface	Contamination Concern	Transport Mechanism
Primary mirror	Exposed to ambient environment Direct view of telescope interior Ground and launch phase particulates Stray light	Molecular deposition Return flux Redistribution Particle cloud
Secondary mirror	Exposed to ambient environment Direct view of telescope interior and spacecraft High laser energy flux	Direct deposition Impingement
Star Trackers	Exposed to ambient environment Susceptible to spacecraft contaminants Susceptible to re-boost contaminants Stray light	Return flux Plume backflow Particulate deposition Particle cloud
Laser windows and transmitting optics	High energy flux Laser internal contaminants LAWS internal contaminants	Diffusion transport Molecular deposition Particle redistribution
Detectors and receiving optics	Low signal level LAWS internal contaminants	Diffusion transport Molecular deposition Particle redistribution
Thermal control surfaces	LAWS external sources Space environmental effects	Molecular deposition Return flux
Cryogenic Surface	LAWS internal sources Cold surface	Molecular deposition Diffusion transport

312599-FW-01

7.5.1 Launch Phase Contamination Concerns

The most noticeable flight-phase contamination events during launch operations that need to be carefully reviewed/addressed are identified below.

- Pre-Launch Standby

  Inclement weather during the pre-launch standby period can induce contaminant ingestion into the payload fairing (PLF) interior through the peripheral vents. The ingestion rate and quantity will depend upon the balance between the external wind environment (gust speed and direction) and the PLF internal purge or air-conditioning flow rate. The resulting LAWS subsystem degradation will be affected by the external air quality, i.e., the contaminant contents, as well as the contaminant distribution on spacecraft surfaces. The wind-ingestion analysis will aid in the establishment of additional contamination protection requirements during the pre-launch standby phase.
- Launch/Ascent

The vibroacoustic level during lift-off can cause particle suspension from the PLF interior surfaces and subsequent redeposition on various sensitive thermal control and optical surfaces. Since the LAWS telescope will be installed on top of the spacecraft with aperture opening pointing up in a launch/ascent configuration (*Figure 7-3*), that vibroacoustically induced particulate contamination will have to be investigated. A parametric analysis, correlating surface particle deposition and surface area obscuration increase with initial PLF cleanliness level, is needed to establish PLF cleanliness and contamination control requirements.

- Booster Motor Staging

  Of primary concern during booster separation is the upper staging motor plume which may recirculate over the core vehicle and enter into the PLF interior through various vent ports. Contaminant distribution on critical surfaces will occur due to internal flow diffusion/convection. However, for an Atlas IIAS launch vehicle, this shall not be a problem, since the Castor IVA booster motors are located far below the vent ports, and no rocket motors are used for separation.

- Stage Separations

  Depending on the launch vehicle used, the stage separations may contain possible contamination events. The first is the retro-rocket firing, which could cause plume impingement, especially if particulate products are involved. This plume impingement phenomenon is affected by the separation trajectory (tipoff rate, misalignment effect, misfiring occurrence) and the firing duration. Secondly, the separation charge operation during stage separation will generate a particulate debris cloud. Inter-particle collisions and the aerodynamic drag of the debris particles could cause some debris particles to reach the spacecraft surface.

Inasmuch as the present contamination analysis encompasses all events from PLF installation through the collision/contamination avoidance maneuver (CCAM), the following upper stage spacecraft integration sources, independent of launch vehicle operations, need to be addressed.

- Propellant venting constraints have been imposed on post upper stage spacecraft separation maneuver operations (one of them being a vent inhibition distance of 500 ft) so that the spacecraft will not be subject to impingement by vented propellant gases. From the spacecraft molecular contamination view point, the main engine propellant vent problem may seem trivial, depending on whether the propellant gas is condensable on any noncryogenic spacecraft surfaces. On the other hand, venting of the hydrazine monopropellant (most likely in liquid form) for any upper stage RCS could cause condensation because of trace contaminants in the propellant.
- Aside from the propellant venting concern voiced in the preceding paragraph, upper stage RCS firing and the attendant plume impingement or backflux during CCAM could cause spacecraft contamination, because trace contaminants in the propellant and from the catalyst bed could survive the chamber combustion environment and be present in the exhaust plume flowfield. Experience with the CCAM problem for the Shuttle launch systems may be used for assessment.

312599-FW-04

Approach:

- Estimate PLF interior GRMS based on available vibroacoustic analysis results.
- Determine particle resuspension quantities from data.
- Predict particle fallout on payload surfaces.

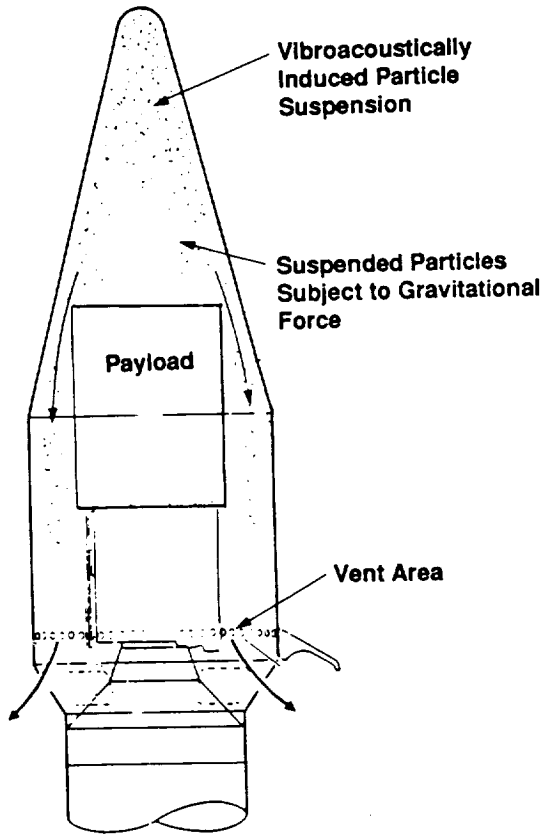

Figure 7-3. Vibroacoustically Induced Particle Redistribution

Other flight-phase contamination sources/events that warrant evaluation include possible contaminant ingestion due to reverse venting during terminal shock traversal, nonmetallic material outgassing during ascent flight, and debris dispersion during upper stage spacecraft separation. Although all the major launch phase contamination issues have been identified, pertinent data on source characteristics and certain flight operational details have not been completely acquired. Therefore, the scope of the study is not fully comprehensive. Future analysis updates shall be performed when up-to-date contamination source data become available.

7.5.2 Orbital Operations Contamination Concerns

The contamination concerns for this phase of the LAWS program include material outgassing during the early phase of the mission; particulate generation during the appendages deployment and spacecraft checkout phase; plume backflow from the orbital reboosts engine firings; and various on-orbit contamination sources due to operational maneuvering of the space vehicle.

The contamination control approach for this orbital operations phase is to use preventive measures and constraints. Design features of the LAWS Instrument include the use of an environmental cover to protect the internal optics; the use of compartmentalization to isolate optics

from potential contamination source from ancillary equipments; and the use of venting path design to reduce the possibility of contamination deposition during pressure transients. Location of external critical surfaces will be chosen to minimize the impact from the external contamination sources.

Contamination analysis will be performed to study the impact of various design options. Operational constraints will be established to reduce contamination impact during periods of high rate of contamination generation. Such measures as pointing the telescope away from contamination sources, or turning on the purge gas system, will be used to ensure that the end-of-life contamination budget will not be exceeded.

A mathematical model for external contamination analysis during orbital operations has been established. *Figure 7-4* depicts the LAWS Instrument external surfaces to be used in on orbit contamination transport analysis. This model will be updated when the details of the spacecraft configuration are made available. For overall system contamination control, ground operational events, such as particle fallout at various facilities and air conditioning (or purge air) flow recirculation (if the air cleanliness is substandard), should also be considered in contaminant buildup estimates and contamination control procedures development.

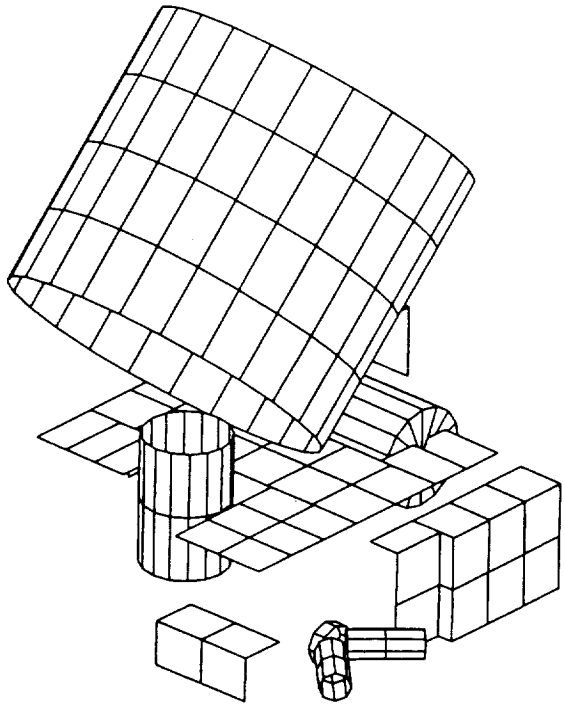

Figure 7-4. LAWS Contamination Math Model

The key analytical tools (computer codes) for performing the LAWS launch-phase and orbital phase contamination analysis are listed in *Table 7-6*.

Similar to the situation for the launch phase analysis, pertinent data for the orbital operation phase analysis have not been completely established. Therefore, only preliminary study can be performed at this time. Future analysis update shall be performed when design features and source characterization data are made available.

Table 7-6. Analytical Tools for Contamination Analysis

312599-FW-06

COMPUTER CODE	FUNCTION AND MODEL
1. Molecular transfer kinetics • Free molecular (MTK)	• Contamination flux transport in space environment • Radiative heating analogy • Surface/gas interaction phenomena • Deposit flux and total deposit
2. Molecular transport with intermolecular collisions • Monte Carlo (MCTK) • Diffusion (SPAR)	• Contamination flux transport in near free-molecular environment • Monte Carlo simulation or diffusion • Surface/gas interaction phenomena same as MTK
3. Rocket propellant thermo-chemistry and nozzle flow (ODK, TDK, CONTAM 3)	• Thermal chemical equilibrium and kinetics • Nozzle flow characterization • Gas and multi-phase flow
4. Rocket plume flowfield and plume impingements (MOC, RAMP, PLIMP,CONTAM 3)	• Method-of-characteristics • Two-phase flow; nozzle frictional effects • Plume flowfield and impingement properties
5. Return flux (MOLESCAT)	• Molecular backscatter of outgassed species • Bhatnagar-Gross-Krook model: collisions between outgassed and ambient molecules: self-collisions of outgassed molecules
6. Plume backflux (GAPS, BKFLW)	• Free-molecular distribution from outer plume (Bird's criterion) • Monte Carlo simulation (GAPS); simplified model (BKFLW)
7. Deposit-induced surface change (DISC)	• Maxwell's solution for wave propagation through multilayer medium, such as substrate, coating, and contaminant film
8. Particle cloud dispersion (PT)	• Particle trajectories from vehicle in flight • Particle cloud definition • Aerodynamic forces and orbital dynamics
9. Venting/purging (NCELL)	• Venting/purging of spacecraft • Dynamic equilibrium (MASS, MOMEN, ENGY, SPECIES) in multiple chambers
10. MIE scattering (MIESCA) MIE scattering & diffraction (LIESCA)	• Light scattering by spherical or cylindrical particles (MIE solution) • Particle-induced optical surface degradation
11. Spacecraft charging (NASCAP)	• Spacecraft charging characteristics in a space plasma environment
12. Particle redistribution (PRD)	• Particles on surfaces resuspend and redistribute by vibroacoustic excitation • Surface cleanliness prediction

Appendix A

Functional Specification
LAWS Laser Breadboard

LMSC-HSV SPEC F312362
Rev. B
1 April 1991

FUNCTIONAL SPECIFICATION

LASER ATMOSPHERIC WIND SOUNDER (LAWS) BREADBOARD

Lockheed
Missiles & Space Company, Inc.
4800 Bradford Blvd., Huntsville, AL 35807

A-3

LMSC-HSV SPEC F312362
Rev. B
1 April 1991

LAWS LASER BREADBOARD FUNCTIONAL SPECIFICATION

S.C. Kurzius
Laser Responsible
Equipment Engineer

APPROVED:

W.E. Jones
Program Manager

D.J. Wilson
Deputy Program Manager/
Chief Engineer

CONTENTS

LMSC-HSV SPEC F312362
Rev. B
1 April 1991

1. SCOPE

This laser breadboard functional specification establishes the performance, design, development, and verification requirements for the LAWS laser breadboard that will be used to test parts of the LAWS transmitter.

2. APPLICABLE DOCUMENTS

The following documents form a part of this specification to the extent specified herein.

2.1 Government Documents

Phase I Final Report.

2.2 LMSC Documents

LMSC/HSV SOW F312354 Rev. A - LAWS Laser Breadboard SOW, January 1991, and the applicable LMSC documents cited therein (SOW Para. 2.2).

2.3 Subcontractor Documents

None.

3. REQUIREMENTS

3.1 Laser Breadboard Definition. The LAWS laser breadboard is a frequency stable pulsed CO_2 laser system that will be used to demonstrate critical parts of the LAWS transmitter.

3.1.1 Breadboard Diagram. The LAWS laser breadboard shall consist of the following systems, identified in Figure 1.

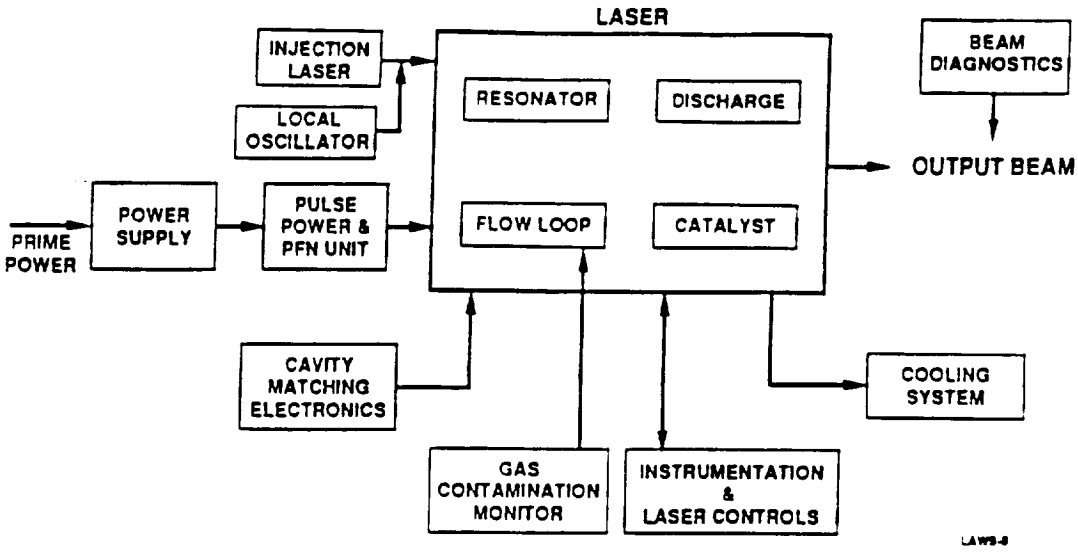

Figure 1. Laser Breadboard Block Diagram

3.1.1.1 Active Optical Control System. The optical coherence system shall be comprised of the following breadboard subsystems:

a. Resonator
b. Injection Laser
c. Cavity Matching Electronics
d. Beam Diagnostics
e. Local Oscillator

3.1.1.2 Pulsed Discharge and Gain Control System. The pulsed discharge and gain control system shall be comprised of the following breadboard subsystems:

a. Discharge
b. Pulse Power and Pulse Forming Network (PFN)
c. Power Supply
d. Instrumentation and Laser Controls.

3.1.1.3 Laser Flow & Gas Control System. The laser flow and gas control System shall be comprised of the following breadboard subsystems:

a. Flow Loop and Gas Supply
b. Catalyst
c. Gas Contamination Monitor
d. Cooling System.

3.1.2 Interface Definition

3.1.2.1 Power Source Interface. The LAWS laser breadboard shall operate with power sources of 220 ±10 V.

3.1.2.2 Coolant Interface. TBD

3.1.2.3 Lidar Interface. TBD

3.2 Characteristics. This paragraph specifies the characteristics of the laser breadboard. Specifications of the Phase I selected design configuration are appended in Section 10 for reference.

3.2.1 Performance

3.2.1.1 Warmup. The LAWS laser breadboard shall operate as specified herein with an overall system warm-up time not to exceed 15 min.

3.2.1.2 Wall Plug Efficiency. The LAWS laser breadboard shall operate with a discharge efficiency consistent with a LAWS system laser final design wall plug efficiency of not less than 5 percent.

3.2.1.3 Energy per Pulse. The LAWS laser breadboard shall have a laser beam output energy per pulse of not less than 15 J (goal: 20 J).

3.2.1.4 Pulsewidth. The LAWS laser breadboard laser beam output pulsewidth (FWHM) shall be within the range of 2 to 3 μs.

3.2.1.5 Pulse Shape. The LAWS laser breadboard laser beam output pulse shape shall have less than 10 percent of the energy in the gain switched spike and less than 20 percent of the energy in the tail. The tail shall be down not less than 20 dB from the main pulse intensity after two pulse widths.

3.2.1.6 Laser Beam Mode. The LAWS laser breadboard laser shall have not less than 95 percent of the output beam energy in a single longitudinal and single transverse mode.

3.2.1.7 Wavelength. With a pulse laser working gas mixture containing $^{12}C^{16}O_2$, the LAWS laser breadboard laser output beam shall have a wavelength of 10.59 ±0.01 μm.

3.2.1.8 Wavelength with Isotope. With a pulse laser working gas mixture containing the isotope $^{12}C^{18}O_2$, the LAWS laser breadboard laser output beam shall have a wavelength of 9.11 ±0.01 μm.

3.2.1.9 Chirp. The LAWS laser breadboard laser output beam shall have less than 200 kHz chirp.

3.2.1.10 Beam Quality. The LAWS laser breadboard laser output beam quality ratio shall be less than 1.2 (goal:1.1) relative to a plane wave of the same dimensions. Beam quality is defined as

$$BQ = \exp\left\{\frac{1}{2}\left[\frac{2}{\lambda}\ OPD\right]^2\right\}$$

where

OPD = rms optical path difference across the laser beam

λ = wavelength.

3.2.1.11 Beam Dimensions. The laser breadboard output beam dimensions shall be square.

3.2.1.12 Beam Polarization. The laser breadboard laser output beam polarization shall be not less than 95 percent linear.

3.2.1.13 Beam Jitter. The laser breadboard laser output beam jitter shall be less than 100 urad (goal: 25 urad).

3.2.1.14 Beam Energy Stability. The laser breadboard pulse-to-pulse laser output beam energy shall not fluctuate more than 10 percent.

3.2.1.15 Divergence. The laser breadboard laser output beam divergence shall be less than 1.2 times the diffraction limit.

3.2.1.16 Pulse Rate Frequency. In performance test mode, the laser breadboard laser beam output pulse rate frequency (PRF) shall be variable from 1 Hz to not less than 10 Hz.

3.2.1.17 Pulse on Command Delay. Reserved.

3.2.1.18 Intracavity Beam Mode: The laser breadboard resonator intracavity beam shall have not less than 90 percent of its energy in the lowest order cavity mode.

3.2.1.19 Life Test Pulse Rate Frequency: The nominal laser breadboard laser beam PRF shall be designed with a goal of 20 Hz at an energy per pulse of 20 J

while operating in a life test mode. In the life test mode, the LAWS laser breadboard need not meet performance specifications of paras. 3.2.1.1 through 3.2.1.18 herein.

3.2.1.20 Life. The laser breadboard shall have as a goal an operational life with maintenance of not less than 3×10^8 shots while maintained under the ground based operating environment specified in para. 3.2.4 herein.

3.2.2 Physical

3.2.2.1 Weight. Reserved.

3.2.2.2 Head Dimensions. The laser breadboard head dimensions shall not be greater than 1.1 m x 2.2 m x 1.1 m.

3.2.2.3 Breadboard Dimensions. The laser breadboard volume shall not be greater than 10 m^3, consistent with commercial transport requirements.

3.2.2.4 Structural Characteristics. The laser breadboard shall have structural characteristics enabling it to meet operating and non operating environment requirements specified in para. 3.2.4 herein.

3.2.2.5 Material Compatibility. The laser breadboard shall contain only materials which are compatible with each other and with the environments specified in para. 3.2.4 herein. Specifically, the laser breadboard design shall minimize potential oxygen isotope contamination of working gas mixtures containing the isotope $^{12}C^{18}O_2$.

3.2.2.6 Leakage. The laser breadboard flow loop leakage rate shall be less than 1×10^{-2} torr per hour for a period of at least 30 days.

3.2.2.7 Connectors. Connectors shall preclude incorrect installation or application. When applicable, connectors shall contain physical alignment guides.

3.2.2.8 Guards. Critical and vulnerable items on the laser breadboard shall be located or shielded in accordance with standard laboratory practices.

3.2.3 Maintainability

3.2.3.1 Design Requirements

3.2.3.1.1 Corrective Maintenance. The laser breadboard design shall allow for easy access and corrective maintenance.

3.3.3.1.2 Protective Features. The laser breadboard design shall include protective features necessary to prevent a safety hazard for maintenance actions.

3.2.3.1.3 Verification. The laser breadboard design shall provide a capability for functional verification.

3.2.3.1.4 Maintenance Points. The laser breadboard design shall include maintenance points for the laser breadboard gas system, including those for filling or purging, in accessible locations.

3.2.3.2 Support Equipment

3.2.3.2.1 Safety. The use of support equipment shall not introduce a safety hazard.

3.2.3.2.2 Verification of Status. The operational status of all support equipment shall be verifiable.

3.2.4 Environmental Conditions. The laser breadboard storage and operational environments are those found in ground based offices and laboratories.

3.2.5 Transportability. Shipping containers, packaging, and other safeguards shall protect the laser breadboard from normal risks incident to transportation, storage, and handling of scientific hardware.

3.3 Design and Construction

3.3.1 Materials, and Parts. Reserved.

3.3.2 Electromagnetic Radiation. Reserved.

3.3.3 Nameplates. Nameplates or product markings shall identify the laser breadboard and each of its major components. Identification shall include product name and fixed asset owner.

3.3.4 Safety. The design of the laser breadboard shall address safe operational conditions such that failures which may occur will not cause major damage to interfacing equipment.

3.3.4.1 Hazardous Material. Materials which present toxic hazards to personnel shall be avoided in the design of the laser breadboard. Where use of toxic materials cannot be avoided, manufacturing and processing controls shall be implemented such that environmental limits specified by the Occupational Safety and Health Act (OSHA) shall not be violated. Identified carcinogenic materials shall not be used in any phase of development. Suspected carcinogenic material(s) shall be identified and require LMSC approval prior to use in any phase of development.

3.3.4.2 Dangerous Components

3.3.4.2.1 Covers. The laser breadboard shall protect personnel from accidental contact with potentially dangerous parts such as high voltage components.

3.3.4.2.2 Identification of Dangerous Components. The laser breadboard shall label dangerous components sufficiently to reasonably ensure safety from accidental contact.

3.3.4.2.3 Safety Interlocks. Parts of the laser breadboard which present a danger of electrocution shall have interlocks to prevent access when the part is energized.

3.3.4.3 Failure Criteria. The laser breadboard shall be designed such that no single failure or combination of two failures result in a catastrophic event capable of causing injury or loss of life to personnel. The laser breadboard shall be designed such that no single failure results in a critical event capable of major damage to facilities or other breadboard components.

3.4 Documentation

Reserved.

3.5 Furnished Component Characteristics

3.5.1 LMSC Furnished Injection Laser. The laser breadboard injection laser will be a continuous wave (cw) CO_2 laser.

3.5.1.1 Injection Laser Power. The laser breadboard injection laser power output will be not less than 10 W.

3.5.1.2 Injection Laser Beam Diameter. The laser breadboard injection laser output beam diameter will be 2.5 $\pm$0.5 mm.

3.5.1.3 Injection Laser Valves. The laser breadboard injection laser will be sealed.

3.5.1.4 Injection Laser Beam Mode. The laser breadboard injection laser output beam will have 98 percent of its energy in a TEM_{00} mode.

3.5.1.5 Injection Laser Line Selection. The laser breadboard injection laser will be able to select the 10.59 μm line when utilizing a tube filled with a $^{12}C^{16}O_2$ mixture and the 9.11 μm line when using a $^{12}C^{18}O_2$ mixture. Two tubes shall be provided, one to operate at 10.59 μm and one to operate at 9.11 μm. A grating will be incorporated for line selection.

3.5.1.6 Injection Frequency Stability. Reserved.

3.5.1.7 Injection Laser Beam Polarization. The laser breadboard injection laser output beam will have a linear polarization of not less than 95 percent.

3.5.2 Government Furnished Catalyst Characteristics. Reserved. However, the breadboard flow loop design is to be based on a GFE catalyst impregnated on a monolith support structure in the main flow loop, i.e., a design without a bypass flow loop.

APPENDIX

10. PHASE I SELECTED DESIGN SPECIFICATIONS

10.1 Scope. Specifications based on the Phase I selected design configuration are as summarized below. It is recognized however that elements of this Phase I design are subject to revision in Phase II engineering trade studies. Therefore, the specifications below are of use primarily as initial design points.

10.2 Power Resonator Performance

10.2.1 PZT Control. The laser breadboard resonator PZT cavity length tuning device will have a preprogrammed mirror acceleration/deceleration that minimizes feedback mirror relocation and have a maximum settling time of 5 ms.

10.2.2 PZT Tuning Range. The laser breadboard resonator PZT cavity length tuning range will be not less than 25 μm.

10.3 Flow Loop Performance. The laser breadboard flow loop will provide homogeneous gas flow within the discharge cavity.

10.3.1 Gas Temperature. The laser breadboard laser gas temperature will be 293 $\pm$20 K prior to discharge.

10.3.2 Gas Homogeneity. The relative density variation is not to exceed 1×10^{-3}.

10.4 Pulse Power. The laser breadboard pulse power unit will consist of a full voltage pulse forming network (PFN) and a thyratron discharge switch. The laser discharge voltage will not be greater than 40 kV.

10.5 Resonator. The laser breadboard resonator will be a confocal unstable resonator with square mirrors configured as shown in Figure 2.

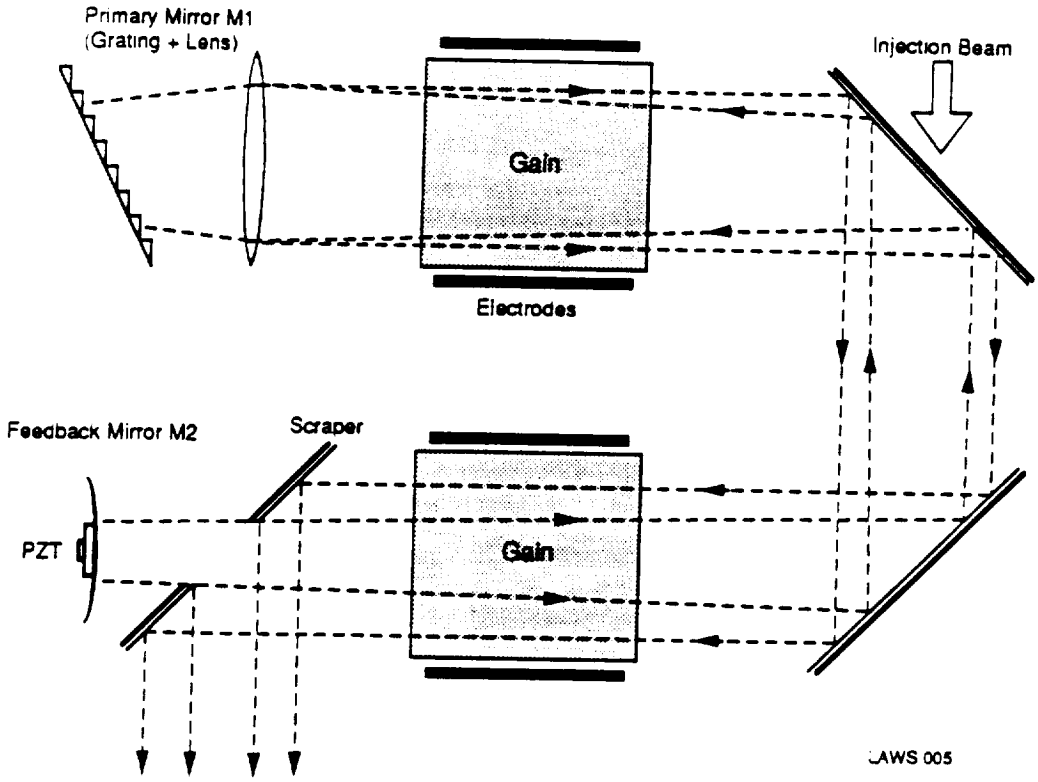

Figure 2. Laser Resonator Configuration

10.5.1 Cavity Magnification. The laser breadboard resonator cavity magnification will be 2.25 ±0.25.

10.5.2 Equivalent Fresnel Number. The laser breadboard resonator equivalent Fresnel number will be 2.4 +0.1.

10.5.3 Cavity Length. The laser breadboard resonator cavity length will be 2.2 ±.02 m.

10.5.4 Cavity Beam Size. The laser breadboard resonator cavity beam size will be 4 ± .1 cm x 4 ±.1 cm.

10.5.5 Primary Mirror Curvature. The laser breadboard resonator effective primary mirror curvature (grating + lens) will be 17.5 ±.1 m.

10.5.6 Feedback Mirror Curvature. The laser breadboard resonator feedback mirror curvature will be -7.7 ±.1 m.

10.5.7 Mirror Construction. The laser breadboard resonator feedback and two turning mirrors will be copper plated and liquid cooled.

10.5.8 Piezo Translation. The laser breadboard resonator cavity length will be tunable by a piezo-electric translation (PZT) device mounted on the feedback mirror.

10.5.9 Grating. The laser breadboard resonator will have a blazed grating for beam wavelength selection.

10.5.10 Windows. The laser breadboard windows will be anti-reflection coated.

10.6 Discharge Cavity

10.6.1 Laser Excitation. The laser breadboard power laser excitation will be via a surface corona ultraviolet (UV) pre-ionized glow discharge.

10.6.2 Specific Loading. The laser breadboard specific loading will be 100 to 175 Joule per liter atmosphere (J/liter-atm).

10.6.3 Gain Length. The laser breadboard resonator gain length will be 1.50 ±0.1 m.

10.7 Flow Loop

10.7.1 Gas Mixture. The laser breadboard working gas mixture will be 50 ±25 percent He, 25 ±10 percent CO_2, remainder N_2, with residual gasses less than 0.1 percent.

10.7.2 Gas Pressure. The laser breadboard working gas pressure will be greater than 0.2 and less than 0.5 atmospheres (atm).

10.7.3 Cavity Flush Factor. The laser breadboard power laser cavity flow flush factor will be greater than 2.5.

10.7.4 Cavity Acoustic Transits. Acoustic pulse transits within the discharge cavity of the laser breadboard will be greater than 50 across the acoustic mufflers.

10.7.5 Catalyst. The laser catalyst will be an in-the-flow-loop monolith or honeycomb structure.

Appendix B

Enhanced LAWS Laser Test Results From ID Program

The LAWS laser hardware has been further optimized and operated under the Textron ID Program Z773 to obtain enhanced performance. *Figure B-1* depicts operations at 330 and 380 Torr at specific energy loadings from 60 to 90 J/L-atm. Note the increase in measured efficiency as pressure and energy loading is increased, with essential agreement between code predictions and test data. The figure depicts a demonstration of operations to upwards of 10 J output for the LAWS laser. Note the measured discharge efficiencies of 8 to 10 percent. The top two figures validate the model (o), with actual test data (x) at the two different operating pressures. The bottom figure extrapolates to 20 J output at the 130 J/L-atm/475 Torr design point from the validated model. Arc-free design loading will be achievable through a minor modification of the current electrode dielectric configuration by either an increase in separation of side-by-side electrodes by approximately 1 mm, or by test of the dielectric material prior to machining to eliminate minor voids in strategic regions.

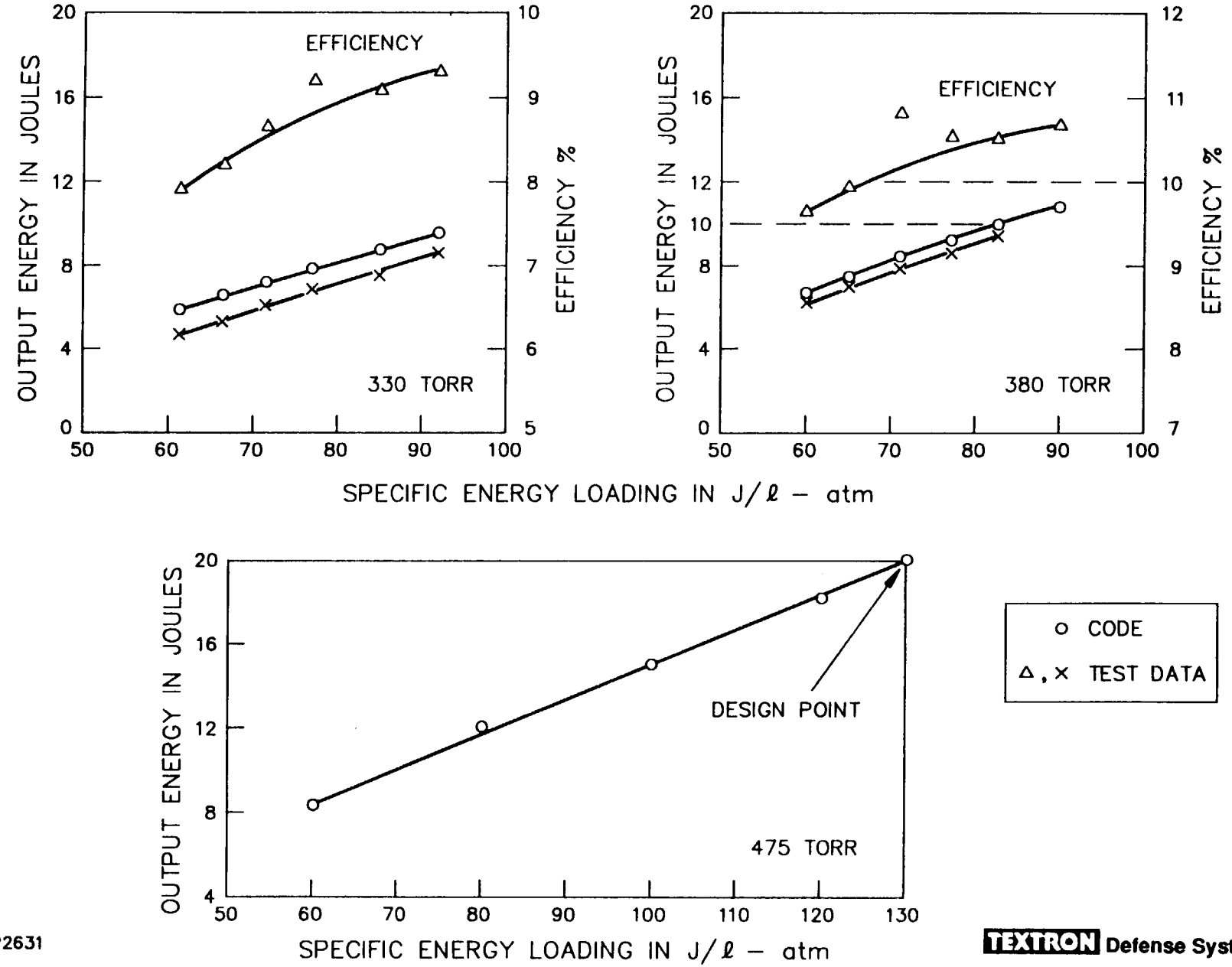

Figure B1. 10 J Output Demonstrated at 10% Efficiency